Late Cretaceous and Paleocene Lissamphibia and Squamata of Montana and the end-Cretaceous mass extinction

David G. DeMar, Jr.

A dissertation

submitted in partial fulfillment of the

requirements for the degree of

Doctor of Philosophy

University of Washington

2016

Reading Committee:

Gregory P. Wilson, Chair

Christian A. Sidor

Adam D. Leaché

James D. Gardner

Program Authorized to Offer Degree:

Biology

University of Washington

Abstract

Late Cretaceous and Paleocene Lissamphibia and Squamata of Montana and the end-Cretaceous mass extinction

David G. DeMar, Jr.

Chair of the Supervisory Committee:
Professor Gregory P. Wilson, Chair
Department of Biology

Late Cretaceous and Paleocene lissamphibians (e.g., salamanders and albanerpetontids) and squamates (e.g., lizards and snakes) are common components of the nonmarine vertebrate fossil record of North America. However, within the context of the Cretaceous-Paleogene (K-Pg) mass extinction (ca. 66 million years ago) those clades have received little attention relative to other aspects of the continental biota (e.g., dinosaurs, mammals). This dissertation represents the first comprehensive study of salamander (Caudata) and salamander-like lissamphibians (Allocaudata: Albanerpetontidae) and nonmarine squamates leading up to and across the K-Pg boundary. The primary impetus behind these studies was to better determine the timing, mode, and severity of lissamphibian and squamate extinctions and to address the proposed causal mechanisms of the

mass extinction and their ancillary effects prior to (e.g., climate change, Deccan Traps volcanism, acid rain) and at the K-Pg boundary (e.g., bolide impact, thermal pulse).

To assess lissamphibian and squamate diversity patterns leading up to and across the K-Pg boundary, my coauthors and I documented temporal species richness, taxonomic composition, and turnover. The larger lissamphibian dataset (2021 specimens versus 200 in squamates) allowed for additional quantitative measures of diversity to be calculated including faunal evenness, heterogeneity indices, and relative abundance distributions. Species-level diversity was recorded from a succession of ≥ 45 temporally constrained vertebrate microfossil localities of the uppermost Cretaceous Hell Creek and lowermost Paleocene Tullock formations of Garfield County, northeastern Montana, USA.

Results of the caudate and allocaudate study revealed a stepwise pattern of species loss during the last ca. 200 k.y. of the Cretaceous (based on new and revised age determinations of the study area). Five of nine species were either extirpated (33%) from the local area or went extinct (22%) at or near the K-Pg boundary. Declines in species diversity and significant changes in community structure coincided with those species losses. Combined, these results suggest growing ecological stress in the local caudate and allocaudate faunas prior to the bolide impact at the K-Pg boundary.

Squamates suffered high species extinctions (81%) during the last ca. 200 k.y. of the Cretaceous which were concentrated nearer the K-Pg boundary. Though species extinctions were highest across the K-Pg boundary, low to high levels of turnover (appearances and disappearances) in

the squamate faunas of northeastern Montana occurred throughout most of the depositional duration of the Hell Creek Formation (ca. 1.9 Ma). Coincident with a moderate level of local squamate turnover that occurred more than ca. 300 k.y. before the K-Pg boundary was the loss of chamopsiids and platynotans possessing monocuspid and fang-like teeth, respectively, from the lower to upper halves of the Hell Creek Formation. A similar but less pronounced biostratigraphic pattern has been observed in other aspects of the local vertebrate faunas (euselachians, lissamphibians, turtles, and mammals).

The caudate fauna of the earliest Paleocene satisfies several expectations of early post-extinction recovery faunas in being species depauperate (five species), predominated by a "bloom" taxon (*Opisthotriton kayi*), and invaded by immigrants (*Proamphiuma cretacea*). A Lazarus taxon (the caudate *Prodesmodon copei*) reappeared as early as the Pu2/3 of the local section. The squamate fauna during that interval possessed two chamopsiid lizards. Chamopsiids are part of a clade thought to have gone extinct during the K-Pg mass extinction. These new records suggest that chamopsiids were a "dead clade walking" as they failed to recover in abundance or diversity following the extinction.

Several new fossil lissamphibians and squamates were documented in this dissertation including a new fossil salamander (proteid) and several lizards (indeterminate iguanomorph, six scincomorphs, and five anguimorphs) from the Hell Creek Formation. Results of my systematic and phylogenetic work demonstrate that the Hell Creek Formation of the study area contains the taxonomically richest caudate and squamate assemblages known from the Mesozoic of North America. My coauthored description and phylogenetic analysis of a new stem iguanian lizard

from the slightly older deposits of the Two Medicine Formation (Campanian) of northwestern Montana has yielded important insights into the evolution of Iguanomorpha during the Late Cretaceous. The new taxon, *Magnuviator ovimonsensis* gen. et sp. nov., represents the oldest unequivocal iguanomorph from North America and is the sister taxon to a clade of paracontemporaneous iguanomorphs (Temujiniidae) from the Gobi Desert of Mongolia. Its phylogenetic relationships imply that crown iguanians were likely absent from North America prior to the K-Pg boundary despite previous claims. Combined, these systematic and phylogenetic studies add to the growing taxonomic inventory of the lissamphibian and squamate fossil record and enhance our understanding of their evolution within Montana, across the Western Interior of North America, and across the northern landmasses of Laurasia during the Late Cretaceous and early Paleocene.

TABLE OF CONTENTS

LIST OF FIGURES

CHAPTER 2: EXTINCTION AND SURVIVAL OF SALAMANDER AND SALAMANDER-LIKE AMPHIBIANS ACROSS THE CRETACEOUS-PALEOGENE BOUNDARY IN NORTHEASTERN MONTANA, USA

CHAPTER 5: A NEW LATE CRETACEOUS (CAMPANIAN) STEM IGUANIAN FROM NORTHWESTERN MONTANA, USA

LIST OF TABLES

CHAPTER 4: A NEW FOSSIL SALAMANDER (CAUDATA: PROTEIDAE) FROM THE UPPER CRETACEOUS (MAASTRICHTIAN) HELL CREEK FORMATION, MONTANA, USA

CHAPTER 5: A NEW LATE CRETACEOUS (CAMPANIAN) STEM IGUANIAN FROM NORTHWESTERN MONTANA, USA

ACKNOWLEDGEMENTS

This dissertation would not have seen the light of day were it not for the support of numerous individuals and institutions.

My committee chair, Gregory P. Wilson, has been a trusted advisor, colleague, and friend during my years as a graduate student at the University of Washington. He has granted me the freedom to explore several research projects without restraint yet provided me with the necessary guidance to see many of them to fruition. Greg leads by example and has taught me how to be a careful scientist in and out of the field. For that, I am thankful and honored to be among those who have received their Ph.D. under his tutelage.

To the other members of my supervisory committee at the University of Washington, Christian A. Sidor, Adam D. Leaché, Elizabeth A. Nesbitt, and Patricia A. Kramer , I thank you for your academic guidance, patience, and moral support. I further thank Christian for providing me with extra field experience (albeit in the middle of Seattle!). I would like to thank my external supervisory committee member, James D. Gardner, for accepting my initial request to join my supervisory committee and for being a valued colleague, coauthor, and friend. His technical knowledge of lissamphibians and squamates, sage advice, and witty emails were always welcomed.

I would like to thank my coauthors Grace Carter, Jack Conrad, Jason Head, David Varricchio, and Gregory Wilson for their contributions to some of the chapters included in this dissertation. However, any mistakes or misinterpretations within this dissertation are entirely mine. I also would like to thank James Gardner for giving me the opportunity to coauthor a

review paper on fossil lissamphibians from North America. That review greatly improved my understanding of the clade and, in turn, improved the quality of my dissertation.

I wish to thank the current and past Wilson lab graduate students who have helped me with all aspects of being a graduate student and for their astute scientific knowledge, friendship, patience, and moral support: Meng Chen, Lauren DeBey, Jonathan Calede, Stephanie Smith, Alexandria Brannick, and Luke Weaver. I also would like to thank Brody Hovatter, Garrett Mercier, and Marlena Staton for their logistical and research support and the numerous undergraduates who have brought to my attention the specimens incorporated into my dissertation.

I am grateful for the many friends, fellow graduate students, and postdocs at the University of Washington who have given me advice, a critical manuscript review, or simply shared a laugh or two with me: Charles "Chuck" Beightol, Camilla Crifò, Regan Dunn, Jared Grummer, Elisha Harris, Adam Huttenlocker, Winifred Kehl, Sterling Nesbitt, Brandon Peecook, Carolina Gomez Posada, and Linda Tsuji. I also wish to thank the staff members in the Department of Biology who have made my life easier when in need of departmental, technical, or logistical support: Karen Bergeron, Toby Bradshaw, Michele Conrad, Brianna Divine, Rodney Dungo, Marissa Heringer, Dave Hurley, Ron Killman, Patti Owens, and Sarah O'Hara.

I am indebted to the following individuals for access to museum displays and collections, photographs of published and unpublished specimens for comparative purposes, and technical and research support: Ana Balcarcel, Michael Caldwell, Regan Dunn, Ron Eng, James Gardner, Patricia Holroyd, Logan Ivy, Adam Leaché, Murat Maga, Carl Mehling, Mark Norell, Randall Nydam, Jason Pardo, Karen Peterson, Patricia Roath, Sharlene Santana, John Scannella, Pavel Skutschas, Abby Vander Linden, David Wake, and the numerous staff and volunteer members of

the UWBM, UCMP, MOR, RTMP, UALVP, and the AMNH who have aided me in one way or another.

I am grateful to the following individuals who have provided me guidance, financial support, and/or aid in and out of the field including many respected research collaborators: Geb Bennett, William A. Clemens, Denver Fowler, Mark Goodwin, Jack Horner, Jason Moore, Nathan Myhrvold, Cory Redman, Paul Renne, Courtney Sprain, and Tom Tobin. I am also indebted to a number of individuals for their volunteer aid in the field: Corinna Casey, David Grossnickle, Geoff Harrison, Don and Kathy Hopkins, Kathryn Hoppe, Richard and Liz Meyn, Michael Poltenovage, and Gregg Wilson. Bashira Chowdhury deserves special recognition for her tireless efforts in helping me in the field for three field seasons. "Just one more shovel full" was her favorite thing to say while bagging sediment in the field. I imagine several additional quality specimens (or "fossil gold") came from that extra effort. Bruce Crowley also was a tremendous aid in the field and has prepared a number of important fossils for me including the holotype specimen of the Egg Mountain iguanomorph described in *Chapter Five*.

I thank the following researchers, scientists, and individuals for their extra guidance and mentorship prior to and during my time at the University of Washington: Sue Ann Bilbey, Dennis Braman, Brent Breithaupt, Donald Brinkman, Mark Clementz, Jack Conrad, Dee Hall, Evan Hall, Jason Head, Randall Nydam, Ray Rogers, Julia Sankey, Caroline Strömberg, Kelli Trujillo, and David Varricchio.

I thank the following artists and scientific illustrators for "bringing back to life" the extinct vertebrates I am most passionate about. Jack Conrad, Misaki Ouchida, and Morgan Turner provided most of the two-dimensional anatomical drawings and the life reconstruction of the Egg Mountain iguanomorph. Kailey Kimball and Chad Littlewood, two staff members of

The Reptile Zoo in Monroe, WA granted Misaki and I access to a live iguanian for reference. Donna Braginetz illustrated the life reconstruction of the extinct salamander *Opisthotriton kayi* featured in the lower right hand corner on the cover of the GSA Special Paper 503. Russell Hawley illustrated the paleocommunities of the Mesaverde Formation, WY in my 2006 and 2008 coauthored papers.

I am deeply grateful to the people of Jordan, Montana and the surrounding areas of Garfield County for their generosity, hospitality, and/or access to their private lands: K.L. and Cherylle Bliss, Daniel Burgess, Gene and Karla Christensen, John Coldwell, Bob and Jane Engdahl, Shane Harbaugh, Harold and Jean Isaacs, John and Kathy McKeever, Jana Olson, Lori and Clyde Phipps, Amy Sinks, Dale and Jane Tharp, Jay and Gail Twitchell, and Judd and Eva Twitchell.

I thank the following land permitting agencies and personnel who have provided logistical support and special use permits for the collection of vertebrate fossils: Doug Melton, Greg Liggett, and the Bureau of Land Management; Matt DeRosier and the Charles M. Russell National Wildlife Refuge; Patrick Rennie and the Montana Department of Natural Resources and Conservation; and Craig Putchat, Dave Andrus, and Montana Fish, Wildlife, and Parks. I also would like to thank the staff at Hell Creek State Park including Mary Pat Watson and Jerry.

Financial support was provided by the National Science Foundation Graduate Research Fellowship Program (DGE-0718124), the University of Washington Department of Biology and the UW Graduate School, the University of California Museum of Paleontology Doris O. and Samuel P. Welles Research Fund, the American Museum of Natural History and Richard Gilder Graduate School, and the Society of Vertebrate Paleontology.

My family and loved ones have been a major source of inspiration, motivation, and support during my time as a college student. First, I want to thank my fish, Costi, for keeping me company during the lonely times these last several years. To my siblings, Connie, Michael, Amy, Kim, Jessica, Kevin, Megan, and Anthony, and my nieces and nephews, thank you for lending an ear and the occasional phone call or text message. I sincerely thank my mom and dad for keeping my head above water during the difficult times in my life and for believing in me even when I did not. I am forever grateful for your unconditional love and support. Thank you for keeping me on track and for the extra push that led to the completion of my graduate studies. I especially would like to thank my son, Jamie, for his patience and understanding during my absence from home over the last decade. Thanks bud for the help in the field, for sorting and finding that rare snake vertebra from Hot Feet, and for always only being a phone call away. To my fiancée, Gina Bailey, thank you for your patience, emotional support, and the occasional much needed distraction during these last several months while finishing my dissertation. I look forward to us sharing many new experiences and in forging a lifelong and loving relationship.

CHAPTER 1:

INTRODUCTION AND OVERVIEW

Of the 'big five' mass extinctions recorded in Earth's history (Raup and Sepkoski 1982), the Cretaceous-Paleogene (K-Pg) mass extinction represents the most well known and recent (ca. 66 million years ago). This event is most famous for the extinction of non-avian dinosaurs although many other forms of life also suffered extinction (e.g., marine and flying reptiles [Bardet 1994; Butler et al. 2009], ammonoids [Ward 1996]) or suffered major losses in taxonomic richness or diversity (e.g., plants [Wilf and Johnson 2004], insects [Labandeira et al. 2002], squamates [Archibald and Bryant 1990; Longrich et al. 2012], mammals [Wilson 2005, 2014]). The K-Pg mass extinction has been intensely studied over the past several decades (see reviews in Archibald 1996, 2011), yet considerable debate remains regarding the tempo (catastrophic vs. gradual) and mode (single vs. multiple causes) of this event (Archibald et al. 2010; Schulte et al. 2010). The catastrophic extinction scenario solely due to a bolide impact (Alvarez et al. 1980) and its proposed ancillary effects (e.g., thermal pulse [Robertson et al. 2004], acid rain [Retallack 2004]) *at the K-Pg boundary* contrasts with a more gradual extinction scenario wherein environmental perturbations such as volcanism (Courtillot et al. 1996; Keller et al. 2009), marine regression (Bakker 1986; Archibald 1996, 2011), and climate change (e.g., Li and Keller 1998; Wilf et al. 2003; Nordt et al. 2003; Tobin et al. 2012, 2014) *leading up to the K-Pg boundary* stressed biotic communities prior to the bolide impact. These scenarios remain to be fully tested among all aspects of the continental biota, particularly from terrestrial vertebrate faunas. In this dissertation, I examined the fates of salamanders and albanerpetontids (Lissamphibia) and lizards and snakes (Squamata) during this pivotal event in vertebrate evolution (*Chapters Two* and *Three*, respectively). Given their temperature-dependent physiologies lissamphibians and squamates serve as excellent model organisms for testing environmental and climate-related mechanisms of the K-Pg mass extinction.

A critical component to better determining the timing of lissamphibian and squamate extinctions and for differentiating between the two main K-Pg extinction scenarios was the development of a high-resolution chronostratigraphic framework. The geologic exposures of the Hell Creek and Tullock formations in Garfield County, northeastern Montana are ideal for documenting terrestrial vertebrate dynamics during the K-Pg interval (e.g., Clemens 2002; papers in Wilson et al. 2014a). The study area includes over 300 taxonomically diverse and well-sampled vertebrate microfossil localities that span ca. 3.1 myr (ca. 68–64.9 Ma) leading up to and across the K-Pg boundary. These localities have been placed within a high-resolution temporal framework based on bio-, magneto-, and lithostratigraphy, and radiometric age determinations (Archibald 1982; Archibald et al. 1982; Swisher et al. 1993; Clemens 2002; Wilson 2004, 2005, 2014). Updates to the chronostratigraphic framework (Renne et al. 2013; LeCain et al. 2014; Sprain et al. 2015) and identification of several K-Pg boundary claystones in the local area (e.g., Hartman et al. 2014; Moore et al. 2014) make it possible to more precisely determine the timing of faunal turnover during the study interval and to better address the competing K-Pg mass extinction scenarios and the ensuing recovery phase.

In addition to documenting lissamphibian and squamate diversity dynamics leading up to and across the K-Pg boundary, I described and/or phylogenetically analyzed several new taxa including a salamander (*Chapter Four*; DeMar 2013) and several lizards (*Chapter Three*) on the basis of isolated bones from the Hell Creek and Tullock formations and on the basis of two nearly complete skeletons from the Campanian-age Two Medicine Formation of northwestern Montana (*Chapter Five;* see also DeMar et al. 2015). The Two Medicine lizard has phylogenetic implications for the K-Pg mass extinction study on squamates (*Chapter Three*). These new taxa

add to the growing list of lissamphibian and squamate species known from the Late Cretaceous of North America (see recent reviews by Gardner and DeMar 2013 and Nydam 2013).

Chapter Two (Wilson et al. 2014b) documents the survival and extinction of salamander (Caudata) and salamander-like lissamphibians (Allocaudata: Albanerpetontidae) within the chronostratigraphic framework described above. This coauthored study is the first to document high-resolution temporal patterns of species richness, evenness, relative abundance distributions, taxonomic composition, and turnover in those clades leading up to and across the K-Pg boundary. Anurans (frogs and toads) were excluded from this study due to time constraints but currently are under study by G. Mercier, G. P. Wilson, and I (e.g., Mercier et al. 2014).

Results demonstrate that during the last ca. 400 k.y. of the Cretaceous (ca. 200 k.y. based on new radiometric age determinations; see Sprain et al. 2015) caudate and allocaudate diversity declined (species richness, evenness, community structure) which was coincident with increasing disappearance rates. Fifty-five percent of species were lost during that interval though only 22% went extinct at or near the K-Pg boundary. The earliest Paleocene caudate assemblage was species depauperate and predominated by a single "bloom" taxon. A single caudate immigrant joined the survivors immediately after the K-Pg boundary. The overall diversity pattern implies growing ecological stress in the lissamphibian assemblages leading up to the K-Pg boundary and provides support in favor of the multi-cause K-Pg extinction scenario.

My contributions to *Chapter Two* (Wilson et al. 2014b) involved: 1) systematic study and taxonomic updates and additions to the fossil lissamphibian database originally assembled by my coauthors (G. P. Wilson and G. Carter); 2) conducted or aided in the quantitative analyses; 3) wrote or aided in writing parts of the manuscript (e.g., systematics of fossil lissamphibians; interpretations regarding extinction selectivity); 4) photographed most figured specimens and

assembled voucher specimen plates and aided in figure and table creation; 5) conducted field work in the study area to boost sample sizes; and 6) provided financial support through grants to me.

Chapter Three documents lizard and snake turnover and extinctions leading up to and across the K-Pg boundary within the same chronostratigraphic framework. Many of the same methodologies and quantitative measures of diversity used in the lissamphibian study (*Chapter Two*; Wilson et al. 2014b) were also applied to the lizard and snake data though the smaller sample sizes (200 specimens across 45 localities) limited my ability to apply them all (i.e., species evenness, relative abundance distributions). Nevertheless, the assembled squamate database is the largest of its kind for documenting their diversity dynamics leading up to and across the K-Pg boundary. Several new lizards were described in the Appendix to *Chapter Three*.

Chapter Four (DeMar 2013) is a description and phylogenetic analysis of a new species of salamander from the Hell Creek Formation of Garfield County, northeastern Montana. I recognized the new species, *Paranecturus garbanii*, from the large sample of salamander specimens studied in *Chapter Two* (Proteidae gen. et sp. nov. of Wilson et al. 2014b). The new species is based on isolated atlantes and trunk vertebrae from several vertebrate microfossil localities. I assessed the phylogenetic relationships of *P. garbanii* through a cladistic analysis of 13 caudate taxa and 23 vertebral characters and found it to be the oldest member of Proteidae.

Chapter Five is a description and phylogenetic analysis of a new Late Cretaceous (Campanian) stem iguanian lizard from the Egg Mountain locality of the Two Medicine Formation, Montana. The description of the new taxon, *Magnuviator ovimonsensis* gen. et sp. nov., was augmented by computed and microcomputed tomography scans (CT and μCT,

respectively) and three dimensional reconstructions of the skeletons. That data allowed for a more comprehensive morphological description and improved the number of character states scored for our phylogenetic analysis.

Using the character/taxon data matrix of Gauthier et al. (2012), my coauthors (J. Conrad, J. Head, D. Varricchio, G. P. Wilson) and I recovered the new taxon as a stem iguanian (Iguanomorpha sensu Conrad 2008) and sister to Temujiniidae, a contemporaneous family of Late Cretaceous iguanomorphs from Mongolia. Our results imply Laurasian faunal exchange among iguanomorphs during the Cretaceous and suggest that crown iguanians were absent from North America prior to the K-Pg boundary (contra Gao and Fox 1996; Longrich et al. 2012). *Magnuviator* was a relatively large iguanomorph that inhabited a semi-arid environment and may have preyed on wasps at Egg Mountain.

My contributions to *Chapter Five* involved all aspects of the study: 1) described the holotype and paratype specimens; 2) created three-dimensional reconstructions of the holotype and paratype specimens; 3) scored characters and ran the phylogenetic analyses; 4) created the strict consensus apomorphy list; 5) measured specimens; 6) assembled or aided in the assembly of all figures; 7) created the outline drawings of the holotype skeleton; 8) photographed the specimens; 9) advised on the life reconstruction of the new taxon; and, 10) wrote the manuscript.

Chapter Six provides a summary of the main conclusions of my dissertation.

Combined, these chapters highlight the rich fossil record of lissamphibians and squamates from the Late Cretaceous of Montana and provide new insights into their evolution and extinction during the end-Cretaceous mass extinction.

REFERENCES CITED

Alvarez, L. W., W. Alvarez, F. Asaro, and H. V. Michel. 1980. Extraterrestrial cause for the Cretaceous-Tertiary extinction. Science 208:1095–1108.

Archibald, J. D. 1982. A study of Mammalia and geology across the Cretaceous-Tertiary boundary in Garfield County, Montana. University of California Publications in Geological Sciences 122:1–286.

Archibald, J. D. 1996. Dinosaur Extinction and the End of an Era: What the Fossils Say. 237 pp. Columbia University Press, New York.

Archibald, J. D. 2011. Extinction and Radiation: How the Fall of Dinosaurs Led to the Rise of Mammals. 108 pp. The Johns Hopkins University Press, Baltimore, Maryland.

Archibald, J. D., and L. J. Bryant. 1990. Differential Cretaceous/Tertiary extinctions of nonmarine vertebrates; Evidence from northeastern Montana; pp. 549–562 in V. L. Sharpton, and P. D. Ward (eds.), Global catastrophes in Earth history; An interdisciplinary conference on impacts, volcanism, and mass mortality. Geological Society of America Special Paper 247, Boulder, Colorado.

Archibald, J. D., R. F. Butler, E. H. Lindsay, W. A. Clemens, and L. Dingus. 1982. Upper Cretaceous-Paleocene biostratigraphy and magnetostratigraphy, Hell Creek and Tullock formations, northeastern Montana. Geology 10:153–159.

Archibald, J. D., W. A. Clemens, K. Padian, T. Rowe, N. MacLeod, P. M. Barrett, A. Gale, P. Holroyd, H.-D. Sues, N. C. Arens, J. R. Horner, G. P. Wilson, M. B. Goodwin, C. A. Brochu, D. L. Lofgren, S. H. Hurlbert, J. H. Hartman, D. A. Eberth, P. B. Wignall, P. J. Currie, A. Weil, G. V. R. Prasad, L. Dingus, V. Courtillot, A. Milner, A. Milner, S.

Bajpai, D. J. Ward, and A. Sahni. 2010. Cretaceous Extinctions: Multiple Causes. Science 328:973.

Bakker, R. T. 1986. The Dinosaur Heresies: New Theories Unlocking the Mystery of the Dinosaurs and Their Extinction. 481 pp. William Marrow and Company, New York.

Bardet, N. 1994. Extinction events among Mesozoic marine reptiles. Historical Biology 7:313–324.

Butler, R. J., P. M. Barrett, S. Nowbath, and P. Upchurch. 2009. Estimating the effects of sampling biases on pterosaur diversity patterns: implications for hypotheses of bird/pterosaur competitive replacement. Paleobiology 35:432–446.

Clemens, W. A. 2002. Evolution of the mammalian fauna across the Cretaceous-Tertiary boundary in northeastern Montana and other areas of the Western Interior; pp. 217–245 in J. H. Hartman, K. R. Johnson, and D. J. Nichols (eds.), The Hell Creek Formation and the Cretaceous-Tertiary boundary in the northern Great Plains: An integrated continental record of the end of the Cretaceous. Geological Society of America Special Paper 361, Boulder, Colorado.

Conrad, J. L. 2008. Phylogeny and systematics of Squamata (Reptilia) based on morphology. Bulletin of the American Museum of Natural History 310:1–182.

Courtillot, V., J. J. Jaeger, Z. Yang, G. Féraud, and C. Hofmann. 1996. The influence of continental flood basalts on mass extinctions: Where do we stand?; pp. 513–525 in G. Ryder, D. Fastovsky, and S. Gartner (eds.), The Cretaceous-Tertiary Event and Other Catastrophes in Earth History. Geological Society of America Special Paper 307, Boulder, Colorado.

DeMar, D. G., Jr. 2013. A new fossil salamander (Caudata, Proteidae) from the Upper Cretaceous (Maastrichtian) Hell Creek Formation, Montana, U.S.A. Journal of Vertebrate Paleontology 33:588–598.

DeMar, D. G., Jr. J. L. Conrad, J. J. Head, D. J. Varricchio, and G. P. Wilson. 2015. Phylogenetics and paleobiology of a Late Cretaceous stem iguanian from Montana. Journal of Vertebrate Paleontology, Program and Abstracts, 2015, 115.

Gao, K., and R. C. Fox. 1996. Taxonomy and evolution of Late Cretaceous lizards (Reptilia: Squamata) from western Canada. Bulletin of Carnegie Museum of Natural History 33:1–107.

Gardner, J. D., and D. G. DeMar, Jr. 2013. Mesozoic and Palaeocene lissamphibian assemblages of North America: a comprehensive review. Palaeobiodiversity and Palaeoenvironments 93:459–515.

Gauthier, J. A., M. Kearney, J. A. Maisano, O. Rieppel, and A. D. B. Behlke. 2012. Assembling the squamate tree of life: Perspectives from the phenotype and the fossil record. Bulletin of the Peabody Museum of Natural History 53:3–308.

Hartman, J. H., R. D. Butler, M. W. Weiler, and K. K. Schumaker. 2014. Context, naming, and formal designation of the Cretaceous Hell Creek Formation lectostratotype, Garfield County, Montana; pp. 89–121 in G. P. Wilson, W. A. Clemens, J. R. Horner, and J. H. Hartman (eds.), Through the End of the Cretaceous in the Type Locality of the Hell Creek Formation in Montana and Adjacent Areas. Geological Society of America Special Paper 503, Boulder.

Keller, G., A. Sahni, and S. Bajpai. 2009. Deccan volcanism, the KT mass extinction and dinosaurs. Journal of Biosciences 34:709–728.

Labandeira, C. C., K. R. Johnson, and P. Lang. 2002. Preliminary assessment of insect herbivory across the Cretaceous-Tertiary boundary: Major extinction and minimum rebound; pp. 297–327 in J. H. Hartman, K. R. Johnson, and D. J. Nichols (eds.), The Hell Creek Formation and the Cretaceous-Tertiary Boundary in the Northern Great Plains: An Integrated Continental Record of the End of the Cretaceous. Geological Society of America Special Papers 361, Boulder.

LeCain, R., W. C. Clyde, G. P. Wilson, and J. Riedel. 2014. Magnetostratigraphy of the Hell Creek and lower Fort Union Formations in northeastern Montana; pp. 137–147 in G. P. Wilson, W. A. Clemens, J. R. Horner, and J. H. Hartman (eds.), Through the End of the Cretaceous in the Type Locality of the Hell Creek Formation in Montana and Adjacent Areas. Geological Society of America Special Paper 503, Boulder.

Li, L., and G. Keller. 1998. Abrupt deep-sea warming at the end of the Cretaceous. Geology 26:995–999.

Longrich, N. R., B. A. S. Bhullar, and J. A. Gauthier. 2012. Mass extinction of lizards and snakes at the Cretaceous–Paleogene boundary. Proceedings of the National Academy of Sciences 109:21396–21401.

Mercier, G., D. G. DeMar, Jr. and G. P. Wilson. 2014. Frogs and toads (Lissamphibia, Anura) during the end-Cretaceous mass extinction: Evidence from the fossil record of northeastern Montana. Journal of Vertebrate Paleontology, Program and Abstracts, 2014, 187.

Moore, J. R., G. P. Wilson, M. Sharma, H. R. Hallock, D. R. Braman, and P. R. Renne. 2014. Assessing the relationships of the Hell Creek–Fort Union contact, Cretaceous-Paleogene boundary, and Chicxulub impact ejecta horizon at the Hell Creek Formation

lectostratotype, Montana, USA; pp. 123–135 in G. P. Wilson, W. A. Clemens, J. R. Horner, and J. H. Hartman (eds.), Through the End of the Cretaceous in the Type Locality of the Hell Creek Formation in Montana and Adjacent Areas. Geological Society of America Special Paper 503, Boulder.

Nordt, L., S. Atchley, and S. Dworkin. 2003. Terrestrial evidence for two greenhouse events in the latest Cretaceous. GSA Today 13:4–9.

Nydam, R. L. 2013. Squamates from the Jurassic and Cretaceous of North America. Palaeobiodiversity and Palaeoenvironments 93:535–565.

Raup, D. M., and J. J. Sepkoski, Jr. 1982. Mass extinction in the marine fossil record. Science 215:1501–1503.

Renne, P. R., A. L. Deino, F. J. Hilgen, K. F. Kuiper, D. F. Mark, W. S. Mitchell, III, L. E. Morgan, R. Mundil, and J. Smit. 2013. Time scales of critical events around the Cretaceous-Paleogene boundary. Science 339:684–687.

Retallack, G. J. 2004. End-Cretaceous acid rain as a selective extinction mechanism between birds and dinosaurs; pp. 35–64 in P. J. Currie, E. B. Koppelhus, M. A. Shugar, and J. L. Wright (eds.), Feathered Dragons. Indiana University Press, Bloomington.

Robertson, D. S., M. C. McKenna, O. B. Toon, S. Hope, and J. A. Lillegraven. 2004. Survival in the first hours of the Cenozoic. Geological Society of America Bulletin 116:760–768.

Schulte, P., L. Alegret, I. Arenillas, J. A. Arz, P. J. Barton, P. R. Bown, T. J. Bralower, G. L. Christeson, P. Claeys, C. S. Cockell, G. S. Collins, A. Deutsch, T. J. Goldin, K. Goto, J. M. Grajales-Nishimura, R. A. F. Grieve, S. P. S. Gulick, K. R. Johnson, W. Kiessling, C. Koeberl, D. A. Kring, K. G. MacLeod, T. Matsui, J. Melosh, A. Montanari, J. V. Morgan, C. R. Neal, D. J. Nichols, R. D. Norris, E. Pierazzo, G. Ravizza, M. Rebolledo-Vieyra,

W. U. Reimold, E. Robin, T. Salge, R. P. Speijer, A. R. Sweet, J. Urrutia-Fucugauchi, V. Vajda, M. T. Whalen, and P. S. Willumsen. 2010. The Chicxulub asteroid impact and mass extinction at the Cretaceous-Paleogene boundary. Science 327:1214–1218.

Sprain, C. J., P. R. Renne, G. P. Wilson, and W. A. Clemens. 2015. High-resolution chronostratigraphy of the terrestrial Cretaceous-Paleogene transition and recovery interval in the Hell Creek region, Montana. Geological Society of America Bulletin.

Swisher, C. C., III , L. Dingus, and R. F. Butler. 1993. 40Ar/39Ar dating and magnetostratigraphic correlation of the terrestrial Cretaceous-Paleogene boundary and Puercan Mammal Age, Hell Creek-Tullock formations, eastern Montana. Canadian Journal of Earth Sciences 30:1981–1986.

Tobin, T. S., G. P. Wilson, J. M. Eiler, and J. H. Hartman. 2014. Environmental change across a terrestrial Cretaceous-Paleogene boundary section in eastern Montana, USA, constrained by carbonate clumped isotope paleothermometry. Geology.

Tobin, T. S., P. D. Ward, E. J. Steig, E. B. Olivero, I. A. Hilburn, R. N. Mitchell, M. R. Diamond, T. D. Raub, and J. L. Kirschvink. 2012. Extinction patterns, δ18O trends, and magnetostratigraphy from a southern high-latitude Cretaceous-Paleogene section: links with Deccan volcanism. Palaeogeography, Palaeoclimatology, Palaeoecology 350–352:180–188.

Ward, P. D. 1996. Ammonoid Extinction; pp. 815–824 in N. H. Landman, K. Tanabe, and R. A. Davis (eds.), Ammonoid Paleobiology. Plenum Press, New York.

Wilf, P., and K. R. Johnson. 2004. Land plant extinction at the end of the Cretaceous: A quantitative analysis of the North Dakota megafloral record. Paleobiology 30:347–368.

Wilf, P., K. R. Johnson, and B. T. Huber. 2003. Correlated terrestrial and marine evidence for global climate changes before mass extinction at the Cretaceous-Paleogene boundary. Proceedings of the National Academy of Sciences of the United States of America 100:599–604.

Wilson, G. P. 2004. A quantitative assessment of mammalian change leading up to and across the Cretaceous-Tertiary boundary in northeastern Montana, Ph.D. Dissertation, pp. 412. University of California.

Wilson, G. P. 2005. Mammalian faunal dynamics during the last 1.8 million years of the Cretaceous in Garfield County, Montana. Journal of Mammalian Evolution 12:53–75.

Wilson, G. P. 2014. Mammalian extinction, survival, and recovery dynamics across the Cretaceous-Paleogene boundary in northeastern Montana; pp. 365–392 in G. P. Wilson, W. A. Clemens, J. R. Horner, and J. H. Hartman (eds.), Through the end of the Cretaceous in the type locality of the Hell Creek Formation in Montana and adjacent areas. Geological Society of America Special Paper, Boulder, Colorado.

Wilson, G. P., W. A. Clemens, J. R. Horner, and J. H. Hartman eds. 2014a. Through the End of the Cretaceous in the Type Locality of the Hell Creek Formation in Montana and Adjacent Areas. Geological Society of America Special Paper 503.

Wilson, G. P., D. G. DeMar, Jr., and G. Carter. 2014b. Extinction and survival of salamander and salamander-like amphibians across the Cretaceous-Paleogene boundary in northeastern Montana, USA; pp. 271–297 in G. P. Wilson, W. A. Clemens, J. R. Horner, and J. H. Hartman (eds.), Through the end of the Cretaceous in the type locality of the Hell Creek Formation in Montana and adjacent areas. Geological Society of America Special Paper 503, Boulder, Colorado.

CHAPTER 2:

EXTINCTION AND SURVIVAL OF SALAMANDER AND SALAMANDER-LIKE AMPHIBIANS ACROSS THE CRETACEOUS-PALEOGENE BOUNDARY IN NORTHEASTERN MONTANA, USA[1]

[1]A version of this chapter has been published. The official citation is listed below.

Wilson, G. P., D. G. DeMar, Jr., and G. Carter. 2014. Extinction and survival of salamander and salamander-like amphibians across the Cretaceous-Paleogene boundary in northeastern Montana, USA; pp. 271–297 in G. P. Wilson, W. A. Clemens, J. R. Horner, and J. H. Hartman (eds.), Through the end of the Cretaceous in the type locality of the Hell Creek Formation in Montana and adjacent areas. Geological Society of America Special Paper 503, Boulder, Colorado. DOI:10.1130/2014.2503(10).

ABSTRACT

Modern amphibians (lissamphibians) are highly sensitive indicators of environmental disturbance. As such, fossil lissamphibians are an excellent model for testing causal hypotheses of the Cretaceous-Paleogene mass extinction and secondary effects of Deccan volcanism and a bolide impact (e.g., acid rain). We quantitatively analyzed high-resolution temporal changes in diversity and community structure of a succession of salamander and salamander-like lissamphibian assemblages from the Hell Creek Formation and Tullock Member of the Fort Union Formation of Garfield County, northeastern Montana (ca. 67.5–65.3 Ma). Richness, evenness, and taxonomic composition remained stable through the lower Hell Creek Formation. Peak richness (11 species) occurred in the middle of the formation coincident with a short term drop in evenness. Following a return to preexisting levels of evenness, diversity progressively declined in the upper third of the formation. This pattern reflects plummeting relative abundances of *Scapherpeton tectum* and a stepwise disappearance of five species, of which three represent extirpation (33%) and two represent extinction (22%). These results suggest that ecological instability increased in the local fauna during the last ~400 k.y. of the Cretaceous. Temporal correlation with local, regional, and global changes in other aspects of the terrestrial (mammals, plants) and marine (planktonic foraminifera, mollusks) biota and environment (volcanism, paleotemperature) implies a global phenomenon (late Maastrichtian event). The post-Cretaceous-Paleogene "survival" fauna from the lowermost Tullock Member was taxonomically depauperate and predominated by the "bloom taxon" *Opisthotriton kayi*. Together, our results lend growing support in favor of a complex multiple-cause scenario for the Cretaceous-Paleogene mass extinction event.

INTRODUCTION

Since Alvarez et al. (1980), researchers have hotly debated the tempo and mode of the Cretaceous-Paleogene mass extinction event (for reviews, see Powell 1998; Archibald 2011). Some have argued for a geologically sudden mass extinction event that resulted from a large bolide impact and its ancillary effects (e.g., global wildfire, acid rain, thermal pulse, prolonged darkness) at the Cretaceous-Paleogene boundary (e.g., Robertson et al. 2004; Fastovsky and Sheehan 2005; Goldin and Melosh 2009; Schulte et al. 2010). While there are multiple lines of compelling evidence for a large bolide impact at the Cretaceous-Paleogene boundary (Schulte et al. 2010), evidence also exists for other significant environmental perturbations that occurred shortly before and at the Cretaceous- Paleogene boundary (Deccan volcanism—Keller et al. 2009; marine regression—Archibald 1996; climate change—Wilf et al. 2003; Tobin et al. 2012). Other researchers have thus argued that a more likely scenario involves multiple perturbations that combined to cause the Cretaceous-Paleogene mass extinction event (see Wilson 2014; Archibald et al. 2010). Most recently, the multiple-cause scenario has taken the form of a press-pulse model (White and Saunders 2005; Arens and West 2008). Under this model, press mechanisms, such as climate change, sea level change, and volcanism, operated over longer temporal scales (10 thousand years [k.y.] to 1 million years [m.y.]) to stress biotic communities during the latest Cretaceous, leaving them vulnerable to pulse mechanisms, such as a large bolide impact or a surge of volcanism, which occurred over shorter temporal scales (1 day to <10 k.y.) at or very near the Cretaceous-Paleogene boundary. Despite the abundance of literature on the Cretaceous-Paleogene mass extinction, few studies have directly tested these scenarios, particularly with the fossil record of the continental biota.

Most studies of the continental biota have relied upon taxonomic presence-absence data of "before" and "after" units immediately across the Cretaceous-Paleogene boundary (e.g., Archibald and Bryant 1990). These data have been used to estimate proportional rates of extinction at the scale of geologic formations and map the distribution of extinctions among higher taxa. In turn, they have provided important measures of the severity of the mass extinction event and a means for testing the congruence of causal hypotheses and the pattern of differential survival (e.g., Table 6.1 in Archibald 1996). Unfortunately, this approach provides only limited information regarding the timing of extinctions, which is vital to differentiating between the aforementioned extinction scenarios, and neglects relative abundance data, which are a major component of biological diversity (Magurran 2004). Although Archibald and Bryant (1990) measured relative abundances, they only distinguished between "common" and "rare" taxa in their results. Other studies have shown that trends in richness and relative abundances are often decoupled or discordant, revealing important insights about extinction and recovery dynamics (McKinney et al. 1998; McElwain et al. 2009). Thus, testing the Cretaceous-Paleogene extinction scenarios requires quantification of high-resolution temporal patterns of biotic diversity leading up to and across the Cretaceous-Paleogene boundary.

In this study, we compile a well-constrained stratigraphic succession of vertebrate microfossil assemblages that spans ~2.2 m.y. across the Cretaceous-Paleogene boundary (ca. 67.5–65.3 Ma). The fossil assemblages derive from exposures of the Hell Creek Formation and the lowermost Tullock Member of the Fort Union Formation in Garfield County, northeastern Montana (Fig. 2.1). In particular, we focus on the salamanders and salamander-like lissamphibians (caudates and allocaudates, respectively) within these assemblages. Developmental and ecophysiological traits of modern lissamphibians (frogs, salamanders,

caecilians), such as the lack of a cleidoic egg, highly permeable skin allowing for ion, water, and gas exchange, a biphasic life cycle, and strict ectothermy, influence their biogeography, abundances, and sensitivity to climate change and environmental perturbations (Lillywhite 2010). In fact, caudates and lissamphibians in general are commonly viewed as ecological indicators or "canaries in a coal mine" that reflect the overall health of an ecosystem (Morell 1999; Wake and Vredenburg 2008). They thus represent excellent models for examining ecological and evolutionary dynamics leading up to and across the Cretaceous-Paleogene boundary.

With the aim of testing the extinction scenarios, we quantitatively analyzed temporal trends in species richness, evenness, relative abundance distributions, taxonomic composition, and turnover in a fossil database of salamanders and salamander-like lissamphibians. Results show that during the last ~400 k.y. of the Cretaceous, five of nine (56%) caudate and allocaudate species were lost in a stepwise fashion from local assemblages, of which three lineages reappeared as Lazarus taxa (sensu Flessa and Jablonski 1983) in the study area or elsewhere in North America in the early and late Paleocene. Significant changes in diversity and community structure also preceded the Cretaceous-Paleogene boundary and temporally correlate with similar changes in other components of the local vertebrate fauna, the regional paleoflora, the global marine biota, and proxies for global environmental conditions. These results lend growing support in favor of a complex multiple-cause scenario for the Cretaceous-Paleogene mass extinction event.

Institutional Abbreviations

DMNH—Denver Museum of Nature and Science (formerly the Denver Museum of Natural History), Denver, Colorado, USA. MOR—Museum of the Rockies, Montana State University, Bozeman, Montana, USA. UCMP—University of California Museum of Paleontology, Berkeley, California, USA. UWBM—University of Washington Burke Museum of Natural History and Culture, Seattle, Washington, USA.

Other Abbreviations

AIC—Akaike's information criterion. FRPF—fossil recovery potential functions. LME—late Maastrichtian event. NALMA—North American land mammal "age". Pu—Puercan NALMA. RAD—relative abundance distribution.

Previous work on salamanders and salamander-like lissamphibians across the Cretaceous-Paleogene Boundary

The fate of caudate and allocaudate faunas across the Cretaceous-Paleogene boundary has been examined in previous studies within the wider context of vertebrate faunas. In their analysis of the UCMP vertebrate fossil database from the Hell Creek Formation and Tullock Member of the Fort Union Formation of Garfield and McCone Counties in northeastern Montana, Archibald and Bryant (1990) documented the Cretaceous-Paleogene survivorship of five of seven caudate and allocaudate species (100% of the common species). Because these changes were recorded at the scale of geologic formations and NALMA, it was not precisely known when these changes occurred relative to the Cretaceous-Paleogene boundary and the ~1.9 m.y. depositional duration of the Hell Creek Formation in the study area (see also Bryant 1989). The Pearson et al. (2002) study is one of the few that has examined high-resolution temporal

patterns in a succession of vertebrate assemblages leading up to the Cretaceous-Paleogene boundary, although they did not extend their study into the Paleocene. They compiled a database of stratigraphic occurrences of vertebrate taxa through the Hell Creek Formation in the Williston Basin of southwestern North Dakota and northwestern South Dakota. The duration of Hell Creek deposition in their study area is estimated to be ~1.36 m.y. (Hicks et al. 2002) versus ~1.9 m.y. in northeastern Montana (Wilson 2014). Of the 321 caudate specimens from 19 stratigraphic horizons in the Pearson et al. (2002) database, 172 specimens were identifiable to three species, namely *Scapherpeton tectum*, *Opisthotriton kayi*, and *Habrosaurus dilatus*. The most common caudate, *Scapherpeton tectum*, and *Opisthotriton kayi* occurred throughout the Hell Creek Formation and to within ~3 m of the Cretaceous-Paleogene boundary in the study area, whereas *Habrosaurus dilatus* was restricted to the upper half of the section. Notably, eight caudate and allocaudate species that occur in the Hell Creek Formation of northeastern Montana (this study) were not found in their sections. The absence of these mostly rare and/or small-bodied taxa may signify temporal, biogeographic, and/or paleoenvironmental differences between the two study areas; however, they are more likely due to the small lissamphibian sample sizes and limited use of screen washing in the Pearson et al. (2002) study. We expect that recent extensive screen washing efforts in the North and South Dakota study area should alleviate most of these differences.

Lillegraven and Eberle (1999) also examined changes in a stratigraphic succession of Lancian and Puercan vertebrate faunas of the Ferris Formation in the Hanna Basin of south-central Wyoming. They recorded *Habrosaurus dilatus* through most of the Lancian time in the Ferris Formation, whereas *Scapherpeton tectum* only occurred immediately below the Lancian-Puercan zone of uncertainty (ca. Cretaceous-Paleogene boundary). Lissamphibians were not

reported from the Puercan of the Ferris Formation, but again small fossil sample sizes in this study limit the robustness of the results. Caudates and allocaudates have also been reported from a number of other Lancian vertebrate microfossil assemblages in the Western Interior of North America (e.g., Estes 1964; Carpenter 1979; Breithaupt 1982; Cifelli et al. 1999), sometimes in large quantities (e.g., the Lance local fauna). However, because most of these assemblages do not occur in stratigraphic succession with other assemblages or because they lack well-constrained chronostratigraphic data relative to the Cretaceous-Paleogene boundary, they are of limited value in understanding diversity dynamics up to and across the Cretaceous-Paleogene boundary at the scale of this study.

MATERIALS and METHODS

In this section, we provide the details of the fossil database and chronostratigraphic framework used in the analyses, and the computational methods used to infer changes in taxonomic diversity and community structure across the Cretaceous-Paleogene boundary in the study area. Fossil Database and Chronostratigraphic Framework Fossil caudates and allocaudates used in this study were collected from exposures of the uppermost Cretaceous Hell Creek Formation and the lowermost Paleocene Tullock Member of the Fort Union Formation of Garfield County, northeastern Montana. Hereafter, we abbreviate the latter stratigraphic unit as the Tullock Member. Specimens were drawn from vertebrate microfossil collections made beginning in 1972 under the guidance of William A. Clemens of the UCMP (e.g., Archibald and Bryant 1990) and more recently through crews led by one of us (Wilson) while affiliated with the UCMP (1998–2004), DMNH (2005–2007), and UWBM (2008–present) (Wilson 2005, 2014).

We only included specimens that were identifiable to the species level and that derive from localities that were both surface collected and screen washed and occur in a detailed stratigraphic framework. Fossil anurans (frogs) were omitted from this study but will be included in future iterations.

The resulting fossil caudate and allocaudate database consists of 2021 specimens, of which 1491 are from 67 Lancian localities and 530 are from an early Puercan (Pu1) locality (UCMP locality V74111). The Lancian localities sample 49 distinct horizons and span ~75 m of the ~89.5-m-thick Hell Creek Formation in the study area. The early Puercan specimens are from the lowermost Tullock Member less than 3 m above the Cretaceous-Paleogene boundary. Specimens from UCMP localities V73085 (Flat Creek 3) and V73087 (Flat Creek 5) were combined into a single assemblage because they are thought to represent the same local fauna (Archibald 1982). This approach was also deemed appropriate for DMNH localities 3302 (Hot Feet General), 3304 (Hot Feet Sharon's Spot), 3305 (Hot Feet Phyllis' Layer), and 3327 (Hot Feet Pat's General), which occur in the same stratigraphic horizon and laterally span ~30 m of exposure. Because fossil sample size varies throughout the section, some quantitative analyses (i.e., rarefaction, heterogeneity estimates, and relative abundance distributions) were restricted to six well-sampled assemblages (UCMP localities V99220, V99369, V74111; UWBM locality C1153; Flat Creek assemblage; Hot Feet assemblage). Each of these six assemblages has ≥138 specimens and we consider them to be well sampled (see Table 2.1 for details). The higher-level systematics of caudates used here is based on Milner (2000) and Heatwole and Carroll (2000, their Appendix 2). We follow other workers (e.g., Fox and Naylor 1982; McGowan and Evans 1995; Gardner 2001) in regarding albanerpetontids as a distinct clade of salamander-like lissamphibians (Order Allocaudata: Family Albanerpetontidae; Fox and Naylor 1982; for a

review, see Gardner and Böhme 2008). Descriptions and diagnoses of common North American Late Cretaceous and early Paleocene salamanders and albanerpetontids can be found in the literature. In particular, we refer the reader to Estes (1981) and Holman (2006) for a broad overview and to the following references for each genus: *Opisthotriton* (Estes 1964, 1969a; Gardner 2000c), *Prodesmodon* (Estes 1964; Naylor 1979; Gardner 2000c), *Habrosaurus* (Estes 1964; Gardner 2003a), *Scapherpeton* (Estes 1964, 1969a; Gardner 2000c), *Lisserpeton* (Estes 1965; Gardner 2000c), *Piceoerpeton* (Naylor and Krause 1981; Naylor 1983; Gardner 2012), *Proamphiuma* (Estes 1969b; Gardner 2003b), and *Albanerpeton* (Fox and Naylor 1982; Gardner 2000a). A new genus and species of proteid was recognized during this study and is here referred to as Proteidae gen. et sp. nov. It is formally described elsewhere (*Paranecturus garbanii*: DeMar 2013; *Chapter Four*). Specimens from the database also include previously undescribed elements of *Habrosaurus prodilatus* and geographic and temporal range extensions of two taxa (DeMar 2011).

Images of voucher specimens are included in Figures 2.2 and 2.3. Summary statistics of anatomical elements in the database appear in Table 2.2. The majority of specimens are atlantes and trunk vertebrae; caudal vertebrae are far less abundant. Tooth-bearing elements are common and include premaxillae, maxillae, vomers, and dentaries. Associations of isolated vertebral and skull elements are reliably known for the batrachosauroidid *Opisthotriton* (Estes 1975), the sirenid *Habrosaurus* (Estes 1964; Gardner 2003a), and to a lesser degree for scapherpetontids (e.g., *Scapherpeton*, *Lisserpeton*; Gardner 2005). Identifications of some fossils from the uppermost 13.8 m of the Hell Creek Formation are based on the UCMP online vertebrate collections database (www.ucmp.berkeley.edu/science/vertebrate_coll.php). The chronostratigraphic framework for this study is based on that described in Wilson (2005) and

updated in Wilson (2014). Fossil localities were incorporated into the chronostratigraphic framework based on measured stratigraphic positional data as described in Wilson (2005, 2014). Stratigraphic positions are reported in meters above or below the Cretaceous-Paleogene boundary (e.g., −35 m for a locality 35 m below the Cretaceous-Paleogene boundary). Figure 2.4 shows the level of sampling through the section. Sample sizes from the middle third of the Hell Creek Formation are being bolstered through ongoing collection in this part of the section. Numerous additional specimens are known from the upper third of the Hell Creek Formation, but they have yet to be examined and incorporated into this database.

Taxonomic Richness

Taxonomic richness of caudates and allocaudates was calculated as: (1) the raw number of species per locality; (2) the species-level and generic-level standing richness (i.e., number of species or genera that first appear or last appear in a stratigraphic horizon plus those that range through the horizon); and (3) the expected number of species in 136 specimen subsamples of the six most fossiliferous assemblages (Table 2.1). Expected species richness was calculated via rarefaction analysis using Analytic Rarefaction version 1.3 (Holland 2003), which is based on the rarefaction equations of Tipper (1979). Expected species richness values and rarefaction curves with 95% confidence intervals are meant to account for variation in sample size (Raup 1975; Tipper 1979) in the six well-sampled assemblages (Table 2.1) that span the section.

Relative Abundances and Heterogeneity Measures

We used two approaches to calculate relative abundances of individuals within caudate and allocaudate species in the Hell Creek Formation and the lowermost Tullock Member. In one

approach, we only used the six well-sampled assemblages (Table 2.1); these span the stratigraphic interval of interest. In the other approach, we subdivided the Hell Creek Formation and the lowermost Tullock Member into 10 m stratigraphic intervals. Only one 10 m bin in the Hell Creek Formation (−30 m to −40 m) did not have adequate sampling for the analysis (<20 specimens). In our analysis, we used eight bins, of which one had 60 specimens and all others had at least 167 specimens. The former approach minimizes the effects of time averaging and is likely more ecologically relevant, whereas the latter approach provides larger sample sizes and a more stratigraphically even treatment of the interval of interest. In all cases, counts were based on the number of identifiable specimens per taxon (NISP) method rather than the minimum number of individuals (MNI) method. This approach was deemed most appropriate because most fossil localities in the study area derive from deposits with a low probability of skeletal association (e.g., channels, crevasse splays; Badgley 1986). Some workers have recommended using the minimum number of elements (MNE) method in cases where breakage of elements is more likely to occur, for example, through the process of screen washing (Badgley 1986). Brinkman (1990) noted the tendency of hour-glass–shaped lissamphibian trunk vertebrae to break at their midline and recommended consideration of half-centra as elements. We less commonly observed midline breakage among scapherpetontid trunk vertebrae, whereas the long, slender trunk vertebrae of *Opisthotriton* showed a greater degree of midline breakage. Because most fragmentary specimens that are identifiable to *Opisthotriton* were from the anterior section, overestimation of the abundance of this taxon from counting anterior and posterior half-centra is likely minimal. On this basis, we follow previous studies in using the NISP approach for lissamphibians despite the occurrence of breakage as a complicating factor (Brinkman 1990). We also note that in our database, species of *Habrosaurus* are almost entirely represented by tooth-

bearing elements, whereas *Albanerpeton* is identified solely on these elements; as a consequence, their abundances are probably underestimated relative to taxa that are represented more commonly by vertebrae. Future efforts will attempt to quantify and account for this discrepancy. Although fidelity of relative abundances in the fossil record is subject to sampling and taphonomic biases (Behrensmeyer et al. 1992; Blob and Badgley 2007; Rogers and Brady 2010), the effect of differences in taphonomic filters among assemblages is reduced when considering fossils of similar size and shape, such as those included here (Blob and Fiorillo 1996). We calculated relative abundances based on the total number of individuals in an assemblage, but we only plotted relative abundances of the four most common species in the section (*Opisthotriton*, *Scapherpeton*, *Habrosaurus*, *Lisserpeton*).

For each of the six well-sampled assemblages (Table 2.1), we combined richness and relative abundance data to calculate four heterogeneity indices (evenness, equitability, Simpson's, Berger-Parker) and 95% confidence intervals, using PAST (Paleontological Statistics Software Package; Hammer et al. 2001). These heterogeneity indices measure diversity in slightly different ways by emphasizing richness, dominance, and rarity to varying degrees. Evenness and equitability indices are derived from Shannon's index (H), which is based in information statistics (for a review, see Magurran 2004). Simpson's and Berger-Parker indices are sometimes referred to as dominance measures (the inverse of evenness) because they place less emphasis on richness than the other measures and more emphasis on the most common species.

To more fully investigate community structure, we also constructed relative abundance distributions (RADs; Magurran 2004) for each of the six well-sampled assemblages (Table 2.1). These are log-linear plots of the rank abundance versus percent relative abundance for all species

in a community. RAD shape (e.g., steepness of slope) may provide information regarding the ecological stability of a community and thereby reveal trends in deterioration and recovery of communities leading up to and across the Cretaceous-Paleogene boundary (McElwain et al. 2009). We generated the RADs and tested their fit to five ecological and theoretical models that represent different assumptions about niche apportionment. These analyses were done using Vegan 1.17–1 (Oksanen et al. 2010) for the statistical program R, version 2.10.1 (R Development Core Team, 2009), with Akaike's information criterion (AIC) as the measure of most likely fit among the five models. For a more thorough explanation of the methods and models, see Wilson (2014, and references therein).

Taxonomic Composition and Turnover

We tabulated biostratigraphic ranges for all species in the Hell Creek Formation and lowermost Tullock Member. The 50% stratigraphic confidence intervals are derived from two one-tailed calculations for the end points of the observed ranges. These calculations are based on the stratigraphic distribution of fossil localities and number of specimens recovered within the local section, using Wilf and Johnson's (2004) expansion of the Strauss and Sadler (1989) method. Wilf and Johnson's calculations incorporate "fossil recovery potential functions" (FRPFs; Marshall 1997), which specify potential for fossil recovery as a function of stratigraphic position. As in the Wilson studies (2005, 2014), we developed FRPFs from the total number of identifiable specimens in a taxon's observed stratigraphic range. As a result, confidence intervals for biostratigraphic ranges adjacent to well-sampled parts of the stratigraphic section are smaller than those calculated from a random distribution method. Some confidence intervals extend indefinitely above or below the sampled stratigraphic interval.

From the biostratigraphic range data, we calculated turnover events in 5 m stratigraphic bins (e.g., the highest Lancian 5 m bin includes all specimens that occur between 0 and 5 m below the Cretaceous-Paleogene boundary). A species was considered present in a stratigraphic interval if it occurred in a locality from that stratigraphic interval (true occurrence) or in localities above and below that stratigraphic interval (range-through occurrence). A range-through occurrence implies that the absence of a species from the stratigraphic interval is more likely due to sampling error than to true short-term absence, although this may not always be the case. The range-through method may produce edge effects, including artifactually higher numbers of appearances and disappearances at the bottom and top of the stratigraphic section, respectively, where the method cannot be applied (Foote 2000). These effects are minimized in this study because the fossil localities nearest the bottom and top of the section are fairly well sampled.

We calculated turnover rates at the species level as per-taxon rates (Foote 2000) and proportional rates per bin, with the assumption that durations represented by the 5 m bins are uniform throughout the section (~108 k.y.). Estimated per-capita turnover rates (λ = appearance, μ = disappearance) were calculated according to Foote (2000).

RESULTS

The results are subdivided by the major analyses: taxonomic richness, relative abundances and heterogeneity measures, and taxonomic composition and turnover.

Taxonomic Richness

The raw number of species (filled circles, Fig. 2.5) varies among fossil localities within a stratigraphic horizon and throughout the section. The maximum raw number of species for each horizon increases from the lower to the middle part of the Hell Creek Formation, and then it declines thereafter into the uppermost Hell Creek Formation and the lowermost Tullock Member. The standing richness data at both the species (Fig. 2.5, gray shade) and genus level (Fig. 2.5, dashed line) largely mirror this pattern. Results from the rarefaction analysis also reflect this pattern (Fig. 2.5, diamonds; see also Table 2.1). After accounting for differences in sample sizes, the expected richnesses of the lowermost (−76 m) and upper Hell Creek assemblages (−19.5, −5 m) are significantly lower than the middle Hell Creek assemblage (−41 m), and the expected richness of the Pu1 assemblage (+3 m) immediately across the Cretaceous-Paleogene boundary is significantly lower than all but the uppermost Hell Creek assemblage (−5 m). The expected richness of UCMP locality V99369 (−59 m) from the lower middle Hell Creek is not statistically different from the middle Hell Creek value (−41 m). The strong positive correlation ($r = 0.862$, $p < 0.001$) between the log number of lissamphibian specimens and the raw richness per locality shown in Figure 2.6 indicates that sampling intensity plays a significant role in the observed raw richness and standing richness patterns. Only two localities with greater than 100 specimens fall outside the 95% confidence intervals: UWBM locality C1153 from the

middle of the Hell Creek Formation (Lancian) has significantly higher richness (n = 11) than expected, whereas UCMP locality V74111 from the lowermost Tullock Member (Pu1) has significantly lower richness (n = 5) than expected. Rarefaction curves (Fig. 2.7) confirm the depressed richness of the Pu1 locality. By 100 sampled specimens, the richness of UCMP locality V74111 levels off slightly above four species, whereas Lancian Hell Creek assemblages tend to plateau later (>100 specimens) and at higher levels of richness (6–10 species).

Relative Abundances and Heterogeneity Measures

The four heterogeneity indices from each of the six well-sampled assemblages (Table 2.1) show a common trend in diversity leading up to and across the Cretaceous-Paleogene boundary (Fig. 2.8). Heterogeneity was relatively high for much of the Hell Creek Formation, but minima occurred in the middle (UWBM locality C1153) and uppermost parts (UCMP localities V73085, V73087) of the formation; thereafter, all but the evenness values (Fig. 2.8A) decreased across the Cretaceous-Paleogene boundary in the lowermost Tullock Member Pu1 assemblage (UCMP locality V74111). The significance of the pattern as gauged by 95% confidence intervals varies slightly among the heterogeneity indices. The evenness value for the middle Hell Creek assemblage is significantly lower than all other assemblages. For the equitability and Simpson indices (Figs. 2.8B and 2.8C), values from the middle Hell Creek assemblage (UWBM locality C1153) and the uppermost Hell Creek assemblage (UCMP localities V73085, V73087) are not significantly different from each other, though they are significantly lower than other Hell Creek assemblages. According to the dominance measures (Simpson's, Berger-Parker; Figs. 2.8C and 2.8D), the heterogeneity of the lowermost Tullock assemblage (UCMP locality V74111) is significantly lower than those for all Hell Creek

assemblages; for the information indices, it is statistically distinct from all assemblages (equitability) and from all but the uppermost Hell Creek assemblage (evenness).

The RADs from each of the six well-sampled assemblages (Table 2.1) show temporal changes in community structure that are similar to but more detailed than those seen from the heterogeneity indices (Fig. 2.9). Among Lancian assemblages, the differences between the percent abundances of species of successive rank tend to be relatively small. As a consequence, the fitted lines for most of these assemblages are gently sloping. One exception is the assemblage from the middle of the Hell Creek Formation (UWBM locality C1153), which has an initially steep slope followed by a large number of rare taxa (n = 9; <5% relative abundance). Additionally, the assemblage from the uppermost part of the Hell Creek Formation (UCMP localities V73085, V73087) has a fitted line of notably steeper slope. This trend continued across the Cretaceous-Paleogene boundary to the Pu1 assemblage, which has an even steeper fitted curve. The models that best fit the abundance data vary among localities (Table 2.3) without a discernible pattern. In stratigraphic order, the Zipf model fits the lowest Lancian assemblage (UCMP locality V99220) slightly better than the log-normal model does; the geometric model is the best fit for UCMP locality V99369; the abundance data of Lancian assemblages from the middle and upper Hell Creek Formation (UWBM locality C1153 and DMNH localities 3302, 3304, 3305, 3327, respectively) are best fit by the Zipf model; the geometric model is the best fit for the uppermost Hell Creek assemblage (UCMP localities V73085, V73087); and the Zipf model provides the best fit for the Pu1 assemblage from the lowermost Tullock Member (UCMP locality V74111).

In all but the lowermost Hell Creek assemblage (UCMP locality V99220), the batrachosauroidid *Opisthotriton kayi* is the most common species, followed by the

scapherpetontid *Scapherpeton tectum*. This abundance ranking differs from observations by Bryant (Bryant 1989, p. 32) wherein *Scapherpeton* was considered "the most common salamander in the Hell Creek and Tullock formations in the study area." This discrepancy might be due to differences in sampling methodologies or sample sizes (see Bryant 1989; Archibald and Bryant 1990). Only in the lowermost Hell Creek assemblage (UCMP locality V99220) is *Scapherpeton tectum* the most common species, followed by *Opisthotriton kayi*, *Habrosaurus* dilatus, and *Lisserpeton bairdi*. Figure 2.10 provides another view of the relative abundance trends (10 m bins), revealing a strong inverse relationship between *Scapherpeton tectum* and *Opisthotriton kayi*. Through the Hell Creek Formation and across the Cretaceous-Paleogene boundary into the Tullock Member, percent relative abundance of *Scapherpeton* decreases from ~60% to 6%, whereas percent abundance of *Opisthotriton* increases from 17% to 88% over the same span. The other common taxa, *Habrosaurus dilatus* and the scapherpetontid *Lisserpeton bairdi*, maintain low (<15%) and slightly decreasing percent relative abundances through the section.

Taxonomic Composition and Turnover

Among the 11 Lancian lissamphibian species in the database, four caudates range through the Hell Creek Formation and across the Cretaceous-Paleogene boundary into the Tullock Member (Fig. 2.11): the batrachosauroidid *Opisthotriton kayi* (Figs. 2.2I–2.2J), the scapherpetontids *Lisserpeton bairdi* (Figs. 2.2A–2.2B) and *Scapherpeton tectum* (Figs. 2.2C–2.2D), and the sirenid *Habrosaurus dilatus* (Figs. 2.3I–2.3J). Two other scapherpetontids (*Piceoerpeton naylori* and Scapherpetontidae gen. et. sp. A; Figs. 2.2E–2.2F and 2.2M–2.2O, respectively) are only found within the Hell Creek Formation, though upper stratigraphic

confidence limits for both taxa extend across the Cretaceous-Paleogene boundary. The presence of *Piceoerpeton willwoodense* in the late Paleocene and early Eocene of North America (Meszoely 1967; Estes and Hutchison 1980; Naylor and Krause 1981) implies that the *Piceoerpeton* lineage survived the end Cretaceous mass extinction. As an aside, Gardner (2012) questioned Bryant's (1989) identification of an atlantal centrum from the Hell Creek Formation as cf. *Piceoerpeton* (UCMP 123524). Because we have not seen this specimen to confirm the identification, we have chosen to exclude it from our database.

The sirenid *Habrosaurus prodilatus* (Figs. 2.3A–2.3H) was previously only known from older Judithian-age deposits of the Dinosaur Park Formation in Alberta (Gardner 2003a). Here, we note its co-occurrence with *H. dilatus* and extend its temporal and biogeographic range to the lower half of the Hell Creek Formation in the study area (see also DeMar, 2011). The upper 50% confidence limit for the stratigraphic range of *H. prodilatus* implies that it likely went extinct well before the Cretaceous-Paleogene boundary.

Estes (1969b), Estes and Berberian (1970), and Gardner (2003b) reported occurrences of *Proamphiuma cretacea* from the Bug Creek Anthills of McCone County, northeastern Montana. This locality is no longer considered Cretaceous in age. Instead, it is interpreted as a Paleocene channel deposit that formed during incision of Hell Creek Formation strata (Lofgren et al. 1990). As such, Bug Creek specimens of *P. cretacea* may have either been reworked from Cretaceous-aged deposits or deposited during the earliest Paleocene, or both. We identified several trunk vertebrae of *P. cretacea* in assemblages from the Tullock Member, of which the stratigraphically lowest occurs in UCMP locality V74111 (+3 m; Pu1 NALMA) and provides the first unequivocal evidence of Paleocene-aged *P. cretacea* (Figs. 2.2P–2.2R; see also DeMar 2011).

The batrachosauroidid *Prodesmodon copei* (Figs. 2.2K–2.2L) is known from three fossil assemblages that together span most of the Hell Creek Formation. Note that Bryant (1989) identified voucher specimens of *P. copei* (UCMP 130687, vertebrae) from the uppermost Hell Creek Formation (UCMP locality V75162), but we re-identified these as squamate vertebrae and in turn removed them from our analyses. Despite the very low percent relative abundance of *P. copei* (~1%), its upper 50% stratigraphic confidence limit implies that it survived the Cretaceous-Paleogene event. This agrees with our recent discovery of *P. copei* (UCMP 557548) from an undifferentiated Pu2/3 locality (UCMP locality V72126) of the Tullock Member within the study area. A reported but undocumented occurrence of this taxon (i.e., no voucher specimen listed, described, or figured) from the late Puercan (Pu2/3) Purgatory Hill locality of the middle part of the Tullock Member of McCone County, Montana (Van Valen and Sloan 1965; Estes 1981), would, if confirmed, be consistent with the survival of *P. copei* into the Paleocene.

Necturus krausei (the genus *Necturus* is extant) from the late Paleocene–age (Tiffanian NALMA) Ravenscrag Formation of Saskatchewan, Canada, was previously the oldest known member of the Proteidae (Naylor 1978). Our reported occurrence of Proteidae gen. et sp. nov. (Figs. 2.2G–2.2H) in the latest Cretaceous Hell Creek Formation represents a substantial temporal range extension for the family (~5 m.y.) and implies survivorship of Proteidae across the Cretaceous-Paleogene boundary (see DeMar 2013).

Two albanerpetontids are reported from the study area. *Albanerpeton galaktion* has previously been reported from older and contemporaneous deposits elsewhere (Fox and Naylor 1982; Gardner 2000a). We record *A. galaktion* (Figs. 2.3K–2.3L) from the lower half of the Hell Creek Formation (−59 and −41.2 m; Fig. 2.11), representing its first reported appearance in the study area. The better-known *A. nexuosum* (amended from *A. nexuosus* by Folie and Codrea

2005; Figs. 2.3M–2.3N) is identified from several localities in the upper half of the Hell Creek Formation. Two specimens (UCMP 556657, 556564) from UCMP locality V99369 (−59 m) may belong to *A. nexuosum* and thus extend its stratigraphic range lower in the section, but due to poor preservation, we conservatively identify these as *Albanerpeton* sp. indet. Likewise, several specimens (UCMP 123309, 123490, 123493) from the uppermost portions of the Hell Creek Formation (UCMP locality V73087) may belong to *A. galaktion*, thus extending its range higher up in section, but again, poor preservation prevents a species-level identification. Although we can infer that the genus *Albanerpeton* survived the Cretaceous-Paleogene boundary based on its occurrences in the late Paleocene of North America (e.g., Paskapoo Formation of Alberta, Canada; Gardner 2000b; Gardner and Böhme 2008) and through the Cenozoic into the Pliocene of Europe (e.g., Venczel and Gardner 2005), its presence in the Paleocene deposits of the local section is inconclusive. A poorly preserved maxilla (UCMP 556631) from the lowermost Tullock Member (UCMP locality V74111) exhibits some features reminiscent of albanerpetontids, but we presently cannot rule out other taxonomic affinities (e.g., unidentified caudate or anuran).

Rates of turnover per 5 m bin are unexceptional through most of the Hell Creek Formation (Fig. 2.12). The high proportional rate of appearance at the base of the section (Fig. 2.12B) is an artifact of the method for calculating proportional rates. Two moderate spikes in appearance rates (proportional and per-capita) occur in the lower half of the formation, represented by the first appearances of four rare species (*Prodesmodon copei*, Scapherpetontidae gen. et sp. A, *Albanerpeton galaktion*, *A. nexuosum*). With better fossil sampling, these taxa may range to the base of the section. Disappearance rates are also negligible during the same interval, save the spike that occurs at −41 m. This resulted from the local disappearance, and possible

extinction, of *Habrosaurus prodilatus* and *Albanerpeton galaktion*. The one prolonged surge in turnover rates occurs in the uppermost 20 m of the Hell Creek Formation. Rates of disappearances (per-capita) increased leading up to the Cretaceous-Paleogene boundary from 0.11 to 0.12 within 14.5 m of the Cretaceous-Paleogene boundary and then by more than fourfold (0.52) in the penultimate bin (Fig. 2.12A). Proportional rates of disappearances over the same interval show a similar trend (11.1%, 12.5%, 42.9%, respectively), but when correcting for pseudoextinctions (i.e., *Albanerpeton*, *Prodesmodon*, *Piceoerpeton*), the proportional rate does not spike in the penultimate bin (14.3%; Fig. 2.12B). Overall, this represents the steady loss of five out of nine species (56%) during this interval. However, upper confidence limits for the stratigraphic ranges of some of the relevant taxa (Fig. 2.11) imply that some disappearances might have been concentrated closer to the Cretaceous-Paleogene boundary.

DISCUSSION AND CONCLUSIONS

Lead-Up to the Cretaceous-Paleogene Boundary: Declining Diversity

Our data show that the diversity of caudate and allocaudate assemblages of northeastern Montana changed through time leading up to the Cretaceous-Paleogene boundary. In the middle of the Hell Creek Formation (−41 m), which corresponds to ~800–900 k.y. before the Cretaceous-Paleogene boundary and the latter part of magnetochron C30n, the caudate and allocaudate fauna reached a short-lived peak in taxonomic richness (11 species). This is in part due to a narrow stratigraphic overlap of *Habrosaurus prodilatus* and *Albanerpeton galaktion*, which made their last appearances, and *Albanerpeton nexuosum*, which made its first unequivocal appearance at this point in the local section. A large concurrent drop in evenness, as

inferred by decreasing heterogeneity values and steepening RAD slopes, implies a significant change in community structure as well. *Opisthotriton kayi* replaced *Scapherpeton tectum* as the most ecologically abundant taxon, climbing from 49% and 33% in the preceding intervals to nearly 80% of all caudate and allocaudate individuals. By consequence, the newly added species were rare, with relative abundances less than 5%. Apart from the high species richness, this middle Hell Creek caudate and allocaudate fauna strongly resembled the post–Cretaceous-Paleogene survival fauna (see following). In fact, the evenness value (Fig. 2.8A) for this middle Hell Creek assemblage is lower than the Pu1 survival fauna. These changes were transitory, with a return to preexisting levels of richness, evenness, and community structure in the next well-sampled stratigraphic horizon (−19.5 m).

It is unclear whether this faunal shift in the middle of the Hell Creek Formation reflects a response to a brief environmental perturbation or an anomaly in the fossil database. Deccan flood basalt volcanism, which likely had an impact on latest Cretaceous global atmospheric content and climates (e.g., Self et al. 2006; Tobin et al. 2012), began on the Indian subcontinent in magnetochron C30n; however, the main eruptive phase occurred later, during the Cretaceous part of C29r (e.g., Chenet et al. 2009). Regionally, leaf margin analysis of paleofloras from southwestern North Dakota indicates a cool interval in the latter part of C30n that spanned this short-lived change in the caudate and allocaudate fauna. Higher species richness during a cooler interval would be consistent with modern caudate biogeography, wherein most species inhabit the cooler and temperate climates of eastern and western North America and temperate Eurasia (Crump 2010). Gardner and Böhme (2008) likewise suggested that albanerpetontids, like many extant lissamphibians, might have favored lower or more moderate temperatures.

At this time, we hesitate to interpret this faunal change as a response to a modest drop in paleotemperatures, noting that fossil samples from the middle of the Hell Creek Formation in northeastern Montana (−40 to −50 m bin) currently derive from a single locality (UWBM locality C1153). Although the caudate and allocaudate sample from this locality is substantial in size (N = 235 specimens), it may be an oddity from a unique depositional environment or taphonomic filter. The mammalian fossil sample from this locality is presently too small (N = 14 specimens) to offer further insight, but study of the sedimentology and taphonomy of the site is currently under way by one of us (DeMar). Thus, we await the results of that study and samples from additional localities in this and adjacent stratigraphic bins to test the robustness of this abrupt shift in the caudate and allocaudate fauna.

Following a return to preexisting levels of richness, evenness, and community structure (at −19.5 m; Hot Feet assemblage), the caudate and allocaudate faunas underwent a protracted decline during the last ~400 k.y. of the Cretaceous that continued across the Cretaceous-Paleogene boundary. Local richness decreased in a stepwise fashion from nine to four species as rates of disappearance increased leading up to the Cretaceous-Paleogene boundary. During this interval, there was also a statistically significant decline in heterogeneity values, a steepening of RAD slopes, and a statistically significant increase in the abundance of *Opisthotriton kayi* relative to *Scapherpeton tectum* and other lissamphibians. These changes imply growing instability in the structure of caudate and allocaudate paleocommunities. This trend appears robust across multiple stratigraphic horizons and in multiple well-sampled localities.

As discussed in Wilson (2014), the initiation of these changes in caudate and allocaudate assemblages occurred during an episode of increased atmospheric pCO_2 and estimated mean annual temperatures (e.g., Li and Keller 1998), referred to as the late Maastrichtian event (Nordt

et al. 2003). The late Maastrichtian event, which interrupted a general Maastrichtian cooling trend (Barrera and Savin 1999), has been recorded globally in marine deposits via stable isotopic analysis ($\delta^{18}O$, $\delta^{13}C$) of foraminifera (Li and Keller 1998; Wilf et al. 2003; MacLeod et al. 2005) and macrofauna (Tobin et al. 2012) and regionally in terrestrial deposits of western North America via isotopic analysis of paleosol carbonates (Nordt et al. 2003) and leaf margin analysis of paleofloras (Wilf et al. 2003). Although estimates of its timing and magnitude vary with ocean depth, geography, and climate proxy, data from paleofloras of nearby North Dakota suggest that the warming event, which may have been precipitated by CO_2 released from the main pulse of Deccan volcanism (Ravizza and Peucker-Ehrenbrink 2003; Self et al. 2006; Chenet et al. 2009; Tobin et al. 2012), began ~500–600 k.y. before the Cretaceous-Paleogene boundary. Temperatures remained elevated by ~5–6 °C until a dramatic cooling interval lowered temperatures by ~7 °C within the last ~100 k.y. of the Cretaceous (Wilf et al. 2003).

Peak warming occurred ~200–300 k.y. before the Cretaceous-Paleogene boundary and coincident with the transition from the HC II megafloral zone to what has been interpreted as the immigration of a species-rich, warm-adapted flora (HC III flora; Wilf et al. 2003). It may also correlate with a significant concentration of late Maastrichtian palynological disappearances (RT3-level) recorded in northern Canada (Sweet and Braman 2001). In the marine realm, changes in the species richness, relative abundances, and geographic ranges of planktonic foraminifera (Kucera and Malmgren 1998) and extinctions in molluscs (Tobin et al. 2012) have been temporally correlated with the late Maastrichtian event and interpreted as responses to biotic stress conditions caused by episodes of Deccan volcanism (Keller 2003). In northeastern Montana, mammalian faunas initially experienced modest turnover followed by sustained declines in mean individual body size and evenness of local faunas and relative abundances of

metatherians. These mammalian faunal changes began in the middle to upper third of the Hell Creek Formation and intensified up section, culminating in the extinction of 75% of all mammalian species within the last 10 m of the formation (Wilson 2014). The temporally correlated and wide-reaching nature of these biotic changes makes plausible their connection to the late Maastrichtian event and its associated environmental changes. The implied level of biotic stress in vertebrate faunas of northeastern Montana prior to the Cretaceous-Paleogene boundary would also be consistent with environmental instability inferred from a short interval of fluctuating $\delta^{13}C$ values of sedimentary organic material in the upper Hell Creek Formation of nearby North Dakota (Arens and Jahren 2002).

Although the stepwise loss of 56% of caudate and allocaudate species within the last ~20 m of the local section temporally correlates with the global and regional warming of the late Maastrichtian event and the sudden cooling event that followed (Li and Keller 1998; Nordt et al. 2003; Wilf et al. 2003), an alternative interpretation is that the pattern of turnover only appears stepwise due to sampling artifacts, namely, the Signor-Lipps effect (Signor and Lipps 1982). If this were the case, the true pattern of turnover would be more concentrated closer to the Cretaceous-Paleogene boundary. The pattern of expected richness, however, casts doubt on this scenario by showing a significant decline between −41 m and −5 m. Moreover, two of the involved species (*Albanerpeton galaktion*, Proteidae gen. et sp. nov.) have an upper 50% stratigraphic confidence limit that predicts their true disappearances no less than 5 m below the top of the Hell Creek Formation and more than ~100 k.y. before the Cretaceous-Paleogene boundary. For the other species involved, although their last appearances successively occur at −14.5 m (Scapherpetontidae gen. et sp. A) and −5.2 m (*Prodesmodon copei*, *Piceoerpeton* naylori, *Albanerpeton nexuosum*), their upper stratigraphic confidence limits extend across the

Cretaceous-Paleogene boundary and into the Tullock Member. Central to this issue is the fossil sampling profile in the last 10 m of the Hell Creek Formation: Whereas the sample sizes in the penultimate stratigraphic bin (−10 m to −5 m) are large (267 specimens), the stratigraphically highest bin (−5 m to 0 m) includes only 25 specimens, all from one locality (UCMP locality V75162). Thus, while we expect that targeted collecting in this interval will improve our ability to discriminate among alternative extinction patterns, at present the weight of the data support a protracted pattern of caudate and allocaudate turnover accompanied by declining heterogeneity values and declining relative abundances of *Scapherpeton* during the last ~400 k.y. of the Cretaceous.

Cretaceous-Paleogene Extinction

Despite uncertainties in the timing of these events, the caudate and allocaudate assemblages experienced significant turnover near the Cretaceous-Paleogene boundary (−20 m to 0 m). The local disappearance of 56% of all species in the section corresponds to 22% species-level extinction. Although *Piceoerpeton naylori* is absent from Paleocene strata in the study area, the lineage reappeared elsewhere in the late Paleocene of Wyoming and Montana (see Results: Taxonomic Composition and Turnover). Likewise, *Albanerpeton* sp. and indeterminate albanerpetontids from the middle and late Paleocene of Alberta (Gardner and Böhme 2008) suggest that at least one *Albanerpeton* lineage (likely *A. nexuosum*) survived the Cretaceous-Paleogene boundary. Furthermore, the reappearance of *Prodesmodon copei* in the middle of the Tullock Member (Pu2/3) indicates its survival. Thus, these three lineages were temporarily extirpated from northeastern Montana or had very low abundances, but they did not go extinct in the Cretaceous-Paleogene mass extinction.

The overall survivorship pattern of caudates and allocaudates largely agrees with that presented in Archibald and Bryant (1990) for northeastern Montana. Our slightly lower extinction rate (22% vs. 28.6%) derives from updates to the systematic paleontology (i.e., new taxa, re-identifications). As noted by Archibald and Bryant (1990), the Cretaceous-Paleogene survivors tend to be the most common species in the caudate and allocaudate assemblages from the Hell Creek Formation. Indeed, all four of the local survivors (*Opisthotriton kayi*, *Scapherpeton tectum*, *Lisserpeton bairdi*, *Habrosaurus* dilatus) not only range through most of the Hell Creek Formation, but they also occur in 23–41 of the 49 stratigraphic horizons and account for more than 95% of all Hell Creek specimens. The Cretaceous-Paleogene victims never constituted more than 7% of all specimens in any one 10 m stratigraphic bin. The Cretaceous-Paleogene survivors also have geographic ranges across much of the Western Interior of North America in the Lancian, whereas the victims are restricted to the study area. Although not amenable to statistical analysis, the apparent pattern of endemics as victims (although both endemics are newly recognized species) agrees with ecological and paleontological studies that suggest that abundant and widespread taxa are less vulnerable to background extinction than are rare and geographically restricted taxa (e.g., Jablonski 2005; Molles 2005; Payne and Finnegan 2007), and it contrasts with cases in which such factors do not confer an advantage during times of mass extinction (e.g., Jablonski 1986, 1989; Lockwood 2003; Payne and Finnegan 2007).

Among higher-level taxa from the Hell Creek assemblages of northeastern Montana, all four caudate families (i.e., Batrachosauroididae, Scapherpetontidae, Sirenidae, Proteidae) survived the Cretaceous-Paleogene event. At the species level, one of four scapherpetontids suffered extinction. One scapherpetontid and one batrachosauroidid were extirpated near the

Cretaceous-Paleogene boundary. The lone sirenid from the upper Hell Creek Formation persisted into the Paleocene. The newly recognized proteid species suffered extinction, but Proteidae reappeared in the late Tiffanian NALMA in the form of *Necturus krausei* (Naylor 1978). Allocaudates, represented by a single albanerpetontid in the upper Hell Creek Formation (*Albanerpeton nexuosum*), were extirpated. Together, these data offer no strong support for taxonomic selectivity among caudates and allocaudates during the Cretaceous-Paleogene mass extinction event.

Investigating body-size selectivity among fossil caudates and allocaudates is challenging due to the habitat-dependent and indeterminate growth strategies of modern lissamphibians (Sebens 1987). Moreover, the fossil localities used in this study, though collected via similar methods (surface and screen washing), do not derive from isotaphonomic deposits (e.g., channel lags vs. crevasse splays). As a result, we would expect the distribution and frequency of fossil sizes to vary across localities; however, because the size range represented by caudate and allocaudate specimens in our study is small, the differences are likely negligible (Blob and Fiorillo 1996). Previous investigations into the taphonomy of vertebrate microfossil localities within the Hell Creek Formation of northeastern Montana support this conclusion (L. Wilson 2008) and have found no directed taphonomic trends through the section that might bias our interpretations of caudate and allocaudate body size trends (Wilson 2005).

Acknowledging these concerns, we recognize a body size pattern among caudates and allocaudates that might reflect selectivity in survivorship across the Cretaceous-Paleogene boundary. Qualitative estimates of maximum body size indicate that the three Cretaceous-Paleogene survivors (*Habrosaurus*, *Scapherpeton*, *Lisserpeton*) were large relative to other Lancian caudates (Estes 1964; Holman 2006). For example, Estes (1981) estimated that

Habrosaurus dilatus might have reached a total body length of 160 cm, based on the maximum length of its trunk vertebrae (~2 cm). Scapherpetontidae gen. et sp. A, though known from only a few specimens, has trunk vertebrae that are similar in size to those of the other relatively large scapherpetontids *Scapherpeton* and *Lisserpeton*. *Opisthotriton kayi*, which is the most abundant species in the local section, was intermediate in body size relative to other Lancian caudates (Estes 1964), with a maximum estimated total body length of ~35 cm. Among the victims, *Piceoerpeton naylori* might have been intermediate in body size, but the remainder (Proteidae gen. et sp. nov., *Albanerpeton*) were small (~10–20 cm total body length), based on maximum vertebral dimensions or complete skeletons (e.g., McGowan and Evans 1995; DeMar 2013; *Chapter Four*). The overall pattern might indicate that larger body size among Lancian caudates and allocaudates provided an important advantage in Cretaceous-Paleogene survival (e.g., longer estivation times; Gehlbach et al. 1973). This would contrast with studies suggesting that large body size is a selective disadvantage during times of background extinction (e.g., Jablonski 1996); however, it should be noted that caudates and allocaudates are small relative to other aspects of the Lancian vertebrate fauna (e.g., nonavian dinosaurs, crocodiles). Future research will aim to quantify and test the robustness of this pattern and investigate plausible advantages of larger body size in Cretaceous-Paleogene caudates and allocaudates.

Ecomorphological traits of Lancian caudates and allocaudates that reflect diet and life habit provide no clear evidence of selectivity in Cretaceous-Paleogene survivorship among these groups. Fossil batrachosauroidids, scapherpetontids, sirenids, and proteids were paedomorphic and likely fully aquatic, as suggested by their somewhat elongate bodies and reduced limbs (e.g., Estes 1964; Gardner 2000c). Albanerpetontids are generally regarded as having been predominantly terrestrial with specializations for fossoriality and terrestrial locomotion, based on

their robustly built skulls, interdigitating intermandibular joint, modified cervical vertebrae, dermal scales, and powerful limbs and girdles (e.g., see Gardner and Böhme 2008, and references therein). In terms of dietary habits, modern caudates are viewed as generalist predators that prey upon arthropods, mollusks, annelids, and small vertebrates (Solé and Rödder 2010). Most Lancian caudates have relatively simple, pointed, unicuspid teeth that suggest that they too were generalist predators, though there is notable morphological variation among them. For example, *Opisthotriton* has pedicellate teeth (i.e., having a basal pedicel and a distal crown separated by a zone of weakness; Holman 2006), which suggest it may have fed on soft-bodied organisms. The stout, non-pedicellate, bulbous teeth of *Habrosaurus dilatus* suggest a diet of hard-bodied arthropods and mollusks (Estes 1964; Gardner 2003a). Albanerpetontids possess pleurodont, tricuspid, non-pedicellate teeth (Milner 2000) with shearing capabilities (Gardner 2001), which also suggest a diet consisting mainly of hard-bodied organisms (Fox and Naylor 1982). Although the dental morphological adaptations of caudates and allocaudates overlap, the prey items available to each might have differed depending on their preferred habitat (i.e., aquatic and terrestrial, respectively). However, there does not appear to be a strong pattern of selectivity along this axis in the pattern of Cretaceous-Paleogene survivorship of caudates and allocaudates.

On a broader scale, aspects of the inferred ecologies of Lancian caudates and allocaudates likely contributed to their lower rate of Cretaceous-Paleogene extinction relative to some other Lancian vertebrates (e.g., squamates, mammals: Archibald and Bryant 1990; Wilson 2014). For instance, Robertson et al. (2004) argued that a severe thermal pulse would have occurred within the first few hours after the bolide impact, and survivors would have needed to find shelter from its effects in water or below ground surface (but see Goldin and Melosh [2009] for a model that

predicts a less severe thermal pulse). Batrachosauroidids, scapherpetontids, sirenids, and proteids are considered obligate aquatic taxa (Estes 1975, 1976; Naylor 1978; Gardner 2003a) and would have been sheltered from the immediate effects of a thermal pulse by staying submerged under water. Although the inferred fossorial nature of *Albanerpeton* appears to have had little effect on its local survival, the aquatic lifestyles of Lancian caudates, along with their probable ability to estivate, would have also provided an advantage in this regard. This is consistent with previous observations that freshwater taxa suffered far less extinction (10%) than those from the terrestrial realm (88%; Archibald and Bryant 1990; Sheehan and Fastovsky 1992). Likewise, as dietary generalists that could have fed among the detritus, they might have been less prone to extinction than specialist feeders, such as herbivorous nonavian dinosaurs (Sheehan and Hansen 1986; Sheehan et al. 1996).

Cretaceous-Paleogene Survival: Depauperate Fauna with Opisthotriton kayi *as Bloom Taxon*

During the first ~100–200 k.y. after the Cretaceous-Paleogene mass extinction, the Pu1 caudate and allocaudate assemblage (UCMP locality V74111) of northeastern Montana was taxonomically depauperate and highly uneven. Other Pu1 assemblages known from the study area appear to be consistent with this pattern, but they require more detailed study and additional sampling to fully corroborate this result. Mammal data from Pu1 assemblages show a similar pattern of low evenness (Wilson 2014). Despite the large sample size of caudates (530 specimens) from UCMP locality V74111, only four local survivor taxa occur in this assemblage (*Opisthotriton kayi*, *Scapherpeton tectum*, *Lisserpeton bairdi*, *Habrosaurus* dilatus) with one (*O. kayi*) making up ~88% of all individuals. A single immigrant, *Proamphiuma* cretacea, made its first appearance in the study area, but it was extremely rare (0.4%). This pattern of diversity is

reminiscent of those found among modern communities after an ecological disturbance or during the early stages of ecological succession (Magurran 2004). It also closely matches descriptions of survival biotas in the "standard model" of postextinction biotic recovery (Harries et al. 1996; Erwin 1998): a taxonomically impoverished biota that is numerically dominated by one or a few opportunistic generalists or bloom taxa. The survival biota of the "standard model" also usually includes an influx of postextinction immigrants (but see Jablonski 1998). Immigrants were a strong component of the Pu1 mammalian survival fauna in northeastern Montana (Weil and Clemens 1998; Clemens 2010; Wilson 2014), but this does not seem to have been the case in the Pu1 caudate survival fauna. It is not wholly unexpected, seeing that modern lissamphibians are poor dispersers (Crnobrnja-Isailovic 2007; Wells 2007) and consequently have low species turnover rates, as indicated by their high beta diversity (Qian 2009).

Most of the local survivors persisted well into the Paleocene (e.g., *L. bairdi*—Torrejonian; *O. kayi*, *S. tectum*, and *H. dilatus*—Tiffanian; Gardner 2000c; Holman 2006); none appears to have suffered the fate of what Jablonski (2002) called "dead clades walking"—taxa that survive mass extinctions only to decline in richness, become marginalized, or simply fail to diversify during the recovery interval. With the exception of the relatively rapid reappearance of the Lazarus taxon *Prodesmodon* during the early Paleocene (Pu2/3 NALMA), major changes in the caudate and allocaudate fauna of North America did not occur until the late Paleocene. *Albanerpeton* and *Piceoerpeton*, as additional examples of Lazarus taxa typical of postextinction recoveries (Erwin 2001), did not reappear until the Torrejonian and Tiffanian NALMAs, respectively. Concurrent with the reappearances of *Piceoerpeton* and *Albanerpeton*, two new caudate families appeared in North America: the Cryptobranchidae and Dicamptodontidae (Milner 2000; Holman 2006). It should be noted that prior to this study (see DeMar 2013;

Chapter Four), the Proteidae also was considered to have made their first appearance in North America during the Tiffanian NALMA (Naylor 1978). Overall, these changes occurred over a period of ~5 m.y. Thus, the Cretaceous-Paleogene extinction event incurred minor losses to the caudate and allocaudate fauna of northeastern Montana, and the available fossil record indicates that these losses were not immediately followed by the rapid turnover via speciation or high rates of immigration typical of other postextinction recoveries and radiations (e.g., mammals; Clemens 2002; Wilson 2014). Despite the immigration event of *Proamphiuma* and the relatively rapid reappearance of *Prodesmodon* into northeastern Montana, the Lazarus pattern and diversification in North America ~5 m.y. after the Cretaceous-Paleogene boundary imply a delayed recovery and diversification for the caudate and allocaudate fauna; however, until the nonmammalian vertebrate fauna of the intervening interval has been more thoroughly documented, this scenario remains provisional.

Role of Acid Rain in the Cretaceous-Paleogene Extinction

Caudates and allocaudates suffered a lower rate of extinction at or near the Cretaceous-Paleogene boundary (2 of 9 species [22%]) than did many vertebrate groups in northeastern Montana (e.g., 21 of 28 mammal species were lost [75%]; Wilson 2014). The level of extinction reported here is less than reported by Archibald and Bryant (1990, who reported 28.6% for caudates and allocaudates), and it is lower than expected in light of the reputation of modern lissamphibians as sensitive indicators of ecological instability and environmental disturbance (e.g., Wake 1991; Alford and Richards 1999). Several authors (Archibald and Bryant 1990; Weil 1994; Archibald 1996) have noted the inconsistency of the lissamphibian survivorship pattern in relation to predictions of global acid rain at the Cretaceous-Paleogene boundary as well as

predictions of other harmful agents, such as large volumes of NO_2 gas and increased exposure to ultraviolet-B radiation due to temporary loss of the atmospheric ozone shield (Prinn and Fegley 1987; Kring 2007).

Rainout of nitric acid would have resulted from the large amount of nitric oxide that was allegedly produced in the atmosphere by the kinetic energy from both the bolide entry and the impact ejecta plume of water vapor and rock (Lewis et al. 1982; Prinn and Fegley 1987). Vaporization of anhydrite evaporites at the impact site may have contributed sulfuric acid to the rainout as well (Sigurdsson et al. 1992; Brett 1992; Kring et al. 1996). Because the amount of each acid produced depends on a number of bolide and impact site parameters (see, e.g., Prinn and Fegley 1987), theoretical estimates vary considerably (see Table 2.2 in Retallack, 2004). Prinn and Fegley (1987) estimated that an asteroid impact would lead to acid rain with pH ≈ 0–1 at the impact site and pH ≈ 4–5 globally; estimates for a cometary impact are considerably lower (pH ≈ 0–1.5 at the impact site and globally). Empirical data interpreted as evidence of acid rain include paleosol features (e.g., kaolinitic composition) of the Cretaceous-Paleogene boundary clay in northeastern Montana (Retallack et al. 1987; Retallack 1996, 2004), nitrogen enrichment of the Cretaceous-Paleogene boundary clay of New Zealand (Gilmour et al. 1990), and elevated strontium isotope ratios of fossil foraminifera (Hess et al. 1986; MacDougall 1988; Vonhof and Smit 1997). Estimates of acid production from these data agree with the lower end of the theoretical estimates and, based on limits of acidification implied by the paleosol data, suggest a pH of 4 as the lower bound for acid rain at the Cretaceous-Paleogene boundary in northeastern Montana (Retallack 2004).

Retallack (2004) proposed additional constraints on the pH of the acid rain based on the differing sensitivities of modern freshwater organisms to acidification of their environments. For

example, acid tolerances reported for shelled mollusks range between pH 5.5 and 8.0; those reported for fish range between pH 4.2 and 8.0; and those reported for lissamphibians range between pH 3.4 and 8.0 (Howells 1995; figure 2.7 in Retallack, 2004). With these ranges and the then-available fossil data from northeastern Montana (Archibald and Bryant 1990; Hartman 1998), Retallack (2004) argued that major levels of extinction among mollusks and moderate to low levels among fish and lissamphibians suggested that the acid rain at the Cretaceous-Paleogene boundary ranged between pH 4 and 5.5.

Maruoka and Koeberl (2003) went further in proposing that the effect of acid rain on the freshwater biota might have been neutralized by the buffering capacity of a calcium-enriched impact vapor plume. The calcium enrichment of the vapor plume is predicted on the basis of abundant carbonate sediments at the impact target in Chicxulub. Prinn and Fegley (1987) earlier recognized this neutralization potential but believed that it would have probably had only a small effect. Instead, they argued that the acid buffering capacities of the lakes and rivers where acid rain would have fallen would have had the biggest influence on pH of the water and the duration of the acid effect. Bailey et al. (2005) experimentally supported this hypothesis and, in turn, suggested that the effects of acid rain would have varied geographically with the $CaCO_3$ content of the fluvial and lacustrine catchment sediments in different regions. Whereas the sandstones, siltstones, and mudstones of the Hell Creek Formation in northeastern Montana would have provided little acid-buffering capacity (Bailey et al. 2005), according to Retallack (2004), the calcareous smectitic paleosols near the Cretaceous-Paleogene boundary would have prevented the pH from dropping below 4. These prospects of acid neutralization and buffering continue to be invoked to minimize the severity of acid rain and thereby negate its role as a selective agent

against caudates and allocaudates at the Cretaceous-Paleogene boundary (Retallack 2004; Fastovsky and Sheehan 2005).

We disagree with this resolution and, in particular, argue that Retallack's (2004) biological assay is a critical oversimplification. Moderate acidic conditions of pH 4.0–5.5 would incur a substantial and perceptible degree of harm to modern lissamphibians. Considerable variation in acid tolerances of lissamphibians has been reported among species, populations, and ontogenetic stages (for a review, see Pierce 1985). Though much of this research has focused on frogs, studies of salamanders suggest a similar degree of variation within this group and that, as a whole, they tend to be less tolerant of acid than frogs (Table 1 in Pierce 1985, and references therein). Thus, despite the limits of acid tolerances reported by Retallack (2004, his figure 2.7), some species, populations, and ontogenetic stages of modern salamanders would be affected by acid rain with pH 4.0–5.5. Moreover, although mortality tends to reach 100% as pH approaches lower tolerance limits of a taxon (e.g., 4.0–5.0 for the salamander *Ambystoma*; Pough and Wilson 1977; Cook 1983), less acidic conditions can lead to lower but still significant mortality rates (e.g., 50% for pH 5.0–7.0 in *Ambystoma maculatum*) as well as nonlethal effects, such as diminished growth rates and developmental abnormalities, which may reduce the survivorship of a population or species (Pierce 1985, and references therein; for additional effects, see also Wells 2007).

Using phylogeny to infer the acid tolerances of latest Cretaceous caudates and allocaudates of northeastern Montana is less than optimal, especially with regards to allocaudates, which have an uncertain phylogenetic position within lissamphibians (Milner 2000; Gardner and Böhme 2008); however, latest Cretaceous caudates include representatives of the extant Proteidae and Sirenidae, the extinct Batrachosauroididae, which is possibly the sister

taxon to the extant Proteidae, and the extinct Scapherpetontidae, which is generally placed among crown group salamanders (Urodela; Estes 1981; Gardner 2000c; but see Milner 2000). We therefore infer that latest Cretaceous caudates and allocaudates of northeastern Montana had at least a similar range of acid tolerances, sources of variation in those tolerances, and range of effects to acidification as is found in modern lissamphibians. On this basis, if theoretical and empirical estimates for acid rain at the Cretaceous-Paleogene boundary in northeastern Montana are correct, we would expect that acid rain would have had significant impact on the Cretaceous-Paleogene survivorship of caudates and allocaudates.

Officer et al. (1987) predicted that Deccan volcanism would include massive fluxes of volatiles (H_2SO_4, HCl, CO_2) that would also ultimately result in global acid rain and possibly a decrease in atmospheric ozone before the Cretaceous-Paleogene boundary. Self et al. (2006) estimated that a single eruption would emit up to 35,000 Tg of SO_2 over the course of a decade. The alternating episodes of eruptions and hiatuses from the main phase of Deccan volcanism during the last ~500–600 k.y. of the Cretaceous would have had enormous and lasting impact on the atmosphere (Self et al. 2006). The elevated strontium isotope ratios from ~300–400 k.y. before the Cretaceous-Paleogene boundary (Nelson et al. 1991; Vonhof and Smit 1997) seem to support this claim, although there is no reported evidence of acid rain before the Cretaceous-Paleogene boundary in northeastern Montana (Retallack et al. 1987; Retallack 1996, 2004).

Results of the analysis of the caudate and allocaudate fauna of northeastern Montana (this study) include evidence of moderate levels of taxonomic disappearances and declines in heterogeneity and abundances that are indicative of environmental stress leading up to and at the Cretaceous-Paleogene boundary. As such, they may be consistent with acid rain resulting from both Deccan volcanism during the last ~400 k.y. of the Cretaceous and a bolide impact at the

Cretaceous-Paleogene boundary. However, considerable work remains to be done to determine (1) whether acid rain was associated with the volatile flux from the Deccan volcanism; (2) whether it was associated with the Cretaceous-Paleogene boundary in northeastern Montana and elsewhere; and (3) whether, in either case, it in particular caused the changes in the lissamphibian faunas of northeastern Montana. Future work will aim to more specifically test this hypothesis by looking for signatures of acid trauma in the latest Cretaceous caudate and allocaudate fauna (developmental abnormalities, reduction in growth rates).

Implications for the Cretaceous-Paleogene Extinction Scenario

Our study of the caudate and allocaudate fauna is one of a few that have quantitatively analyzed high-resolution temporal patterns of both presence-absence data and relative abundance data in continental vertebrates leading up to and across the Cretaceous-Paleogene boundary. These two types of data offer complementary viewpoints of extinction: Presence-absence data form the basis for estimating the timing, severity, and selectivity of extinctions, whereas relative abundance data reflect the ecological stability of species and paleocommunities, thus providing insight into extinction vulnerabilities and the ecological process of extinction (McKinney 1997). As a result, this study provides a more comprehensive approach to discriminating between competing scenarios for the Cretaceous-Paleogene mass extinction event than has been presented in most previous work on continental vertebrates.

Coupled with results from other such studies, the results presented here lend growing support in favor of a complex multiple-cause scenario for the Cretaceous-Paleogene mass extinction event. The stepwise pattern of extinctions and extirpations, the sharp drop in the relative abundance of *Scapherpeton*, and the decline in diversity, as measured by heterogeneity

indices, of the caudate and allocaudate fauna of northeastern Montana point to ecological instability during the final ~400 k.y. of the Cretaceous. If these or similar patterns were not found in other taxa, geographic regions, and paleoenvironmental settings, they could be cast aside as anomalous. However, the caudate and allocaudate trends temporally correlate with, for example, ecological instability in the mammalian fauna of northeastern Montana (Wilson 2014), turnover in the paleoflora of nearby North Dakota (i.e., HC II to HC III flora; Wilf et al. 2003; Wilf and Johnson 2004) and palynoflora of northern Canada (i.e., RT3-level; Sweet and Braman 2001), symptoms of elevated biotic stress in the marine biota (e.g., planktonic foraminifera; Keller 2003), and probable causes in the form of the late Maastrichtian event and Deccan volcanism. Consequently, compelling evidence exists that this was a global rather than local phenomenon that preceded the Cretaceous-Paleogene boundary bolide impact.

We make no claim that the biotic changes that have been recorded during the lead-up to the Cretaceous-Paleogene boundary were more severe than those that occurred across the Cretaceous-Paleogene boundary; this is borne out by examples from the caudate and allocaudate fauna (this study), the mammalian fauna (Wilson 2014), the paleoflora (Wilf et al. 2003; Wilf and Johnson 2004), and the planktonic foraminifera (Keller 2003). Rather, we argue that the first phase, the ecological instability, may have helped precipitate the second phase, the mass extinction. Recent theoretical and empirical research in ecology (for reviews, see, e.g., Scheffer et al. 2001; Scheffer and Carpenter 2003; Huggett 2005) suggests that ecosystems may respond in a nonlinear fashion to gradual accumulation of environmental perturbations. That is, the biotic changes will be minor or imperceptible until the perturbations, additively or synergistically, surpass some "ecological threshold," which in turn leads to large and sudden biotic changes. Barnosky (2008) invoked "ecological thresholds" in explaining how the synergistic effects of

multiple events (human impact, climate change) culminated in the Quaternary megafaunal extinction. Likewise, Arens and West (2008) detailed a "press-pulse" model for the Cretaceous-Paleogene mass extinction event, in which longer-term environmental disturbances, such as volcanism and climate change, additively destabilized biotic communities in advance of the "knock-out" blow from the bolide impact at the Cretaceous-Paleogene boundary. Moreover, Mitchell et al. (2012) used food-web models to show how changes in trophic structure of terrestrial communities during the Late Cretaceous might have lowered the collapse threshold for Maastrichtian communities. Although the data presented here and in other studies (e.g., Keller 2003; Wilson 2014) strongly resemble the patterns predicted by these models, key aspects require further investigation, namely, the robustness and pervasiveness of the pre–Cretaceous-Paleogene biotic patterns, the temporal correlations among them, the severity of the proposed environmental perturbations, and the mechanistic relationship between the latest Cretaceous ecological instability and the more severe concentration of extinctions across the Cretaceous-Paleogene boundary. We urge further work on these topics and stress the need to document and understand the variability of these patterns among biotic groups and across geographic areas.

ACKNOWLEDGMENTS

We wish to acknowledge the many students, staff, and volunteers at the University of California Museum of Paleontology (UCMP), Denver Museum of Nature and Science (DMNH), and University of Washington Burke Museum of Natural History and Culture who assisted with the collection and curation of the specimens used in this study. We would also like to thank the people of Garfield County, Montana, for their generosity and hospitality during the course of the fieldwork that was essential to this study. The Bureau of Land Management, Charles M. Russell Wildlife Refuge, Montana Department of Natural Resources and Conservation, and Montana Fish, Wildlife, and Parks provided logistical support and special use permits for the collection of vertebrate fossils. William A. Clemens, Harley J. Garbani, James Gardner, Joseph Hartman, Pat Holroyd, Jack Horner, and Caroline Strömberg provided invaluable help and encouragement throughout this study. We thank James Gardner, Michael Newbrey, and one anonymous reviewer for their insightful comments and suggestions. We also thank members of the Wilson Laboratory who provided comments and reviews of earlier drafts of this manuscript. Financial support for this research was provided by the University of California at Berkeley, the UCMP, the Doris O. and Samuel P. Welles Research Fund (to DeMar), the National Science Foundation Graduate Research Fellowship (to DeMar, grant DGE-0718124), the DMNH, and the University of Washington Department of Biology.

REFERENCES CITED

Alford, R. A., and S. J. Richards. 1999. Global amphibian declines: A problem in applied ecology. Annual Review of Ecology and Systematics 30:133–165.

Alvarez, L. W., W. Alvarez, F. Asaro, and H. V. Michel. 1980. Extraterrestrial cause for the Cretaceous-Tertiary extinction. Science 208:1095–1108.

Archibald, J. D. 1982. A study of Mammalia and geology across the Cretaceous-Tertiary boundary in Garfield County, Montana. University of California Publications in Geological Sciences 122:1-286.

Archibald, J. D. 1996. Dinosaur Extinction and the End of an Era: What the Fossils Say. 237 pp. Columbia University Press, New York.

Archibald, J. D. 2011. Extinction and Radiation: How the Fall of Dinosaurs Led to the Rise of Mammals. 108 pp. The Johns Hopkins University Press, Baltimore, Maryland.

Archibald, J. D., and L. J. Bryant. 1990. Differential Cretaceous/Tertiary extinctions of nonmarine vertebrates; Evidence from northeastern Montana; pp. 549–562 in V. L. Sharpton, and P. D. Ward (eds.), Global catastrophes in Earth history; An interdisciplinary conference on impacts, volcanism, and mass mortality. Geological Society of America Special Paper 247, Boulder, Colorado.

Archibald, J. D., W. A. Clemens, K. Padian, T. Rowe, N. MacLeod, P. M. Barrett, A. Gale, P. Holroyd, H.-D. Sues, N. C. Arens, J. R. Horner, G. P. Wilson, M. B. Goodwin, C. A. Brochu, D. L. Lofgren, S. H. Hurlbert, J. H. Hartman, D. A. Eberth, P. B. Wignall, P. J. Currie, A. Weil, G. V. R. Prasad, L. Dingus, V. Courtillot, A. Milner, A. Milner, S.

Bajpai, D. J. Ward, and A. Sahni. 2010. Cretaceous Extinctions: Multiple Causes. Science 328:973.

Arens, N. C., and A. H. Jahren eds (2002) Chemostratigraphic correlation of four fossil-bearing sections in southwestern North Dakota. Geological Society of America Special Paper 361, Boulder, Colorado.

Arens, N. C., and I. D. West. 2008. Press-Pulse: A general theory of mass extinction? Paleobiology 34:456–471.

Badgley, C. 1986. Counting individuals in mammalian fossil assemblages from fluvial environments. Palaios 1:328–338.

Bailey, J. V., A. S. Cohen, and D. A. Kring. 2005. Lacustrine fossil preservation in acidic environments: Implications of experimental and field studies for the Cretaceous-Paleogene boundary acid rain trauma. Palaios 20:376–389.

Barnosky, A. D. 2008. Megafauna biomass tradeoff as a driver of Quaternary and future extinctions. Proceedings of the National Academy of Sciences of the United States of America 105:11543–11548.

Barrera, E., and S. M. Savin. 1999. Evolution of late Campanian-Maastrichtian marine climates and oceans; pp. 245–282 in E. Barrera, and C. C. Johnson (eds.), Evolution of the Cretaceous Ocean-Climate System. Geological Society of America Special Paper 332, Boulder, Colorado.

Behrensmeyer, A. K., R. W. Hook, C. Badgley, J. A. Boy, R. E. Chapman, P. Dodson, R. A. Gastaldo, R. W. Graham, L. D. Martin, P. E. Olsen, R. A. Spicer, R. E. Taggart, and M. V. H. Wilson eds (1992) Paleoenvironmental contexts and taphonomic modes. University of Chicago Press, Chicago.

Blob, R. W., and C. Badgley. 2007. Numerical methods for bonebed analysis; pp. 333–396 in R. R. Rogers, D. A. Eberth, and A. R. Fiorillo (eds.), Bonebeds: Genesis, Analysis, and Paleobiological Significance. University of Chicago Press, Chicago.

Blob, R. W., and A. R. Fiorillo. 1996. The significance of vertebrate microfossil size and shape distributions for faunal abundance reconstructions: A Late Cretaceous example. Paleobiology 22:422–435.

Breithaupt, B. H. 1982. Paleontology and paleoecology of the Lance Formation (Maastrichtian), east flank of Rock Springs Uplift, Sweetwater County, Wyoming. Contributions to Geology 21:123–151.

Brett, R. 1992. The Cretaceous-Tertiary extinction: A lethal mechanism involving anhydrite target rocks. Geochimica et Cosmochimica Acta 56:3603–3606.

Brinkman, D. B. 1990. Paleoecology of the Judith River Formation (Campanian) of Dinosaur Provincial Park, Alberta, Canada: Evidence from vertebrate microfossil localities. Palaeogeography, Palaeoclimatology, Palaeoecology 78:37–54.

Bryant, L. J. 1989. Non-dinosaurian lower vertebrates across the Cretaceous-Tertiary boundary in northeastern Montana. University of California Publications in Geological Sciences 134:1–107.

Carpenter, K. 1979. Vertebrate fauna of the Laramie Formation (Maestrichtian), Weld County, Colorado. Contributions to Geology 17:37–49.

Chenet, A.-L., V. Courtillot, F. Fluteau, M. Gérard, X. Quidelleur, S. F. R. Khadri, K. V. Subbarao, and T. Thordarson. 2009. Determination of rapid Deccan eruptions across the Cretaceous-Tertiary boundary using paleomagnetic secular variation: 2. Constraints from

analysis of eight new sections and synthesis for a 3500-m-thick composite section:. Journal of Geophysical Research 114:1–38.

Cifelli, R. L., R. L. Nydam, J. G. Eaton, J. D. Gardner, and J. I. Kirkland. 1999. Vertebrate faunas of the North Horn Formation (Upper Cretaceous-Lower Paleocene), Emery and Sanpete Counties, Utah; pp. 377–388 in D. D. Gillette (ed.), Vertebrate Paleontology in Utah. Utah Geological Survey Miscellaneous Publication 99-1.

Clemens, W. A. 2002. Evolution of the mammalian fauna across the Cretaceous-Tertiary boundary in northeastern Montana and other areas of the Western Interior; pp. 217–245 in J. H. Hartman, K. R. Johnson, and D. J. Nichols (eds.), The Hell Creek Formation and the Cretaceous-Tertiary boundary in the northern Great Plains: An integrated continental record of the end of the Cretaceous. Geological Society of America Special Paper 361, Boulder, Colorado.

Clemens, W. A. 2010. Were immigrants a significant part of the earliest Paleocene mammalian fauna of the North American Western Interior? Vertebrata PalAsiatica 48:285–307.

Cook, R. P. 1983. Effects of acid precipitation on embryonic mortality of *Ambystoma* salamanders in the Connecticut Valley of Massachusetts. Biological Conservation 27:77–88.

Crnobrnja-Isailovic, J. 2007. Cross-section of a refugium: Genetic diversity of amphibian and reptile populations in the Balkans; pp. 327–337 in S. Weiss, and N. Ferrand (eds.), Phylogeography of Southern European Refugia. Springer, Dordrecht, The Netherlands.

Crump, M. L. 2010. Amphibian diversity and life history; pp. 3–19 in C. K. Dodd, Jr. (ed.), Amphibian Ecology and Conservation. Oxford University Press, New York.

DeMar, D. G.. Jr. 2011. New taxonomic, paleobiogeographic, and biostratigraphic records of fossil salamanders (Caudata) from the Hell Creek and Tullock Formations of Garfield County, Montana. Journal of Vertebrate Paleontology 31:98A.

DeMar, D. G., Jr. 2013. A new fossil salamander (Caudata, Proteidae) from the Upper Cretaceous (Maastrichtian) Hell Creek Formation, Montana, U.S.A. Journal of Vertebrate Paleontology 33:588–598.

Erwin, D. H. 1998. The end and the beginning: Recoveries from mass extinctions. Trends in Ecology & Evolution 13:344–349.

Erwin, D. H. 2001. Lesson from the past: Biotic recoveries from mass extinctions. Proceedings of the National Academy of Sciences of the United States of America 98:5399–5403.

Estes, R. 1964. Fossil vertebrates from the Late Cretaceous Lance Formation eastern Wyoming. University of California Publications in Geological Sciences 49:1–187.

Estes, R. 1965. A new fossil salamander from Montana and Wyoming. Copeia 1:90–95.

Estes, R. 1969a. The Batrachosauroididae and Scapherpetontidae, Late Cretaceous and Early Cenozoic salamanders. Copeia 2:225–234.

Estes, R. 1969b. The fossil record of amphiumid salamanders. Breviora 322:1–11.

Estes, R. 1975. Lower vertebrates from the Fort Union Formation, Late Paleocene, Big Horn Basin, Wyoming. Herpetologica 31:365–385.

Estes, R. 1976. Middle Paleocene lower vertebrates from the Tongue River Formation, southeastern Montana. Journal of Paleontology 50:500–520.

Estes, R. 1981. Gymnophiona, Caudata. 115 pp. Gustav Fischer Verlag, Stuttgart.

Estes, R., and P. Berberian. 1970. Paleoecology of a Late Cretaceous vertebrate community from Montana. Breviora 343:1–35.

Estes, R., and J. H. Hutchison. 1980. Eocene lower vertebrates from Ellesmere Island, Canadian Arctic Archipelago. Palaeogeography, Palaeoclimatology, Palaeoecology 30:325–347.

Fastovsky, D. E., and P. M. Sheehan. 2005. The extinction of the dinosaurs in North America. GSA Today 15:4–9.

Flessa, K. W., and D. Jablonski. 1983. Extinction is here to stay. Paleobiology 9:315–321.

Folie, A., and V. Codrea. 2005. New lissamphibians and squamates from the Maastrichtian of Haţeg Basin, Romania. Acta Palaeontologica Polonica 50:57–71.

Foote, M. 2000. Origination and extinction components of taxonomic diversity: General problems; pp. 74–102 in D. H. Erwin, and S. L. Wing (eds.), Deep Time: Paleobiology's Perspective. The Paleontological Society, Supplement to v. 26, no. 4, Lawrence, Kansas.

Fox, R. C., and B. G. Naylor. 1982. A reconsideration of the relationships of the fossil amphibian *Albanerpeton*. Canadian Journal of Earth Sciences 19:118–128.

Gardner, J. D. 2000a. Albanerpetontid amphibians from the Upper Cretaceous (Campanian and Maastrichtian) of North America. Geodiversitas 22:349–388.

Gardner, J. D. 2000b. Revised taxonomy of albanerpetontid amphibians. Acta Palaeontologica Polonica 45:55–70.

Gardner, J. D. 2000c. Systematics of albanerpetontids and other lissamphibians from the Late Cretaceous of Western North America In Department of Biological Sciences, Vol. Ph.D., pp. 577. University of Alberta, Edmonton.

Gardner, J. D. 2001. Monophyly and the affinities of albanerpetontid amphibians (Temnospondyli; Lissamphibia). Zoological Journal of the Linnean Society 131:309–352.

Gardner, J. D. 2003a. Revision of *Habrosaurus* Gilmore (Caudata; Sirenidae) and relationships among sirenid salamanders. Palaeontology 46:1089–1122.

Gardner, J. D. 2003b. The fossil salamander *Proamphiuma cretacea* Estes (Caudata: Amphiumidae) and relationships within the Amphiumidae. Journal of Vertebrate Paleontology 23:769–782.

Gardner, J. D. 2005. Lissamphibians; pp. 186–199 in P. J. Currie, and E. B. Koppelhus (eds.), Dinosaur Provincial Park: A Spectacular Ancient Ecosystem Revealed. Indiana University Press, Bloomington.

Gardner, J. D. 2012. Revision of *Piceoerpeton* Meszoely (Caudata: Scapherpetontidae) and description of a new species from the late Maastrichtian and ?early Paleocene of western North America. Bulletin de la Société Géologique de France 6:611–620.

Gardner, J. D., and M. Böhme. 2008. Review of the Albanerpetontidae (Lissamphibia), with comments on the paleoecological preferences of European Tertiary albanerpetontids; pp. 178–218 in J. T. Sankey, and S. Baszio (eds.), Vertebrate Microfossil Assemblages: Their Role in Paleoecology and Paleobiogeography. Indiana University Press, Bloomington.

Gehlbach, F. R., R. Gordon, and J. B. Jordan. 1973. Aestivation of the salamander, Siren intermedia. American Midland Naturalist 89:455-463.

Goldin, T. J., and H. J. Melosh. 2009. Self-shielding of thermal radiation by Chicxulub impact ejecta: Firestorm or fizzle? Geology 37:1135–1138.

Gilmour, I., W. S. Wolbach, and E. Anders. 1990. Early environmental effects of the terminal Cretaceous impact; pp. 383–390 in V. L. Sharpton, and P. D. Ward (eds.), Global catastrophes in Earth history; An interdisciplinary conference on impacts, volcanism, and mass mortality. Geological Society of America Special Paper 247, Boulder, Colorado.

Hammer, Ø., D. A. T. Harper, and P. D. Ryan. 2001. PAST: Paleontological Statistics Software Package for education and data analysis. Palaeontologia Electronica 4:1–9.

Harries, P. J., E. G. Kauffman, and T. A. Hansen. 1996. Models for biotic survival following mass extinction; pp. 41–60 in M. B. Hart (ed.), Biotic Recovery from Mass Extinction Events. Geological Society Special Publication 102, London.

Hartman, J. H. 1998. The biostratigraphy and paleontology of latest Cretaceous and Paleocene freshwater bivalves from the western Williston Basin, Montana, U.S.A.; pp. 317–345 in P. A. Johnston, and J. W. Haggart (eds.), Bivalves: An Eon of Evolution--Paleobiological Studies Honoring Norman D. Newell. University of Calgary Press, Calgary.

Heatwole, H., and R. L. Carroll, eds. eds (2000) Amphibian Biology Vol. 4: Palaeontology, The Evolutionary History of Amphibians, Vol. 4. Surrey Beatty & Sons, Chipping Norton.

Hess, J., M. L. Bender, and J.-G. Schilling. 1986. Evolution of the ratio of Strontium-87 to Strontium-86 in seawater from Cretaceous to present. Science 231:979–984.

Hicks, J. F., K. R. Johnson, J. D. Obradovich, L. Tauxe, and D. Clark. 2002. Magnetostratigraphy and geochronology of the Hell Creek and basal Fort Union Formations of southwestern North Dakota and a recalibration of the age of the Cretaceous-Tertiary boundary; pp. 35–55 in J. H. Hartman, K. R. Johnson, and D. J. Nichols (eds.), The Hell Creek Formation and the Cretaceous-Tertiary boundary in the northern Great Plains: An integrated continental record of the end of the Cretaceous. Geological Society of America Special Paper 361, Boulder, Colorado.

Holland, S. M. 2003. Analytic Rarefaction 1.3. http://www.uga.edu/~strata/software/.

Holman, J. A. 2006. Fossil Salamanders of North America. 232 pp. Indiana University Press, Bloomington.

Howells, G. P. 1995. Acid Rain and Acid Waters. 262 pp. Ellis Horwood, New York.

Huggett, A. J. 2005. The concept and utility of 'ecological thresholds' in biodiversity conservation. Biological Conservation 124:301–310.

Jablonski, D. 1986. Background and mass extinctions: The alternation of macroevolutionary regimes. Science 231:129–133.

Jablonski, D. 1989. The biology of mass extinction: A palaeontological view. Philosophical Transactions of the Royal Society of London, Series B 325:357–368.

Jablonski, D. 1996. Body size and macroevolution; pp. 256–289 in D. Jablonski, D. H. Erwin, and J. H. Lipps (eds.), Evolutionary Paleobiology. University of Chicago Press, Chicago.

Jablonski, D. 1998. Geographic variation in the molluscan recovery from the end-Cretaceous extinction. Science 279:1327–1330.

Jablonski, D. 2002. Survival without recovery after mass extinctions. Proceedings of the National Academy of Sciences of the United States of America 99:8139–8144.

Jablonski, D. 2005. Mass extinctions and macroevolution. Paleobiology 31(suppl.):192–210.

Keller, G. 2003. Biotic effects of impacts and volcanism. Earth and Planetary Science Letters 215:249–264.

Keller, G., A. Sahni, and S. Bajpai. 2009. Deccan volcanism, the KT mass extinction and dinosaurs. Journal of Biosciences 34:709–728.

Kring, D. A. 2007. The Chicxulub impact event and its environmental consequences at the Cretaceous-Tertiary boundary. Palaeogeography, Palaeoclimatology, Palaeoecology 255:4–21.

Kring, D. A., H. J. Melosh, and D. M. Hunten. 1996. Impact-induced perturbations of atmospheric sulfur. Earth and Planetary Science Letters 140:201–212.

Kucera, M., and B. A. Malmgren. 1998. Terminal Cretaceous warming event in the mid-latitude South Atlantic Ocean: Evidence from poleward migration of Contusotruncana contusa (planktonic foraminifera) morphotypes. Palaeogeography, Palaeoclimatology, Palaeoecology 138:1–15.

Lewis, J. S., G. Hampton Watkins, H. Hartman, and R. G. Prinn. 1982. Chemical consequences of major impact events on Earth; pp. 215–221 in L. T. Silver, and P. H. Schultz (eds.), Geological implications of impacts of large asteroids and comets on the Earth. Geological Society of America Special Paper 190, Boulder, Colorado.

Li, L., and G. Keller. 1998. Abrupt deep-sea warming at the end of the Cretaceous. Geology 26:995–999.

Lillegraven, J. A., and J. J. Eberle. 1999. Vertebrate faunal changes through Lancian and Puercan time in southern Wyoming. Journal of Paleontology 73:691–710.

Lillywhite, H. B. 2010. Physiological ecology: field methods and perspective; pp. 363–386 in C. K. Dodd, Jr. (ed.), Amphibian ecology and conservation: A handbook of techniques. Oxford University Press, New York.

Lockwood, R. 2003. Abundance not linked to survival across the end-Cretaceous mass extinction: Patterns in North American bivalves. Proceedings of the National Academy of Sciences of the United States of America 100:2478–2482.

Lofgren, D. L., C. L. Hotton, and A. C. Runkel. 1990. Reworking of Cretaceous dinosaurs into Paleocene channel deposits, upper Hell Creek Formation, Montana. Geology 18:874–877.

MacDougall, J. D. 1988. Seawater strontium isotopes, acid rain, and the Cretaceous-Tertiary boundary. Science 239:485–487.

MacLeod, K. G., B. T. Huber, and C. Isaza-Londoño. 2005. North Atlantic warming during global cooling at the end of the Cretaceous. Geology 33:437–440.

Magurran, A. E. 2004. Measuring Biological Diversity. 256 pp. Blackwell Publishing, Malden, Massachusetts.

Marshall, C. R. 1997. Confidence intervals on stratigraphic ranges with nonrandom distribution of fossil horizons. Paleobiology 23:165–173.

Maruoka, T., and C. Koeberl. 2003. Acid-neutralizing scenario after the Cretaceous-Tertiary impact event. Geology 31:489–492.

McElwain, J. C., P. J. Wagner, and S. P. Hesselbo. 2009. Fossil plant relative abundances indicate sudden loss of Late Triassic biodiversity in East Greenland. Science 324:1554–1556.

McGowan, G. J., and S. E. Evans. 1995. Albanerpetontid amphibians from the Cretaceous of Spain. Nature 373:143–145.

McKinney, F. M., S. Lidgard, J. J. Sepkoski, Jr., and P. D. Taylor. 1998. Decoupled temporal patterns of evolution and ecology in two post-Paleozoic clades. Science 281:807–809.

McKinney, M. L. 1997. Extinction vulnerability and selectivity: Combining ecological and paleontological views. Annual Review of Ecology and Systematics 28:495–516.

Meszoely, C. A. M. 1967. A new cryptobranchid salamander from the Early Eocene of Wyoming. Copeia 1967:346–349.

Milner, A. R. 2000. Mesozoic and Tertiary Caudata and Albanerpetontidae; pp. 1413–1444 in H. Heatwole, and R. L. Carroll (eds.), Amphibian Biology Vol. 4, Palaeontology, The Evolutionary History of Amphibians. Surrey Beatty & Sons, Chipping Norton.

Mitchell, J. S., P. Roopnarine, and K. D. Angielczyk. 2012. Late Cretaceous restructuring of terrestrial communities facilitated the end-Cretaceous mass extinction in North America. Proceedings of the National Academy of Sciences of the United States of America 109:18857–18861.

Molles, M. C., Jr. 2005. Ecology: Concepts and Applications, Third Edition. 622 pp. McGraw-Hill Companies, Inc., New York.

Morell, V. 1999. Frogs: canaries in the hot zone? Science 284:729.

Naylor, B. G. 1978. The earliest known *Necturus* (Amphibia, Urodela), from the Paleocene Ravenscrag Formation of Saskatchewan. Journal of Herpetology 12:565–569.

Naylor, B. G. 1979. The Cretaceous salamander *Prodesmodon* (Amphibia: Caudata). Herpetologica 35:11–20.

Naylor, B. G. 1983. New salamander (Amphibia: Caudata) atlantes from the upper Cretaceous of North America. Journal of Paleontology 57:48–52.

Naylor, B. G., and D. W. Krause. 1981. *Piceoerpeton*, a giant early Tertiary salamander from western North America. Journal of Paleontology 55:507–523.

Nelson, B. K., G. K. MacLeod, and P. D. Ward. 1991. Rapid change in strontium isotopic composition of sea water before the Cretaceous/Tertiary boundary. Nature 351:644–647.

Nordt, L., S. Atchley, and S. Dworkin. 2003. Terrestrial evidence for two greenhouse events in the latest Cretaceous. GSA Today 13:4–9.

Officer, C. B., A. Hallam, C. L. Drake, and J. D. Devine. 1987. Late Cretaceous and paroxysmal Cretaceous/Tertiary extinctions. Nature 326:143–149.

Ogg, J. G., and A. G. Smith. 2004. The geomagnetic polarity time scale; pp. 63-86 in F. M. Gradstein, J. G. Ogg, and A. Smith (eds.), A Geologic Time Scale 2004. Cambridge University Press, Cambridge.

Oksanen, J., F. G. Blanchet, R. Kindt, P. Legendre, R. G. O'Hara, G. L. Simpson, P. Solymos, M. Henry, H. Stevens, and H. Wagner. 2010. Vegan: Community Ecology Package R package version 1.17–1.

Payne, J. L., and S. Finnegan. 2007. The effect of geographic range on extinction risk during background and mass extinction. Proceedings of the National Academy of Sciences of the United States of America 104:10506–10511.

Pearson, D. A., T. Schaefer, K. R. Johnson, D. J. Nichols, and J. P. Hunter. 2002. Vertebrate biostratigraphy of the Hell Creek Formation in southwestern North Dakota and northwestern South Dakota; pp. 145–167 in J. H. Hartman, K. R. Johnson, and D. J. Nichols (eds.), The Hell Creek Formation and the Cretaceous-Tertiary boundary in the northern Great Plains: An integrated continental record of the end of the Cretaceous. Geological Society of America Special Paper 361, Boulder, Colorado.

Pierce, B. A. 1985. Acid tolerance in amphibians. BioScience 35:239–243.

Pough, F. H., and R. E. Wilson. 1977. Acid precipitation and reproductive success of Ambystoma salamanders. Water, Air, and Soil Pollution 7:307–316.

Powell, J. L. 1998. Night Comes to the Cretaceous: Dinosaur Extinction and the Transformation of Modern Geology. 250 pp. Freeman and Company, New York.

Prinn, R. G., and B. Fegley, Jr. 1987. Bolide impacts, acid rain, and biospheric traumas at the Cretaceous-Tertiary boundary. Earth and Planetary Science Letters 83:1–15.

Qian, H. 2009. Global comparisons of beta diversity among mammals, birds, reptiles, and amphibians across spatial scales and taxonomic ranks. Journal of Systematics and Evolution 47:509–514.

R Development Core Team, 2009, R: A Language and Environment for Statistical Computing: Vienna, Austria, R Foundation for Statistical Computing; www.r-project.org (accessed August 2010).

Raup, D. M. 1975. Taxonomic diversity estimation using rarefaction. Paleobiology 1:333–342.

Ravizza, G., and B. Peucker-Ehrenbrink. 2003. Chemostratigraphic evidence of Deccan volcanism from the marine Osmium isotope record. Science 302:1392–1395.

Renne, P. R., C. C. Swisher, III, A. L. Deino, D. B. Karner, T. L. Owens, and D. J. DePaolo. 1998. Intercalibration of standards, absolute ages and uncertainties in $^{40}Ar/^{39}Ar$ dating. Chemical Geology (Isotope Geoscience section) 145:117–152.

Retallack, G. J. 1996. Acid trauma at the Cretaceous-Tertiary boundary in eastern Montana. GSA Today 6:1–7.

Retallack, G. J. 2004. End-Cretaceous acid rain as a selective extinction mechanism between birds and dinosaurs; pp. 35–64 in P. J. Currie, E. B. Koppelhus, M. A. Shugar, and J. L. Wright (eds.), Feathered Dragons. Indiana University Press, Bloomington.

Retallack, G. J., G. D. Leahy, and M. D. Spoon. 1987. Evidence from paleosols for ecosystem changes across the Cretaceous/Tertiary boundary in eastern Montana. Geology 15:1090–1093.

Robertson, D. S., M. C. McKenna, O. B. Toon, S. Hope, and J. A. Lillegraven. 2004. Survival in the first hours of the Cenozoic. Geological Society of America Bulletin 116:760–768.

Rogers, R. R., and M. E. Brady. 2010. Origins of microfossil bonebeds: Insights from the Upper Cretaceous Judith River Formation of north-central Montana. Paleobiology 36:80–112.

Scheffer, M., and S. R. Carpenter. 2003. Catastrophic regime shifts in ecosystems: Linking theory to observation. Trends in Ecology and Evolution 18:648–656.

Scheffer, M., S. R. Carpenter, J. A. Foley, C. Folke, and B. Walker. 2001. Catastrophic shifts in ecosystems. Nature 413:591–596.

Schulte, P., L. Alegret, I. Arenillas, J. A. Arz, P. J. Barton, P. R. Bown, T. J. Bralower, G. L. Christeson, P. Claeys, C. S. Cockell, G. S. Collins, A. Deutsch, T. J. Goldin, K. Goto, J. M. Grajales-Nishimura, R. A. F. Grieve, S. P. S. Gulick, K. R. Johnson, W. Kiessling, C. Koeberl, D. A. Kring, K. G. MacLeod, T. Matsui, J. Melosh, A. Montanari, J. V. Morgan, C. R. Neal, D. J. Nichols, R. D. Norris, E. Pierazzo, G. Ravizza, M. Rebolledo-Vieyra, W. U. Reimold, E. Robin, T. Salge, R. P. Speijer, A. R. Sweet, J. Urrutia-Fucugauchi, V. Vajda, M. T. Whalen, and P. S. Willumsen. 2010. The Chicxulub asteroid impact and mass extinction at the Cretaceous-Paleogene boundary. Science 327:1214–1218.

Sebens, K. P. 1987. The ecology of indeterminate growth in animals. Annual Review of Ecology and Systematics 18:371–407.

Self, S., M. Widdowson, T. Thordarson, and A. E. Jay. 2006. Volatile fluxes during flood basalt eruptions and potential effects on the global environment: A Deccan perspective. Earth and Planetary Science Letters 248:518–532.

Sheehan, P. M., P. J. Coorough, and D. Fastovsky. 1996. Biotic selectivity during the K/T and Late Ordovician extinction events; pp. 477–489 in G. Ryder, D. Fastovsky, and S. Gartner (eds.), The Cretaceous-Tertiary Event and Other Catastrophes in Earth History. Geological Society of America Special Paper 307, Boulder, Colorado.

Sheehan, P. M., and D. E. Fastovsky. 1992. Major extinctions of land-dwelling vertebrates at the Cretaceous-Tertiary boundary, eastern Montana. Geology 20:556–560.

Sheehan, P. M., and T. A. Hansen. 1986. Detritus feeding as a buffer to extinction at the end of the Cretaceous. Geology 14:868–870.

Signor, P. W., III, and J. H. Lipps. 1982. Sampling bias, gradual extinction patterns and catastrophes in the fossil record; pp. 291–296 in L. T. Silver, and P. H. Schultz (eds.), Geological implications of impacts of large asteroids and comets on the Earth. Geological Society of America Special Paper 190, Boulder, Colorado.

Sigurdsson, H., S. D'Hondt, and S. Carey. 1992. The impact of the Cretaceous/Tertiary bolide on evaporite terrane and generation of major sulfuric acid aerosol. Earth and Planetary Science Letters 109:543–559.

Solé, M., and D. Rödder. 2010. Dietary assessments of adult amphibians; pp. 167–184 in C. K. Dodd, Jr. (ed.), Amphibian ecology and conservation. Oxford University Press, New York.

Strauss, D., and P. M. Sadler. 1989. Classical confidence intervals and bayesian probability estimates for ends of local taxon ranges. Mathematical Geology 21:411–427.

Sweet, A. R., and D. R. Braman. 2001. Cretaceous-Tertiary palynofloral perturbations and extinctions within the *Aquilapollenites* phytogeographic province. Canadian Journal of Earth Sciences 38:249–269.

Swisher, C. C., III , L. Dingus, and R. F. Butler. 1993. $^{40}Ar/^{39}Ar$ dating and magnetostratigraphic correlation of the terrestrial Cretaceous-Paleogene boundary and Puercan Mammal Age, Hell Creek-Tullock formations, eastern Montana. Canadian Journal of Earth Sciences 30:1981–1986.

Tipper, J. C. 1979. Rarefaction and rarefiction: The use and abuse of a method in paleoecology. Paleobiology 5:423–434.

Tobin, T. S., P. D. Ward, E. J. Steig, E. B. Olivero, I. A. Hilburn, R. N. Mitchell, M. R. Diamond, T. D. Raub, and J. L. Kirschvink. 2012. Extinction patterns, $\delta^{18}O$ trends, and magnetostratigraphy from a southern high-latitude Cretaceous-Paleogene section: links with Deccan volcanism. Palaeogeography, Palaeoclimatology, Palaeoecology 350–352:180–188.

Van Valen, L., and R. E. Sloan. 1965. The earliest primates. Science 150:743–745.

Venczel, M., and J. D. Gardner. 2005. The geologically youngest albanerpetontid amphibian, from the lower Pliocene of Hungary. Palaeontology 48:1273–1300.

Vonhof, H. B., and J. Smit. 1997. High-resolution late Maastrichtian-early Danian oceanic $^{87}Sr/^{86}Sr$ record: Implications for Cretaceous-Tertiary boundary events. Geology 25:347–350.

Wake, D. B. 1991. Declining amphibian populations. Science 253:860.

Wake, D. B., and V. T. Vredenburg. 2008. Are we in the midst of the sixth mass extinction? A view from the world of amphibians. Proceedings of the National Academy of Sciences of the United States of America 105:11466–11473.

Weil, A. 1994. K/T survivorship as a test of acid rain hypotheses. Geological Society of America Abstracts with Programs 26:A–335.

Weil, A., and W. A. Clemens. 1998. Aliens in Montana: Phylogenetically and biogeographically diverse lineages contributed to an earliest Cenozoic community. Geological Society of America Abstracts with Programs 30:69–70.

Wells, K. D. 2007. The Ecology and Behavior of Amphibians. 1148 pp. University of Chicago Press, Chicago, Illinois.

White, R. V., and A. D. Saunders. 2005. Volcanism, impact and mass extinctions: Incredible or credible coincidences? Lithos 79:299–316.

Wilf, P., and K. R. Johnson. 2004. Land plant extinction at the end of the Cretaceous: A quantitative analysis of the North Dakota megafloral record. Paleobiology 30:347–368.

Wilf, P., K. R. Johnson, and B. T. Huber. 2003. Correlated terrestrial and marine evidence for global climate changes before mass extinction at the Cretaceous-Paleogene boundary. Proceedings of the National Academy of Sciences of the United States of America 100:599–604.

Wilson, G. P. 2004. A quantitative assessment of mammalian change leading up to and across the Cretaceous-Tertiary boundary in northeastern Montana, Ph.D. dissertation, pp. 412. University of California.

Wilson, G. P. 2005. Mammalian faunal dynamics during the last 1.8 million years of the Cretaceous in Garfield County, Montana. Journal of Mammalian Evolution 12:53–75.

Wilson, G. P. 2014. Mammalian extinction, survival, and recovery dynamics across the Cretaceous-Paleogene boundary in northeastern Montana; pp. 365–392 in G. P. Wilson, W. A. Clemens, J. R. Horner, and J. H. Hartman (eds.), Through the end of the Cretaceous in the type locality of the Hell Creek Formation in Montana and adjacent areas. Geological Society of America Special Paper, Boulder, Colorado.

Wilson, L. E. 2008. Comparative taphonomy and paleoecological reconstruction of two microvertebrate accumulations from the Late Cretaceous Hell Creek Formation (Maastrichtian), eastern Montana. Palaios 23:289–297.

FIGURES for CHAPTER 2

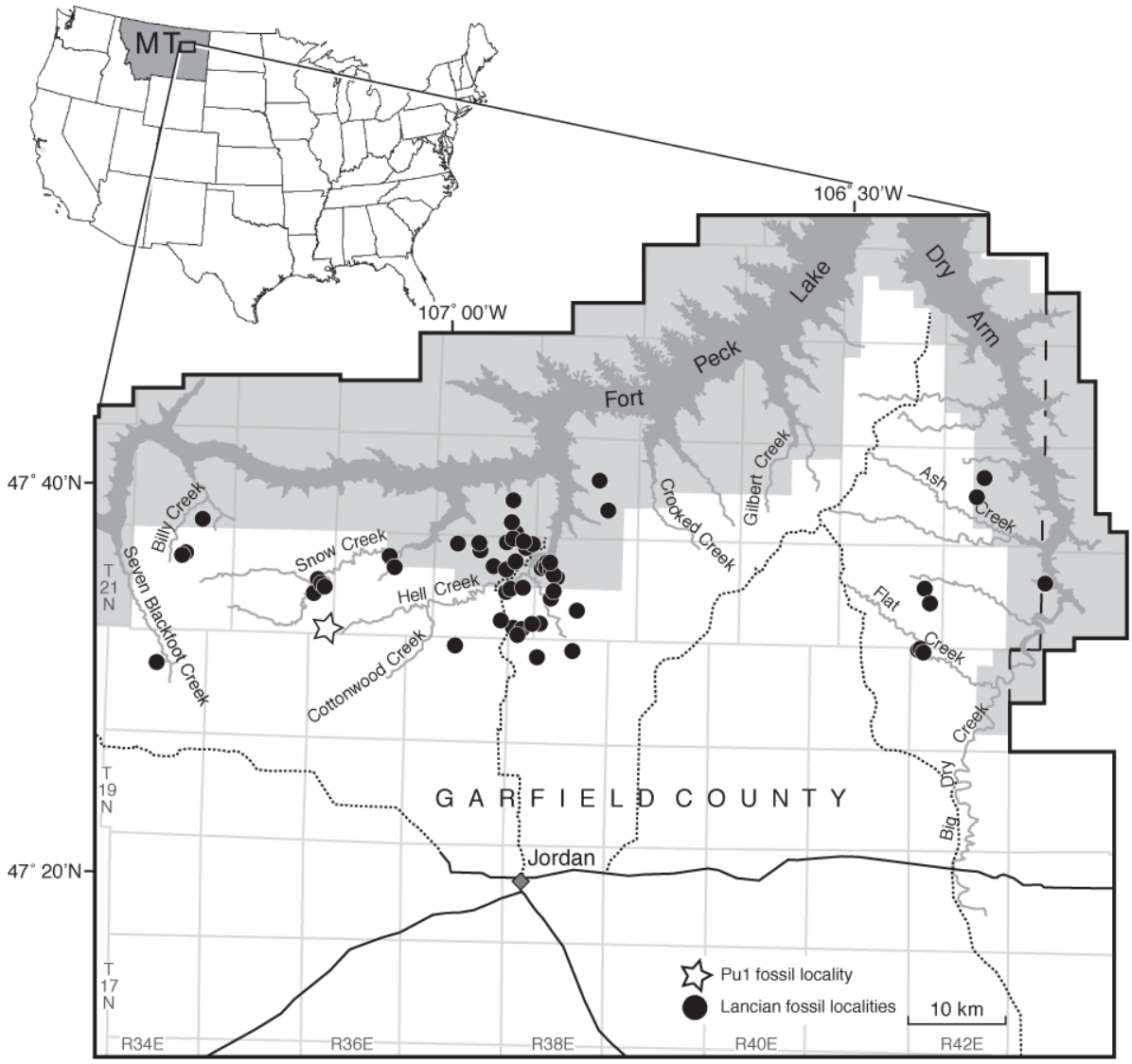

Figure 2.1. Map of caudate and allocaudate fossil localities from the Hell Creek Formation and Tullock Member exposures of Garfield County, northeastern Montana. The light-gray shaded area represents the Charles M. Russell Wildlife Refuge, solid black lines represent paved roads, dotted lines are unpaved roads, and dashed lines demarcate county lines. Amphibian fossil

localities used in the study are represented by filled circles (Lancian) and an open star (Pu1 [early Puercan] interval).

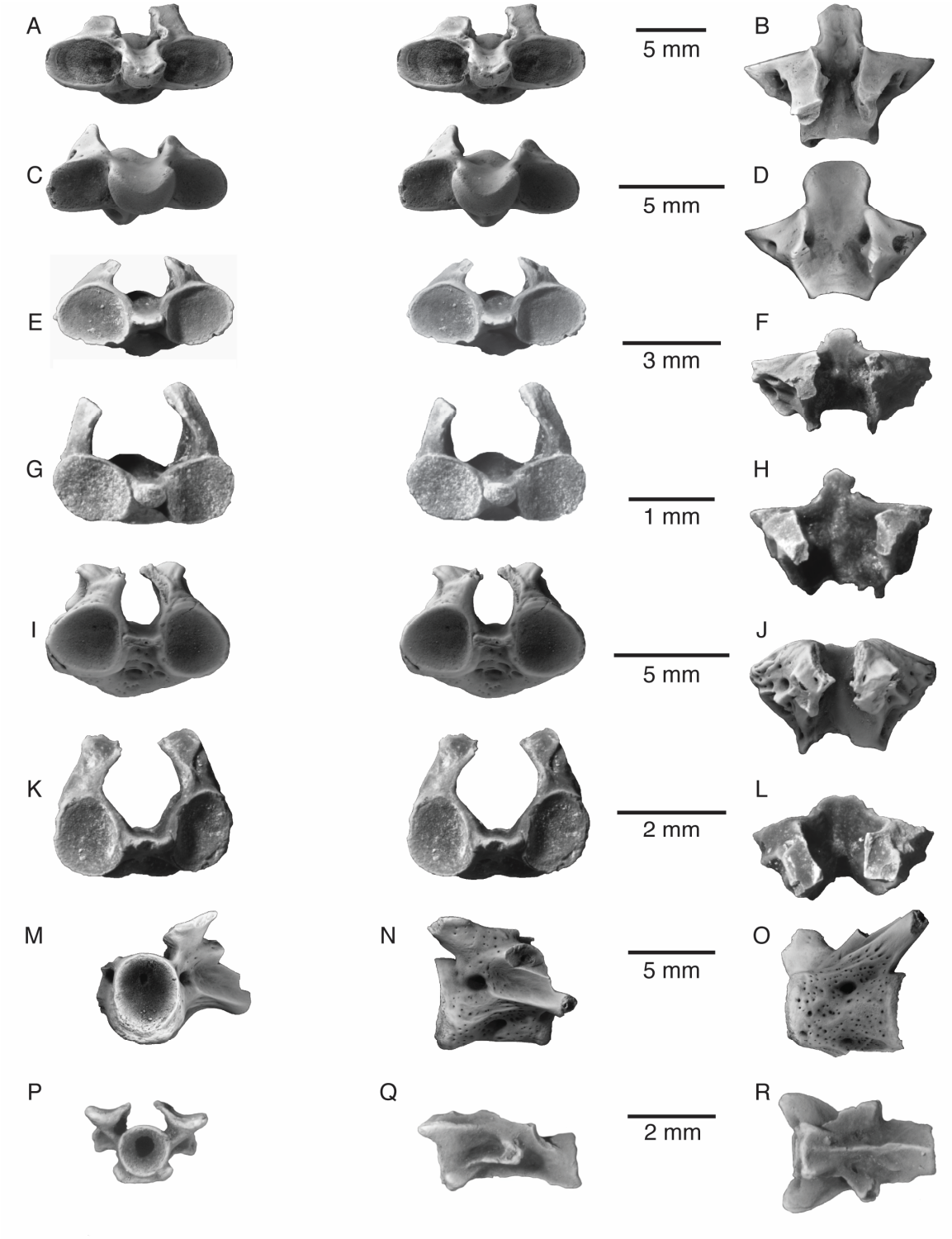

Figure 2.2. Caudate atlantes and trunk vertebrae from the Hell Creek Formation of Garfield County, northeastern Montana. Atlantes, each missing the upper part of the neural arch roof, in stereo anterior views and dorsal views, respectively: (**A**, **B**) *Lisserpeton bairdi* (UCMP 191281)

from UCMP locality V99230; (**C**, **D**) *Scapherpeton tectum* (MOR 4189) from MOR locality HC-597; (**E**, **F**) *Piceoerpeton naylori* (MOR 5366) from MOR locality HC-591; (**G**, **H**) Proteidae gen. et sp. nov. (UWBM 93370) from UWBM locality C1153; (**I**, **J**) *Opisthotriton kayi* (UCMP 191407) from UCMP locality V99370; and (**K**, **L**) *Prodesmodon copei* (UWBM 93332) from UWBM locality C1153. Fragmentary trunk vertebra in anterior (**M**), left-lateral (**N**), and ventral (**O**) views of Scapherpetontidae gen. et sp. A (UWBM 93382) from UWBM locality C1151. Fragmentary trunk vertebra in anterior (**P**), left-lateral (**Q**), and ventral (**R**) views of *Proamphiuma cretacea* (UCMP 192529) from UCMP locality V74111 in the Tullock Member of Garfield County, northeastern Montana.

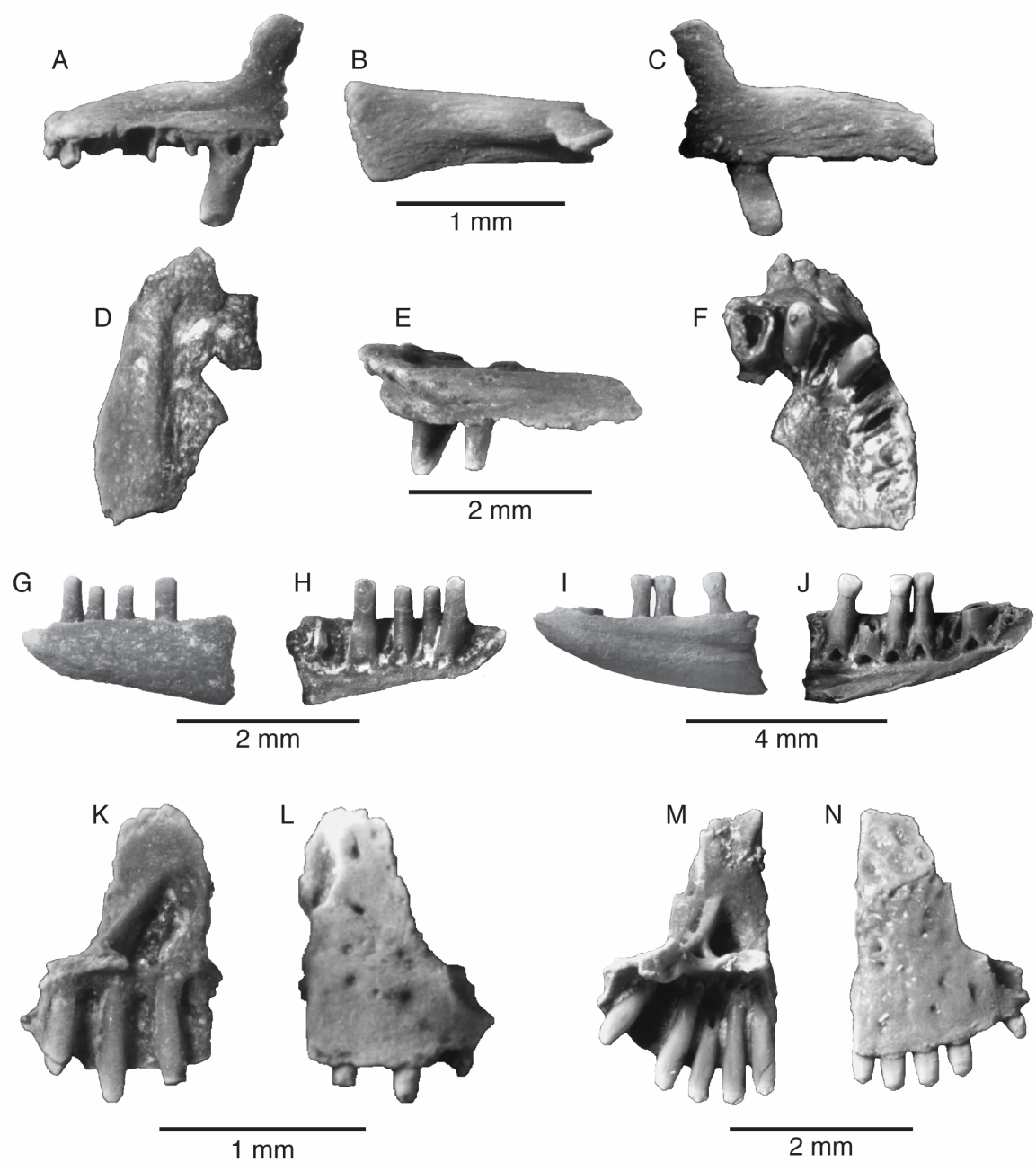

Figure 2.3. Sirenid and albanerpetontid tooth-bearing elements from the Hell Creek Formation of Garfield County, northeastern Montana. An anterior fragment of a right maxilla in lingual (**A**), dorsal (**B**), and labial (**C**) views of *Habrosaurus prodilatus* (UWBM 93403) from UWBM locality C1153. A near-complete left vomer of *Habrosaurus prodilatus* (UCMP 556520) from UCMP locality V99220 in dorsal (**D**), lateral (**E**), and occlusal (**F**) views. An anterior fragment

of a left dentary of *Habrosaurus prodilatus* (UCMP 556621) from UCMP locality V99220 in labial (**G**) and lingual (**H**) views. An anterior fragment of a left dentary of *Habrosaurus dilatus* (UWBM 93373) from UWBM locality C1153 in labial (**I**) and lingual (**J**) views. A near-complete left premaxilla of *Albanerpeton galaktion* (UCMP 556656) from UCMP locality V99369 in lingual (**K**) and labial (**L**) views. A near-complete left premaxilla of *Albanerpeton nexuosum* (DMNH 55222) from DMNH locality 3304 in lingual (**M**) and labial (**N**) views.

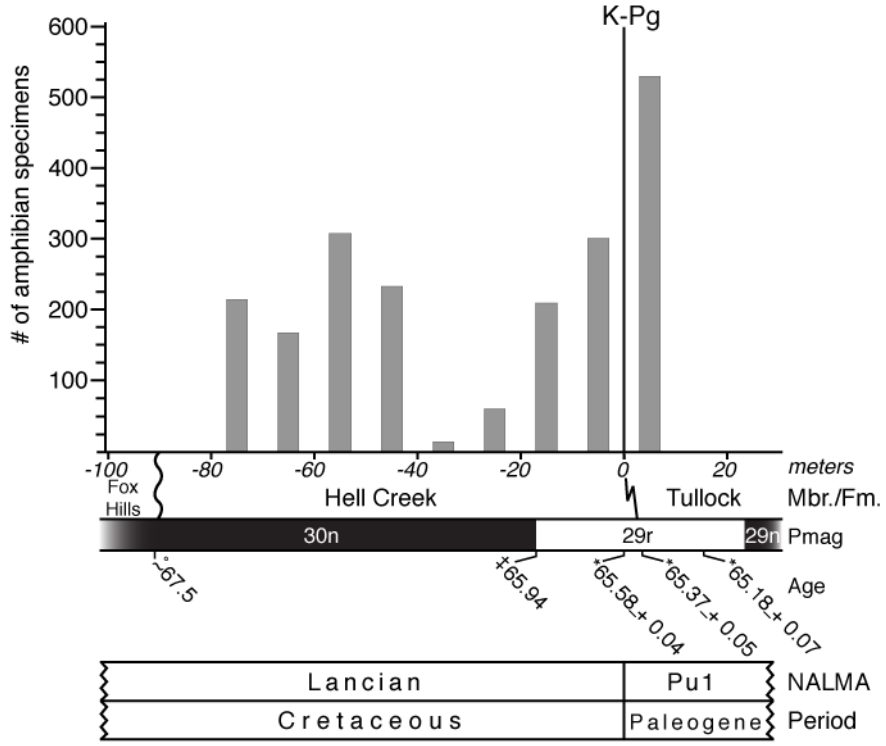

Figure 2.4. Caudate and allocaudate fossil sample sizes through the Hell Creek Formation and lowermost Tullock Member of Garfield County, northeastern Montana. Fossil sample sizes are based on 10 m bins. The chronostratigraphic framework is based on the following data: Ar/Ar radiometric ages (*) from Swisher et al. (1993) and revised by Renne et al. (1998) and Wilson (2004, 2005); ages for magnetochron boundaries (‡) from Ogg and Smith (2004); and the estimated age of the base of the Hell Creek Formation (†) from Wilson (2014). K-Pg—Cretaceous-Paleogene boundary; Pu1—early Puercan; NALMA—North American land mammal "age."

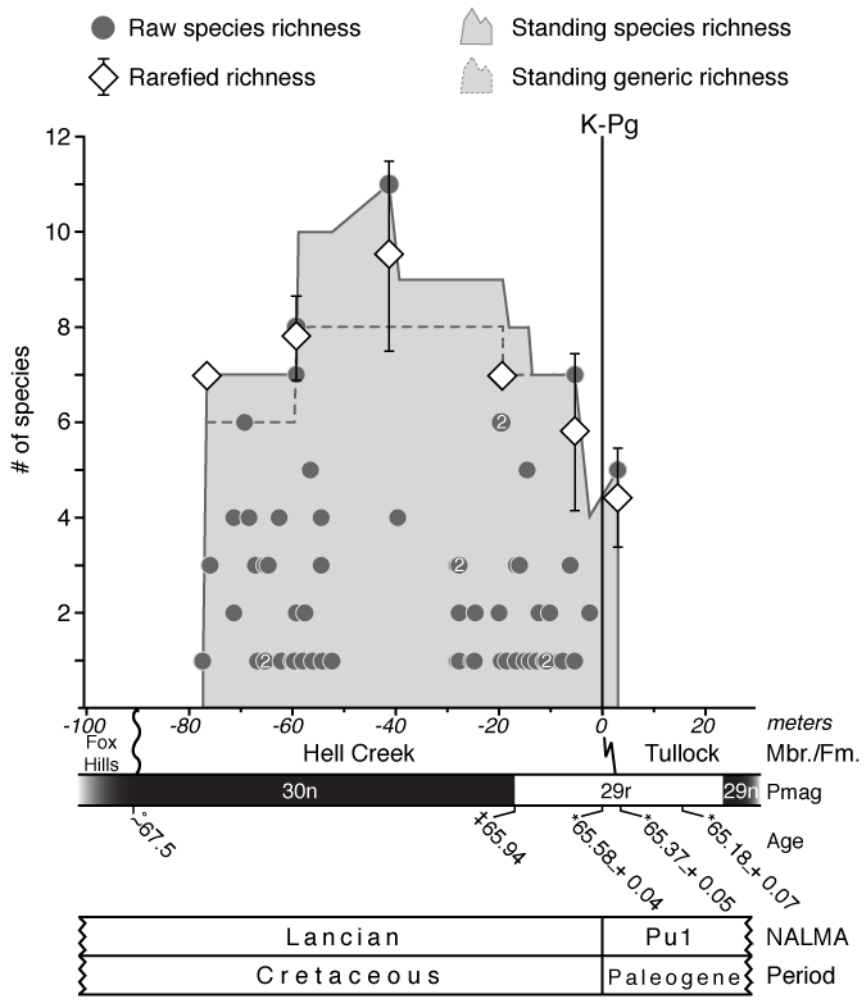

Figure 2.5. Caudate and allocaudate taxonomic richness through the Hell Creek Formation (Lancian) and lowermost Tullock Member (early Puercan [Pu1]) of Garfield County, northeastern Montana. Richness is represented as (1) raw numbers of species at individual localities (filled circles; if more than one locality at the same horizon has the same richness, the number of localities is listed within the circle); (2) standing species richness through the section (gray shade under solid line); (3) standing generic richness through the section (area under dashed line); and (4) expected numbers of species (open diamonds and 95% confidence intervals) from rarefaction analysis of 136-specimen samples from select localities (see Table 2.1

for details). For an explanation of the chronostratigraphic framework, see caption for Figure 2.4. K-Pg— Cretaceous-Paleogene boundary; NALMA—North American land mammal "age."

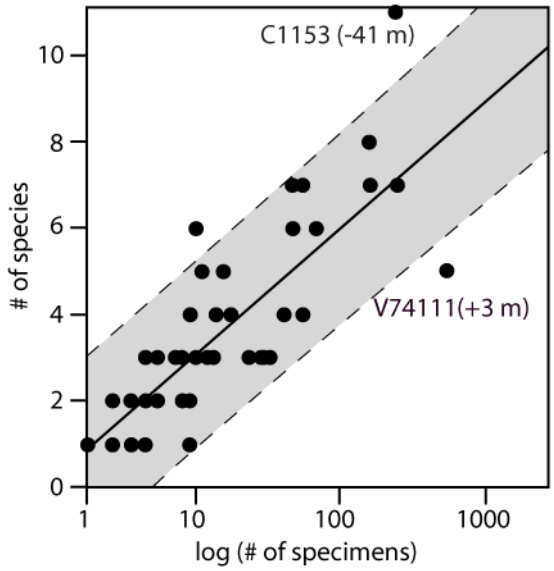

Figure 2.6. Log-linear correlation of caudate and allocaudate fossil sample sizes and species richness for localities from the Hell Creek Formation (Lancian) and lowermost Tullock Member (early Puercan [Pu1]) of Garfield County, northeastern Montana ($r = 0.862$, $p < 0.001$). The 95% confidence interval is shaded gray. Outliers of adequate sample sizes (>100 specimens) are identified by their locality numbers and stratigraphic position relative to the Cretaceous-Paleogene boundary.

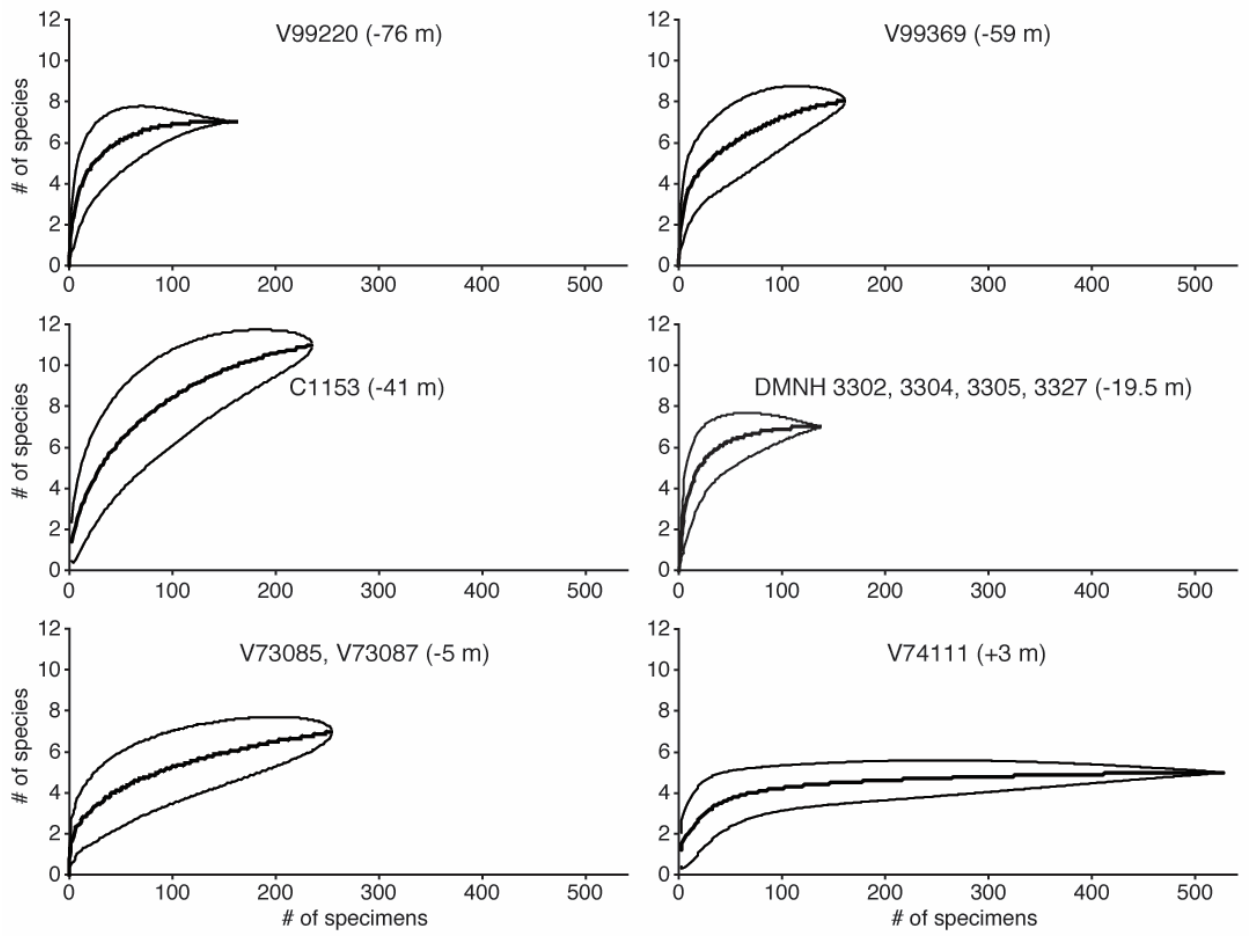

Figure 2.7. Rarefaction curves for six well-sampled caudate and allocaudate assemblages from the Hell Creek Formation (Lancian) and lowermost Tullock Member (early Puercan [Pu1]) of Garfield County, northeastern Montana. Bold lines represent the expected number of species for each sample size in each assemblage. Thin lines represent 95% confidence intervals. All assemblages are Lancian in age, except UCMP locality V74111 (Pu1), and are identified by their locality numbers and stratigraphic position relative to the Cretaceous-Paleogene boundary (see Table 2.1 for details).

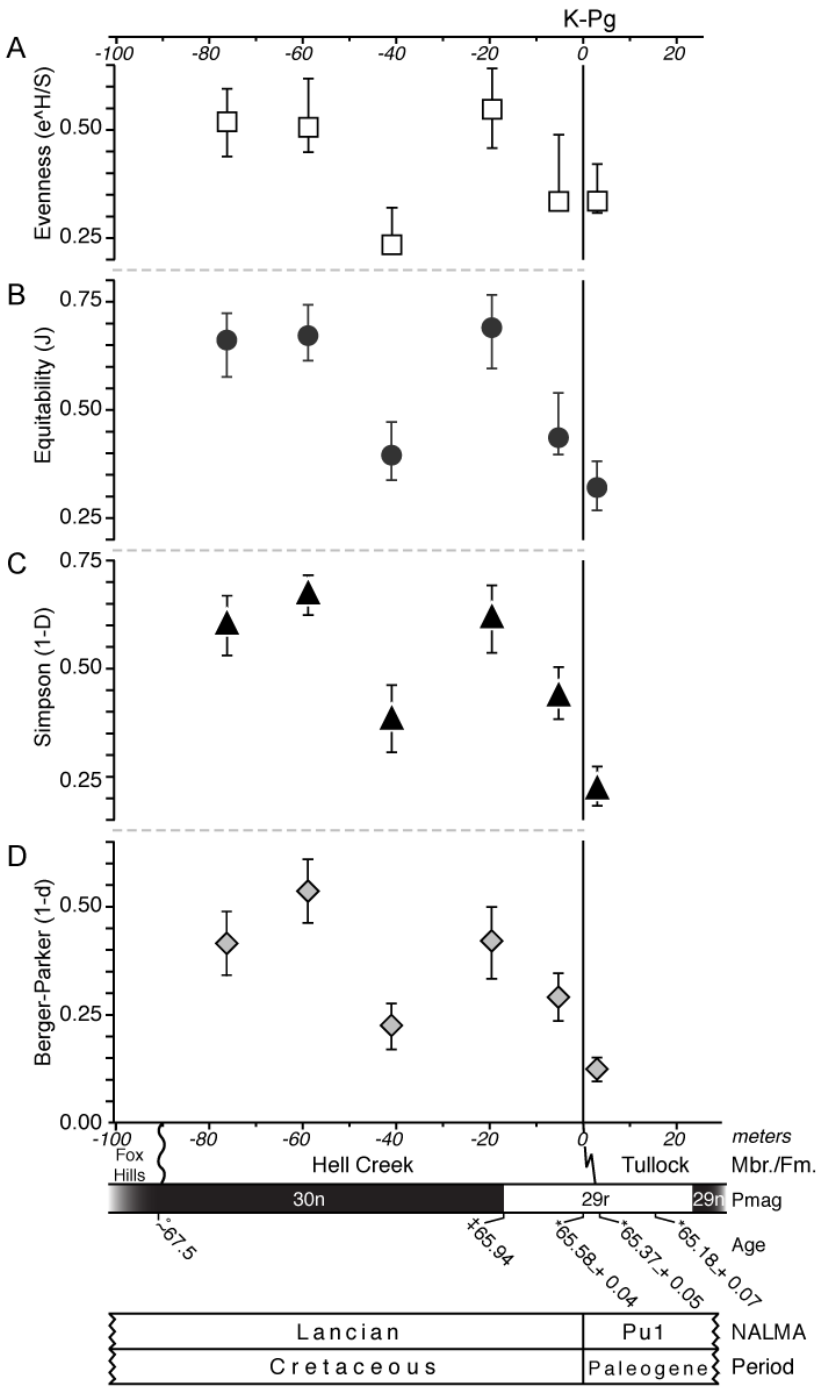

Figure 2.8. Heterogeneity indices and 95% confidence intervals for six well-sampled caudate and allocaudate assemblages from the Hell Creek Formation (Lancian) and lowermost Tullock Member (early Puercan [Pu1]) of Garfield County, northeastern Montana. From left to right, the

localities are UCMP locality V99220 (−76.4 m), UCMP locality V99369 (−59.0 m), UWBM locality C1153 (−41.2 m), DMNH localities 3302, 3304, 3305, and 3327 (−19.5 m), UCMP localities V73085 and V73087 (−5.2 m), and UCMP locality V74111 (+2.9 m) (see Table 2.1 for details). Evenness (**A**) and equitability (**B**) are derived from Shannon's index, whereas Simpson's (**C**) and Berger-Parker (**D**) indices are dominance measures. For an explanation of the chronostratigraphic framework, see caption for Figure 2.4. Values for all indices range from 0.00 to 1.00 and are plotted at the same scale, though the range of values shown differs among indices. K-Pg— Cretaceous-Paleogene boundary; NALMA—North American land mammal "age."

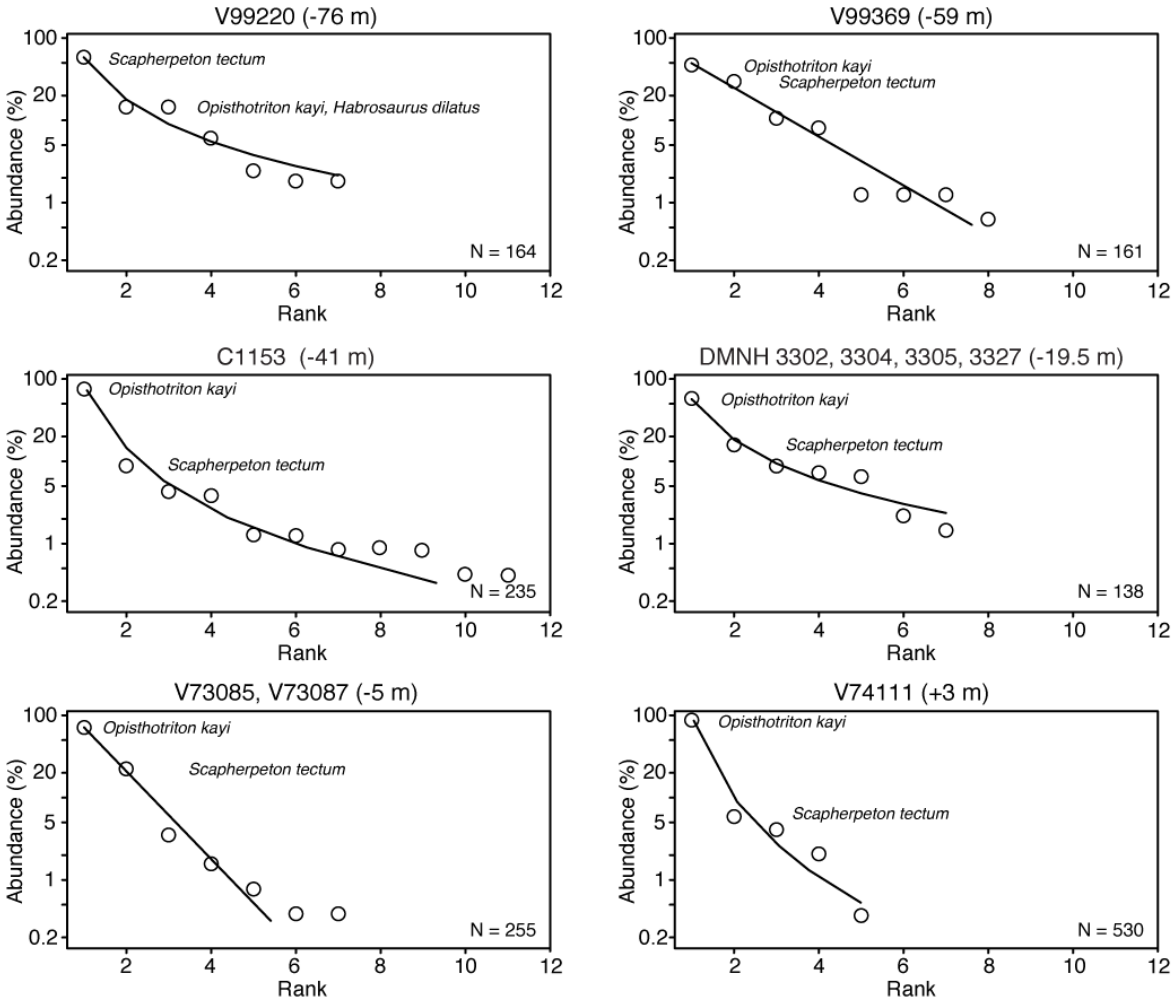

Figure 2.9. Relative abundance distributions (RADs) for six well-sampled caudate and allocaudate assemblages from the Hell Creek Formation (Lancian) and lowermost Tullock Member (early Puercan [Pu1]) of Garfield County, northeastern Montana. Boxes include a log-linear plot of percent abundance versus rank abundance for each species (open circles) in an assemblage and a line or curve representing the best-fit model for the data (see Table 2.3). For each assemblage, the two most abundant taxa and the total fossil sample size (N) are indicated. All assemblages are Lancian in age, except UCMP locality V74111 (Pu1), and are identified by locality numbers and stratigraphic position relative to the Cretaceous-Paleogene boundary (see Table 2.1 for details).

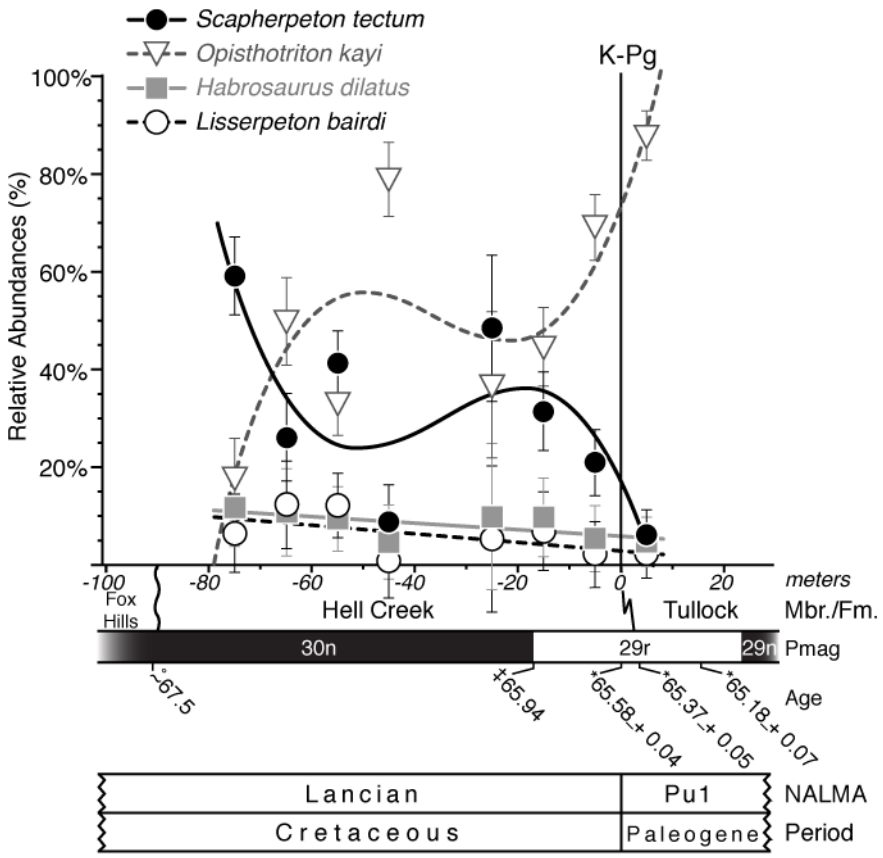

Figure 2.10. Relative abundances of the four most abundant caudate species for eight well-sampled 10 m bins from the Hell Creek Formation (Lancian) and lowermost Tullock Member (early Puercan [Pu1]) of Garfield County, northeastern Montana. The 95% confidence intervals (cross-bars) were calculated for each value (see Methods). Least squares regression found cubic fits for the *Scapherpeton tectum* ($r = 0.657$, $p < 0.194$) and *Opisthotriton kayi* data ($r = 0.705$, $p < 0.146$) and linear fits for the *Habrosaurus dilatus* ($r = 0.412$, $p < 0.086$) and the *Lisserpeton bairdi* data ($r = 0.376$, $p < 0.106$). None was statistically significant. K-Pg—Cretaceous-Paleogene boundary; NALMA—North American land mammal "age."

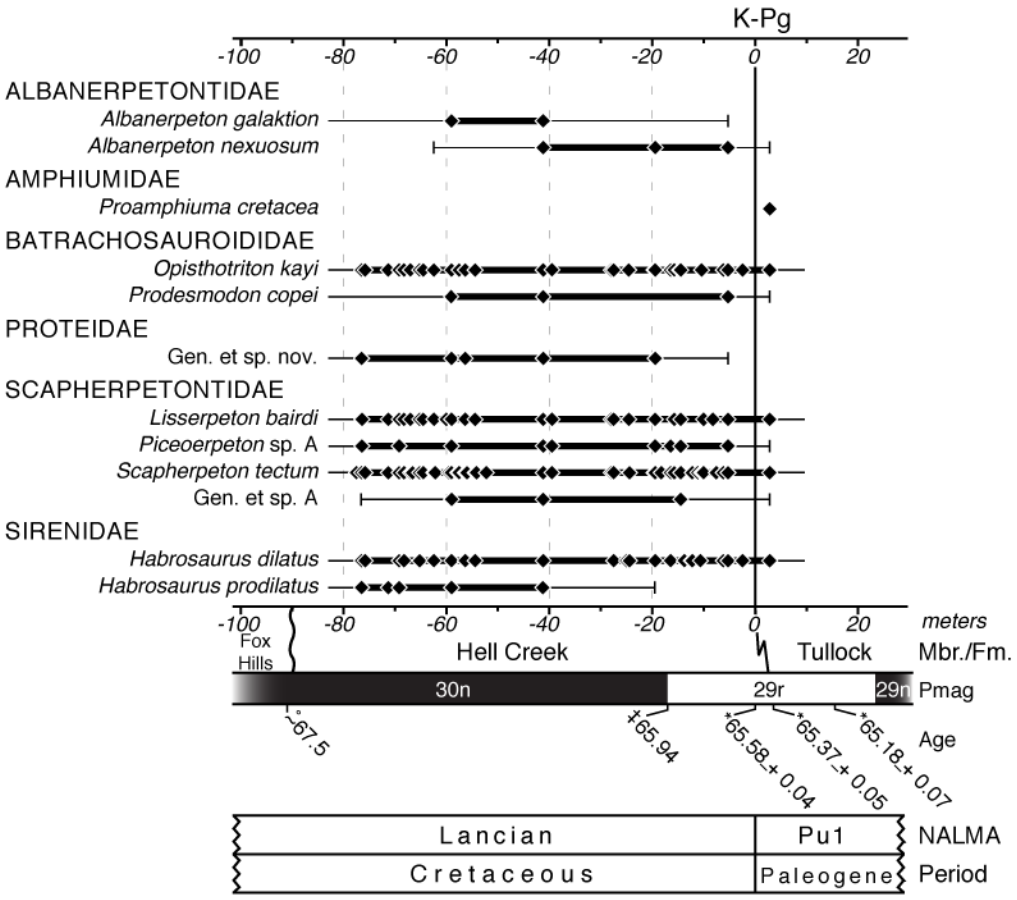

Figure 2.11. Biostratigraphic ranges with 50% confidence intervals for caudate and allocaudate species from the Hell Creek Formation (Lancian) and lowermost Tullock Member (early Puercan [Pu1]) of Garfield County, northeastern Montana. Diamonds represent actual occurrences, thick lines represent inferred range-through occurrences, thin lines with vertical cross-bars represent 50% confidence intervals, and thin lines without cross-bars indicate that the calculated confidence limit extends beyond the sampled interval. For an explanation of the chronostratigraphic framework, see caption for Figure 2.4. K-Pg— Cretaceous-Paleogene boundary; NALMA—North American land mammal "age."

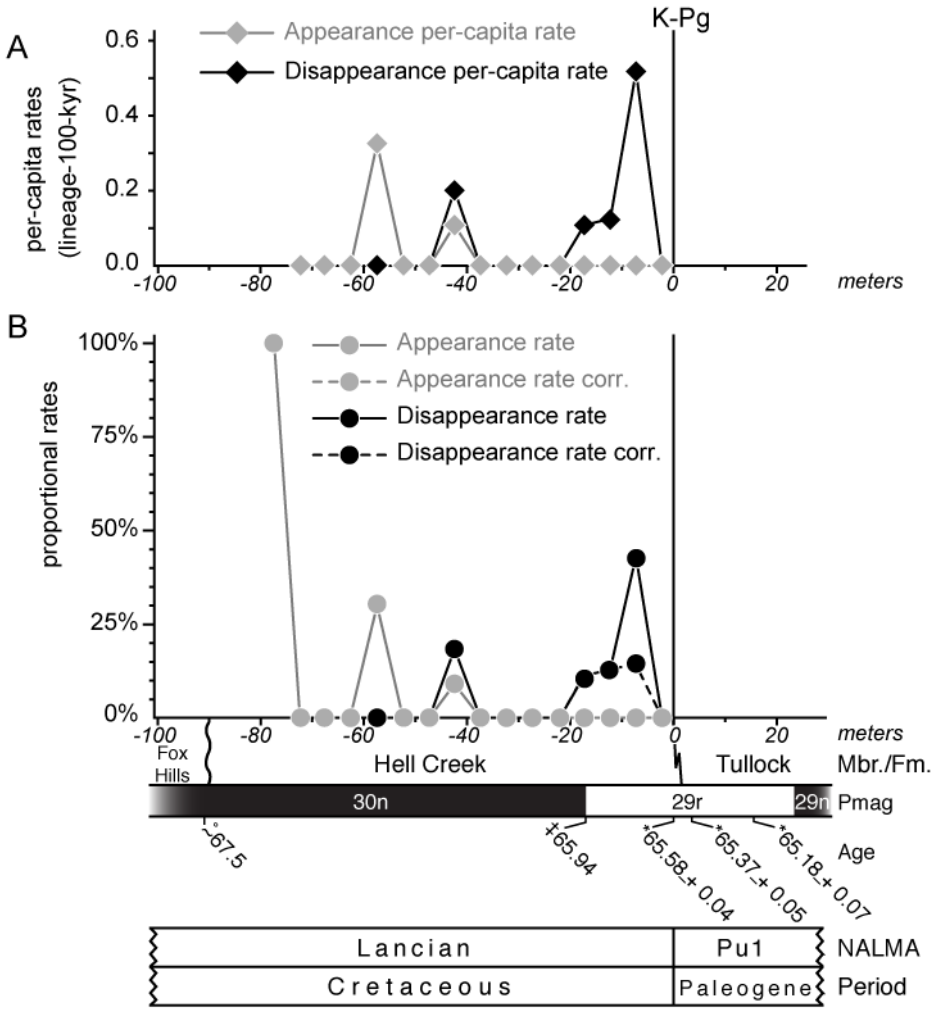

Figure 2.12. Per-capita rates (**A**) and proportional rates (**B**) of caudate and allocaudate turnover for 5 m bins through the Hell Creek Formation of Garfield County, northeastern Montana. Per-capita rates (diamonds) are in lineage-100-k.y. units. For an explanation of the chronostratigraphic framework see caption for Figure 2.4. K-Pg—Cretaceous-Paleogene boundary; NALMA—North American land mammal "age"; Pu1—early Puercan.

TABLES for CHAPTER 2

TABLE 2.1. SUMMARY STATISTICS OF THE SIX MOST FOSSILIFEROUS CAUDATE AND ALLOCAUDATE ASSEMBLAGES FROM THE HELL CREEK FORMATION (LANCIAN) AND LOWERMOST TULLOCK MEMBER (PU1) OF GARFIELD COUNTY, NORTHEASTERN MONTANA

Institution	Loc. no.	Alt. loc. no.	Fossil assemblage	Height (m)	S	N	E	U95%	L95%
UCMP	V99220	MOR HC-583; UWBM C1103	Tuma	-76.4	7	164	7.0	7.2	6.8
UCMP	V99369	MOR HC-293; UWBM C1115	Celeste's Magnificent Microsite	-59.0	8	161	7.7	8.7	6.6
UWBM	C1153	UCMP V82022	Hartless	-41.2	11	235	9.5	11.5	7.5
DMNH	3302	N.A.*	Hot Feet	-19.5	7	138	7.0	7.0	7.0
	3304	N.A.	Hot Feet						
	3305	UWBM C1529	Hot Feet						
	3327	N.A.	Hot Feet						
UCMP	V73085	N.A.	Flat Creek	-5.2	7	255	5.8	7.5	4.2
	V73087	UWBM C1614	Flat Creek						
UCMP	V74111	MOR FU-655; UWBM C1369	Worm Coulee 1	2.9	5	530	4.4	5.5	3.4

Note: Loc. no. = locality number; Alt. loc. no. = alternate museum locality number; Fossil assemblage = refers to a fossil assemblage from either a single locality or a group of closely associated localities; Height (m) = stratigraphic height in meters relative to Hell Creek-Tullock contact (~K-Pg boundary); S = raw number of species; N = number of individual specimens; E = estimated number of species at 136 specimens via rarefaction analysis; U95% = estimated number of species based on the upper 95% confidence interval via rarefaction analysis; L95% = estimated number of species based on the lower 95% confidence interval via rarefaction analysis.

*N.A. = no alternate locality number.

TABLE 2.2.SUMMARY STATISTICS OF CAUDATE AND ALLOCAUDATE FOSSIL SPECIMENS FROM THE HELL CREEK FORMATION (LANCIAN) AND LOWERMOST TULLOCK MEMBER (PU1) OF GARFIELD COUNTY, NORTHEASTERN MONTANA

Taxon	Element									Total (n)†	% total (n)§
	Atlas vertebra	Trunk vertebra	Caudal vertebra	Dentary	Premaxilla	Maxilla	Vomer	Pterygoid	Tooth-bearing*		
Albanerpeton galaktion	–	–	–	1	1	1	–	–	–	3	0.15
Albanerpeton nexuosum	–	–	–	1	2	2	–	–	–	5	0.25
Proamphiuma cretacea	–	2	–	–	–	–	–	–	–	2	0.10
Opisthotriton kayi	72	986	7	95	5	9	15	2	–	1191	58.93
Prodesmodon copei	2	3	–	–	–	–	–	–	–	5	0.25
Proteidae gen. et sp. nov.	28	–	–	–	–	–	–	–	–	28	1.39
Lisserpeton bairdi	87	17	–	1	2	–	–	–	–	107	5.29
Piceoerpeton sp. A	9	7	–	–	–	–	–	–	–	16	0.79
Scapherpeton tectum	94	333	–	60	5	11	–	–	3	506	25.04
Scapherpetontidae gen. et sp. A	–	5	–	–	–	–	–	–	–	5	0.25
Habrosaurus dilatus	1	18	–	95	19	1	8	–	3	145	7.17
Habrosaurus prodilatus	–	–	–	3	1	2	1	–	1	8	0.40
Total (n)**	293	1371	7	256	35	26	24	2	7	2021	–
% total (n) ††	14.50	67.84	0.35	12.67	1.73	1.29	1.19	0.10	0.35	–	100.00

*Refers to a fragmentary tooth-bearing element that is not identifiable to a specific tooth-bearing bone (e.g., dentary).

†Total number (n) of specimens per taxon.

§Percent total number (n) of specimens per taxon.

**Total number (n) of specimens per element across all taxa.

††Percent total number (n) of specimens per element across all taxa.

TABLE 2.3. MEASURE OF MODEL FIT FOR RELATIVE ABUNDANCE DISTRIBUTIONS (RADS) FOR SIX WELL-SAMPLED CAUDATE AND ALLOCAUDATE ASSEMBLAGES FROM THE HELL CREEK FORMATION (LANCIAN) AND LOWERMOST TULLOCK MEMBER (PU1) OF GARFIELD COUNTY, NORTHEASTERN MONTANA.

Institution	Loc. no.	S	N	RAD Model AIC*				
				Broken-stick	Log-normal	Geometric	Zipf	Zipf-Mandelbrot
UCMP	V99220	7	164	67.20	42.16	44.93	**41.42**	43.08
UCMP	V99369	8	161	72.58	47.62	**38.81**	58.22	42.80
UWBM	C1153	11	235	299.02	68.37	119.21	**52.05**	54.05
DMNH	3302, 3304 3305, 3327	7	138	55.60	39.36	44.65	**36.89**	38.89
UCMP	V73085 V73087	7	255	200.97	41.80	**35.97**	47.63	38.08
UCMP	V74111	5	530	437.16	64.53	88.05	**46.15**	48.15

Note: Loc. no. = locality number; S = raw species richness; N = number of individual specimens.

*AIC = Akaike's information criterion. The best fit model (bold) per assemblage was determined by the lowest AIC value.

CHAPTER 3:

SQUAMATE TURNOVER AND EXTINCTIONS LEADING UP TO AND ACROSS THE CRETACEOUS-PALEOGENE BOUNDARY IN NORTHEASTERN MONTANA, USA

ABSTRACT

The Cretaceous-Paleogene (K-Pg) mass extinction led to a major decline in squamate (lizards, snakes) richness across the K-Pg boundary. However, the timing and pattern of those extinctions remain poorly resolved. To more precisely determine the timing and magnitude of squamate turnover and extinctions leading up to and across the K-Pg boundary, I examined nonmarine squamate diversity dynamics (richness, taxonomic composition, turnover) on the basis of specimens derived from 45 temporally constrained vertebrate microfossil localities (39 stratigraphic horizons) that span most of the Hell Creek and overlying Tullock formations in Garfield County, northeastern Montana, USA. The sample contains 200 specimens diagnostic at the genus or species level, from which I recognize 33 distinct taxa (31 lizards, 2 snakes). Twelve taxa represent previously undescribed species of scincomorphs and anguimorphs from the Hell Creek Formation including an indeterminate iguanomorph. Six Hell Creek taxa represent new paleobiogeographic and/or temporal records of known taxa. Combined, these new records place the Hell Creek Formation as the taxonomically richest squamate assemblage known from the latest Cretaceous of North America accounting for 30 of the 44 diagnosable or potentially diagnosable species. Biostratigraphic occurrences revealed a doubling in range through species richness (six to twelve species) from the lower half of the Hell Creek Formation. Species richness remained relatively stable (average = 11 species) throughout much of the remaining thickness of the Hell Creek Formation with a peak richness value of 13 species in the middle of the unit. Though eight species range through most of the Hell Creek Formation, substantial turnover occurred in the formation. A loss in monocuspid and fang-like tooth morphologies in

squamates is coincident with taxonomic turnover in chamopsiids and platynotans, respectively, from the lower to upper halves of the Hell Creek Formation.

Within the uppermost ~15 m of the Hell Creek Formation, range through and raw species richnesses sharply declined as per-capita and proportional rates of disappearances increased leading up to the K-Pg boundary. Eighty-one percent of squamate species from that stratigraphic interval went extinct across the K-Pg boundary. Most borioteiioids (Chamopsiidae + Polyglyphanodontini) and all platynotans (e.g., *Paraderma bogerti*, *Palaeosaniwa* sp.) were extinguished at or near the K-Pg boundary; the occurrences of two indeterminate chamopsiids low in the Tullock Formation represent the first known survivors of that clade. The Contogeniidae, Xenosauridae, and Anguidae each had a single species cross the K-Pg boundary. These higher-level extinction patterns support previous reports and improve the temporal resolution of squamate species turnover and extinctions leading up to and during the end-Cretaceous mass extinction. These results strongly resemble the timing and/or magnitude of extinctions observed among other aspects of the local vertebrate fauna (e.g., lissamphibians, mammals).

INTRODUCTION

Documentation of nonmarine vertebrate extinctions during the Cretaceous-Paleogene (K-Pg) mass extinction is largely based on the continental fossil record from the Western Interior of North America (see reviews by Archibald 1996, 2011). At least a dozen Maastrichtian and Paleocene age geologic formations are known to preserve fossil squamates (see Nydam 2013: table 1 and references therein). Here I focus on the Hell Creek Formation and the overlying Tullock Formation, which together are the best-studied nonmarine units for understanding K-Pg patterns of extinction and recovery (Archibald 1996, 2011; Clemens 2002; Wilson et al. 2014a; Fastovsky and Bercovici 2015) and which continue to yield important chronostratigraphic, geochemical, sedimentological, and paleontological data (e.g., Renne et al. 2013; Sprain et al. 2015; Tobin et al. 2014; Wilson et al. 2014a and papers therein) for improving our understanding of the K-Pg event.

Terrestrial squamate diversity dynamics leading up to and across the K-Pg boundary are poorly resolved relative to other small tetrapods in my study area of northeastern Montana (Garfield and McCone counties) and throughout the Western Interior of North America (e.g., mammals: Wilson 2005, 2014; caudates and allocaudates: Wilson et al. 2014b; *Chapter Two*). Most early studies of latest Cretaceous and early Paleocene nonmarine squamates of North America centered principally on their systematics (e.g., Estes 1964, 1969a, b, 1975, 1976, 1983; Estes et al. 1969; Estes and Berberian 1970). Those studies provided the systematic foundation for fossil squamate identifications and subsequent determination of squamate extinction patterns across the K-Pg boundary (e.g., Sullivan 1987; Bryant 1989). More recent systematic and phylogenetic work has added a plethora of new fossil squamates to the known record from the

Late Cretaceous and Paleocene of North America (e.g., Denton and O'Neill 1995; Gao and Fox 1996; Nydam et al. 2000; Nydam and Cifelli 2005; Nydam and Voci 2007; Nydam et al. 2007, 2010, 2013a; Nydam and Fitzpatrick 2009; Longrich et al. 2012b; DeMar and Wilson 2013; DeMar et al. 2015; see Nydam 2013b and references therein for a comprehensive review). The work presented here draws from these studies and adds to the rich and growing squamate fossil record of North America. My systematic work (see Appendix to *Chapter Three*) provides the basis for some of the raw data presented herein for documenting terrestrial squamate diversity patterns leading up to and across the K-Pg boundary in northeastern Montana.

Past studies of squamate extinctions across the K-Pg boundary relied largely upon presence/absence data from specimens found above or below the K-Pg boundary or both. For example, Archibald and Bryant (1990) documented formational-level patterns of non-dinosaurian and non-mammalian vertebrate extinctions, including squamates, across the K-Pg boundary based on specimens housed in the collections at the University of California Museum of Paleontology (UCMP). More recent analyses of entire vertebrate faunas from within a biostratigraphically constrained framework leading up to (Pearson et al. 2002) and across the K-Pg boundary (Lillegraven and Eberle 1999) have shown more precisely when squamate extinctions may have occurred. Pearson et al. (2002) documented 134 lepidosaurian (lizard) specimens from 16 vertebrate microfossil localities (13 horizons) in the Hell Creek Formation of southwestern North Dakota. Unfortunately, all of the specimens (isolated vertebrae) could not be identified below the level of Lepidosauria indeterminate (family, genus, or species). Snakes were not recorded in their study. Nevertheless, squamates were shown to occur from near the base of the Hell Creek Formation from 81.5 m to 4.15 m below the K-Pg boundary with the highest concentration of squamate-bearing localities recorded within the upper third in their local

section. Lillegraven and Eberle (1990) conducted a similar study of the biostratigraphic distributions of vertebrates from the uppermost Cretaceous and lowermost Paleocene deposits of the Ferris Formation, southeastern Wyoming. Among the squamates, only the chamopsiid *Leptochamops denticulatus*, the anguid *Odaxosaurus piger*, and several indeterminate squamates were documented. *L. denticulatus* was shown to occur in the Cretaceous portion of the Ferris Formation and to within 15 m below the "zone of uncertainty" (~K-Pg boundary). *O. piger* and the indeterminate squamates spanned the "zone of uncertainty" with the latter taxa ranging to the top of the studied interval and into the Puercan 3 North American Land Mammal Age.

Longrich et al. (2012b) conducted the most recent investigation of squamate extinctions across the K-Pg boundary. Their combined dataset included published squamate records and museum-based observations of specimens collected across several geologic formations of the Western Interior of North America (Utah to Alberta). They recorded a total of 30 latest Cretaceous (Maastrichtian) squamate species. With an estimated temporal range for each taxon, they calculated species-level extinctions across the K-Pg boundary. They recorded an 83% extinction rate and claimed that those extinctions were coincident with the Chicxulub bolide impact at the K-Pg boundary. Although Longrich et al.'s study benefited from regional sampling, limited sample sizes (one recorded occurrence per geologic unit or locality) and relatively low temporal resolution (taxon occurrences binned between ≤200 kyr to >2.5 myr before K-Pg boundary; their table S2) likely led to inflated and concentrated levels of extinction at the K-Pg boundary and coincident with the bolide impact..

With the aim of reinvestigating the timing and pattern of squamate extinctions leading up to and across the K-Pg boundary, I documented high-resolution biostratigraphic occurrences of latest Cretaceous and early Paleocene squamates based largely on a new and unstudied collection

of specimens from the Hell Creek and Tullock formations of northeastern Montana, USA. Species richness, taxonomic composition, and turnover were calculated through the section. Results revealed considerable turnover throughout the Hell Creek Formation with increasing disappearance rates approaching the K-Pg boundary. Moderate turnover and compositional differences in the squamate faunas with a concurrent loss of tooth types from the lower and upper halves of the Hell Creek Formation suggests that not all squamate species from the Hell Creek Formation were victims of the Cretaceous-Paleogene mass extinction.

Institutional Abbreviations

BMRP—Burpee Museum of Natural History, Rockford, Illinois, USA

DMNH—Denver Museum of Nature and Science (formerly the Denver Museum of Natural History), Denver, Colorado, USA

MOR—Museum of the Rockies, Montana State University, Bozeman, Montana, USA

UALVP—University of Alberta Laboratory for Vertebrate Paleontology, Edmonton, Alberta, Canada

UCMP—University of California Museum of Paleontology, Berkeley, California, USA

UWBM—University of Washington Burke Museum, Seattle, Washington, USA

Other Abbreviations

K-Pg—Cretaceous-Paleogene; La—Lancian NALMA; NALMA—North American Land Mammal Age; Pu—Puercan NALMA; SVL—snout-vent length; To—Torrejonian NALMA.

MATERIALS and METHODS

Fossil Squamate Database

Terrestrial squamate specimens used in this study include screenwashed jaws, cranial elements, vertebrae, and osteoderms. A smaller sample of surface collected material also was included. The specimens derive from the upper Cretaceous (Maastrichtian) Hell Creek Formation and the overlying lower Paleocene (Danian) Tullock Formation (referred to as a member of the Fort Union Formation by some authors; see Clemens 2002 for an explanation) of Garfield County, northeastern Montana, USA (Fig. 3.1). These specimens are curated into the collections at the UCMP, UWBM, MOR, and DMNH, and most were collected by crews led by Dr. William A. Clemens (UCMP), Dr. Gregory P. Wilson (UCMP, DMNH, and UWBM), and, more recently, me (UWBM). Except where noted, I only included specimens identifiable to the species level and from localities placed within the detailed stratigraphic framework assembled by previous authors (e.g., Archibald 1982; Clemens 2002; Wilson 2005, 2014; Wilson et al. 2014b; *Chapter Two*).

Among a total of nearly 600 squamate specimens, 200 were identifiable to species. Twenty-seven of those specimens were previously described (Balsai 2001; Nydam et al. 2000; Nydam and Fitzpatrick 2009; Longrich et al. 2012b) or were voucher specimens in other studies (Bryant 1989; Archibald and Bryant 1990; Longrich et al. 2012b). I identified and described the other 174 specimens (e.g., see Appendix to *Chapter Three*). Of the 200 specimens, 162 are from 37 localities (33 horizons) of the Hell Creek Formation and 38 specimens are from eight Tullock Formation localities (six horizons). Squamates span ~74 m of the ~89.5-m-thickness of the Hell Creek Formation. Specimens from the Tullock Formation occur at fewer localities throughout

the ~80-m-thick formation (Pu1–To1; thickness based on Sprain et al. 2015, fig. 6). I consider specimens from two Flat Creek area localities (UCMP loc. V73087 [Flat Creek 5] and UWBM loc. C1505 [Flat Creek Cimo]) as part of the same local fauna because the localities are at the same stratigraphic level and in close proximity to one another (<50 m) (cf. Archibald 1982; Wilson et al. 2014b; *Chapter Two*). I refer to specimens from UCMP localities V72128, V72129, and V73080 within the thick Garbani Channel complex of the Tullock Formation collectively as the Garbani local fauna (sensu Clemens 2002; Clemens and Wilson 2004, fig. 2).

I use the higher-level systematics of squamates that is based principally on studies by Conrad (2008), Nydam et al. (2007), Nydam et al. (2010), and Nydam (2013b). The taxonomic framework is listed in Table 1. Following Nydam (2013b), I use the Borioteiioidea (sensu Nydam et al. 2007) to refer to the North American radiation of teiid-like lizards that comprise Chamopsiidae (sensu Nydam et al. 2010) and Polyglyphanodontini (sensu Nydam et al. 2007). I did not adopt the Polyglyphanodontia (sensu Gauthier et al. 2012) because it is based solely on Late Cretaceous taxa from Asia except for *Polyglyphanodon sternbergi* from the Maastrichtian of Utah (Gilmore 1942a). Descriptions and diagnoses of known North American Late Cretaceous and early Paleocene squamates can be found in the literature. See Estes (1983) and Nydam (2013b) for broad taxonomic overviews and the following references for each genus relevant to this study: *Chamops segnis*, *Leptochamops denticulatus*, *Meniscognathus altmani*, and *Haptosphenus placodon* (Estes 1964; Gao and Fox 1996), *Leptochamops thrinax* (Gao and Fox 1991, 1996), *Socognathus unicuspis* (Gao and Fox 1991, 1996; Nydam et al. 2010), *Socognathus brachyodon* (Longrich et al. 2012b), *Peneteius aquilonius* (Estes 1969a; Nydam et al. 2000), *Contogenys sloani* (Estes 1969b; Gao and Fox 1996; Nydam and Fitzpatrick 2009), *Odaxosaurus piger* (Gilmore 1928; Estes 1964; Gao and Fox 1996), *Odaxosaurus priscus* (Gao and Fox 1996),

cf. *Gerrhonotus* sp. (Estes 1964), *Proxestops jepseni* (Gilmore 1942b; Gauthier 1982; = *P. silberlingii* of Sullivan 1991), *Machaerosaurus torrejonensis* (Gilmore 1928; Sullivan 1982, 1991), *Exostinus lancensis* (Gilmore 1928; Estes 1964; Gao and Fox 1996), *Parasaniwa wyomingensis* (Gilmore 1928; Estes 1964; Gao and Fox 1996), *Paraderma bogerti* (Estes 1964; Pregill et al. 1986; Gao and Fox 1996), *Palaeosaniwa canadensis* (Gilmore 1928; Estes 1964; Gao and Fox 1996; Balsai 2001), *Labrodioctes montanensis* (Gao and Fox 1996; see Balsai 2001 for possible synonymy with *Palaeosaniwa canadensis*), *Cemeterius monstrosus* (Longrich et al. 2012b), *Coniophis precedens* (Marsh 1892; Rage 1984; Holman 2000; Longrich et al. 2012a; Caldwell et al. 2015: table 2), and *Cerberophis robustus* (Longrich et al. 2012b; = Boidae indet. of Bryant 1989).

In this study, I recognized one indeterminate iguanomorph and eleven new and diagnosable scincomorphs and anguimorphs (see bold taxa in Table 3.1) and figured, described, and discussed them in the Appendix to *Chapter Three*. I used morphological and dental terminology and modes of tooth implantation from Gao and Fox (1996). I proposed holotypes for most of these taxa. Formal descriptions and erection of new taxa will appear elsewhere.

Voucher specimens of known taxa are listed and figured in the Appendix to *Chapter Three*. None of these specimens previously has been figured, although one (UCMP V130723) is a voucher specimen of Bryant (1989, p. 48; *Palaeosaniwa* sp., Appendix to *Chapter Three*, Fig. A3.16K–L). I dusted all specimens with magnesium under a fume hood (except UCMP V130723), and photographed and measured each specimen in multiple views using a LEICA MZ95 microscope and Clemex Captiva software (v. 7.0.700).

I identified each specimen to species principally on the basis of characters from maxillae, dentaries, and vertebrae. In general, a combination of tooth and jaw morphology is necessary for

species-level identifications of Late Cretaceous and Paleocene squamates. For many worn and fragmentary jaw specimens, only higher-level identifications were possible (e.g., Anguimorpha: Anguidae; Scincomorpha: Chamopsiidae); in turn, they were excluded from the analyses. I included cranial elements or osteoderms in the analyses, if the ornamentation was similar to that of identifiable maxillae (e.g., Platynota gen. et sp. undetermined C; see below). Premaxillae, frontals, parietals, jugals, pterygoids, ilia, a femur, and osteoderms were excluded from the analyses because of the uncertainty surrounding their taxonomic identities.

Osteoderms referred to *Odaxosaurus piger* (e.g., Estes 1964) are abundant throughout the Hell Creek and Tullock formations in the study area (e.g., see Appendix to *Chapter Three*, Fig. A3.14K–L). Referral of those elements to *O. piger* is considered tentative by some authors (Armstrong-Ziegler 1980; Gao and Fox 1996; Nydam 2013a, b) because osteoderms have not been found in direct association with taxonomically identifiable jaws of *O. piger* (in contrast with the geologically younger *Glyptosaurus sylvestris* from the Eocene of Wyoming; Sullivan 1986). Furthermore, *Gerrhonotus*-like taxa (e.g., cf. *Gerrhonotus* sp. of Estes 1964) that presumably have osteoderms commonly co-occur with *O. piger* in multiple upper Cretaceous units (e.g., Lance, Hell Creek, and Fruitland formations: Estes 1964; Bryant 1989; Armstrong-Ziegler 1980, respectively) and, thus, the osteoderms cannot confidently be referred to *O. piger*. The presence of an undetermined anguid and gerrhonotine in the study area (e.g., Table 3.1 and Appendix to *Chapter Three*) further prohibits assigning the osteoderms to *O. piger*. For these reasons, the isolated osteoderms here are referred only to Anguidae indet. I excluded the anguid osteoderms from the species-level stratigraphic distributions though they are useful at the family level. In contrast, the osteoderms referred to Platynota gen. et sp. undetermined C (Fig. A3.8I–J) were used for species-level stratigraphic occurrences because their unique and easily identifiable

nodose ornamentation allows them to be associated with the more diagnostically informative maxilla (Fig. A3.8A–D) of that taxon. A number of non-anguid anguimorph osteoderms similar to those identified by Nydam et al. (2013, fig. 9n–o) and Brinkman (2002, p. 89, f–h) from other upper Cretaceous units (e.g., Aguja and Dinosaur Park formations, respectively) also occur in the Hell Creek Formation, but I did not include them in my analyses as their taxonomic affinities are not well understood.

Chronostratigraphic Framework

I updated the previous chronostratigraphic framework for the study area (see Wilson 2005, 2014) with new stratigraphic placements of the paleomagnetic chron boundaries (LeCain et al. 2014) and new high-resolution $^{40}Ar/^{39}Ar$ age determinations for a tuff associated with the K-Pg boundary (Renne et al. 2013) and tuffs associated with superpositional lignite beds in the Hell Creek and Tullock formations (i.e., Null, IrZ, Z, MCZ, HFZ, Y, X, W, V, and U coals; see Sprain et al. 2015 and references therein). These new age determinations make it possible to more precisely determine the timing of faunal turnover during the study interval and to better address the competing hypotheses of the K-Pg mass extinction and the ensuing recovery phase. The updated age for the base of the Hell Creek Formation (~68.0 Ma.) is based on the ~1.93 m.y. depositional duration of the Hell Creek Formation derived from estimated sedimentation rates of the formation (see Wilson 2014 for details).

North American Land Mammal ages (NALMAs) are based on first, last, and unique biostratigraphic occurrences of fossil mammals in the Western Interior of North America (Lillegraven and McKenna 1986; Cifelli et al. 2004; Lofgren et al. 2004). Three NALMAs occur in the study interval: the Lancian (La) NALMA (latest Maastrichtian) and the Puercan (Pu) and

Torrejonian (To) NALMAs (earliest Paleocene). Although the Lancian and Puercan boundary may not exactly coincide with the K-Pg boundary (see Fox 1989; Lofgren et al. 2004), these units allow temporal correlations with other Latest Cretaceous and early Paleocene fossil assemblages throughout the Western Interior. The Puercan and Torrejonian NALMAs are each subdivided into three interval zones (Pu1–3 and To1–3, respectively). Locally, the Pu2 has not been recognized (e.g., Lofgren et al. 2004) and only the first Torrejonian subzone (To1) is represented in the study interval. The Puercan and Torrejonian boundaries in Figures 3.2–3.6 are placed according to Sprain et al. (2015, fig. 6).

Updates to the study system also include the addition of six recently discovered squamate-bearing localities analyzed here. Five of these localities are from the Hell Creek Formation (UWBM locs. C1191 [Turtle Cove], C1401 [Impossible Ridge], C1492 [Lizard Flats], C1672 [Kafir = MOR HC-800], and C1957 [How's the View? = MOR HC-1105]) and one is from the Tullock Formation (UWBM C1912 [Stonehenge = MOR FU-1040]). I placed these localities into the local composite section on the basis of high-accuracy (≤0.30 m) elevational data obtained using a Trimble 2008 GeoExplorer XH GPS unit at each locality and the geographically nearest formational contact (Fox Hills-Hell Creek or Hell Creek-Tullock; Wilson 2014). I used lithological descriptions of the Fox Hills-Hell Creek formational contact by Jensen and Varnes (1964) and those of the Hell Creek-Tullock formational contact by Moore et al. (2014 and references therein; see also Tobin et al. 2014). Although the Hell Creek-Tullock contact is diachronous from west to east (see Clemens 2002), it is closely associated with an impact claystone that marks the K-Pg boundary in the central part of the study area (e.g., Flag Butte; Moore et al. 2014). As such, stratigraphic positions of all localities are reported in meters above or below the K-Pg boundary.

Here I subdivide the Hell Creek Formation into two informal stratigraphic intervals to allow for ease of discussion of the squamate assemblages leading up to the K-Pg boundary. The lower half is bounded by some of the best-sampled localities in the section including Tuma (−74.1 m) and Hartless (−41.2 m), whereas the upper half of the Hell Creek Formation is bounded by Hauso 1 and Flat Creek 5 (−6.3 and −5.2 m, respectively) just below the K-Pg boundary. Squamate faunas from the lower and upper halves of the Hell Creek Formation correspond to the "La1" and "La2" mammalian faunas of Wilson (2014). Squamate turnover through the Tullock Formation is discussed relative to the Pu1–3 and To1 NALMA subintervals.

Due to the relatively small sample sizes per locality (i.e., most have fewer than 10 specimens), specimens were summed per 10-m-bin to demonstrate the overall level of sampling through the Hell Creek and Tullock formations (Fig. 3.1). Bin sizes and their stratigraphic placements follow Wilson (2014) and Wilson et al. (2014b; *Chapter Two*). An average of 23 squamate specimens per each of the seven 10-m-bins of the Hell Creek Formation was calculated. The stratigraphically lowest Tullock Formation locality (UCMP loc. V74111) of the study area has produced more than 500 salamander (Wilson et al. 2014b; *Chapter Two*) and nearly 900 mammal specimens (Wilson 2014), but has produced only a few indeterminate squamate fossils. Only two other lower Tullock Formation localities (UCMP locs. V74110 and V77087) have produced squamate specimens of interest (i.e., two indeterminate chamopsiids). An average of 6.3 specimens per each of the six 10-m-bins of the Tullock Formation was calculated. These low sample sizes, particularly from the Tullock Formation, are likely due to poor squamate preservation and the uncertainty of associations between diagnostic and putatively referred specimens (e.g., holotype dentary of *Odaxosaurus piger* to referred osteoderms). As a result of these fossil preservation issues, I do not use quantitative measures of

diversity that are particularly sensitive to small samples sizes, including heterogeneity indices (e.g., evenness, Simpson's Diversity Index) and relative abundance distributions. These were used by Wilson (2014) and Wilson et al. (2014b; *Chapter Two*) for their studies on mammals and caudates and allocaudates, respectively. Nevertheless, the database assembled for this study is the largest of its kind to date and allows me to document species richness, taxonomic composition, and turnover leading up to and across the K-Pg boundary.

Taxonomic Richness

Squamate richness was calculated as the raw number of species per locality and as standing species richness (i.e., number of species that first appear or last appear in a stratigraphic horizon plus those that range through the horizon). The per-locality stratigraphic resolution follows Wilson (2014) and Wilson et al. (2014b) and allowed for ease of stratigraphic and temporal correlations to be made with the local mammalian and lissamphibian assemblages, respectively. Fourteen singleton taxa (i.e., taxa that only occur at a single locality or horizon) are excluded from the standing species richness estimates but are included in Figure 3.3 (see stars) for completeness. To account for the occurrence of an indeterminate species of *Socognathus* at −41.2 m (Fig. A3.13M–P), I added one species to each standing species richness estimate for the eight stratigraphic horizons occurring between −59 m (last known occurrences of *S. unicuspis* and *S. brachyodon*) and −41.2 m.

To document higher-level taxonomic richness of squamates leading up to and across the K-Pg boundary, I calculated proportional range-through abundances per stratigraphic horizon for each of the six major taxonomic groups. Singleton occurrences of higher-level taxa (e.g., Iguanomorpha) were excluded. These abundances were calculated for each stratigraphic horizon as the number of species per major taxonomic group divided by the total number species present or range through, multiplied by 100. I tallied proportional abundances for the Borioteiioidea (Chamopsiidae + Polyglyphanodontini), Contogeniidae, Xenosauridae, Anguidae, Platynota, and Serpentes. These data offer a broader perspective of taxonomic turnover.

Taxonomic Composition and Turnover

I assembled biostratigraphic occurrences and ranges for all squamate species through the Hell Creek and Tullock formations. Confidence intervals (CI) at the 50% and 95% levels were estimated above and below the end points of all taxa possessing multiple stratigraphic occurrences using two one-tailed calculations. This methodology follows that of Wilson (2014) and Wilson et al. (2014b; *Chapter Two*), which is a version of the Strauss and Sadler (1989) method modified by Wilf and Johnson (2004) to include "fossil recovery potential functions" (FRFPs; Marshall 1997). The total number of specimens and the distribution of fossil localities affect the upper and lower bounds of each CI such that more densely sampled taxa in better sampled intervals will have smaller confidence intervals. Some taxa have CIs extending beyond the stratigraphic limits of the study area, a likely consequence of low sample sizes (e.g., in Pu1 interval). See Wilson (2014) and references therein for a more thorough discussion of this methodology.

Squamate turnover leading up to the K-Pg boundary was calculated from the biostratigraphic ranges of taxa per 5-m-bin of the Hell Creek Formation for both true and range-through occurrences per Wilson (2014) and Wilson et al. (2014b; *Chapter Two*). Range-through edge effects (see Foote 2000) artificially inflate appearance and disappearance rates at the top and bottom of the observed stratigraphic interval and, unlike the well-sampled lissamphibian and mammalian assemblages (Wilson 2014; Wilson et al. 2014b; *Chapter Two*), these edge effects occur here due to the low sample sizes.

Per-taxon and proportional turnover rates were calculated at the species level (Foote 2000) per 5-m bin. The duration of each bin is assumed to be uniform and represents ~108 k.y. Singletons are excluded. As in Wilson (2014) and Wilson et al. (2014b; *Chapter Two*), estimated per-capita turnover rates were calculated according to Foote (2000).

RESULTS

Taxonomic Richness

Raw species richness varies throughout the stratigraphic interval (Fig. 3.3). Peak raw richness occurs at the Hartless (n = 10 species; N = 37 specimens; −41.2 m) and CMM (n = 8 + 3 singletons; N = 20; −59 m) localities in the lower half of the Hell Creek Formation. These values are slightly higher than those from the upper half (e.g., Bryant 1989; Archibald and Bryant 1990), such as Hauso 1 (n = 8 + 1 singleton; N = 18; −6.3 m) and Flat Creek 5 (n = 5 + 1 singleton; N = 12; −5.2 m) near the K-Pg boundary. The stratigraphically lowest locality in the section, Tuma (−76.4 m), has a total of six taxa with an additional three singletons (N = 15 specimens). All other localities have four or fewer raw taxa with a few localities also containing

or represented exclusively by a singleton. Standing species richness abruptly doubles from six species near the base of the Hell Creek Formation (−76.4 m; Tuma) to 12 species at −59 m (CMM + JPC). From there, a small decrease in standing richness occurs before reaching a peak richness value of 13 species near the middle of the formation (−41.2 m; Hartless). Standing richness remains elevated between 11 and 12 species for the succeeding ~26 m in the upper half of the Hell Creek Formation. Following this zone of peak standing richness, the number of taxa sharply declines in the upper ~15 m of the Hell Creek Formation and across the K-Pg boundary into the lowermost Tullock Formation. Peak richness values (raw and standing) in the Tullock Formation (three and four taxa, respectively) are approximately one-third of those in the Hell Creek Formation and remain depressed throughout the Puercan (Pu1–3) and early Torrejonian (To1; not shown) NALMAs.

Among the higher-level taxa, borioteiioids (Chamopsiidae + Polyglyphanodontini) and platynotan lizards are the most species rich in the Hell Creek Formation. Excluding singletons, these two groups proportionately make up the entire squamate assemblage (66.7% and 33.3%, respectively) in the lowermost ~9.4 m of the study interval (−76.4 to −67 m). Proportional taxonomic richness remains high for those groups, 28.6% to 66.7% (average value = 42.3%) for borioteiioids and 25.0% to 55.6% (average value = 35.6%) for platynotans across their known biostratigraphic ranges. Anguids and xenosaurids, both represented by a single range-through taxon (*Odaxosaurus piger* and *Exostinus lancensis*, respectively) appear in the lower half of the Hell Creek Formation and maintain fairly constant but relatively low proportional richnesses (average values = 10.6% and 10.4%, respectively) throughout their biostratigraphic ranges in that unit. Snakes (*Coniophis precedens*, *Cerberophis robustus*) first appear in the middle of the Hell Creek Formation at −41.2 m. They also maintain a relatively low average proportional richness

(11.4%), but it peaks at 16.7% where the two snakes are known to overlap biostratigraphically (−18 m to −15.1 m). The Contogeniidae is the last to appear in the Hell Creek Formation at −6.3 m and is represented by the lone species *Contogenys sloani*. Range-through proportional richnesses for this taxon begin at 10% and peak at 25% as the more species-rich clades begin to fade out within the uppermost Hell Creek Formation. Above the K-Pg boundary contogeniids, xenosaurids, and anguids taxonomically predominate the Tullock Formation. Contogeniids and xenosaurids both have average richness values at 30.6%; whereas anguids have an average of 63.3% with peak richness at 100% at the To1 locality (Horsethief Canyon) in the uppermost Tullock Formation.

Taxonomic Composition

Thirty-three squamate species occur within the stratigraphic interval including one indeterminate iguanomorph, 16 scincomorphs, and 16 anguimorphs (Fig. 3.4). Among Hell Creek Formation scincomorphs, the chamopsiids *Chamops segnis* and *Meniscognathus altmani* (Fig. A3.10A–J), have the greatest stratigraphic ranges and occur at more localities than all other scincomorphs. *M. altmani* previously was unknown from the study area (Bryant 1989; Longrich et al. 2012b), but here is shown to occur at seven localities. Among the anguimorphs, the platynotan lizards *Parasaniwa wyomingensis*, *Paraderma bogerti*, *Palaeosaniwa* sp., and Platynota gen. et sp. undet. C (Figs. A3.16 and A3.8, respectively), range through more than half of the thickness of the Hell Creek Formation. Only three taxa, namely the scincomorph *Contogenys sloani* (Contogeniidae; cf. Fig. A3.18) and the anguimorphs *Exostinus lancensis* (Xenosauridae; Fig. A3.15) and *Odaxosaurus piger* (Anguidae; Fig. A3.14), span the K-Pg boundary and range to the middle of the Tullock Formation (Pu3 NALMA). The lower 50% CI

of *C. sloani* indicates that its range in the Hell Creek Formation is likely restricted to the upper half of the unit.

The remaining squamates appear to have more restricted biostratigraphic ranges, perhaps as a consequence of low sample sizes. The polyglyphanodontine *Peneteius aquilonius* and the chamopsiids *Leptochamops denticulatus* and *Haptosphenus placodon* have ranges restricted to portions of the upper half of the Hell Creek Formation. The 50% CIs of these taxa suggest they range into the lower half of the Hell Creek Formation with that of *L. denticulatus* reaching the base. Similarly, the two snakes of the Hell Creek Formation, *Coniophis precedens* (Fig. A3.9F–I) and *Cerberophis robustus* (Fig. A3.9A–E), have ranges restricted to the upper half or less of the formation. Here, *C. precedens* makes its first appearance in the study area in the form of isolated vertebrae. *C. precedens* likely extends into the lower half based on its 50% CIs; whereas *C. robustus* is limited to the upper third. The 95% CI of *C. robustus* pushes its range down into the lower half (–59 m). All other taxa have 95% CIs that stretch beyond the lower and upper stratigraphic limits of the study interval. *Contogenys sloani* occurs at 6.3 m and 5.2 m below the K-Pg boundary (contra Longrich et al. 2012b; see discussion in Appendix to *Chapter Three* listed under vouchers specimens). Its lower 50% CI extends to near the middle of the Hell Creek Formation. Four singletons also are restricted to the upper Hell Creek Formation, two of which are undetermined new taxa (?Chamopsiidae gen. et sp. undet., Anguidae gen. et sp. undet.; Figs. A3.3I–L and A3.5, respectively). The remaining two singletons, *Obamadon gracilis* (Longrich et al. 2012b) and *Colpodontosaurus cracens* (Fig. A3.16A–D), are known only from a single locality in the upper half of the formation. *C. cracens* previously was unknown from the study area (Bryant 1989; Longrich et al. 2012b). Biostratigraphic range CIs could not be determined for any of these or the other singleton taxa.

Among the taxa restricted to the lower half of the Hell Creek Formation (including singletons) are those that largely represent novel taxa including Chamopsiidae gen. et sp. undet. A, B, C, and D (Figs. A3.2 and A3.3A–H), Gerrhonotinae gen. et sp. undet. (Fig. A3.6), Platynota gen. et sp. undet. A and B (Fig. A3.7), and Scincomorpha gen. et sp. undet. (Fig. A3.4; see below for likely higher stratigraphic range). The lone indeterminate iguanomorph (Fig. A3.1) occurs at the stratigraphically lowest locality in the section (−76.4 m). *Socognathus brachyodon* (Fig. A3.13A–D), a recently described chamopsiid from the Lance Formation of Wyoming (Longrich et al. 2012b), makes its first appearance in the Hell Creek Formation and occurs at a single lower Hell Creek locality (−59 m). Its congener, *Socognathus unicuspis* (Fig. A3.13G–L), previously was only known from older Judithian-age deposits of central and southern Alberta, Canada (Gao and Fox 1991, 1996; Peng et al. 2001; Nydam et al. 2010); it occurs between −76.4 m and −59 m of the Hell Creek Formation, but with a 50% CI stretching into the middle of the formation. A similar temporal (Judithian) and paleobiogeographic (southern Alberta) distribution has been noted for *Leptochamops thrinax* (Fig. A3.12; Gao and Fox 1991, 1996), although it also is known from the late Campanian-age Mesaverde Formation of central Wyoming (DeMar and Breithaupt 2006). Here, *L. thrinax* is restricted to a narrow stratigraphic interval (−60.1 m to −59 m) in the lower half of the Hell Creek Formation. Its 50% CIs extend beyond the lower limits of the Hell Creek Formation while the upper limit reaches the middle of the unit. The occurrence of *Socognathus* sp. indet. (Fig. A3.13M–P) from the middle of the Hell Creek Formation (−41.2 m) indicates that at least one of the present species (likely *S. unicuspis* based on abundances) has a slightly higher distribution in the formation. The upper 50% CI of *S. unicuspis* corroborates that occurrence. The occurrence of *Socognathus* at the Bug Creek Anthills (BCA) locality, Hell Creek Formation, McCone County, northeastern Montana (Gao and Fox 1996; pers. obs. April,

2014) further extends the stratigraphic range even closer to the K-Pg boundary, but how much closer is uncertain as the locality represents a temporally-mixed latest Cretaceous and early Paleocene fossil assemblage (Lofgren et al. 1990). Similarly, the singleton taxon identified here as Scincomorpha gen. et sp. undet. occurring near the base of the Hell Creek Formation (−76.4 m) also occurs at BCA. That BCA occurrence is based on an undescribed and unnumbered left dentary identified as an "unnamed taxon" in the collections at the UALVP (pers. obs. April, 2014). This occurrence extends the stratigraphic range of this taxon higher in section, but again how high is ambiguous.

I also document fragmentary remains of two indeterminate chamopsiids informally referred to as the "Harley's Point chamopsiid" and the "Hell Hollow chamopsiid" (Fig. A3.17) from the lowermost Tullock Formation (Pu1 NALMA). Both specimens possess some of the diagnostic features of chamopsiid lizards, including the barrel-shaped and tri-cusped teeth with heavy basal cementum (Nydam et al. 2010; see also Estes 1964, 1983; Gao and Fox 1996 with these latter authors referring to chamopsiids as Teiidae). Differences in tooth morphology between these specimens suggest the presence of two distinct chamopsiid lizards in the early Paleocene. The "Hell Hollow chamopsiid" possibly is referable to *Meniscognathus altmani* on the basis of the lingually concave surface of the tooth; whereas the "Harley's Point chamopsiid" shows dental similarities with *Socognathus unicuspis*. *Meniscognathus altmani* ranges through most of the Hell Creek Formation as high as 4.6 m from the K-Pg boundary in the study area. The occurrence of *Socognathus* at the BCA locality demonstrates that the genus also occurs in the upper portions of the Hell Creek Formation though its upper range is less well resolved. A caveat worth noting is that the Hell Hollow Channel locality (UCMP loc. V74110) incises the top of the lower Z coal (Iridium Z [IrZ]; Sprain et al. 2015). A similar field observation by G. P.

Wilson (pers. commun.) has been made for the McKeever Ranch Harley's Point locality (UCMP loc. V77087). Both of those localities have produced Puercan 1 mammalian faunas (Archibald 1982; Clemens 2002; Wilson 2004). If these specimens have not been reworked from Cretaceous sediments, as is likely the case, then they represent the first members of Chamopsiidae to have survived the K-Pg mass extinction.

Three anguimorphs are restricted to the Pu3 NALMA interval of the Tullock Formation: *Proxestops jepseni*, cf. *Machaerosaurus torrejonensis* (Fig. A3.19), and an indeterminate platynotan (Fig. A3.20). The report of a Cretaceous occurrence of *Proxestops* is erroneous (see biostratigraphic range chart in Longrich et al., 2012b, fig. 6). Although not shown in the biostratigraphic range chart (Fig. 3.4), indeterminate anguids that are based on a dentary, maxilla, and 11 osteoderms that possibly belong to *Odaxosaurus*, *Proxestops*, or both are known from the To1 Horsethief Canyon 1 locality (UWBM loc. C1418 = UCMP loc. V73094) of the Tullock Formation. That locality is ~20 m above the Garbani Channel localities (e.g., UCMP loc. V73080; Garbani 13-NW Harley's High).

Taxonomic Turnover

Squamate turnover rates per 5-m bin are fairly substantial and vary through most of the Hell Creek Formation (Fig. 3.5). The high proportional rate of appearance (100%) at the base of the section is an artifact of the method for calculating proportional rates (Fig. 3.5B). Three moderate-sized peaks in per-capita and proportional appearance rates occur in the lower half of the formation at −62.5 m, −57.5 m, and −42.5 m. Appearances occur to within less than 10 m of the K-Pg boundary and rates are generally lower in the upper half of the formation. Squamate disappearances occur throughout most of the Hell Creek Formation. Disappearance rates are

moderate (0.31 to 0.38 per-capita; 20 to 23.1% proportional) in the lower half of the section but spike in the last two 5-m bins (−7.5 m and −2.5 m) nearest the K-Pg boundary (per-capita rates = 0.47 and 0.78, respectively; proportional rates = 36.4% and 57.1%, respectively). A single pseudoextinction of the genus *Coniophis* lowers the disappearance rate to 0 (per-capita and proportional) at −17.5 m (see multi-shaded circle in Fig. 3.5B).

Extinction Rates across the K-Pg boundary

Extinction rates across the K-Pg boundary vary depending on how many taxa are included in the extinction calculations. Four squamates appear to go extinct well in advance of the K-Pg boundary (*Leptochamops thrinax*, *Socognathus unicuspis*, Chamopsiidae gen. et sp. undet. C and D; Fig. 3.4). However, *Socognathus* is known from the stratigraphically higher BCA locality in McCone County (Gao and Fox 1996; pers. obs.) and, thus, extends its stratigraphic range closer to or beyond the K-Pg boundary. Likewise, the indeterminate scincomorph from the base of the Hell Creek Formation also is known from BCA and can be inferred to occur higher in section of the study area. The remaining 15 non-singleton taxa largely have stratigraphic ranges well into the upper portions of the Hell Creek Formation or have 50% CIs that places them close to if not above the K-Pg boundary (Platynota gen. et sp. A). Among the 17 taxa appearing in the upper Hell Creek Formation (including the inferred presence of *Socognathus* and Scincomorpha indet.), 14 appear to go extinct. This corresponds to an 82.4% extinction rate across the K-Pg boundary. Taking the single psuedoextinction of *Coniophis* into account, the extinction rate drops to 76.5%. *Coniophis* is known from the Paleocene and Eocene of North America (e.g., Estes 1976; Gardner and Cifelli 1999; Longrich et al. 2012b; Smith 2013). These rates may be underestimated as four singleton taxa (*Obamadon gracilis*,

?Chamopsiidae gen. et sp. undet., Anguidae gen. et sp. undet., *Colpodontosaurus cracens*) occurring in the upper half of the Hell Creek Formation (−28 m to −5.2 m) are not included in that estimate. When those four taxa and the inferred psuedoextinction of *Coniophis* are included, extinction estimates increase to 81% (17 out of 21 taxa). If the "Harley's Point" and "Hell Hollow" chamopsiids represent Paleocene age lizards then extinction rates drop to between 71.4% and 76.2% assuming one or both of those specimens represent pseudoextinctions of known chamopsiids from the Hell Creek Formation (e.g., *Meniscognathus* or *Socognathus*; see above).

The least conservative extinction estimate applied here is the approach of Longrich et al. (2012b), wherein all taxa occurring during the Lancian NALMA (ca. 69–66 Ma) and those from the early Paleocene are included. Using that approach, I included all taxa from within the Hell Creek Formation, which represents the last ~1.9 m.y. of the Lancian and of the Cretaceous. The extinction rate is 86.7% (26 out of 30; again accounting for the pseudoextinction of *Coniophis*). Thus, depending on how I calculated rates of extinction across the K-Pg boundary (i.e., by stratigraphic, formational, or time interval) local squamate extinctions ranged between 71.4% and 86.7%. My low estimate of 71.4% squamate extinction is similar to that presented by Bryant (1989) and Archibald and Bryant (1990) at 72.7% (8 out of 11 taxa); whereas, my high estimate at 86.7% is similar to but exceeds that of Longrich et al. (2012b) who estimated regional extinction levels at 83%. Longrich et al.'s (2012b) extinction estimate is near but greater than what I consider as the best estimate for squamate extinctions across the K-Pg boundary, which is 81%. My preferred estimate is based on the current state of the data including the newly derived stratigraphic occurrences and ranges and their 50% stratigraphic confidence intervals from the study area. However, additional sampling is needed to better resolve the timing and magnitude of

squamate extinctions across the K-Pg boundary and to ameliorate the Signor-Lipps effect (Signor and Lipps 1982).

DISCUSSION

Here, I discuss patterns of squamate temporal richnesses, biostratigraphy, turnover, and extinctions leading up to and across the K-Pg boundary in the context of previous research on this topic (e.g., Sheehan and Hansen 1986; Bryant 1989; Archibald and Bryant 1990; Sheehan and Fastovsky 1992; Archibald 1996, 2011; Longrich et al. 2012b; Nydam 2013).

Lead up to the Cretaceous-Paleogene boundary: significant turnover and distinct upper and lower Hell Creek squamate faunas

My results show that squamate assemblages underwent consistent turnover during the last ca. 1.9 m.y. of the Cretaceous in northeastern Montana. Moderate to high rates of appearances (excluding proportional rate at base of section) and disappearances are shown to occur or overlap in six and seven of the fifteen 5-m bins, respectively, throughout the Hell Creek Formation, thus indicating high species turnover. Related to the species turnover is the occurrence of distinctive lower and upper Hell Creek squamate faunas (Table 3.2). Of the 20 taxa appearing in the lower Hell Creek Formation, only 10 range into the upper half (50% decline in richness), which includes the inferred occurrences of *Socognathus unicuspis* and Scincomorpha gen. et sp. undet. from the BCA locality. Those 10 taxa from the lower portions of the Hell Creek Formation join 10 taxa currently restricted to the upper Hell Creek, which includes the local first appearances of three clades (Polyglyphanodontini, Contogeniidae, and Serpentes). The biostratigraphic turnover

between the lower and upper Hell Creek squamate faunas occurs between 59 m and 41.2 m below the Hell Creek-Tullock formational contact. For example, the first and last appearances of five species overlap in the middle of the Hell Creek Formation (−41.2 m) corresponding to ca. 300–400 k.y. before the K-Pg boundary.

The lower and upper Hell Creek squamate assemblages stratigraphically correlate to the "La1" and "La2" mammalian faunas of the study area (Wilson 2014, table 1, see also fig. 10). Wilson (2014) documented the occurrences of eight mammals (two are singletons) restricted to the lower and upper halves of the Hell Creek Formation (n = 2 and 6, respectively). A similar pattern has been documented for the caudate and allocaudate assemblages of the study area (Wilson et al. 2014b; *Chapter Two*, Fig. 2.11), wherein, among the 11 lissamphibians documented in the Hell Creek Formation, two (*Albanerpeton galaktion*, *Habrosaurus prodilatus*) are shown to have biostratigraphic ranges restricted to the lower half of the unit and one to the upper half (*Albanerpeton nexuosum*). A second salamander species, cf. *Piceoerpeton* sp. (UCMP 122039; Gardner and DeMar 2013, table 6, appendix 6), also is restricted to the upper Hell Creek Formation (UCMP loc. V78143; –9.5 m). Similar lower and upper restricted biostratigraphic ranges of other vertebrates in the study area include euselachians (sharks and rays; Cook et al. 2014, fig. 5), anurans (frogs and toads; Mercier et al. 2014), and turtles (Holroyd et al. 2014).

Although I could not account for differences in sample sizes, the overall richness pattern leading up to and across the K-Pg boundary largely mirrors that observed in the caudates and allocaudates of the study area (Wilson et al. 2014b; *Chapter Two*), wherein species richness climbed and peaked in the middle of the Hell Creek Formation (−41.2 m). However, unlike in the lissamphibians where richness values drop in a more stepwise fashion in the uppermost 20 m of the Hell Creek Formation, squamate richnesses remained elevated closer to the K-Pg

boundary as seen in the turtle (Holroyd et al. 2014) and mammal assemblages (Wilson 2014). Both squamate and mammalian assemblages show similar rates of disappearances in the two highest 5-m bins (36% and 57% versus 39% and 59%, respectively) and similar extinction rates (81% versus 75%) across the K-Pg boundary, whereas caudates and allocaudates and turtles demonstrate much lower extinction rates (22% and ~8%, respectively).

According to Wilson (2014) and Wilson et al. (2014b; *Chapter Two*), the onset of changes in taxonomic diversity and community structure in the local mammalian and caudate and allocaudate faunas began in the middle to upper third of the Hell Creek Formation, which based on the refined age estimates of the Null coal at ~30 m below the K-Pg boundary (Sprain et al. 2015), represents the last ca. 300–400 k.y. of the Cretaceous (<650 k.y. of Wilson 2014). These changes temporally overlap with a period of elevated paleotemperatures and increased atmospheric pCO_2 known as the late Maastrichtian event (LME; Li and Keller 1998; Nordt et al. 2003). Numerous lines of evidence at a local (bivalve carbonate clumped isotope paleothermometry in study area; Tobin et al. 2014), regional (e.g., leaf margin analysis of North Dakota; Wilf et al. 2003), and global (e.g., invertebrate macrofauna of the Antarctic Peninsula; Tobin et al. 2012) scale document the LME and its impact on marine and terrestrial faunas (see Wilson 2014, Wilson et al. 2014b and *Chapter Two* for a review). During that chronostratigraphic interval, decreasing richness values and increasing disappearance rates in the squamate assemblages suggest the LME may have affected these assemblages similar to the other local vertebrate assemblages (i.e., caudates and allocaudates, turtles, mammals; Holroyd et al. 2014; Wilson 2014; Wilson et al. 2014b; *Chapter Two*).

Cretaceous-Paleogene Extinction

Phylogeny and Extinction Selectivity

Eighty-one percent of squamate species occurring in the upper half of the Hell Creek Formation went extinct near or at the K-Pg boundary. The high level of species extinctions mainly corresponds to the loss of all borioteiioids and stem platynotans, a pattern previously recognized by others at both a local (northeastern Montana) and regional scale (Estes 1983; Bryant 1989; Archibald and Bryant 1990; Longrich et al. 2012b; Nydam 2013). Combined, those two groups account for 82.4% of taxa (14 out of 17) that went extinct at or near the K-Pg boundary or 66.7% of the total number of taxa in the upper third of the Hell Creek Formation (n = 21; see above for details). The local K-Pg survivors include members of the Contogeniidae, Xenosauridae, and Anguidae, which is consistent with results from other studies (Estes 1983; Sullivan 1987; Bryant 1989; Archibald and Bryant 1990; Lillegraven and Eberle 1999; Longrich et al. 2012b; Nydam 2013). The lone iguanomorph at the base of the section likely was not a victim of the K-Pg extinction. Based on the isolated occurrence of the iguanomorph *Pariguana lancensis* from the Lance Formation, it is uncertain whether or not it was a victim of the mass extinction. That taxon's type locality (Bushy Tailed Blowout [UCMP V5711]) falls within the Cretaceous part of magnetochron C29r (Wilson et al. 2010, fig. 1b) and based on the refined age estimate of the base of C29r (LeCain et al. 2014; Sprain et al. 2015) occurred within the last ~200 kyr of the Cretaceous. According to Longrich et al. (2012b), *P. lancensis* is a member of crown Iguanidae (= Pleurodonta of Conrad 2008 and others) and is sister to hoplocercids (e.g., *Morunasaurus* and *Enyaloides*), which would imply that crown iguanians survived the K-Pg mass extinction. However, a phylogenetic analysis by my colleagues and me (DeMar et al. 2015;

Chapter Five), which includes *P. lancensis* and a new stem iguanomorph known from two nearly complete skeletons from the upper Campanian of Montana, casts doubt on the crown affinities of *P. lancensis* (see Fig. 5.10). Like many other Lancian-age squamate species from North America, it was a member of a lineage that went extinct at the end of the Cretaceous. That scenario likely holds true for the other putative iguanomorphs from the Late Cretaceous of North America (see Nydam 2013b for a review of these problematic specimens) including the single indeterminate iguanomorph identified here from near the base of the Hell Creek Formation.

Early arguments regarding the severity of lizard extinctions across the K-Pg boundary were somewhat muted at higher taxonomic levels (Sullivan 1987; Bryant 1989; Archibald and Bryant 1990; Sheehan and Hansen 1986; Sheehan and Fastovsky 1992; Nydam 2002, fig. 10) because many K-Pg victims were considered members of extant families (i.e., Teiidae, Varanidae, Helodermatidae, and Scincidae: Estes 1964, 1983; Pregill et al. 1986; Gao and Fox 1991, 1996; Nydam et al. 2000). Thus, at the family level all squamate lineages appeared to survive the K-Pg mass extinction (e.g., 8 out of 8 families; Archibald and Bryant 1990). However, recent phylogenetic studies have demonstrated that many Lancian squamate species from the Western Interior are members of extinct clades or are basal stem taxa (e.g., Conrad et al. 2011; Gauthier et al. 2012; Yi and Norell 2013). Some of those clades were snuffed out during the K-Pg mass extinction (Longrich et al. 2012b; Nydam 2013b) including Borioteiioidea (Chamopsiidae + Polyglyphanodontini) and the Lancian platynotans from North America (e.g., *Parasaniwa*, *Palaeosaniwa*, and *Paraderma*; Monstersauria of Conrad et al. 2011). A similar scenario seems likely for the Late Cretaceous iguanomorphs of North America (see discussion above).

Abundances, Paleobiogeography, and Extinctions across the K-Pg Boundary

High relative abundances and broad geographic range coverage is often a poor predictor for survivorship during mass extinctions (e.g., Jablonski 1986, 1989; Lockwood 2003; Payne and Finnegan 2007). That prediction holds true for the local squamate faunas of northeastern Montana wherein taxa with higher relative abundances, which were estimated using the number of localities (site occupancy) as a proxy for squamate abundances (e.g., see Jernvall and Fortelius 2004; Holroyd et al. 2014), did not correlate with species survivorship. In fact, the most frequently occurring taxa in the Hell Creek Formation (*Champs segnis*, *Meniscognathus altmani*, *Parasaniwa wyomingensis*, and *Palaeosaniwa* sp.) occur in seven to ten stratigraphic horizons yet are among those that went extinct at or near the K-Pg boundary. This pattern contrasts with the caudate and allocaudate faunas in the local section wherein the four most abundant and frequently occurring species spanned the K-Pg boundary (Wilson et al. 2014b; *Chapter Two*, Fig. 2.11). Two of the local squamate survivors (*Exostinus lancensis*, *Odaxosaurus piger*) each occur at six localities and span most of the formation; whereas *Contogenys sloani* found near the top of the Hell Creek Formation occurs twice. *Meniscognathus altmani* may be a fourth taxon with high site-occupancy (seven occurrences) to have survived the K-Pg mass extinction (i.e., "Hell Hollow chamopsiid" in the lowermost Tullock Formation) though better preserved specimens are needed to corroborate this claim. A Mann-Whitney *U* test demonstrates that the negative correlation between site occupancy and species survivorship through the Hell Creek Formation is not quite statistically significant ($p = 0.07867$; Monte Carlo $p = 0.0759$), even when including all taxa from the unit ($p = 0.1173$; Monte Carlo $p = 0.1142$). These results differ from those of Longrich et al. (2012b) who state that from across the Western Interior of North America the victims of the K-Pg mass extinction occur at fewer localities

(geographic areas) than do the survivors (mean = 2.16 versus 3, respectively), although their results were not statistically significant (Mann-Whitney *U* test; p = 0.5243; Monte Carlo p = 0.5197). Upon updating Longrich et al.'s (2012b) dataset with the revised and new squamate occurrences from this study, I found a statistically significant difference in the mean values of 2.03 versus 3.4 for victims and survivors, respectively (Monte Carlo p = 0.0075). Although the number of taxon occurrences across the Western Interior appear to be a predictor for K-Pg extinction selectivity in squamates at a regional scale (i.e., fewer biogeographic occurrences = higher extinction probability), nearly half (21 of the 44) of the Lancian-age squamates from the Western Interior were only recently identified or described (nine are from Longrich et al. 2012b; 12 are from this study) and most are known only from a single fossil locality or geographic area. Future investigations need to determine if these taxa were truly rare or if they have been overlooked in existing collections.

Pre-K-Pg Boundary Turnover in Squamate Tooth Types

Tooth morphology, which is often linked to diet in squamates (e.g., Hotton 1955; Brizuela and Albino 2009; Meyers et al. 2006), may serve as a proxy for understanding extinction selectivity in squamates prior to and across the K-Pg boundary. For example, many borioteiioids (e.g., *Chamops*, *Haptosphenus*, and *Peneteius*) have similar dentitions to modern teiids (teeth multicuspid, heterodont, subpleurodont, heavy cementum deposits; Estes 1964, 1969) and although those similarities are homoplastic, functionally they provide insights into the diets of borioteiioids (Nydam et al. 2000; Nydam and Cifelli 2002; Nydam 2002). However, because extant lizards exhibit a wide range of ecological and dietary preferences and foraging strategies (e.g., Zug et al. 2001; Pianka and Vitt 2003) some authors have argued that fossil

squamates (mainly lizards) would serve as poor ecological indicators during the mass extinction (Bryant 1989; Archibald 1996, 2011). Nevertheless, I noted a correlation between the loss of specific tooth morphologies and taxonomic turnover from the lower to upper halves of the Hell Creek Formation and across the K-Pg boundary. That correlation may be related to dietary preferences in squamates.

Turnover in tooth types from two major squamate clades (Borioteiioidea and Platynota) occurs in the local section more than 300 k.y. before the K-Pg boundary. Among the borioteiioids (Chamopsiidae + Polyglyphanodontini), the loss of chamopsiids possessing monocuspid teeth with low mesial and distal "shoulders" and weak carinae occurs between the lower and upper halves of the Hell Creek Formation (Chamopsiidae gen. et sp. undet. A, B, C, and D, *Socognathus brachyodon*, *S. unicuspis*; Figs. 6d, A3.2, A3.3A–H, and A3.13). The local loss of these chamopsiids coincides with the appearances of two others (*Haptosphenus placodon*, *Leptochamops denticulatus*; Figs. 3.6b, A3.10K–N, A3.11) and one possible chamopsiid (*Obamadon gracilis*; Fig. 3.6e; Longrich et al. 2012b, fig. 1b and S2), all of which possess well-developed tricuspid teeth and one polyglyphanodontine with transversely expanded, multicusped, molariform teeth (*Peneteius aquilonius*; Fig. 3.6b; Nydam et al. 2000, figs. 1–3). A fifth taxon, ?Chamopsiidae gen. et sp. undet. (Fig. 3.6g), also appeared in the upper Hell Creek and while its teeth are not tricuspid they possess well-defined "shoulders" that flare mesially and distally and are nearly incipiently tricuspid (Fig. A3.3I–J) as in *L. denticulatus*. Although chamopsiids possessing tricuspid teeth also occur in the lower Hell Creek Formation in the local section (i.e., *Chamops segnis*, *Meniscognathus altmani, Leptochamops thrinax*), they do not reach their greatest numbers of occurrences and peak richness until the upper Hell Creek or "La2" interval. Whereas sampling may be an issue, the loss of multiple chamopsiid taxa

possessing monocuspid teeth from the lower to upper Hell Creek Formation suggests that this pattern is real. However, the causality of those taxonomic losses may not be attributed to tooth shape alone if at all. If, for example, the chamopsiids possessing monocuspid teeth form a monophyletic clade within Chamopsiidae, then they likely shared traits in addition to monocuspid teeth (e.g., reproductive biology, foraging strategy, habitat preference) that may have led to their disappearances. Future work will aim to provide a phylogenetic framework to test this hypothesis.

Among the stem platynotans, a similar pattern of turnover in tooth types from the lower to upper portions of the Hell Creek Formation is observed, albeit to a lesser extent. Platynotans, which range through most of the Hell Creek Formation (*Parasaniwa wyomingensis*, *Paraderma bogerti*, *Palaeosaniwa* sp.), possess moderate to robust recurved and trenchant teeth. The teeth of *P. bogerti* also may have an anterior venom groove (Pregill et al. 1986; Gao and Fox 1996; Yi and Norell 2013; see Cifelli and Nydam 1995 and Nydam 2000 for an alternate interpretation); whereas, the teeth of *Palaeosaniwa* are ziphodont and microserrated mesially and distally (Estes 1964; Gao and Fox 1996; Balsai 2001), much like in modern varanids (e.g., *Varanus komodoensis*; D' Amore and Blumenschine 2009). In contrast, Platynota gen. et sp. A possesses recurved, non-trenchant, and fang-like teeth with weakly developed mesial and distal carinae (Figs. 3.6l, A3.7A–I). Platynota gen. et sp. B and C lack well-preserved teeth (Figs. A3.7J – M and A3.8A–D, respectively). However, the mesiodistally restricted tooth bases and the rounded base of the partial crown in Platynota gen. et sp. B implies it possessed teeth more similar to the non-trenchant fang-like form present in Platynota gen. et sp. A than to those present in the other known platynotans (see Appendix to *Chapter Three* for details). If verified, the more gracile fang-like tooth type present in these two stem platynotans would then be restricted to the lower

Hell Creek Formation; this temporal pattern of tooth-type turnover would be similar to that seen in the chamopsiids. Despite these differences in tooth morphology, all platynotan taxa in the Hell Creek Formation likely were capable of preying on small to large vertebrate prey such as frogs, other lizards, and mammals. The total loss of platynotans across the K-Pg boundary may be causally related to their shared diet, but other traits common to this group cannot be ruled out.

Regional turnover in plants (Johnson 2002) and insect foliar damage types (a proxy for insect richness and composition; Labandeira et al. 2002) and the temporally correlated warming event during the last ca. 300–500 k.y. of the Cretaceous (e.g., Wilf et al. 2003; Tobin et al. 2014) may, in part, explain the turnover in the chamopsiids and platynotans possessing monocuspid and fang-like dentitions, respectively. Assuming the differences in tooth shape noted above within those clades reflect differences in diet, then the loss of taxa possessing the monocuspid and fang-like dentitions suggests that certain prey or food items available to them during the time represented by the lower Hell Creek Formation may have become unavailable (extinct or extirpated) during the last ca. 300–400 k.y. of the Cretaceous. Turnover in the megaflora has been documented from the Hell Creek Formation of southwestern North Dakota and northwestern South Dakota (e.g., HCII–HCIII floral zones: Johnson 2002), which, in part, has been interpreted as representing a response to warming temperatures (e.g., Wilf et al. 2013). Similarly, a study on plant-insect associations based on types of insect feeding traces on leaves revealed turnover in insect damage types (external foliage feeding, galling, mining, piercing and sucking) and a stepwise pattern in the loss of intermediate and specialized feeding types leading up to the K-Pg boundary (Labandeira et al. 2002). The turnover in insect feeding types likely corresponded to the turnover in plant and insect diversity which may have cascaded up the food

chain resulting in the extirpation or extinction of some insectivorous squamates in northeastern Montana.

Longrich et al. (2012b) noted a decline in tooth-shape disparity across the K-Pg boundary as a result of the loss of taxa possessing ziphodont, brachyodont, or tricuspid teeth. The decreased tooth-shape disparity corresponds with the extinctions of the two major groups of squamates at or near the K-Pg boundary, namely the stem platynotans (e.g., *Palaeosaniwa*) and the borioteiioideans (e.g., *Chamops*). I document a similar pattern in the loss of these types across the K-Pg boundary.

Tooth structure among the survivors is different than in most non-survivors of the K-Pg mass extinction. Among the survivors, both the contogeniid *Contogenys sloani* and the anguid *Odaxosaurus piger* possess truncate tooth crowns (Fig. 3.6f–g, i–k, respectively). Whereas *C. sloani* possesses teeth with an apical mesiodistal groove and faint to absent vertical striae, the teeth of *O. piger* are more robust with lingually expanded bases and an oblique apical cutting edge with well-developed lingual and labial vertical striae (Estes 1964, 1969; Gao and Fox 1996; Nydam and Fitzpatrick 2009; Fig. A3.14A–J). Estes (1964) suggested that *O. piger* had a durophagous diet and that it likely preyed on hard-shelled arthropods or possibly mollusks. Later interpretations of its ecology suggest it was possibly amphibious or aquatic (Estes and Berberian 1970) or lived along stream banks (Estes pers. commun. as cited in Bryant 1989). *Contogenys* also possesses truncate tooth crowns but the teeth are relatively more gracile and likely not suited for a durophagous diet. The xenosaurid *Exostinus lancensis* possesses teeth with sub-cylindrical shafts and slightly labiolingually compressed recurved crowns with a sharp leading edge (Gao and Fox 1996; Fig. A3.15). The closely related extant xenosaurid *Xenosaurus* (Conrad 2008;

Bhullar 2011) possesses a similar dentition and is known to prey mainly on arthropods (Zug et al. 2001).

Post K-Pg Squamate Faunas: Depauperate and a "Dead Clade Walking"

The local extinction of at least 81% of squamate species across the K-Pg boundary led to a depauperate squamate assemblage in the earliest Paleocene (Pu1–To1). This pattern is not the result of poor sampling effort. The Worm Coulee 1 locality (UCMP loc. V74111) less than three meters above the K-Pg boundary has produced more than 500 salamander and over 900 mammal specimens and an abundance of fish, turtles, champsosaurs, and crocodilians, but it has produced only a few indeterminate squamate specimens. The scarcity of squamates could be a true evolutionary pattern or it may reflect some unknown taphonomic or paleoenvironmental filter. The standing species richness estimate in the lower Tullock Formation (0–30 m; Fig. 3.3) implies that *Contogenys sloani*, *Exostinus lancensis*, and *Odaxosaurus piger* were present, but specimens of those taxa have yet to be found in that part of the stratigraphic section. Alternatively, they may have been temporarily extirpated from the local area during the earliest Paleocene.

Chamopsiids occur in two localities in the Tullock Formation, the Hell Hollow Channel and Harley's Point localities. Both of these localities are channel-lag deposits in the lower part of the formation. The Hell Hollow locality is less than three meters above the K-Pg boundary and is below the HFZ coal, putting it within the first ca. 70 ka of the Paleocene (Sprain et al. 2015). The Harley's Point locality is a stratigraphically thicker channel deposit that spans from the K-Pg boundary to above the HFZ coal, and was likely deposited within the first 300 k.y. of the Paleocene. Champosiids have not been found stratigraphically higher in the local section, despite several well-sampled Pu3 localities (e.g., Garbani Channel localities). Thus, I consider the

Chamopsiidae a “Dead Clade Walking” (sensu Jablonski 2002), having survived the K-Pg mass extinction but failed to diversify in the aftermath.

The near-complete absence of squamates in the early Pu1–?Pu2 interval may represent the temporary extirpation of the remaining local survivors. *Contogenys sloani*, *Exostinus lancensis*, and *Odaxosaurus piger* reappear stratigraphically higher in section (Pu3 NALMA), possibly representing Lazarus taxa (sensu Flessa and Jablonski 1983); an interpretation that is consistent with that for several local caudate species that also reappear in the section (e.g., *Prodesmodon copei*; Wilson et al. 2014b; *Chapter Two*). The snake *Coniophis* may also represent a Lazarus taxon; it is absent from the Paleocene of the local section, but it occurs in Paleocene deposits elsewhere (e.g., Fort Union Formation of southeastern Montana; Estes 1976). Along with the reappearances of the aforementioned taxa are the concurrent first appearances of two other anguid species, *Proxestops jepseni* and cf. *Machaerosaurus torrejonensis*, and an indeterminate platynotan. Fossil remains of *Contogenys sloani*, *E. lancensis*, and the platynotan are rare; whereas dozens of jaws and osteoderms of anguids are present. Although few specimens could be identified to species among the anguids, they were the predominant lizard clade during the Pu3 interval. Similarly, although sample size is small (n = 13), anguids are the only lizards currently recognized from the To1 Horsethief Canyon 1 locality (UWBM C1418 = UCMP V73094) near the top of the Tullock Formation.

These results imply a prolonged recovery for squamates, a temporal pattern similar among the caudate and allocaudate faunas of North America (Wilson et al. 2014b; *Chapter Two*). Mammals in the local area rapidly rebounded in species richness following the mass extinction (Wilson 2014) and within the first ca. 925 k.y. of the Paleocene (Sprain et al. 2015). Given the

paucity of well-preserved squamate specimens from the Tullock Formation it is difficult to make claims regarding their recovery during the earliest phases of the recovery period (Pu1–To1).

It is clear that by the Late Paleocene and Early Eocene squamates were well on their way to a full recovery (e.g., see Sullivan and Lucas 1996, table 1 and discussion; Longrich et al. 2012b, fig. 6). Anguids maintained their position as the predominant group in terms of taxonomic richness during the remainder of the Paleocene and early Eocene with as many as 10 taxa appearing during that interval (e.g., Gauthier 1982; Estes 1983; Sullivan 1986; Longrich et al. 2012b). Platynotans reappeared in the form of the indeterminate platynotan in the Pu3 interval of the Tullock Formation noted here which may represent an earlier linage of *Provaranosaurus acutus* known from the late Paleocene (Tiffanian) of Wyoming (Gilmore 1942). The tentative Paleocene and Eocene records of *Palaeosaniwa* (Sullivan 1982) and *Parasaniwa* (see Estes 1983), respectively, are unsubstantiated (Estes 1983; Gao and Fox 1996). A new species of xenosaur related to *Exostinus lancensis* (*Restes rugosus*) appeared during the Tiffanian of Wyoming (Gilmore 1942b; Gauthier 1982); whereas *Contogenys sloani* is joined by two new contogeniid species (*Palaeoscincosaurus middletoni*, *Contogenys ekalakaensis*) from the Puercan and Torrejonian of northcentral Colorado and southeastern Montana, respectively (Sullivan and Lucas 1996; Nydam and Fitzpatrick 2009). Unambiguous crown iguanians (*Afairiguana avius*, *Babibasiliscus alxi*) did not appear in North America until the Eocene (Conrad et al. 2007; Conrad 2015), although *Swainiguanoides milleri* from the early Paleocene (Torrejonian) of Wyoming (Sullivan 1982) may represent an iguanian (see Nydam 2013b for a discussion regarding its taxonomic affinities). Unequivocal xantusiids (*Palaeoxantusia fera*) and amphisbaenians (e.g., *Oligodontosaurus*, *Plesiorhineura tsentasi*) appeared in Montana, Wyoming, and New Mexico during the Torrejonian and Tiffanian (Estes 1976; Sullivan 1982;

Longrich et al. 2015). The recently described amphisbaenian *Chthonophis subterraneus* (Longrich et al., 2015) may represent a post K-Pg extinction immigrant into northeastern Montana. Its presence in the temporally-mixed latest Cretaceous-earliest Paleocene Bug Creek Anthills locality was interpreted as representing a Pu1 occurrence (Longrich et al. 2015), although additional specimens from temporally constrained localities relative to the K-Pg boundary are required to support that claim. Finally, snakes begin to diversify by at least the Torrejonian (e.g., *Helagras prisciformis*; Sullivan and Lucas 1986).

CONCLUSIONS

Eighty-one percent of squamate species in northeastern Montana went extinction during the Cretaceous-Paleogene mass extinction, most of which occurred among the scincomorph clade Borioteiioidea and the stem platynotans. Numerous undescribed taxa from the Hell Creek Formation and the addition of several known taxa from older and similar-aged deposits from outside of the study area have added resolution to the extinction event and have revealed a unique but broadly similar pattern of faunal change through the Hell Creek Formation as seen in the euselachians, lissamphibians, turtles, and mammals. The high species turnover and the recognition of two distinct squamate faunas of the Hell Creek Formation calls into question the conclusions of Longrich et al. (2012b) who posit that squamates suffered a devastating mass extinction caused solely by and coincident with the Chicxulub bolide impact at the K-Pg boundary. Those two distinct squamate faunas were possibly the result of dietary preferences among squamates based on several chamopsiids possessing monocuspid teeth and two platynotans possessing fang-like teeth that are lost from the lower ("La1") to upper ("La2")

halves of the Hell Creek Formation. Although additional sampling is required to more soundly address that scenario and the timing of squamate turnover and extinctions leading up to and across the K-Pg boundary, the current state of the data and correlations with declines in richness and increased turnover observed in other local vertebrate faunas suggests that these results are merging on a true pattern.

REFERENCES CITED

Alvarez, L. W., W. Alvarez, F. Asaro, and H. V. Michel. 1980. Extraterrestrial cause for the Cretaceous-Tertiary extinction. Science 208:1095–1108.

Archibald, J. D. 1982. A study of Mammalia and geology across the Cretaceous-Tertiary boundary in Garfield County, Montana. University of California Publications in Geological Sciences 122:1–286.

Archibald, J. D. 1996. Dinosaur Extinction and the End of an Era: What the Fossils Say. 237 pp. Columbia University Press, New York.

Archibald, J. D. 2011. Extinction and Radiation: How the fall of dinosaurs led to the rise of mammals. 108 pp. The Johns Hopkins University Press, Baltimore, Maryland.

Archibald, J. D., and L. J. Bryant. 1990. Differential Cretaceous/Tertiary extinctions of nonmarine vertebrates; Evidence from northeastern Montana; pp. 549–562 in V. L. Sharpton, and P. D. Ward (eds.), Global catastrophes in Earth history; An interdisciplinary conference on impacts, volcanism, and mass mortality. Geological Society of America Special Paper 247, Boulder, Colorado.

Archibald, J. D., W. A. Clemens, K. Padian, T. Rowe, N. MacLeod, P. M. Barrett, A. Gale, P. Holroyd, H.-D. Sues, N. C. Arens, J. R. Horner, G. P. Wilson, M. B. Goodwin, C. A. Brochu, D. L. Lofgren, S. H. Hurlbert, J. H. Hartman, D. A. Eberth, P. B. Wignall, P. J. Currie, A. Weil, G. V. R. Prasad, L. Dingus, V. Courtillot, A. Milner, A. Milner, S. Bajpai, D. J. Ward, and A. Sahni. 2010. Cretaceous Extinctions: Multiple Causes. Science 328:973.

Armstrong-Ziegler, J. G. 1980. Amphibia and Reptilia from the Campanian of New Mexico. Fieldiana Geology New Series, No. 4:1–39.

Balsai, M. J. 2001. The phylogenetic position of *Palaeosaniwa* and the early evolution of the platynotan (varanoid) anguimorphs: In Earth and Environmental Sciences, Ph.D. dissertation, pp. 253. University of Pennsylvania, Philadelphia.

Bhullar, B. A. S. 2011. The power and utility of morphological characters in systematics: A fully resolved phylogeny of *Xenosaurus* and its fossil relatives (Squamata: Anguimorpha). Bulletin of the Museum of Comparative Zoology 160:65–181.

Brinkman, D. 2002. An illustrated guide to the vertebrate microfossils from the Dinosaur Park Formation, pp. 137. Royal Tyrrell Museum of Palaeontology.

Brizuela, S., and A. M. Albino. 2009. The dentition of the Neotropical lizard genus *Teius* Merrem 1820 (Squamata Teiidae). Tropical Zoology 22:183–193.

Bryant, L. J. 1989. Non-dinosaurian lower vertebrates across the Cretaceous-Tertiary boundary in northeastern Montana. University of California Publications in Geological Sciences 134:1–107.

Caldwell, M. W., R. L. Nydam, A. Palci, and S. Apesteguía. 2015. The oldest known snakes from the Middle Jurassic-Lower Cretaceous provide insights on snake evolution. Nature Communications 6.

Camp, C. L. 1923. Classification of the lizards. Bulletin of the American Museum of Natural History 48:289–480.

Cifelli, R. L., J. J. Eberle, D. L. Lofgren, J. A. Lillegraven, and W. A. Clemens. 2004. Mammalian biochronology of the latest Cretaceous; pp. 21–42 in M. O. Woodburne

(ed.), Late Cretaceous and Cenozoic mammals of North America: biostratigraphy and geochronology. Columbia University Press, New York.

Clemens, W. A. 2002. Evolution of the mammalian fauna across the Cretaceous-Tertiary boundary in northeastern Montana and other areas of the Western Interior; pp. 217–245 in J. H. Hartman, K. R. Johnson, and D. J. Nichols (eds.), The Hell Creek Formation and the Cretaceous-Tertiary boundary in the northern Great Plains: An integrated continental record of the end of the Cretaceous. Geological Society of America Special Paper 361, Boulder, Colorado.

Clemens, W. A., and G. P. Wilson. 2009. Early Torrejonian mammalian local faunas from northeastern Montana, U.S.A.; pp. 111–158 in Albright, III, L. B. (ed.), Papers on Geology, Vertebrate Paleontology, and Biostratigraphy in Honor of Michael O. Woodburne. Museum of Northern Arizona, Bulletin.

Conrad, J. L. 2008. Phylogeny and systematics of Squamata (Reptilia) based on morphology. Bulletin of the American Museum of Natural History 310:1–182.

Conrad, J. L. 2015. A new Eocene Casquehead lizard (Reptilia, Corytophanidae) from North America. PLoS ONE 10:e0127900.

Conrad, J. L., O. Rieppel, J. A. Gauthier, and M. A. Norell. 2011. Osteology of *Gobiderma pulchrum* (Monstersauria, Lepidosauria, Reptilia). Bulletin of the American Museum of Natural History 362:1–88.

Conrad, J. L., O. Rieppel, and L. Grande. 2007. A Green River (Eocene) polychrotid (Squamata: Reptilia) and a re-examination of iguanian systematics. Journal of Paleontology 81:1365–1373.

Cook, T. D., M. G. Newbrey, D. B. Brinkman, and J. I. Kirkland. 2014. Euselachians from the freshwater deposits of the Hell Creek Formation of Montana; pp. 229–246 in G. P. Wilson, W. A. Clemens, J. R. Horner, and J. H. Hartman (eds.), Through the End of the Cretaceous in the Type Locality of the Hell Creek Formation in Montana and Adjacent Areas. Geological Society of America Special Paper 503, Boulder.

Cope, E. D. 1886. Thirteenth contribution to the herpetology of tropical America. Proceedings of the American Philosophical Society, Philedelphia 23:271–287.

D' Amore, D. C., and R. J. Blumenschine. 2009. Komodo monitor (*Varanus komodoensis*) feeding behavior and dental function reflected through tooth marks on bone surfaces, and the application to ziphodont paleobiology. Paleobiology 35:525–552.

DeMar, D. G., Jr., and B. H. Breithaupt. 2006. The nonmammalian vertebrate microfossil assemblages of the Mesaverde Formation (Upper Cretaceous, Campanian) of the Wind River and Bighorn Basins, Wyoming; pp. 33–53 in S. G. Lucas, and R. M. Sullivan (eds.), Late Cretaceous vertebrates from the Western Interior. New Mexico Museum of Natural History and Science Bulletin 35.

DeMar, D. G., Jr., and G. P. Wilson. 2013. Squamate turnover in the 2 million years leading up to and across the K-Pg boundary in northeastern Montana: evidence for a complex extinction scenario. Journal of Vertebrate Paleontology, Program and Abstracts, 2013, 114.

DeMar, D. G., Jr., J. L. Conrad, J. J. Head, D. J. Varricchio, and G. P. Wilson. 2015. Phylogenetics and paleobiology of a Late Cretaceous stem iguanian from Montana. Journal of Vertebrate Paleontology, Program and Abstracts, 2015, 115.

Denton, R. K., and R. C. O'Neill. 1995. *Prototeius stageri*, gen. et sp. nov., a new teiid lizard from the Upper Cretaceous Marshalltown Formation of New Jersey, with a preliminary phylogenetic revision of the Teiidae. Journal of Vertebrate Paleontology 15:235–253.

Duméril, A. M. C., and G. Bibron. 1839. Erpétologie générale ou histoire naturelle compléte des reptiles. 854 pp. Roret, Paris.

Estes, R. 1964. Fossil vertebrates from the Late Cretaceous Lance Formation eastern Wyoming. University of California Publications in Geological Sciences 49:1–187.

Estes, R. 1969a. Relationships of two lizards (Sauria, Teiidae). Breviora 317:1–8.

Estes, R. 1969b. A scincoid lizard from the Cretaceous and Paleocene of Montana. Breviora 331:1–9.

Estes, R. 1975. Lower vertebrates from the Fort Union Formation, Late Paleocene, Big Horn Basin, Wyoming. Herpetologica 31:365–385.

Estes, R. 1976. Middle Paleocene lower vertebrates from the Tongue River Formation, southeastern Montana. Journal of Paleontology 50:500–520.

Estes, R. 1983. Sauria Terrestria, Amphisbaenia; pp. 249, Handbuch der Paläoherpetologie, Teil 10A. Gustav Fischer Verlag, Stuttgart.

Estes, R., and P. Berberian. 1970. Paleoecology of a Late Cretaceous vertebrate community from Montana. Breviora 343:1–35.

Estes, R., P. Berberian, and C. A. M. Meszoely. 1969. Lower Vertebrates from the Late Cretaceous Hell Creek Formation, McCone County, Montana. Breviora 337:1–33.

Fastovsky, D. E., and A. Bercovici. 2015. The Hell Creek Formation and its contribution to the Cretaceouse-Paleogene extinction: A short primer. Cretaceous Research 57:368–390.

Flessa, K. W., and D. Jablonski. 1983. Extinction is here to stay. Paleobiology 9:315–321.

Foote, M. 2000. Origination and extinction components of taxonomic diversity: General problems; pp. 74-102 in D. H. Erwin, and S. L. Wing (eds.), Deep Time: Paleobiology's Perspective. The Paleontological Society, Supplement to v. 26, no. 4, Lawrence, Kansas.

Fox, R. C. 1989. The Wounded Knee Local Fauna and mammalian evolution near the Cretaceous-Tertiary boundary, Saskatchewan, Canada. Palaeontographica Abteilung A 208:11–59.

Fürbringer, M. 1900. Zur vergleichenden Anatomie Brustschulterapparates und der Schultermuskeln. Janaische Zeitschrift für Naturwissenschaft 34:215–718.

Gao, K., and R. C. Fox. 1991. New teiid lizards from the Upper Cretaceous Oldman Formation (Judithian) of southwestern Alberta, Canada, with a review of the Cretaceous record of teiids. Annals of Carnegie Museum 60:145–162.

Gao, K., and R. C. Fox. 1996. Taxonomy and evolution of Late Cretaceous lizards (Reptilia: Squamata) from western Canada. Bulletin of Carnegie Museum of Natural History 33:1–107.

Gardner, J. D., and R. L. Cifelli. 1999. A primitive snake from the Cretaceous of Utah. Special Papers in Palaeontology 60:87–100.

Gardner, J. D., and D. G. DeMar. 2013. Mesozoic and Palaeocene lissamphibian assemblages of North America: a comprehensive review. Palaeobiodiversity and Palaeoenvironments 93:459–515.

Gauthier, J. A. 1982. Fossil xenosaurid and anguid lizards from the early Eocene Wasatch Formation, southeast Wyoming, and a revision of the Anguiodea. Contributions to Geology 21:7–54.

Gauthier, J. A., M. Kearney, J. A. Maisano, O. Rieppel, and A. D. B. Behlke. 2012. Assembling the squamate tree of life: Perspectives from the phenotype and the fossil record. Bulletin of the Peabody Museum of Natural History 53:3–308.

Gilmore, C. W. 1928. Fossil lizards of North America. Memoirs of the National Academy of Sciences 22:1–201.

Gilmore, C. W. 1942a. Osteology of *Polyglyphanodon*, an Upper Cretaceous lizard from Utah. Proceedings of the United States National Museum 92:229–265.

Gilmore, C. W. 1942b. Paleocene Faunas of the Polecat Bench Formation, Park County, Wyoming Part II. Lizards. Proceedings of the American Philosophical Society 85:159–167.

Holman, J. A. 2000. Fossil Snakes of North America: Origin, Evolution, Distribution, Paleoecology. 376 pp. Indiana University Press, Bloomington.

Holroyd, P. A., G. P. Wilson, and J. H. Hutchison. 2014. Temporal changes within the latest Cretaceous and early Paleogene turtle faunas of northeastern Montana; pp. 299–312 in G. P. Wilson, W. A. Clemens, J. R. Horner, and J. H. Hartman (eds.), Through the End of the Cretaceous in the Type Locality of the Hell Creek Formation in Montana and Adjacent Areas. Geological Society of America Special Paper 503, Boulder.

Hotton III, N. 1955. Survey of adaptive relationships of dentition to diet in the North American Iguanidae. American Midland Naturalist 53:88–114.

Jensen, F. S., and H. D. Varnes. 1964. Geology of the Fort Peck Area, Garfield, McCone, and Valley Counties, Montana. U.S. Geological Survey Professional Paper 414F:1–49.

Jernvall, J., and M. Fortelius. 2004. Maintenance of trophic structure in fossil mammal communities: Site occupancy and taxon resilience. The American Naturalist 164:614–624.

Jablonski, D. 1986. Background and mass extinctions: The alternation of macroevolutionary regimes. Science 231:129–133.

Jablonski, D. 1989. The biology of mass extinction: A palaeontological view. Philosophical Transactions of the Royal Society of London, Series B 325:357–368.

Jablonski, D. 2002. Survival without recovery after mass extinctions. Proceedings of the National Academy of Sciences of the United States of America 99:8139–8144.

LeCain, R., W. C. Clyde, G. P. Wilson, and J. Riedel. 2014. Magnetostratigraphy of the Hell Creek and lower Fort Union Formations in northeastern Montana; pp. 137–147 in G. P. Wilson, W. A. Clemens, J. R. Horner, and J. H. Hartman (eds.), Through the End of the Cretaceous in the Type Locality of the Hell Creek Formation in Montana and Adjacent Areas. Geological Society of America Special Paper 503, Boulder.

Li, L., and G. Keller. 1998. Abrupt deep-sea warming at the end of the Cretaceous. Geology 26:995–999.

Lillegraven, J. A., and J. J. Eberle. 1999. Vertebrate faunal changes through Lancian and Puercan time in southern Wyoming. Journal of Paleontology 73:691–710.

Lillegraven, J. A., and M. C. McKenna. 1986. Fossil mammals from the “Mesaverde” Formation (Late Cretaceous, Judithian) of the Bighorn and Wind River basins, Wyoming, with definitions of Late Cretaceous North American Land Mammal “ages”. American Museum Novitates 2840:1–68.

Linnaeus, C. v. 1758. Systema naturae per regna tria naturae, secundum classes, ordines, genera, species, cum characteribus, differentiis, synonymis, locis. 824 pp. Salvii Nat., Holmiae [Stockholm].

Lockwood, R. 2003. Abundance not linked to survival across the end-Cretaceous mass extinction: Patterns in North American bivalves. Proceedings of the National Academy of Sciences of the United States of America 100:2478–2482.

Lofgren, D. L., C. L. Hotton, and A. C. Runkel. 1990. Reworking of Cretaceous dinosaurs into Paleocene channel deposits, upper Hell Creek Formation, Montana. Geology 18:874–877.

Lofgren, D. L., J. A. Lillegraven, W. A. Clemens, P. D. Gingerich, and T. E. Williamson. 2004. Paleocene biochronology: the Puercan through Clarkforkian Land Mammal Ages; pp. 43–105 in M. O. Woodburne (ed.), Late Cretaceous and Cenozoic mammals of North America: Biostratigraphy and geochronology. Columbia University Press, New York.

Longrich, N. R., B. A. S. Bhullar, and J. A. Gauthier. 2012a. A transitional snake from the Late Cretaceous Period of North America. Nature 488:205–208.

Longrich, N. R., B. A. S. Bhullar, and J. A. Gauthier. 2012b. Mass extinction of lizards and snakes at the Cretaceous–Paleogene boundary. Proceedings of the National Academy of Sciences 109:21396–21401.

Longrich, N. R., J. Vinther, R. A. Pyron, D. Pisani, and J. A. Gauthier. 2015. Biogeography of worm lizards (Amphisbaenia) driven by end-Cretaceous mass extinction. Proceedings of the Royal Society B 282:20143034.

Marsh, O. C. 1892. Notice of new reptiles from the Laramie Formation American Journal of Science 43:449–453.

Marshall, C. R. 1997. Confidence intervals on stratigraphic ranges with nonrandom distribution of fossil horizons. Paleobiology 23:165–173.

Mercier, G., D. G. DeMar, Jr. and G. P. Wilson. 2014. Frogs and toads (Lissamphibia, Anura) during the end-Cretaceous mass extinction: Evidence from the fossil record of northeastern Montana. Journal of Vertebrate Paleontology, Program and Abstracts, 2014, 187.

Meyers, J. J., A. Herrel, and K. C. Nishikawa. 2006. Morphological correlates of ant eating in horned lizards (*Phrynosoma*). Biological Journal of the Linnean Society 89:13–24.

Moore, J. R., G. P. Wilson, M. Sharma, H. R. Hallock, D. R. Braman, and P. R. Renne. 2014. Assessing the relationships of the Hell Creek–Fort Union contact, Cretaceous-Paleogene boundary, and Chicxulub impact ejecta horizon at the Hell Creek Formation lectostratotype, Montana, USA; pp. 123–135 in G. P. Wilson, W. A. Clemens, J. R. Horner, and J. H. Hartman (eds.), Through the End of the Cretaceous in the Type Locality of the Hell Creek Formation in Montana and Adjacent Areas. Geological Society of America Special Paper 503, Boulder.

Nordt, L., S. Atchley, and S. Dworkin. 2003. Terrestrial evidence for two greenhouse events in the latest Cretaceous. GSA Today 13:4–9.

Nydam, R. L. 2002. Lizards of the Mussentuchit local fauna (Albian–Cenomanian boundary) and comments on the evolution of the Cretaceous lizard fauna of North America. Journal of Vertebrate Paleontology 22:645–660.

Nydam, R. L. 2013a. Lizards and snakes from the Cenomanian through Campanian of Southern Utah: Filling the gap in the fossil record of Squamata from the Late Cretaceous of the Western Interior of North America; pp. 370–423 in A. L. Titus, and M. A. Loewen (eds.),

At the top of the grand staircase: The Late Cretaceous of southern Utah. Indiana University Press, Bloomington.

Nydam, R. L. 2013b. Squamates from the Jurassic and Cretaceous of North America. Palaeobiodiversity and Palaeoenvironments 93:535–565.

Nydam, R. L., and B. M. Fitzpatrick. 2009. The occurrence of *Contogenys*-like lizards in the Late Cretaceous and Early Tertiary of the Western Interior or the U.S.A. Journal of Vertebrate Paleontology 29:677–701.

Nydam, R. L., and R. L. Cifelli. 2002. A new teiid lizard from the Cedar Mountain Formation (Albian–Cenomanian Boundary) of Utah. Journal of Vertebrate Paleontology 22:276–285.

Nydam, R. L., and R. L. Cifelli. 2005. New data on the dentition of the scincomorphan lizard *Polyglyphanodon sternbergi*. Acta Palaeontologica Polonica 50:73–78.

Nydam, R. L., and G. E. Voci. 2007. Teiid-like scincomorphan lizards from the Late Cretaceous (Campanian) of Southern Utah. Journal of Herpetology 41:211–219.

Nydam, R. L., J. A. Gauthier, and J. J. Chiment. 2000. The mammal-like teeth of the Late Cretaceous lizard *Peneteius aquilonius* Estes 1969 (Squamata, Teiidae). Journal of Vertebrate Paleontology 20:628–631.

Nydam, R. L., J. G. Eaton, and J. Sankey. 2007. New taxa of transversely-toothed lizards (Squamata: Scincomorpha) and new information on the evolutionary history of "teiids". Journal of Paleontology 81:538–549.

Nydam, R. L., M. W. Caldwell, and F. Fanti. 2010. Borioteiioidean lizard skulls from Kleskun Hill (Wapiti Formation; Upper Campanian), West-central Alberta, Canada. Journal of Vertebrate Paleontology 30: 1090–1099.

Nydam, R. L., T. B. Rowe, and R. L. Cifelli. 2013. Lizards and snakes of the Terlingua Local Fauna (late Campanian), Aguja Formation, Texas with comments on the distribution of paracontemporaneous squamates throughout the Western Interior of North America. Journal of Vertebrate Paleontology 33:1081–1099.

Oppel, M. 1811. Die Ordnungen, Familien, und Gattungen der Reptilien als Prodrom einer Naturgeschichte derselben. 86 pp. Joseph Lindauer, München.

Payne, J. L., and S. Finnegan. 2007. The effect of geographic range on extinction risk during background and mass extinction. Proceedings of the National Academy of Sciences of the United States of America 104:10506–10511.

Pearson, D. A., T. Schaefer, K. R. Johnson, D. J. Nichols, and J. P. Hunter. 2002. Vertebrate biostratigraphy of the Hell Creek Formation in southwestern North Dakota and northwestern South Dakota; pp. 145–167 in J. H. Hartman, K. R. Johnson, and D. J. Nichols (eds.), The Hell Creek Formation and the Cretaceous-Tertiary boundary in the northern Great Plains: An integrated continental record of the end of the Cretaceous. Geological Society of America Special Paper 361, Boulder, Colorado.

Peng, J., A. P. Russell, and D. B. Brinkman. 2001. Vertebrate microsite assemblages (exclusive of mammals) from the Foremost and Oldman Formations of the Judith River Group (Campanian) of southeastern Alberta: an illustrated guide. Provincial Museum of Alberta Natural History Occasional Paper No. 25:1–54.

Pianka, E. R., and L. J. Vitt. 2003. Lizards: Windows to the evolution of diversity. 333 pp. University of California Press, Berkeley.

Pough, F. H. 1973. Lizard energetics and diet. Ecology 54:837–844.

Pregill, G. K., J. A. Gauthier, and H. W. Greene. 1986. The evolution of helodermatid squamates, with description of a new taxon and an overview of Varanoidea. Transactions of the San Diego Society of Natural History 21:167–202.

Rage, J. C. 1984. Serpentes; pp. 80, Handbuch der Paläoherpetologie, Teil 11. Gustav Fischer Verlag, Stuttgart.

Renne, P. R., A. L. Deino, F. J. Hilgen, K. F. Kuiper, D. F. Mark, W. S. Mitchell, III, L. E. Morgan, R. Mundil, and J. Smit. 2013. Time scales of critical events around the Cretaceous-Paleogene boundary. Science 339:684–687.

Robertson, D. S., M. C. McKenna, O. B. Toon, S. Hope, and J. A. Lillegraven. 2004. Survival in the first hours of the Cenozoic. Geological Society of America Bulletin 116:760–768.

Schulte, P., L. Alegret, I. Arenillas, J. A. Arz, P. J. Barton, P. R. Bown, T. J. Bralower, G. L. Christeson, P. Claeys, C. S. Cockell, G. S. Collins, A. Deutsch, T. J. Goldin, K. Goto, J. M. Grajales-Nishimura, R. A. F. Grieve, S. P. S. Gulick, K. R. Johnson, W. Kiessling, C. Koeberl, D. A. Kring, K. G. MacLeod, T. Matsui, J. Melosh, A. Montanari, J. V. Morgan, C. R. Neal, D. J. Nichols, R. D. Norris, E. Pierazzo, G. Ravizza, M. Rebolledo-Vieyra, W. U. Reimold, E. Robin, T. Salge, R. P. Speijer, A. R. Sweet, J. Urrutia-Fucugauchi, V. Vajda, M. T. Whalen, and P. S. Willumsen. 2010. The Chicxulub asteroid impact and mass extinction at the Cretaceous-Paleogene boundary. Science 327:1214–1218.

Sheehan, P. M., and D. E. Fastovsky. 1992. Major extinctions of land-dwelling vertebrates at the Cretaceous-Tertiary boundary, eastern Montana. Geology 20:556–560.

Sheehan, P. M., and T. A. Hansen. 1986. Detritus feeding as a buffer to extinction at the end of the Cretaceous. Geology 14:868–870.

Signor, P. W., III, and J. H. Lipps. 1982. Sampling bias, gradual extinction patterns and catastrophes in the fossil record; pp. 291–296 in L. T. Silver, and P. H. Schultz (eds.), Geological implications of impacts of large asteroids and comets on the Earth. Geological Society of America Special Paper 190, Boulder, Colorado.

Smith, K. T. 2013. New constraints on the evolution of the snake clades Ungaliophiinae, Loxocemidae and Colubridae (Serpentes), with comments on the fossil history of erycineboids in North America. Zoologischer Anzeiger 252:157–182.

Sprain, C. J., P. R. Renne, G. P. Wilson, and W. A. Clemens. 2015. High-resolution chronostratigraphy of the terrestrial Cretaceous-Paleogene transition and recovery interval in the Hell Creek region, Montana. Geological Society of America Bulletin.

Strauss, D., and P. M. Sadler. 1989. Classical confidence intervals and bayesian probability estimates for ends of local taxon ranges. Mathematical Geology 21:411–427.

Sukhanov, V. B. 1961. Some problems of the phylogeny, and systematics of Lacertilia (seu Sauria). Zoologicheskii Zhurnal 40:73–83.

Sullivan, R. M. 1982. Fossil Lizards from Swain Quarry "Fort Union Formation," Middle Paleocene (Torrejonian), Carbon County, Wyoming. Journal of Paleontology 56:996–1010.

Sullivan, R. M. 1985. A new middle Paleocene (Torrejonian) rhineurid amphisbaenian *Plesiorhineura tsentasi* new genus, new species, from the San Juan Basin, New Mexico. Journal of Paleontology 59:1481–1485.

Sullivan, R. M. 1986. The skull of *Glyptosaurus sylvestris* Marsh, 1871 (Lacertilia: Anguidae) Journal of Vertebrate Paleontology 6:28–37.

Sullivan, R. M. 1987. Reassessment of reptilian diversity across the Cretaceous-Tertiary boundary. 26 pp. Natural History Museum of Los Angeles County, Los Angeles.

Sullivan, R. M. 1991. Paleocene Caudata and Squamata from Gidley and Silberling Quarries, Montana. Journal of Vertebrate Paleontology 11:293–301.

Sullivan, R. M., and S. G. Lucas. 1996. *Palaeoscincosaurus middletoni*, new genus and species (Squamata: ?Scincidae) from the early Paleocene (Puercan) Denver Formation, Colorado Journal of Vertebrate Paleontology 16:666–672.

Tihen, J. H. 1949. The genera of gerrhonotine lizards. American Midland Naturalist 41:580–601.

Tobin, T. S., P. D. Ward, E. J. Steig, E. B. Olivero, I. A. Hilburn, R. N. Mitchell, M. R. Diamond, T. D. Raub, and J. L. Kirschvink. 2012. Extinction patterns, $\delta^{18}O$ trends, and magnetostratigraphy from a southern high-latitude Cretaceous-Paleogene section: links with Deccan volcanism. Palaeogeography, Palaeoclimatology, Palaeoecology 350–352:180–188.

Tobin, T. S., G. P. Wilson, J. M. Eiler, and J. H. Hartman. 2014. Environmental change across a terrestrial Cretaceous-Paleogene boundary section in eastern Montana, USA, constrained by carbonate clumped isotope paleothermometry. Geology.

Wilf, P., and K. R. Johnson. 2004. Land plant extinction at the end of the Cretaceous: A quantitative analysis of the North Dakota megafloral record. Paleobiology 30:347–368.

Wilf, P., K. R. Johnson, and B. T. Huber. 2003. Correlated terrestrial and marine evidence for global climate changes before mass extinction at the Cretaceous-Paleogene boundary. Proceedings of the National Academy of Sciences of the United States of America 100:599–604.

Wilson, G. P. 2004. A quantitative assessment of mammalian change leading up to and across the Cretaceous-Tertiary boundary in northeastern Montana, Ph.D. Dissertation, pp. 412. University of California.

Wilson, G. P. 2005. Mammalian faunal dynamics during the last 1.8 million years of the Cretaceous in Garfield County, Montana. Journal of Mammalian Evolution 12:53–75.

Wilson, G. P. 2013. Mammals across the K/Pg boundary in northeastern Montana, U.S.A.: Dental morphology and body-size patterns reveal extinction selectivity and immigrant-fueled ecospace filling. Paleobiology 39:429–469.

Wilson, G. P. 2014. Mammalian extinction, survival, and recovery dynamics across the Cretaceous-Paleogene boundary in northeastern Montana; pp. in G. P. Wilson, W. A. Clemens, J. R. Horner, and J. H. Hartman (eds.), Through the end of the Cretaceous in the type locality of the Hell Creek Formation in Montana and adjacent areas. Geological Society of America Special Paper, Boulder, Colorado.

Wilson, G. P., W. A. Clemens, J. R. Horner, and J. H. Hartman eds. 2014a. Through the End of the Cretaceous in the Type Locality of the Hell Creek Formation in Montana and Adjacent Areas. Geological Society of America Special Paper 503.

Wilson, G. P., D. G. DeMar, and G. Carter. 2014b. Extinction and survival of salamander and salamander-like amphibians across the Cretaceous-Paleogene boundary in northeastern Montana, USA. Geological Society of America Special Papers 503:271–297.

Yi, H.-Y., and M. A. Norell. 2013. New materials of *Estesia mongoliensis* (Squamata: Anguimorpha) and the evolution of venom grooves in lizards. American Museum Novitates 3767:1–33.

Zug, G. R., L. J. Vitt, and J. P. Caldwell. 2001. Herpetology: An introductory biology of amphibians and reptiles. 630 pp. Academic Press, San Diego.

FIGURES for CHAPTER 3

Figure 3.1. Map of North America (A) and the state of Montana, USA (B). Shaded areas within A and B represent Montana and Garfield County, respectively.

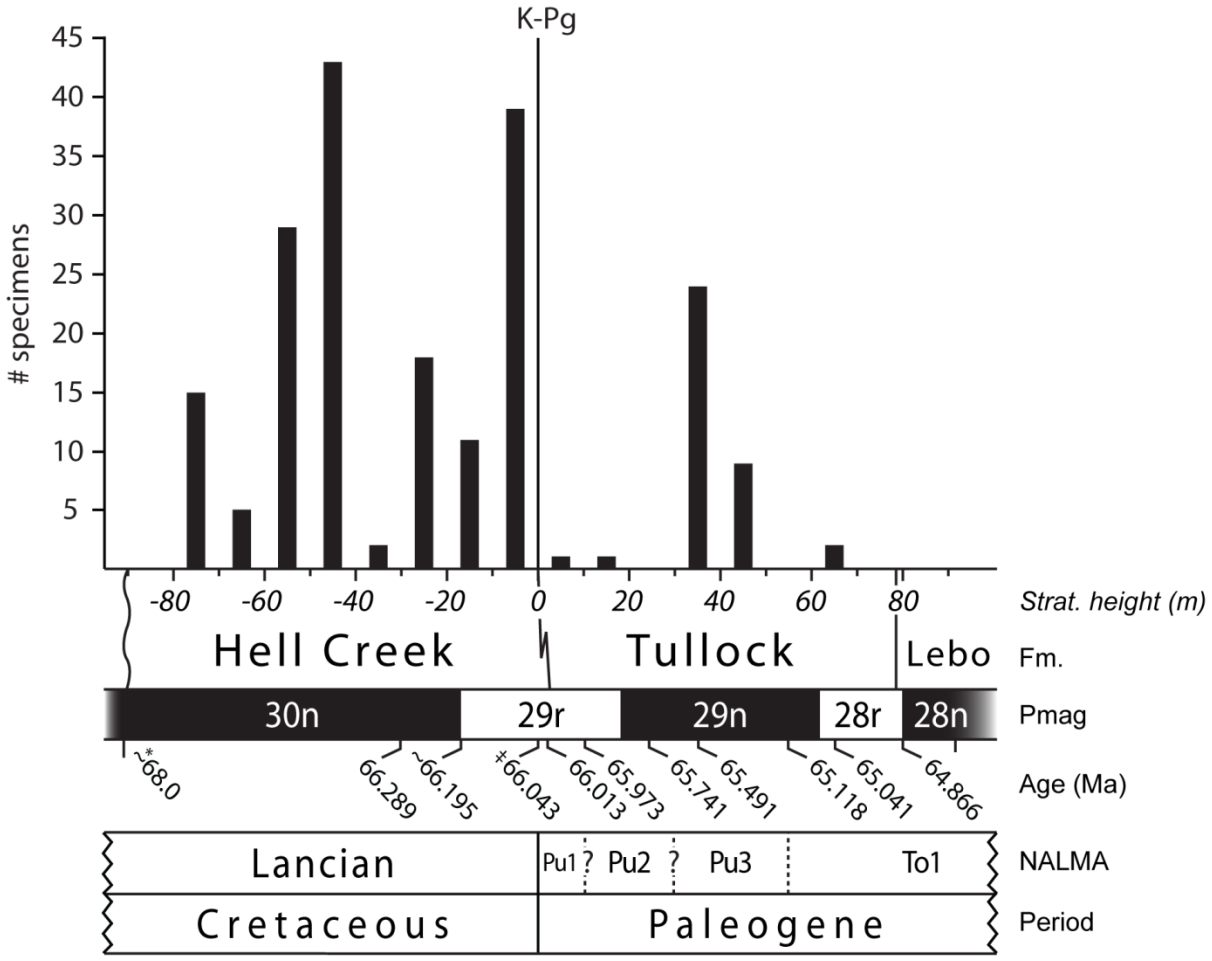

Figure 3.2. Squamate fossil sample sizes through the Hell Creek and Tullock formations of Garfield County, northeastern Montana. Fossil sample sizes are based on 10 m bins. The chronostratigraphic framework is based on the following data: Ar/Ar radiometric ages from Renne et al. (2013; ‡) and Sprain et al. (2015); placement of paleomagnetic polarity chrons follows LeCain et al. (2014), except the C28r/C28n boundary, which follows Swisher et al. (1993); maximum age for the C30n/C29r magnetochron boundary follows Sprain et al. (2015); and the estimated age of the base of the Hell Creek Formation (*) is revised from Wilson (2014). K-Pg—Cretaceous-Paleogene boundary; To1—Torrejonian; NALMA—North American land mammal "age".

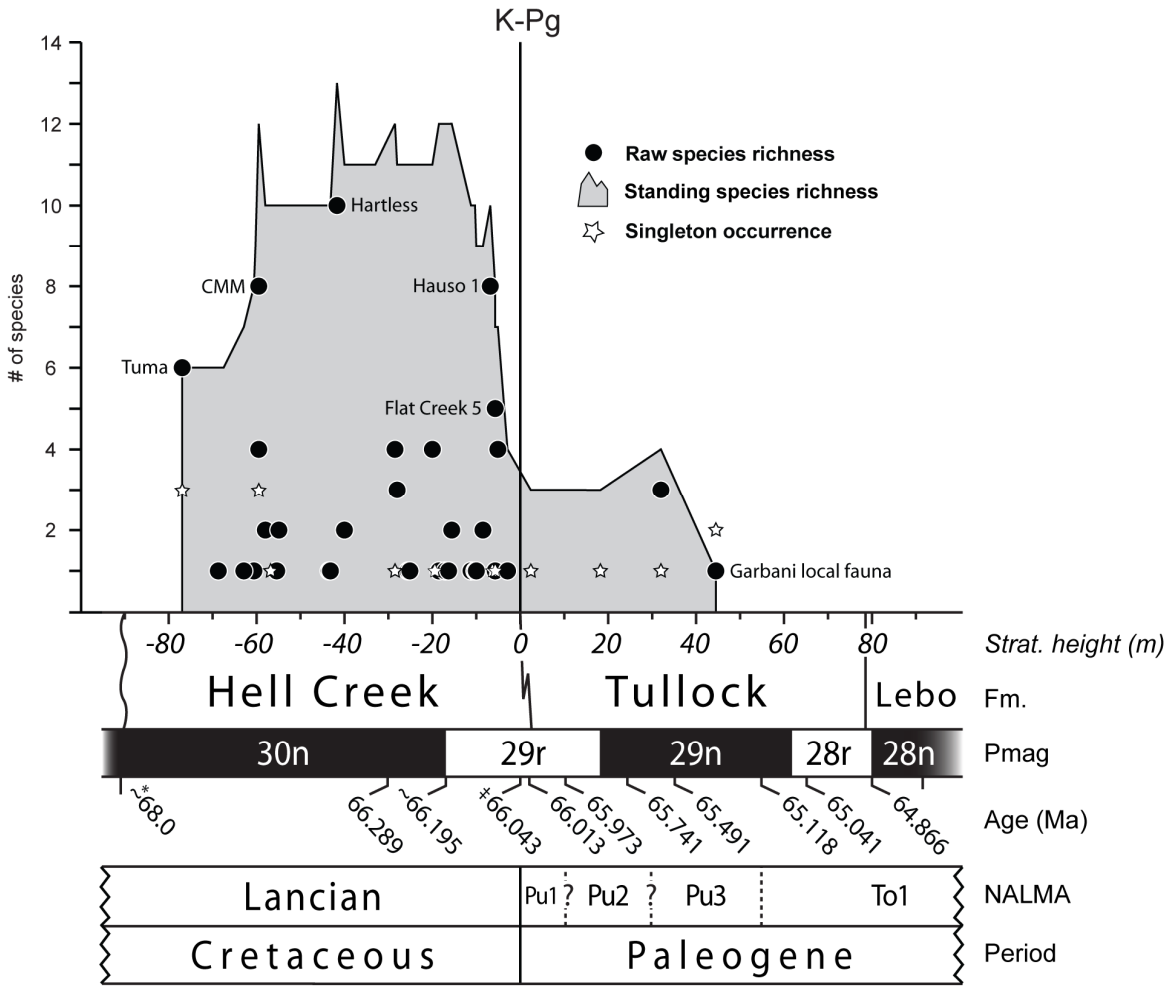

Figure 3.3. Squamate taxonomic richness through the Hell Creek and Tullock formations of Garfield County, northeastern Montana. Richness is represented as (1) raw numbers of species at individual localities (filled circles); (2) standing species richness through the section (gray shade under solid line); and (3) number of singleton taxa not included in the standing species richness plot (white stars). The five most species rich localities of the Hell Creek Formation are labeled next to their corresponding filled circle. The Garbani local fauna also is labeled. For an explanation of the chronostratigraphic framework, see caption for Figure 2. K-Pg—Cretaceous-Paleogene boundary; Pu1–3—Puercan; NALMA—North American land mammal "age"; To1—Torrejonian.

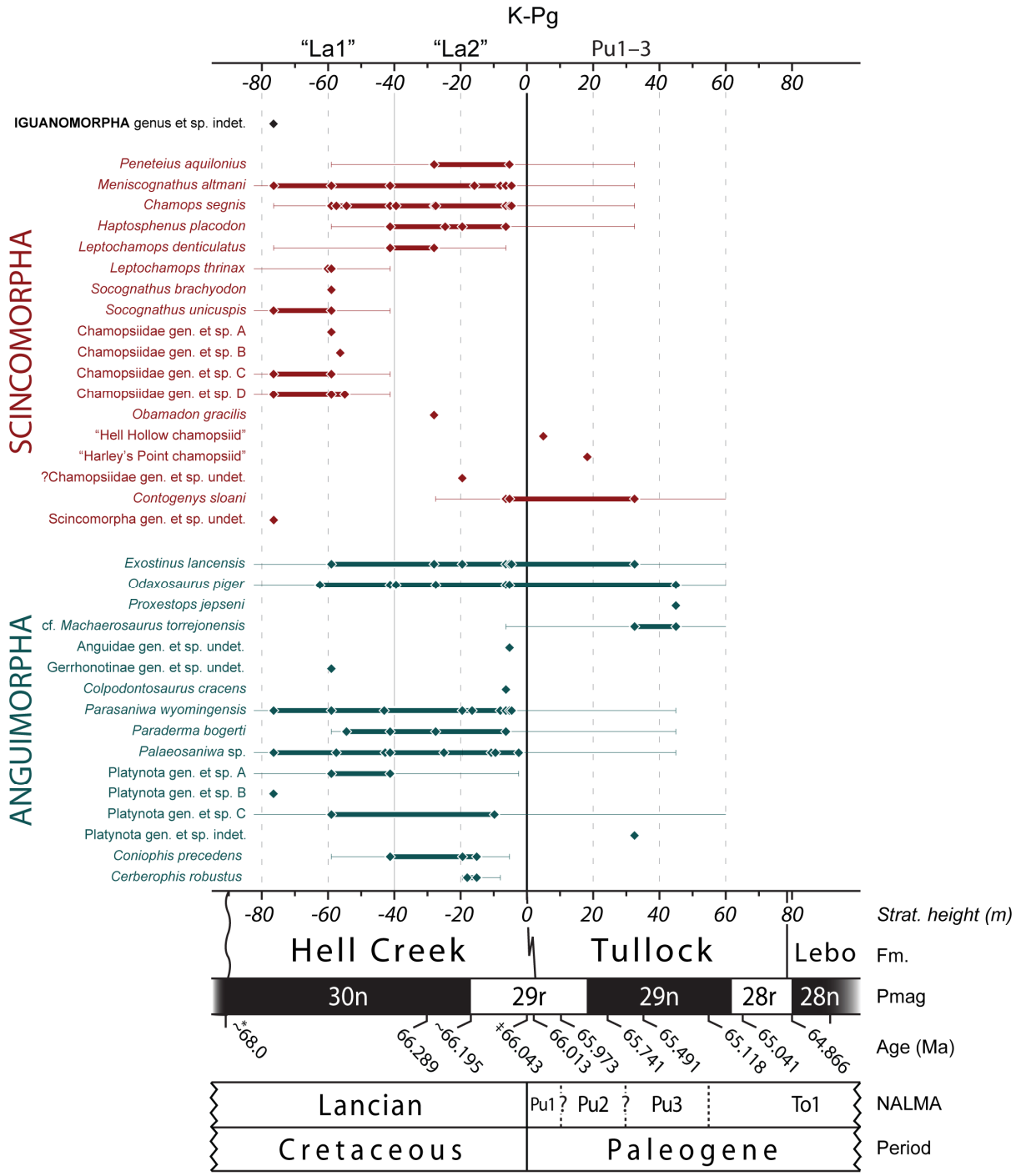

Figure 3.4. Biostratigraphic ranges with 50% confidence intervals for squamate species from the Hell Creek (Lancian) and Tullock formations (Puercan 1–3 [Pu1–3]) of Garfield County, northeastern Montana. Diamonds represent actual occurrences, thick lines represent inferred range-through occurrences, thin lines with vertical cross-bars represent 50% confidence

intervals, and thin lines without cross-bars indicate that the calculated confidence limit extends beyond the sampled interval. Colors represent the major taxonomic groups: **Black** = Iguanomorpha; **Red** = Scincomorpha; **Blue** = Anguimorpha. For an explanation of the chronostratigraphic framework, see caption for Figure 2. “La1” and “La2” refer to the informal subdivisions of the Lancian North American Land Mammal age (NALMA) per Wilson (2014). K-Pg—Cretaceous-Paleogene boundary; To1—Torrejonian; NALMA—North American land mammal “age”.

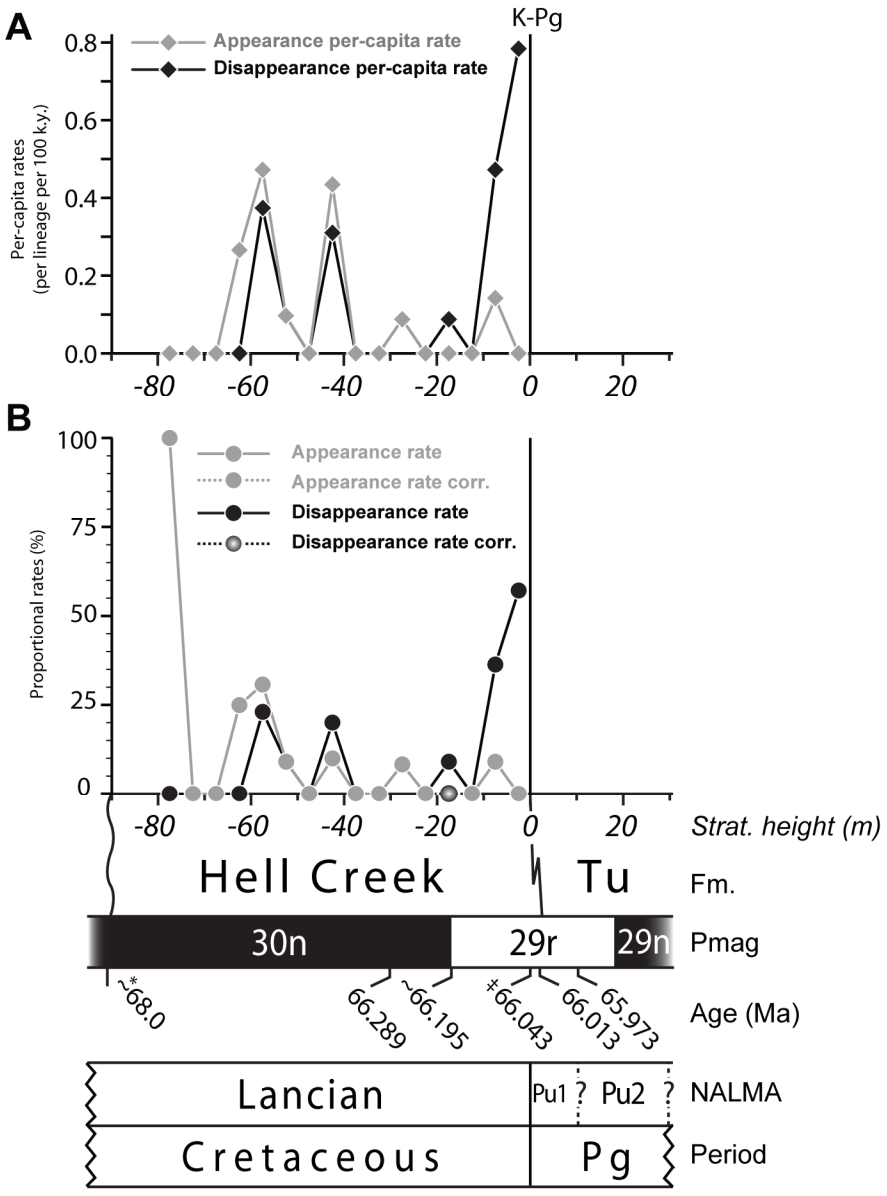

Figure 3.5. Per-capita rates (A) and proportional rates (B) of squamate turnover for 5 m bins through the Hell Creek Formation of Garfield County, northeastern Montana. Per-capita rates (diamonds) are in lineage-100-k.y. units. Proportional rates (circles) are presented as uncorrected (solid lines) and corrected (dashed lines) for inferred pseudo-extinction. For an explanation of the chronostratigraphic framework see caption for Figure 2. K-Pg—Cretaceous-Paleogene

boundary; Pg—Paleogene; Pu1 and Pu2—Puercan; NALMA—North American land mammal "age"; Tu—Tullock.

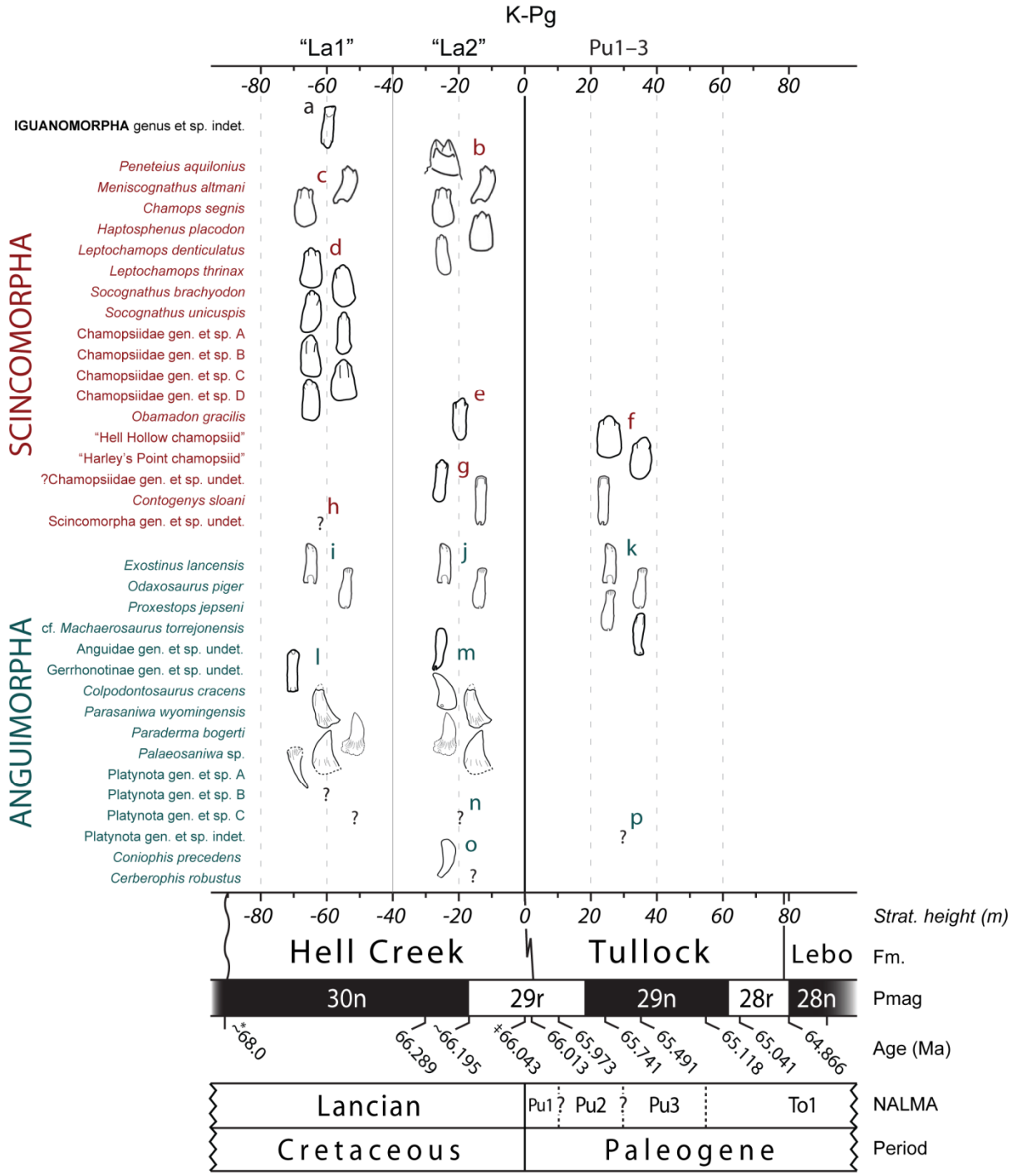

Fig. 3.6. Biostratigraphic distributions of squamate tooth types from the Hell Creek (Lancian) and Tullock formations (Puercan 1–3 [Pu1–3]) of Garfield County, northeastern Montana. Representative tooth outlines are from posterior teeth of the dentary except where noted. "La1"

and “La2” refer to the informal subdivisions of the Lancian North American Land Mammal age (NALMA) per Wilson (2014). Colors represent the major taxonomic groups: **Black** = Iguanomorpha; **Red** = Scincomorpha; **Blue** = Anguimorpha. Tooth outlines are staggered from left to right and top to bottom and are in line with their corresponding taxon listed to the left: **a**. Iguanomorpha genus et sp. indet. (maxillary tooth); **b**. *Peneteius aquilonius*, *Meniscognathus altmani*, *Chamops segnis*, *Haptosphenus placodon*, and *Leptochamops denticulatus*; **c**. *M. altmani* and *C. segnis*; **d**. *Leptochamops thrinax*, *Socognathus brachyodon*, *S. unicuspis*, Chamopsiidae gen. et sp. undet. A, B, C, and D; **e**. *Obamadon gracilis*; **f**. “Hell Hollow chamopsiid”, “Harley’s Point chamopsiid”, and *Contogenys sloani*; **g**. ?Chamopsiidae gen. et sp. undet. and *Contogenys sloani*; **h**. Scincomorpha gen. et sp. indet.; **i** and **j**. *Exostinus lancensis* and *Odaxosaurus piger*; **k**. *E. lancensis*, *O. piger*, *Proxestops jepseni*, and cf. *Machaerosaurus torrejonensis*; **l**. Gerrhonotinae gen. et sp. undet. (maxillary tooth), *Parasaniwa wyomingensis*, *Paraderma bogerti*, *Palaeosaniwa* sp., Platynota gen. et sp. undet. A (maxillary tooth), B, and C. **m**. Anguidae gen. et sp. undet., *Colpodontosaurus cracens*, *P. wyomingensis*, *P. bogerti*, and *Palaeosaniwa* sp.; **n**. Platynota gen. et sp. undet. C; **o**. *Coniophis precedens* and *Cerberophis robustus*; and, **p**. Platynota gen. et sp. indet. Tooth outlines of *P. aquilonius*, *M. altmani*, *C. segnis*, *H. placodon*, *L. denticulatus*, *C. sloani*, *E. lancensis*, *O. piger,* and *P. bogerti* are from Nydam 2002 (fig. 9 and references therein); *O. gracilis* after Longrich et al. (2012b); *C. cracens* and *P. wyomingensis* after Estes (1964); *Palaeosaniwa* sp. after Balsai (2001; *P. canadensis*); and, *C. precedens* after Longrich et al. (2012a); all others after personal photographs of type, proposed type, or referred specimens. Teeth are not to scale. For an explanation of the chronostratigraphic framework, see caption for Figure 3.2. K-Pg—Cretaceous-Paleogene boundary; To1—Torrejonian; NALMA—North American land mammal “age”.

TABLES for CHAPTER 3

Table 3.1. Systematic paleontology and faunal list of squamates from the Hell Creek and Tullock formations, Garfield County, northeastern Montana.

REPTILIA Linnaeus 1758
SQUAMATA Oppel 1811
IGUANOMORPHA Sukhanov 1961 (sensu Conrad 2008)
Genus and species indeterminate
SCINCOGEKKONOMORPHA Sukhanov 1961 (sensu Conrad 2008)
SCINCOMORPHA Camp 1923
CONTOGENIIDAE Nydam and Fitzpatrick 2009
Contogenys sloani Estes 1969
Family incertae sedis
Genus and species undetermined
BORIOTEIIOIDEA Nydam et al. 2007
CHAMOPSIIDAE sensu Nydam et al. 2010
Chamops segnis Marsh 1892
*Meniscognathus altmani** Estes 1964
Haptosphenus placodon Estes 1964
Leptochamops denticulatus Estes 1964
Leptochamops thrinax† Gao and Fox 1991
Socognathus unicuspis† Gao and Fox 1991
Socognathus brachyodon† Longrich et al. 2012b
Genus and species undetermined A
Genus and species undetermined B
Genus and species undetermined C
Genus and species undetermined D
?CHAMOPSIIDAE
Obamadon gracilis Longrich et al. 2012b
Genus and species undetermined
POLYGLYPHANODONTINAE Estes 1983
POLYGLYPHANODONTINI Nydam et al. 2007
Peneteius aquilonius Estes 1969a
ANGUIMORPHA Fürbringer 1900
XENOSAURIDAE Cope 1886
Exostinus lancensis Gilmore 1928

ANGUIDAE Gray 1825
Odaxosaurus piger (Gilmore 1928)
Proxestops jepseni Gauthier 1982
cf. *Machaerosaurus torrejonensis* Gilmore 1928
Genus and species undetermined
GERRHONOTINAE Tihen 1949
Genus and species undetermined
Family incertae sedis[1]
*Colpodontosaurus cracens** Estes 1964
PLATYNOTA Duméril and Bibron 1839
Family incertae sedis
Parasaniwa wyomingensis Gilmore 1928
Paraderma bogerti Estes 1964
Palaeosaniwa sp.
Genus and species undetermined A
Genus and species undetermined B
Genus and species undetermined C
Genus and species indeterminate
SERPENTES Linnaeus, 1758
*Coniophis precedens** Marsh 1892
Cerberophis robustus Longrich et al. 2012b

Taxa in bold are novel and await formal descriptions, diagnoses, and taxonomic nomenclature. Taxa indicated by an asterisk (*) are new to the Hell Creek Formation of the study area. Taxa indicated by a dagger (†) are new to the Hell Creek Formation, two of which (*L. thrinax*, *S. unicuspis*) also represent temporal range extensions from older Campanian age deposits of southern Alberta, Canada, central Wyoming, USA, or both (see text for details). Superscript 1 at Anguimorpha Family incertae sedis follows Nydam 2013b. See Figures A3.1–A3.20 for images of voucher specimens listed in the Appendix to *Chapter Three*.

Table 3.2. Taxonomic composition of lower ("La1") and upper ("La2") Hell Creek Formation squamate assemblages of Garfield County, northeastern Montana. "La1" and "La2" refer to the informal subdivisions of the Lancian North American Land Mammal age (NALMA) per Wilson (2014). Colors represent the major taxonomic groups: **Black** = Iguanomorpha; **Red** = Scincomorpha; **Blue** = Anguimorpha. Arrows indicate taxa ranging from the lower to upper divisions of the Hell Creek Formation. Singletons are indicated with an asterisk (*). A question mark (?) to the right of an arrow (→) indicates the likely continuation of *Socognathus unicuspis* and Scincomorpha gen. et sp. undet. based on their occurrences at the Bug Creek Anthills locality of the Hell Creek Formation, McCone County, Montana. See text for details.

Lower Hell Creek or "La1"		Upper Hell Creek or "La2"
Iguanomorpha gen. et sp. indet.*		
		Peneteius aquilonius
Chamops segnis	→	***Chamops segnis***
Meniscognathus altmani	→	***Meniscognathus altmani***
		Haptosphenus placodon
		Leptochamops denticulatus
Chamopsiidae A*		
Chamopsiidae B*		
Chamopsiidae C		
Chamopsiidae D		
Leptochamops thrinax		
Socognathus unicuspis	→	**?**
Socognathus brachyodon*		
		Obamadon gracilis
		?Chamopsiidae gen. et sp. undet.*
		Contogenys sloani
Scincomorpha incertae sedis*	→	**?**
Exostinus lancensis	→	***Exostinus lancensis***
Odaxosaurus piger	→	***Odaxosaurus piger***
		Anguidae gen .et sp. undet.*
Gerrhonotinae gen. et sp. undet.*		
		Colpodontosaurus cracens*
Parasaniwa wyomingensis	→	***Parasaniwa wyomingensis***
Paraderma bogerti	→	***Paraderma bogerti***
***Palaeosaniwa* sp.**	→	***Palaeosaniwa* sp.**
Platynota gen. et sp. A		
Platynota gen. et sp. B*		
Platynota gen. et sp. C	→	**Platynota gen. et sp. C**
		Coniophis precedens
		Cerberophis robustus

APPENDIX to CHAPTER 3:

SYSTEMATIC PALEONTOLOGY OF NEW SQUAMATES FROM THE HELL CREEK FORMATION, GARFIELD COUNTY, MONTANA AND A LIST OF VOUCHER SPECIMENS

Systematic Paleontology

Reptilia

Squamata

Iguanomorpha

Pleurodonta

Genus and species indet.

Fig. A3.1

Referred Specimen: UCMP 556732, anterior portion of right maxilla preserving four teeth and spaces for three others.

Locality and Horizon: Tuma locality (UCMP V99220 = MOR HC-583, UWBM C1103); lower third (−76.4 m) of Upper Cretaceous (Maastrichtian) Hell Creek Formation, Garfield County, northeastern Montana, USA

Known distribution: Known only from referred specimen locality and horizon.

Description: The right maxilla preserves the anterior portion of the nasal process and premaxillary process. The nasal process rises abruptly anteriorly. The labial surface of the maxilla is smooth with three superior alveolar foramina and three smaller ethmoidal foramina located mostly above and between the second and third superior alveolar foramina. In dorsal view, the premaxillary process has a sharp lingual crest (crista transversalis) and a labial crest along the top of the premaxillary process (external ramus) that merge distally with the nasal process to form the margins of a triangular-shaped depression. That depression houses the anterior inferior alveolar foramen (AIAF). Lingually, the nasal process is concave and the dorsal surface of the bone gently slopes lingually.

Four complete teeth, the bases of three others, and spaces for two more are preserved in UCMP 556732. Teeth are pleurodont in their mode of attachment with one half or more of each tooth attached to the lateral parapet of the maxilla. Cementum is lacking at their bases. Resorption pits are present at the bases of several teeth with the tooth at position two having been partially resorbed. Teeth are columnar and not mesiodistally expanded. The first and second preserved teeth (tooth positions two and three, respectively) are slightly procumbent. Teeth at tooth positions five and seven are nearly vertical in their orientation. The apex of the crown in tooth two is short and bluntly rounded and possesses an incipient mesial accessory cusp. The main apical cusp of the third tooth is tall, asymmetric, and hooked distally; the smaller mesial accessory cusp is separated from the main apical cusp by a shallow and narrow vertical lingual and labial groove. The crown of tooth five possesses a wear facet apically and lingually and the cusp pattern of that tooth could not be determined. Tooth seven is tricuspid featuring a well-developed main apical and mesial accessory cusp and a smaller distal accessory cusp. The main apical cusp is tall and slightly hooked distally; the mesial accessory cusp is prominent with a moderately deep labial and lingual groove separating it from the main cusp while the groove separating the distal accessory cusp is shallow and short.

Comments: Referral of UCMP 556732 to Iguanomorpha is tentative given that no unambiguous synapomorphies of that clade (e.g., Gauthier et al. 2012; *Chapter Five*) are present in the specimen. The referral is based principally on tooth morphology and similarities with extant iguanians and other putative Late Cretaceous iguanomorphs from North America (Gao and Fox 1996) and Mongolia (e.g., Gao and Hou 1995; Gao and Norell 2000). The teeth of UCMP 556732 most closely resemble those of two tentative indeterminate pleurodontan iguanians (see Nydam 2013) present in a partial maxilla (UALVP 29908) described by Gao and Fox (1996;

their Iguanidae* new genus and species A) from the upper Santonian–lower Campanian age Milk River Formation, Alberta, Canada and in a partial dentary (SMNH P1927.980; Iguanidae* new genus and species B) from the Maastrichtian age Frenchman Formation, Saskatchewan, Canada. These specimens and UCMP 556732 all possess high-crowned pleurodont teeth with crowns featuring an enlarged main apical cusp and clearly defined accessory cusps offset by lingual and labial grooves. The teeth of UCMP 556732 principally differ from those of the holotype dentary of *Pariguana lancensis* (Longrich et al. 2012), a recently described iguanian from the Maastrichtian age Lance Formation of Wyoming, in having taller main apical and accessory cusps and clearly defined labial and lingual grooves. Nydam (2013) considers the iguanian affinities of *P. lancensis* as tentative as do I (*Chapter Five*).

Scleroglossa

Scincomorpha

Borioteiioidea Nydam et al. 2007

Chamopsiidae sensu Nydam et al. 2010

Genus and species undetermined A

Fig. A3.2A–E

Diagnosis: A chamopsiid lizard that differs from other chamopsiids in having the following combination of characters: robust subdental shelf with medial process at the dentary symphysis; slit-like moderately deep sulcus dentalis; teeth subpleurodont, unevenly spaced, vary in size and orientation, are unicuspid with low “shoulders” and faint apical striae, and possess longitudinal

lingual grooves on either side of the central cusp that extend up to one half of the height of the tooth.

Proposed Holotype: UWBM 104445, partial right dentary with 13 teeth and the bases of four others.

Proposed Type locality and Horizon: Celeste's Magnificent Microsite (CMM; MOR HC-293 = UCMP V99369, UWBM C1115), lower third (−59.0 m) of Upper Cretaceous (Maastrichtian) Hell Creek Formation, Garfield County, northeastern Montana, USA

Known distribution: Known only from proposed type locality and horizon.

Description: The proposed holotype is a right dentary with a nearly complete tooth row missing the ventral margin and posterior region of the bone. The dentary is more or less straight in dorsal view but curves somewhat lingually at the symphysis. Laterally, the dentary is smooth and possesses six unevenly spaced ovoid inferior alveolar foramina that range in size; the anterior most four foramina are subequal in size whereas the fifth foramen is approximately double the size and more elongate. The sixth inferior alveolar foramen is tiny and immediately posterior to the fifth foramen. A moderate-sized ovoid pit is present near the dental parapet on the lateral side of the bone at the level of the last two teeth. It is unclear as to whether or not that feature is natural or preservational. The dental parapet is gently bowed ventrally. In medial view, the subdental shelf is well-developed, deepening posteriorly from the symphysis until tooth position nine and tapers abruptly thereafter to the end of the shelf. A robust medial process of the subdental shelf is present at the symphysis. A slit-like moderately deep sulcus dentalis is present between the base of the teeth and the labial side of the subdental shelf dorsally. Ventrally, the subdental shelf bears a spleniodentary articulation that extends anteriorly to the level of the ninth tooth position; that articulation forms a narrow but deep groove along the posteroventral surface

of the subdental shelf which differs from the flattened and smooth surface of UWBM 104470. The groove is visible in medial and ventral views. The ventral portion of the dentary is missing and thus the size and orientation of the Meckel's canal cannot be determined. The posterior extent of the intramandibular septum and the opening of the posterior interior alveolar foramen occur at the posterior end of the dentary below the last tooth at position 17.

The unicuspid dentary teeth are subpleurodont in their mode of attachment with a small amount of cementum at their base and unevenly spaced along the tooth row. The three mesial-most preserved teeth are mesiodistally narrow and straight and procumbent with a low central cusp. The more distal teeth generally are larger, have mesiodistally expanded bases, and vary significantly in orientation and size. The main central cusp of all but the mesial most two teeth is bordered by low mesial and distal "shoulders" adorned with weakly developed carinae. The carinae extend ventrolingually onto the lingual surface of the teeth for a short distance below the edges of the "shoulders". A long longitudinal lingual groove is present on either side of the main central cusp extending as far down as one half the height of the tooth (tooth position eight) to near the base of others (tooth position 15). In occlusal view, the main central cusp and carinae form a V-shaped apex. Lingually, the apex of the crown is faintly striated. Variation in crown height resulted in a sinuous occlusal surface. Slight apical and more prominent vertical labial wear facets are present on teeth at positions nine, 11, 13, and 15 indicating a shearing-style occlusion with the maxillary teeth. The last tooth at position 17 is likely a replacement tooth given only the top of the crown has erupted.

Comments: UWBM 104445 shares a number of features in common with *Stypodontosaurus melletes* (Gao and Fox 1996) from the Scollard Formation of Alberta including the elongate but robustly built nature of the dentary, the shape of the subdental shelf, and the presence of the

robust mesial process at the symphysis. However, it differs in overall size, tooth form, and in morphological and spatial details of the spleniodentary articulation. UWBM 104445 may represent a new smaller species of *Stypodontosaurus* but currently is assigned only to Chamopsiidae.

Genus and species undetermined B

Fig. A3.2F–H

Diagnosis: A chamopsiid lizard that differs from other chamopsiids in having the following combination of characters: dentary shallow; moderately deep subdental shelf with weak symphysis and small medial expansion; sulcus dentalis narrow and moderately deep; shallow Meckel's canal; teeth subpleurodont, tall, unicuspid, widely and evenly spaced, increase in height and mesiodistal girth distally, possess shallow longitudinal grooves on more distal teeth, and have weak vertical striae lingually at the crown apex..

Proposed Holotype: UCMP 555268, a partial right dentary preserving five complete teeth and the bases of six others.

Proposed Type locality and Horizon: Mo-Hill (UCMP V99230 = MOR HC-598, UWBM C1113), lower third (−56.3 m) of Upper Cretaceous (Maastrichtian) Hell Creek Formation, Garfield County, northeastern Montana, USA

Known distribution: Known only from proposed type locality and horizon.

Description: UCMP 555268 is a right dentary preserving the anterior portion of the jaw anterior to the posterior interior alveolar foramen. The dentary is relatively shallow dorsoventrally. In dorsal view, the dentary is basically straight but curves medially near the symphysis; the lateral

and medial margins of the dentary curve in concert at tooth positions 1–3. Laterally, the bone is smooth and possesses five unevenly-spaced, rounded to ovoid inferior alveolar foramina that increase in size posteriorly. The three anterior most foramina are closely spaced to one another; the fourth and fifth foramina are separated farther from each other than the third foramen is from the fourth. The fifth inferior alveolar foramen is set within a shallow ovoid depression. The dental parapet is approximately straight in lateral view. Medially, the subdental shelf is well developed, moderately deep (e.g., deeper than in UCMP 556701 [4] but shallower than in DD23 [1]) and gently bowed ventrally. The subdental shelf twists such that anteriorly its medial surface is visible in dorsal view whereas posteriorly that surface is hidden by the dorsal ridge bordering the sulcus dentalis. The shelf is deepest just anterior to the ventral spleniodentary articulation at the level of the seventh and eighth tooth positions; the shelf gently rises towards the symphysis just anterior to that point. The spleniodentary articulation on the ventral face of the subdental shelf is narrow anteriorly and widens posteriorly where it is partially separated from the intramandibular septum by a narrow groove. The symphysis is weakly developed with a small medial expansion at the anterior end of the subdental shelf. A narrow and moderately deep sulcus dentalis borders the bases of the teeth medially. Meckel's canal is relatively shallow in comparison to that of other chamopsiids such as *Chamops segnis* (see Estes 1964, pl. 2 bottom) but more similar in depth to those in *Gerontoseps irvinensis* and *Leptochamops thrinax* (e.g., see Gao and Fox 1996, figs. 14b and 16b, respectively). The Meckelian canal anterior to the spleniodentary articulation is relatively narrow and elongate opening mostly medially and only slightly ventrally; the ventral margin of the dentary curves medially towards a plane nearly in line with the medial edge of the subdental shelf.

The teeth are robustly built, tall, unicuspid, and widely spaced. They are subpleurodont in their mode of attachment with > one half of the tooth above the lateral parapet of the jaw. The broken off crowns reveal the teeth to be thick walled when viewed from above. The base of the first tooth is mesiodistally narrow and oval in horizontal cross section with the more distal teeth increasing in diameter and becoming more subcircular. The preserved more distal teeth increase in crown height and mesiodistal girth distally. The mesial most of these teeth at tooth position six is relatively straight and narrow with weakly expanded mesial and distal sides; the more distal teeth progressively become slightly more barrel shaped. The crowns are unicuspid with low mesial and distal "shoulders" adorned with faint carinae that descend from the apex of the main central cusp and curve ventrolingually onto the lingual side of the tooth. The main central cusp at the 7^{th}–10^{th} tooth positions is asymmetric with a longer distally slanted leading edge and a shorter more vertical but mesially oriented distal edge. Bordering the main central cusp on the lingual side of the teeth are shallow longitudinal grooves that widen and extend farther down in the more distal teeth. The tips of the crowns have weak vertical striae lingually A small vertical distolabial wear facet is present on the sixth tooth whereas in the largest tooth at position ten a much smaller wear facet is present on the distal side of the apex of the crown. The bases of the teeth are heavily cemented and lack basal foramina or resorption pits suggesting tooth replacement has ceased and that this specimen is from an adult individual (Nydam et al. 2000; Nydam and Cifelli 2002).

Comments: UCMP 555268 most closely resembles *Gerontoseps irvinensis* from the Campanian age Oldman Formation, Alberta, Canada (Gao and Fox 1991, 1996) but varies in several details of the dentary (e.g., less convex medial and lateral sides in dorsal view) and teeth (e.g., apex of crown asymmetric versus symmetric in *Gerontoseps*). UCMP 555268 may represent a new

species of *Gerontoseps*, but currently is identified as an undetermined genus and species of chamopsiid.

Genus and species undetermined C

Fig. A3.3A–D

Diagnosis: A chamopsiid lizard that differs from other chamopsiids in having the following combination of characters: subdental shelf shallow with parallel dorsal and ventral margins extending along its length; symphysis weakly developed; sulcus dentalis shallow and restricted to symphyseal region; Meckel's canal moderately deep; teeth subpleurodont, unicuspid with a tall central cusp, columnar, unevenly spaced, vary in height and circumference, and lack apical longitudinal striae.

Proposed Holotype: UCMP 235674, partial right dentary preserving four teeth, the bases of six others, and spaces for two more.

Proposed Type locality and Horizon: Celeste's Magnificent Microsite (CMM; UCMP V99369 = MOR HC-293, UWBM C1115), lower third (−59.0 m) of Upper Cretaceous (Maastrichtian) Hell Creek Formation, Garfield County, northeastern Montana, USA

Referred specimens: UCMP 235668, posterior portion of left dentary preserving three teeth, the bases of two others, and spaces for two more. UCMP 235675, partial left maxilla preserving four teeth and the base of another.

Known distribution: Proposed holotype and Tuma (UCMP V99220 = UWBM C1103, MOR HC-583) localities, lower third of the Hell Creek Formation, Garfield County, northeastern Montana, USA

Description: UCMP 235674 is a partial right dentary broken anterior to the posterior interior alveolar foramen and missing the posterior portion of the ventral border of the bone. Laterally, the dentary is smooth and possesses eight unevenly spaced round to ovoid inferior alveolar foramina. Anteriorly, the foramina are paired with each pair consisting of a larger anterior and a smaller posterior foramen. The dental parapet is nearly straight and only slightly bowed ventrally in lateral view. The ventral border of the dentary is bowed ventrally along its preserved length. Medially, the subdental shelf is shallow with dorsal and ventral margins extending essentially parallel to each other along its preserved length. The shelf is gently bowed ventrally for most of its length but ascends abruptly near the symphysis anteriorly. The symphysis is weak lacking a thick ventral bony buttress or a robust medial process of the subdental shelf as seen in some chamopsiids such as *Socognathus* and *Stypodontosaurus* (see also UWBM 104455), respectively. The sulcus dentalis is shallow and restricted to the symphyseal region of the dentary. A shallow groove for the spleniodentary articulation extends anteriorly to the level of the seventh tooth position. Posteriorly, the groove remains shallow, unlike in UWBM 104445, and extends onto the ventral surface of the subdental shelf where it is slightly exposed medially. Meckel's canal is broad along the preserved portion of the bone.

The preserved teeth are unicuspid with a tall sharply pointed central cusp and low mesial and distal "shoulders" adorned with faint carinae extending ventrolingually a short distance from the apex of the central cusp. The tips of the crowns are labiolingually compressed and gently point lingually. Teeth are tall and mesiodistally narrow with a minimal amount of cementum at their base. In lateral view the cementum is visible above the dental parapet at tooth positions 7–10. No apical striae are present on the crowns. The teeth vary in height and in circumference and horizontal cross-sectional shape (subcircular to ovoid) along the tooth row as seen in occlusal

view from the broken bases of several teeth. The lingual face of each tooth is nearly flat or is gently expanded lingually. A large resorption pit is present at the base of tooth nine. A tall vertical wear facet is present on the mesiolabial side of tooth six. The teeth are not crowded and unevenly spaced along the tooth row.

Genus and species undetermined D

Fig. A3.3E–H

Diagnosis: A chamopsiid lizard that differs from other chamopsiids in having the following combination of characters: moderately deep and abruptly tapering subdental shelf; teeth subpleurodont and monocuspid with weakly developed "shoulders"; teeth also are approximately evenly spaced, slightly barrel shaped to straight sided, vary in height, circumference, and orientation with most slanting distally.

Referred specimen: Partial left dentary (UCMP 235669) preserving eight teeth and the base of another; partial left dentaries (UCMP 235679 and UWBM 104458).

Known distribution: Tuma (UCMP V99220 = MOR HC-583, UWBM C1103), Celeste's Magnificent Microsite (CMM; UCMP V99369 = MOR HC-293, UWBM C1115), and Impossible Ridge (UWBM loc. C1401) localities, all from lower third of the Upper Cretaceous (Maastrichtian) Hell Creek Formation, Garfield County, northeastern Montana, USA

Description: UCMP 235669 is a partial left dentary preserving the posterior portion of the bone. The ventral margin of the dentary is missing. Laterally, the dentary is smooth and possesses two ovoid inferior alveolar foramina. The subdental shelf is moderately robust at the mesial most end of the preserved specimen but tapers abruptly distally. A shallow and narrow sulcus dentalis is

present. Ventrally, the subdental shelf is grooved for articulation with the splenial. Although the anterior portion of the dentary is missing it is apparent that the splenial would have only extended mesially to within the posterior two thirds of the dentary (Fig. 3A.3H).

The teeth are borderline pleurodont with one half or more of the crown situated below the lateral parapet of the dentary. The teeth are monocuspid with a low central cusp and poorly developed "shoulders". The teeth vary in height, circumference, and orientation with most teeth slanted slightly distally. The larger teeth have gently expanded midshafts mesiodistally; whereas the smallest teeth are straight sided. The teeth are not crowded and are approximately evenly spaced along the tooth row. A moderate amount of cementum is present at the tooth bases. The broken shaft of the tooth at the second preserved tooth position shows that the tooth is thick walled.

?Chamopsiidae

Genus and species undetermined

Fig. A3.3I–L

Diagnosis: A small possible chamopsiid lizard that differs from other chamopsiids in having the following combination of characters: subdental shelf extremely shallow; sulcus dentalis absent; tongue-in-groove spleniodentary articulation poorly developed or absent; teeth nearly pleurodont, vary in height, circumference, orientation, and curvature, and are closely spaced; tooth row sinuous across apex of teeth; tooth crowns lack striae and possess well-defined mesial and distal "shoulders".

Proposed Holotype: UWBM 104470, a nearly complete left dentary preserving 9 teeth, the bases of 4 others, and space for one more.

Proposed Type locality and Horizon: Hot Feet (UWBM C1529 = DMNH 3305), upper third (−19.5 m) of Upper Cretaceous (Maastrichtian) Hell Creek Formation, Garfield County, northeastern Montana, USA

Known distribution: Known only from proposed type locality and horizon.

Description: UWBM 104470 is an elongate and gracile left dentary missing the symphyseal and posterior portions of the bone. The dentary is straight when viewed from above. Laterally, the dentary is smooth and possesses five rounded inferior alveolar foramina. The two anterior foramina are much smaller than those more posteriorly and are closely spaced and vertically offset from each other. The posterior foramina are approximately evenly spaced and are around mid-height of the dentary. The posterior-most inferior alveolar foramen is positioned between the second and third complete teeth from the rear of the bone. In lateral view, the dorsal margin of the dental parapet and ventral margin of the dentary are bowed ventrally. Medially, the dentary possesses a weakly developed and gently bowed shallow subdental shelf that is slightly deeper anteriorly. The dorsal border of the shelf lacks a sulcus dentalis. Ventrally, the subdental shelf bears a weakly-developed narrow and anteriorly tapering shallow depression for the dorsal spleniodentary articulation, which terminates anteriorly beneath and below the mesial-most complete teeth from the front of the jaw (tooth positions three and six). Posteriorly, that articular surface is flattened and extends to the end of the preserved shelf twisting onto the ventrolingual surface of the shelf becoming visible in medial view below tooth positions 11–14 (i.e., distal-most three and a half teeth). Thus, the splenial abuts the subdental shelf ventrally and appears to lack tongue-in-groove (Nydam et al. 2010) or slot-and-ridge spleniodentary articulation present in chamopsiids (e.g., *Socognathus brachyodon*; Longrich et al. 2012). The posterior interior alveolar foramen opens into the Meckel's canal ventral to the subdental shelf and between tooth

positions 12 and 13. Meckel's canal is restricted and slit-like anterior to the spleniodentary articulation but widens somewhat posteriorly becoming moderately deep but less so than in *Champs* and *Leptochamops*; the canal opens mostly medially.

The teeth are borderline pleurodont in their mode of attachment with slightly more than one half of the crown above the lateral parapet of the dentary. Variation in tooth size, curvature, and orientation occurs along the tooth row. The mesial-most teeth at positions three and six are recurved or bent while the remaining teeth are straight. Crown height varies resulting in a sinuous occlusal surface. The crowns lack striae and are unicuspid, with a central main cusp and well-defined mesial and distal "shoulders" and faint carinae that curve ventrolingually onto the lingual surface of the crown. The teeth are closely spaced but do not touch each other. Basal foramina are absent and only a small amount of cementum is present. Four of the 9 complete teeth have large resorption pits at their bases indicating active tooth replacement. Two teeth possess wear facets that are largely restricted to the occlusal surface of the tooth, unlike those seen in the undetermined chamopsiids described above (i.e., UWBM 104455 and UCMP 235674) suggesting differences in diet or food processing.

Comments: UWBM 104470 may not represent a chamopsiid due to the apparent lack of a tongue-in-groove or slot-and-ridge spleniodentary articulation (Nydam et al. 2010; Longrich et al. 2012). Similarities of this jaw with fossil lacertids from the Eocene of Europe (e.g., *Plesiolacerta lydekkeri*; see Rage 2013, fig. 3c) suggest UWBM 104470 may represent a Cretaceous lacertid though additional study and comparison is needed before this hypothesis can be accepted.

Family incertae sedis

Genus and species undetermined

Fig. A3.4

Diagnosis: A small scincomorph lizard that differs from other Late Cretaceous scincomorphs in having the following combination of characters: subdental shelf moderately robust; weak symphysis; sulcus dentalis extremely narrow and shallow; ventral border of dentary flattened; Meckel's canal constricted and ventrally directed along its length.

Referred specimens: UCMP 235670, partial left dentary preserving a single complete tooth, the bases of seven others, and space for one more. UCMP 235671, a partial right dentary with four complete teeth and the bases of two others. UCMP 235672, partial right dentary with one complete tooth, the bases of seven others, and space for one more.

Locality and Horizon: Tuma (UCMP V99220 = MOR HC-583, UWBM C1103), lower third (−76.4 m) of Upper Cretaceous (Maastrichtian) Hell Creek Formation, Garfield County, northeastern Montana, USA

Known distribution: Reliably known only from the Tuma locality. Also known from the Bug Creek Anthills locality, Hell Creek Formation, McCone County, Montana (see below).

Description: UCMP 235670 is approximately the anterior half of a left dentary preserving a single unicuspid tooth at the sixth tooth position. The dentary is low and elongate with the ventral margin of the bone being nearly parallel along its length with the dental parapet of the jaw. Laterally, the dentary is smooth with four nearly equally spaced inferior alveolar foramina. Medially, the subdental shelf is well developed with approximately parallel dorsal and ventral margins; its deepest point being just posterior to the complete sixth tooth. Anteriorly, the shelf

gently rises toward the weak symphysis. Posterior to the level of the complete tooth, the ventral border of the dentary slightly widens and becomes flat when viewed ventrally. Anterior to that region, the ventral margin is thin and ridge like. The ventromedial border of the dentary and the ventrolateral margin of the subdental shelf are narrowly separated along their length thus forming a narrow Meckel's canal that is open ventrally and slightly medially. The sulcus dentalis is extremely narrow and shallow.

The single preserved tooth is unicuspid and not swollen mesiodistally or expanded lingually. Faint ridges extend down from the apex onto the mesial and distal low "shoulders" of the crown. Striae are absent. In occlusal view, the bases of the teeth increase in diameter and become subcircular rather than ovoid as they are mesially. The bases of the teeth are closely spaced indicating little separation among the crowns.

Comments: None of the available specimens of this taxon are sufficient for designating a holotype but provide enough morphological evidence to support the novelty of it. The flattened ventral margin of the dentary and the slit-like, ventrally-directed Meckel's canal are atypical of chamopsiids and thus UCMP 235670 likely does not belong to that clade. A second occurrence of this taxon from the Bug Creek Anthills of the Hell Creek Formation, McCone County, Montana is based on an uncatalogued and undescribed specimen from the UALVP collections (personal observation, April 2014).

Anguimorpha

Anguidae

Genus and species undetermined

Fig. A3.5

Diagnosis: A small anguid lizard that differs from other anguids in having the following combination of characters: ventrolateral margin of dentary adorned with an approximately horizontal ridge that delineates the dorsolateral face of the bone from the ventrolateral portion; tooth shafts gently expanded lingually; tooth crowns bluntly rounded and lack vertical striae apically.

Proposed Holotype: UCMP 235684, a partial left dentary preserving six teeth, the bases of two others, and spaces for three more.

Proposed Type locality and Horizon: Flat Creek 5 (UCMP V73087 = UWBM C1614), upper third (−5.2 m) of Hell Creek Formation, Garfield County, northeastern Montana, USA

Known distribution: Known only from proposed type locality.

Description: UCMP 235684 is a partial left dentary missing the symphyseal and posterior regions of the bone. In dorsal view the dentary is straight curving only slightly medially starting at the level of the mesial-most vacant tooth space. Laterally, the dentary is smooth with four anteroposteriorly elongate inferior alveolar foramina, the first of which preserving only the posterior half. The dental parapet is straight along its length; the ventral margin of the dentary descends at a shallow angle posteriorly and is straight. Near the base of the dentary is a narrow approximately horizontal ridge that delineates the dorsolateral face of the bone from the ventrolateral portion. That ridge extends for about one half of the length of the preserved

specimen below the first three inferior alveolar foramina. Posteriorly, the ventral margin of the dentary is flat and partially overlaps anteroposteriorly with the ventrolateral ridge described above. Medially, the subdental shelf is broken along its ventral margin for its entire length and likely had a steep face as determined from the angle at which the teeth are implanted near their base. Because of said breakage, the presence, size, or morphology of the notch for the anterior inferior alveolar foramen (internal mental foramen of Estes 1964) of the subdental shelf cannot be determined. Also evident is the lack of a sulcus dentalis. In ventral view, at the posterior extent of the dentary, the intramandibular septum possesses a free ventral margin like in other anguids. Although the dentary is incomplete, it is evident that the intramandibular septum is attached to the lateral wall of the dentary posterior to mid-length of the tooth row as in *Odaxosaurus piger* but unlike that in *O. priscus* (Gao and Fox 1996) and that the Meckelian canal is restricted and oriented ventrally.

The teeth are pleurodont in their mode of attachment (~ one fourth of tooth height above dental parapet). The mesial most three teeth are slightly procumbent; the distal most tooth is vertically oriented. Apically, the crowns are mesiodistally compressed and bluntly rounded in lingual or labial views. No apical striae are present. A faint mesiodistal ridge is present on the last tooth but it is slightly worn with a rounded wear facet distally. The teeth are weakly expanded lingually lacking the prominent lingual expansion present in both currently recognized species of *Odaxosaurus* (Estes 1964; Gao and Fox 1996). Basal foramina are present in all teeth.

Gerrhonotinae

Genus and species undetermined

Fig. A3.6

Diagnosis: A small gerrhonotine anguid lizard that differs from other anguids in having the following combination of characters: maxillary and dentary teeth non-striated; dentary subdental shelf possesses a mesially deep notch forming the dorsal, anterior, and much of the ventral margins of the anterior inferior alveolar foramen; subdental shelf anterior to the subdental shelf notch relatively tall and nearly equal in height to the tooth attachment surface of the dentary.

Proposed Holotype: UCMP 235676, partial right dentary preserving four nearly complete teeth, one partial tooth, and spaces for two others.

Proposed Type locality and Horizon: Celeste's Magnificent Microsite (CMM; UCMP V99369 = MOR HC-293, UWBM C1115), lower third (−59.0 m) of Upper Cretaceous (Maastrichtian) Hell Creek Formation, Garfield County, northeastern Montana, USA

Referred Specimen: UCMP 235677, a partial right maxilla preserving four teeth, the bases of three others, and spaces for 2 more.

Known distribution: Only known from proposed type locality and horizon.

Description: UCMP 235676 is a partial right dentary from the posterior region of the bone. Labially, the dentary is smooth and possesses a single ovoid inferior alveolar foramen at about mid height. Lingually, the sulcus dentalis is absent and the subdental shelf is tall being approximately equal in height to the tooth attachment surface. A deep notch forming the dorsal, anterior, and much of the ventral margins of the anterior inferior alveolar foramen is present at the posterior end of the preserved portion of the subdental shelf. The deep subdental shelf and

the deeply notched subdental shelf are features differentiating UCMP 235676 from specimens of Cretaceous and Paleocene anguids of the Western Interior (see below). Ventrally, the subdental shelf and the ventral margin of the dentary are faceted for articulation with the splenial and are closely juxtaposed forming a narrowly open and ventrally directed Meckel's canal. The intramandibular septum, as seen in lingual and ventral views, has a free ventral border posteriorly as in other anguids.

The dentary teeth of UCMP 235676 are similar in form to those of the maxilla (UCMP 235677; see below) but differ in having approximately two thirds the height of the tooth below the lateral parapet of the jaw and thus are categorized as being pleurodont in their mode of attachment. The most complete tooth mesial to the subdental shelf notch is slightly worn but demonstrates that the crown in not striated and a small rounded central cusp is preserved. Lingually, the teeth are weakly expanded to nearly straight lacking the "strong, shoulder-like, medial expansion" denoted by Gao and Fox (1996, p. 71) in *Odaxosaurus piger* and *O. priscus*. A basal foramen is present at the base of at least the two mesial most teeth.

UCMP 235677 is a partial right maxilla preserving approximately the posterior half of the bone. The nasal process is largely missing. The region posterior to the nasal process dips at a shallow angle posteriorly (more steeply in *Odaxosaurus*) and is preserved with a flattened dorsal margin and with minimal breakage posteriorly. Labially, the maxilla is smooth and possesses four approximately evenly spaced rounded superior alveolar foramina. Three small rounded foramina are present in a triangular-shaped arrangement dorsal to the second superior alveolar foramen from the anterior end of the bone. No osteoderms are present on the labial surface of the maxilla as seen in some specimens of *Odaxosaurus piger* (e.g., see UALVP 29851 in Gao and Fox 1996, fig. 28C). Lingually, the supradental shelf is narrow dorsoventrally and dips ventrally

above the two distal-most tooth spaces; the lingual margin turns labially in that region thus forming a tapering posterior end as seen in dorsal and ventral views. The supradental shelf lacks a sulcus dentalis; the bases of the teeth meet the lingual edge of the supradental shelf. Two posterior inferior alveolar foramina are present which is characteristic of gerrhonotines (Meszoely 1970; Gao and Fox 1996).

The three most complete teeth in UCMP 235677 are positioned below the paired posterior inferior alveolar foramina and are subpleurodont in their mode of attachment. They are evenly spaced and not crowded and possess basal foramina at their bases except for the distal-most tooth. The fifth preserved tooth from the front of the maxilla has a large resorption pit at its base. The three best preserved teeth are approximately vertical in orientation (the more mesial tooth of that group is curved slightly distally) with nearly straight mesial and distal margins and their crowns are labiolingually compressed in mesial and distal views. The two broken and more distal teeth are gently hooked mesially. The complete and unworn crown of the middle tooth is chisel-shaped and possesses a short and blunt central cusp and two smaller mesial and distal cusps that are separated from each other by shallow longitudinal grooves labially and lingually. Unlike in *Odaxosaurus* and cf. *Gerrhonotus* sp., the crowns in UCMP 235677 are smooth and not striated. All teeth are weakly expanded lingually lacking the well-developed lingual expansion of *Odaxosaurus* spp. (see above).

Comments: The presence of two posterior inferior alveolar foramina in UCMP 235677 differs from that in both species of *Odaxosaurus* (*O. piger*, *O. priscus*) which possess a single large inferior alveolar foramen (Gao and Fox 1996). It is, however, similar to some extant species of *Gerrhonotus* and *Diploglossus* (see Meszoely 1970, fig. 7a, c). The presence of two posterior inferior alveolar foramina in cf. *Gerrhonotus* sp. described by Estes (1964) from the Lance

Formation of Wyoming cannot be determined as that taxon is solely based on partial dentaries. Likewise, specimens referred to cf. *Gerrhonotus* sp. from the Medicine Rocks local fauna of the middle Paleocene Tongue River Formation also are based on dentaries (Estes 1976). Longrich et al. (2012) list a maxilla (AMNH 15441) of "*Gerrhonotus*" sp. (= cf. *Gerrhonotus* sp. of Estes 1964) in their supplementary information (see their section 4c under Materials Studied) but did not provide a description, figure, or provenance of that specimen for comparison.

The subdental shelf anterior to the notch for the anterior inferior alveolar foramen is shallower in *O. piger*, *O. priscus*, cf. *Gerrhonotus* sp., and the undetermined anguid from the Milk River Formation, Alberta (e.g., see Estes 1964, fig. 56; Gao and Fox 1996, fig. 30b; Estes 1964, fig. 58; and Gao and Fox 1996, fig. 30g, respectively) as well as anguids from Paleocene localities of the Western Interior including the Paleocene cf. *Gerrhonotus* sp. (Estes 1976, fig. 5c), *Machaerosaurus torrejonensis* (e.g., Sullivan 1982, fig. 14; personal observation of AMNH 15911 and 12066), and *Proxestops silberlingi* (e.g., Sullivan 1991; personal observation of AMNH 2669; = *P. jepseni* of Gauthier 1982). The nearly complete left dentary with 6 complete teeth of "*Gerrhonotus*" sp. figured by Longrich et al. (2012, SI Appendix, section 4b, character 615, bottom) also has a much shallower subdental shelf. However, its specimen number or provenance is uncertain as it was not mentioned by Longrich et al. (2012). It may be the dentary listed as UCMP 49932 (see their SI Appendix, section 4c, Materials Studied), but according to Estes (1964, p. 122) that specimen number belongs to the anterior half of a right dentary with one tooth.

Platynota

Genus and species undetermined A

Fig. A3.7A–I

Diagnosis: A Late Cretaceous platynotan lizard that differs from all other platynotans in having the following combination of characters: maxilla possesses a network of mostly mesiodistally oriented sinuous ridges and grooves and a few small irregular-shaped bony rugosities dorsally; presence of multiple tiny foramina below superior alveolar foramina on labial side of maxilla; maxillary and dentary teeth non-trenchant, recurved, and fang-like with weakly developed mesial and distal non-serrated carinae.

Proposed Holotype: MOR 4109, a partial right maxilla preserving two teeth and bases and spaces for four more.

Proposed Type locality and Horizon: Celeste's Magnificent Microsite (CMM; MOR HC-293 = UWBM C1115, UCMP V99369), lower third (−59.0 m) of Upper Cretaceous (Maastrichtian) Hell Creek Formation, Garfield County, northeastern Montana, USA

Referred Specimen: UWBM 104469, a partial left dentary preserving one nearly complete tooth, the base of one other, and spaces for two more.

Known distribution: Proposed holotype and Hartless (UWBM C1153 = UCMP V82022) localities, lower half of the Hell Creek Formation, Garfield County, northeastern Montana, USA

Description: MOR 4109 is a partial right maxilla preserving approximately the middle third of the bone (between premaxillary process and posterior interior alveolar foramen, both of which are not preserved). The nasal process is broken near its base where it begins to curve lingually. Labially, the maxilla is ornamented with a network of mostly mesiodistally oriented sinuous

ridges and grooves and a few small irregular-shaped bony rugosities dorsally. This pattern differs from the thick hexagonal osteoderms present on the holotype maxilla of *Paraderma bogerti* (UCMP 54261; Estes 1964, fig. 64; see also Pregill et al. 1986, fig. 9 top). At the base of the ornamented surface are three unevenly spaced superior alveolar foramina. Below these foramina and along a dorsoventrally narrow strip, the maxilla is smooth and possesses several tiny foramina, many of which are connected to short and shallow grooves. Several of these tiny foramina also are found near the superior alveolar foramina within the lower third of the ornamented region. The anterior portion of the infraorbital canal is visible in anterior and lateral views; its posterior exit, the posterior interior alveolar foramen, is not preserved. Lingually, the supradental shelf is steeply inclined towards the base of the nasal process and is smooth dorsally. In ventral and dorsal views, the maxilla is nearly straight; the lingual margin of the subdental shelf curves slightly lingually towards the premaxillary process.

Teeth of maxilla are subpleurodont (> one half of tooth below lateral parapet of the maxilla) in their mode of attachment and possess infolded and complex plicidentine at their bases. A basal foramen is present at the base of each tooth on the distolingual side. Longitudinal striae extend apically from the base of each tooth to more than half of the length of the tooth and well past the lateral parapet of the jaw. The teeth are non-trenchant, unlike those in *Palaeosaniwa*, *Paraderma*, and *Parasaniwa*, and are moderately recurved distolingually and possess a weak carina along most of the length of the leading edge of the tooth; the tip of the unbroken tooth has a weak distal carina restricted to near the apex of the crown. Microserrations (as in *Palaeosaniwa*) and venom grooves (as in *Paraderma*) are absent. The teeth are more round than oval in horizontal cross section and taper apically to form a needle-like apex. The tip of the

crown on the mesial most preserved tooth is broken giving it a blunt appearance. The mode of tooth replacement is every other tooth (also seen in Platynota genus and species B; see below).

UWBM 104469 is a fragmentary left dentary preserving a nearly complete tooth and the base of another. The nearly complete tooth is missing its apex and is more round than oval in horizontal cross section, possesses a weak mesial carina, and is distolingually recurved. These features are all consistent with the proposed holotype maxilla (MOR 4109). Therefore, I tentatively refer this specimen to Platynota genus and species A.

Genus and species undetermined B

Fig. A3.7J–M

Diagnosis: A medium-sized Late Cretaceous platynotan lizard that differs from all other platynotans in having the following combination of characters: lateral surface of dentary perforated with numerous shallow pits and mesiodistally oriented narrow and shallow grooves; dentary possesses a sharp mesiodistally oriented ventrolateral ridge; labiolingually expanded teeth with a D-shaped horizontal cross section.

Proposed Holotype: MOR 3437, partial right dentary preserving the bases of six teeth and spaces for three more.

Proposed Type locality and Horizon: Tuma locality (MOR HC-583 = UCMP V99220, UWBM C1103); lower third (−76.4 m) of Upper Cretaceous (Maastrichtian) Hell Creek Formation, Garfield County, northeastern Montana, USA

Known distribution: Known only from referred specimen locality and horizon.

Description: MOR 3437 is a partial right dentary preserving approximately the posterior two-thirds of the bone. The mesial and distal-most portions of the dentary are missing. Labially, the dentary is smooth but perforated with numerous small pits, many of which are confluent with elongate shallow and narrow grooves. A single large and ovoid inferior alveolar foramen is found near the mesial end of the preserved portion of the dentary; it is approximately in line with the mesial-most first empty tooth space between the first and second preserved tooth bases. A second inferior alveolar foramen is partially preserved at the broken distal end of the bone and, based on its mesial and dorsal margins, also is ovoid. A prominent mesiodistally oriented ridge extends along the ventrolateral margin of the dentary which separates the pitted labial face of the bone from a smooth and pit-less ventromedially-directed ventral region of the dentary below the Meckel's canal. Lingually, the subdental shelf is steeply inclined, lacks a sulcus dentalis, and is broadly rounded lingually. The tooth attachment surface of the subdental shelf is approximately twice the height of the smooth ventral portion of the shelf. The tooth attachment surface narrows distally in dorsal view, a consequence of the lateral parapet of the jaw migrating lingually distally which begins to change orientation just distal to the level of the second tooth base. Consequently, the upper third of the lateral surface of the dentary above the level of the inferior alveolar foramina is exposed dorsolaterally. The Meckel's canal is directed mostly ventrally and slightly medially. Because the posterior region of the dentary is missing, the nature of the intramandibular septum could not be determined (i.e., did the septum have a free or fused ventral border as in the Late Cretaceous platynotans *Palaeosaniwa canadensis* or *Parasaniwa wyomingensis*, respectively?).

All dentary teeth are incomplete but preserve the characteristic platynotan infolded and complex plicidentine of the tooth bases. Only one tooth preserves the base of a crown and it is

near the distal portion of the tooth row. The external surface of the crown of that tooth is striated near its base with shallow longitudinal grooves. Where at least part of the base of a tooth is preserved, a small basal foramen is present on the distolingual side. A tooth replacement pattern of approximately every other tooth is present in MOR 3437. Although no complete teeth are preserved in MOR 3437, it is apparent that the teeth are pleurodont in their mode of attachment and are expanded at their bases. In occlusal view, the single partial crown of the tooth near the distal end of the tooth row is labiolingually expanded and D-shaped in horizontal cross-section; the flat side faces distally and the mesial side is convex mesially. The labiolingual expansion of this tooth differs from the more labiolingually compressed and trenchant distal teeth present in *Parasaniwa*, *Palaeosaniwa*, *Paraderma*, and *Labrodioctes* (Estes 1964; Gao and Fox 1996) but more similar to the problematic *Cemeterius monstrosus* (Longrich et al. 2012; provenance and institutional ownership of this specimen is under investigation by me).

Genus and species undetermined C

Fig. A3.8

Diagnosis: A large heavily armored platynotan lizard that differs from all other platynotans in having the following character: maxilla, frontals, and osteoderms possess nodose osteodermal ornamentation with small pores.

Proposed Holotype: Partial left maxilla (UWBM 104471) preserving the bases of two teeth and spaces for two others.

Proposed Type locality and Horizon: Lizard Flats locality (UWBM loc. C1492); upper third (–9.76 m) of Upper Cretaceous (Maastrichtian) Hell Creek Formation, Garfield County, northeastern Montana, USA

Referred Specimens: Partial right frontal (MOR 9101) and two osteoderms (MOR 4874). A partial left and partial right squamosal (BMRP 2007.4.4, 2006.4.306) of the Hell Creek Formation, Carter County, southeastern Montana (see Williamson et al. 2009a, b).

Known distribution: Proposed holotype and Celeste's Magnificent Microsite (CMM; MOR loc. HC-293 = UWBM loc. C1115, UCMP loc. V99369) localities, lower and upper third of the Hell Creek Formation, Garfield County, northeastern Montana, USA BM locs. 2007.1 and 2001.1 of the Hell Creek Formation, Carter County, southeastern Montana.

Description: UWBM 104471 is a left maxilla (Fig. A3.8A–D) preserving approximately the middle third of the bone. No teeth are preserved though the bases are plicidentine. Tooth replacement appears to be every other tooth. Externally the maxilla is ornamented with heavy, nodose osteoderms that are widely separated from each other. The osteoderms are perforated with numerous small pores. Ventral to the ornamented region of the maxilla and below the three preserved superior alveolar foramina it is smooth. The dorsal margin of the maxilla is nearly perpendicular to its lateral face. In lateral view the dorsal margin of the maxilla rises posteriorly at a low angle. Lingually, the maxilla is smooth below its roof and above the tooth row.

The frontals are paired as indicated by the thick midline suture of the right frontal (Fig. A3.8E). A prominent and deep prefrontal facet is present anterolaterally and below the roof of the frontal. The subolfactory process is broken anteriorly but deepens anteriorly below the prefrontal facet. The nodose ornamentation on the roof of the frontal occurs in three parallel rows extending anteroposteriorly.

The osteoderms (Fig. A3.8I–J) are nodose, rectangular, thick, and possess sutural margins. The central node on some osteoderms is keel-like in being enlarged, elongate, and taller than those surrounding it.

Comments: The nodose ornamentation of the maxilla, frontals, and osteoderms differ from those of the other known Late Cretaceous platynotans of North America. All others have flattened and fragmented osteoderms of the maxilla and other bones of the skull (Randall Nydam, pers. commun., Nov. 2015) including those of *Parasaniwa* (e.g., Gao and Fox 1996, figs. 32E, 33A, F), *Paraderma bogerti* (e.g., Gao and Fox 1996, fig. 35; Pregill et al. 1986, fig. 9), *Palaeosaniwa canadensis* (e.g., Balsai 2001), and *Labrodioctes montanensis* (Gao and Fox 1996, fig. 36B-H). Platynota gen. et sp. undet. C was a heavily armored platynotan, more so than in all of the other Late Cretaceous platynotans of North America.

Squamosals previously referred to a juvenile pachycephalosaur dinosaur (Williamson et al. 2009a, figs. 2, 4a) from the Hell Creek Formation of Carter County, southeastern Montana were later identified as belonging to an unrecognized anguimorph (Williamson et al. 2009b). These squamosals possess an identical nodose osteodermal pattern to the maxilla, frontal, and osteoderms noted here and, as such, are attributed to Platynota gen. et sp. undet. C. The referral of one of those squamosals (BMRP 2007.4.4) to *Exostinus lancensis* by Longrich et al. (2012; see Supplementary Information) is incorrect based on the current evidence.

Serpentes

Alethinophidia

Cerberophis robustus Longrich et al. 2012

Fig. A3.9A–E

Referred Specimen: UWBM 104198, partial cervical or anterior precloacal vertebra.

Locality and Horizon: From Mars (UWBM C1151), upper third (−14.5 m) of Upper Cretaceous (Maastrichtian) Hell Creek Formation, Garfield County, northeastern Montana, USA

Known distribution: Scrap Hill (UCMP V80096; type locality at ~ −18 m) and From Mars localities, Hell Creek Formation, Garfield County, northeastern Montana, USA

Description: UWBM 104198 is a partial cervical vertebra measuring 7.1 mm in anteroposterior length (measured between anterior cotyle and posterior condyle). The neural arch and portions of the centrum are missing. Anteriorly, the broken cotyle is deeply cupped. Posteriorly, the condyle is nearly round in posterior view and is separated from the centrum around its perimeter by a groove. A dorsally broad but ventrally narrow subcentral keel is present along the midline of the centrum which is perforated on both sides by two subcentral foramina, one at the base of the keel on the centrum and the other more ventrally placed and on the side of the keel. A well-developed hypapophysis is present at the posterior end of the keel anterior to the condyle. In lateral view, the hypapophysis has a nearly vertical posterior border and a posteriorly descending anterior border which is slightly bowed ventrally.

Discussion: Because of the fragmentary nature of UWBM 104198, its lacks the currently known diagnostic features of *Cerberophis robustus* (Longrich et al. 2012b; = Boidae indet. of Bryant 1989). However, it is referred to that taxon based on similarities in size (7.1 vs. 9 mm in length,

respectively), orientation of the posterior condyle (both facing posteriorly vs. dorsoposteriorly), and in possessing a groove that separates the posterior condyle from the centrum. Both UWBM 104198 and the holotype specimen (UCMP 130696 from UCMP loc. V80096 [Scrap Hill]) also possess a midline ventral keel of the centrum. However, unlike in the holotype, UWBM 104198 possesses an elongate hypapophysis typically found in the cervical series of snakes (Holman 2000; Polly et al. 2001; Smith 2013). Other slight differences arise in the shape and anteroposterior length of the posterior condyle; it is nearly round in posterior view with an equal height-to-width ratio (3.4 mm x 3.4 mm) and slightly more elongate in ventral view in UWBM 104198 versus slightly more dorsoventrally compressed and shorter in the holotype. UWBM also differs from the holotype in possessing a pair of subcentral foramina on both sides of the ventral keel; the holotype possesses only a single foramen to either side of the keel. These differences combined or individually most likely only represent minor variations in morphology exhibited along the vertebral column (i.e., cervical versus anterior trunk) and are not significant enough to eliminate it from belonging to *Cerberophis* let alone erect a new taxon.

The indeterminate boid vertebra (MCZ 3669) from the BCA locality descried and figured by Estes et al. (1969, fig. 4) likely belongs to *Cerberophis* based on overall similarities in morphology and size (centrum length = 8.8 mm).

VOUCHER SPECIMENS OF SQUAMATES FROM THE HELL CREEK FORMATION, GARFIELD COUNTY, NORTHEASTERN, MONTANA, USA

Chamopsiidae/*Chamops segnis*–Partial right maxilla (UCMP 235685, Fig. A3.10A–D) from UCMP loc. V80091 (Thomas 1); partial left maxilla (UWBM 104459) from UWBM loc. C1153 (Hartless, Fig. A3.10E–F); partial left dentary (UCMP 235681) from UCMP loc. V99370 (Just Past Celeste).

Chamopsiidae/*Meniscognathus altmani*–Partial left dentary (UCMP 555565, Fig. A3.10G–J) from UCMP loc. V99226 (Fahrenheit 109); partial left dentary (UWBM 104465) from UWBM loc. C1153 (Hartless); partial right maxilla (UCMP 191501) from UCMP loc. V99220 (Tuma).

Chamopsiidae/*Haptosphenus placodon*–Partial left mandible (UWBM 104460, Fig. A3.10K–N) from UWBM loc. C1153 (Hartless); partial right mandible (UWBM 104461) from UWBM loc. C1529 (Hot Feet).

Chamopsiidae/*Leptochamops denticulatus*–Partial left maxilla (UWBM 104464, Fig. A3.11A–D) from UWBM loc. C1153 (Hartless); partial left and right dentaries (UWBM 104463 and 104462, respectively, Fig. A3.11E–H and I–L), both from UWBM loc. C1153 (Hartless).

Chamopsiidae/*Leptochamops thrinax*–Partial left dentary (MOR 9100, Fig. A3.12A–D) from MOR loc. HC-1105 (How's the View); partial right dentary (UCMP 235678, Fig. A3.12E–H) from UCMP loc. V99369 (Celeste's Magnificent Microsite).

Chamopsiidae/*Socognathus brachyodon*– Partial right dentary (UCMP 556403, Fig. A3.13A–D) from UCMP loc. V99369 (Celeste's Magnificent Microsite).

Chamopsiidae/*Socognathus unicuspis*–Partial left dentary (UCMP 235673, Fig. A3.13G–J) from UCMP loc. V99220 (Tuma); partial left dentary (UCMP 235680, Fig. A3.13K–L) from UCMP loc. V99369 (Celeste's Magnificent Microsite).

Chamopsiidae/*Socognathus* sp. indet.–Partial left dentary (UCMP 235682, Fig. A3.13E–F) from UCMP loc. V99370 (Just Past Celeste); partial left dentary (UCMP 555294) from UCMP loc. V99218 (Andrei's Jaw); partial right maxilla (UWBM 91219, Fig. A3.13M–P) from UWBM loc. C1153 (Hartless).

Polyglyphanodontini/*Peneteius aquilonius* –Partial maxilla (UCMP 123325) described and figured in Nydam et al. (2000, fig. 1D-F) from UCMP loc. V73087 (Flat Creek 5); nearly complete right dentary (UCMP 124744) described and figured in Nydam et al. (2000, fig. 1A-C) from UCMP loc. V74116 (Baldy Butte SW-Blazing Saddle).

?Chamopsiidae/*Obamadon gracilis*–Partial right dentary (UCMP 128873) described and figured in Longrich et al. (2012b, fig. 1b and SI fig. S2) from UCMP loc. V74116 (Baldy Butte SW-Blazing Saddle).

Contogeniidae/*Contogenys sloani*–Partial dentaries (UCMP 130732, 130741) from UCMP locs. V73087 and V77130, respectively, listed in Nydam and Fitzpatrick (2009). UCMP 130732 also is a voucher specimen of Bryant (1989) which was based on Richard Estes's identification in 1984 (see UCMP online vertebrate collections database; accessed 17 November 2015). Longrich et al. (2012) re-identified UCMP 130732 as *Leptochamops denticulatus*. I have not seen UCMP 130732 but follow Bryant (1989) and Nydam and Fitzpatrick (2009) in retaining the original identification of that specimen as *C. sloani*.

Anguidae/*Odaxosaurus piger*–Partial left dentary (UWBM 104467, Fig. A3.14A–D) and maxilla (UWBM 104466, Fig. A3.14E–H) both from UWBM loc. C1153 (Hartless). Nearly

complete osteoderm commonly referred to *O. piger* (MOR 5838, Fig. A3.14K–L) from MOR loc. HC-293 (Celeste's Magnificent Microsite).

Xenosauridae/*Exostinus lancensis*–Partial left maxilla (UWBM 104456, Fig. A3.15) from UWBM loc. C1115 (Celeste's Magnificent Microsite).

Platynota/*Colpodontosaurus cracens*–Partial left dentary (UCMP 235683, Fig. A3.16A–D) from UCMP loc. V77130 (Hauso 1).

Platynota/*Parasaniwa wyomingensis*–Partial left dentary (UCMP 130742, Fig. A3.16E–F) from UCMP loc. V77130 (Hauso 1).

Platynota/*Paraderma bogerti*–Trunk vertebra (UWBM 104468, Fig. A3.16G–J) from UWBM loc. C1153 (Hartless).

Platynota/*Palaeosaniwa sp.*–Trunk vertebra (UCMP 130723, Fig. A3.16K–L) from UCMP loc. V82022 (Hartless); trunk vertebra (UCMP 128970) from UCMP loc. V75162 (Worm Coulee 5). UCMP 130723 also was listed by Bryant (1989, p. 48) as a voucher specimen but was identified as *P. canadensis*.

Serpentes/*Coniophis precedens*–Precloacal vertebrae (UWBM 104191, Fig. A3.9F–I) from UWBM loc. C1153 (Hartless); UWBM 94550 from UWBM loc. C1529 (Hot Feet); and UWBM 104197 from UWBM loc. C1151 (From Mars).

VOUCHER SPECIMENS OF SQUAMATES FROM THE TULLOCK FORMATION, GARFIELD COUNTY, NORTHEASTERN, MONTANA, USA

Chamopsiidae/Genus et sp. indet. ("Harley's Point chamopsiid")–Partial dentary fragment (UWBM 104472, Fig. A3.17A–C) from UWBM loc. C1367 (Harley's Point).

Chamopsiidae/Genus et sp. indet. ("Hell Hollow chamopsiid")–Single isolated tooth and part of a jaw (UCMP 235686, Fig. A3.17D–F) from UCMP loc. V74110 (Hell Hollow-Channel).

Contogeniidae/*Contogenys sloani*–Jaw (UCMP 130733) listed by Nydam and Fitzpatrick (2009, p. 679) from UCMP loc. V74122 (Biscuit Springs); dentary fragment (UCMP 130740) listed by Nydam and Fitzpatrick (2009) from UCMP loc. V74122 (Biscuit Springs). UCMP 130740 previously was listed as a voucher specimen of *Proxestops jepseni* by Bryant (1989, p. 47).

Contogeniidae/*Contogenys* sp.–Partial left dentary (UCMP 235687, Fig. A3.18) from UCMP loc. V74122 (Biscuit Springs).

Anguidae/*Odaxosaurus piger*–Partial right maxilla (UCMP 229335, Fig. A3.14I–J) from UCMP loc. V72129 (Garbani 04-NW-S Level 1).

Anguidae/*Proxestops jepseni*–Osteoderms (UCMP 192511) from UCMP loc. V74122 (Biscuit Springs).

Anguidae/cf. *Machaerosaurus torrejonensis*–Partial right dentary (UCMP 227950, Fig. A3.19) from UCMP loc. V73080 (Garbani 13-NW Harley's High).

Platynota/Genus et sp. indet.–Partial right dentary (UCMP 235688, Fig. A3.20) from UCMP loc. V74122 (Biscuit Springs).

REFERENCES CITED

Balsai, M. J. 2001. The phylogenetic position of Palaeosaniwa and the early evolution of the platynotan (varanoid) anguimorphs: In Earth and Environmental Sciences, Ph.D. dissertation, pp. 253. University of Pennsylvania, Philadelphia.

Bryant, L. J. 1989. Non-dinosaurian lower vertebrates across the Cretaceous-Tertiary boundary in northeastern Montana. University of California Publications in Geological Sciences 134:1–107.

Estes, R. 1964. Fossil vertebrates from the Late Cretaceous Lance Formation eastern Wyoming. University of California Publications in Geological Sciences 49:1–187.

Estes, R. 1976. Middle Paleocene lower vertebrates from the Tongue River Formation, southeastern Montana. Journal of Paleontology 50:500–520.

Estes, R., P. Berberian, and C. A. M. Meszoely. 1969. Lower Vertebrates from the Late Cretaceous Hell Creek Formation, McCone County, Montana. Breviora 337:1–33.

Gao, K., and R. C. Fox. 1991. New teiid lizards from the Upper Cretaceous Oldman Formation (Judithian) of southwestern Alberta, Canada, with a review of the Cretaceous record of teiids. Annals of Carnegie Museum 60:145–162.

Gao, K., and R. C. Fox. 1996. Taxonomy and evolution of Late Cretaceous lizards (Reptilia: Squamata) from western Canada. Bulletin of Carnegie Museum of Natural History 33:1–107.

Gao, K., and L. Hou. 1995. Iguanians from the Upper Cretaceous Djadokhta Formation, Gobi Desert, China. Journal of Vertebrate Paleontology 15:57–78.

Gao, K., and M. A. Norell. 2000. Taxonomic composition and systematics of Late Cretaceous lizard assemblages from Ukhaa Tolgod and adjacent localities, Mongolian Gobi Desert. Bulletin of the American Museum of Natural History 249:1–118.

Gauthier, J. A. 1982. Fossil xenosaurid and anguid lizards from the early Eocene Wasatch Formation, southeast Wyoming, and a revision of the Anguiodea. Contributions to Geology 21:7–54.

Gauthier, J. A., M. Kearney, J. A. Maisano, O. Rieppel, and A. D. B. Behlke. 2012. Assembling the squamate tree of life: Perspectives from the phenotype and the fossil record. Bulletin of the Peabody Museum of Natural History 53:3–308.

Holman, J. A. 2000. Fossil Snakes of North America: Origin, Evolution, Distribution, Paleoecology. 376 pp. Indiana University Press, Bloomington.

Longrich, N. R., B. A. S. Bhullar, and J. A. Gauthier. 2012. Mass extinction of lizards and snakes at the Cretaceous–Paleogene boundary. Proceedings of the National Academy of Sciences 109:21396–21401.

Meszoely, C. A. M. 1970. North American fossil anguid lizards. Bulletin of the Museum of Comparative Zoology 139:87–149.

Nydam, R. L. 2013. Squamates from the Jurassic and Cretaceous of North America. Palaeobiodiversity and Palaeoenvironments 93:535–565.

Nydam, R. L., M. W. Caldwell, and F. Fanti. 2010. Borioteiioidean lizard skulls from Kleskun Hill (Wapiti Formation; Upper Campanian), Westcentral Alberta, Canada. Journal of Vertebrate Paleontology 30:1090–1099.

Nydam, R. L., and R. L. Cifelli. 2002. A new teiid lizard from the Cedar Mountain Formation (Albian–Cenomanian Boundary) of Utah. Journal of Vertebrate Paleontology 22:276–285.

Nydam, R. L., J. G. Eaton, and J. Sankey. 2007. New taxa of transversely-toothed lizards (Squamata: Scincomorpha) and new information on the evolutionary history of "teiids". Journal of Paleontology 81:538–549.

Nydam, R. L., and B. M. Fitzpatrick. 2009. The occurrence of *Contogenys*-like lizards in the Late Cretaceous and Early Tertiary of the Western Interior or the U.S.A. Journal of Vertebrate Paleontology 29:677–701.

Nydam, R. L., J. A. Gauthier, and J. J. Chiment. 2000. The mammal-like teeth of the Late Cretaceous lizard *Peneteius aquilonius* Estes 1969 (Squamata, Teiidae). Journal of Vertebrate Paleontology 20:628–631.

Polly, P. D., J. J. Head, and M. J. Cohn. 2001. Testing modularity and dissociation: The evolution of regional proportions in snakes; pp. 307–335 in M. Zelditch (ed.), Beyond heterochrony: the evolution of development Wiley–Liss, New York.

Pregill, G. K., J. A. Gauthier, and H. W. Greene. 1986. The evolution of helodermatid squamates, with description of a new taxon and an overview of Varanoidea. Transactions of the San Diego Society of Natural History 21:167–202.

Rage, J.-C. 2013. Mesozoic and Cenozoic squamates of Europe. Palaeobiodiversity and Palaeoenvironments 93:517–534.

Smith, K. T. 2013. New constraints on the evolution of the snake clades Ungaliophiinae, Loxocemidae and Colubridae (Serpentes), with comments on the fossil history of erycine boids in North America. Zoologischer Anzeiger 252:157–182.

Sullivan, R. M. 1982. Fossil Lizards from Swain Quarry "Fort Union Formation," Middle Paleocene (Torrejonian), Carbon County, Wyoming. Journal of Paleontology 56:996–1010.

Sullivan, R. M. 1991. Paleocene Caudata and Squamata from Gidley and Silberling Quarries, Montana. Journal of Vertebrate Paleontology 11:293–301.

Williamson, T. E., T. D. Carr, S. A. Williams, and K. Tremaine. 2009a. Early ontogeny of pachycephalosaurine squamosals as revealed by juvenile specimens from the Hell Creek Formation, eastern Montana. Journal of Vertebrate Paleontology 29:291–294.

Williamson, T., K. Smith, S. Williams, G. I. Bennett, and K. Tremaine. 2009b. Putative young pachycephalosaur squamosals are from a lizard. Journal of Vertebrate Paleontology, Abstracts of Papers 29:201A.

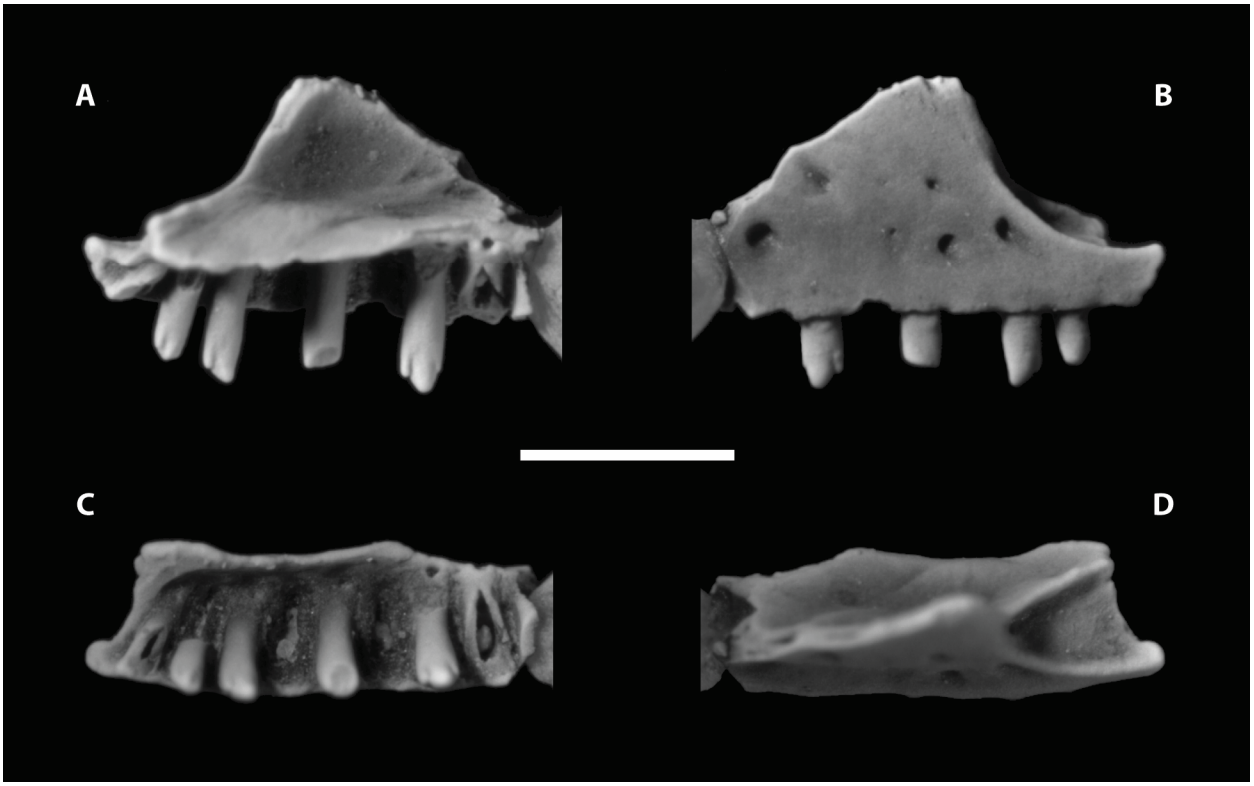

Figure A3.1. Iguanomorpha genus and species indeterminate from the Hell Creek Formation, Garfield County, northeastern Montana. An anterior fragment of a right maxilla (UCMP 556732) from UCMP loc. V99220 in lingual (**A**), labial (**B**), ventral (**C**), and dorsal (**D**) views. Scale bar equals 1 mm.

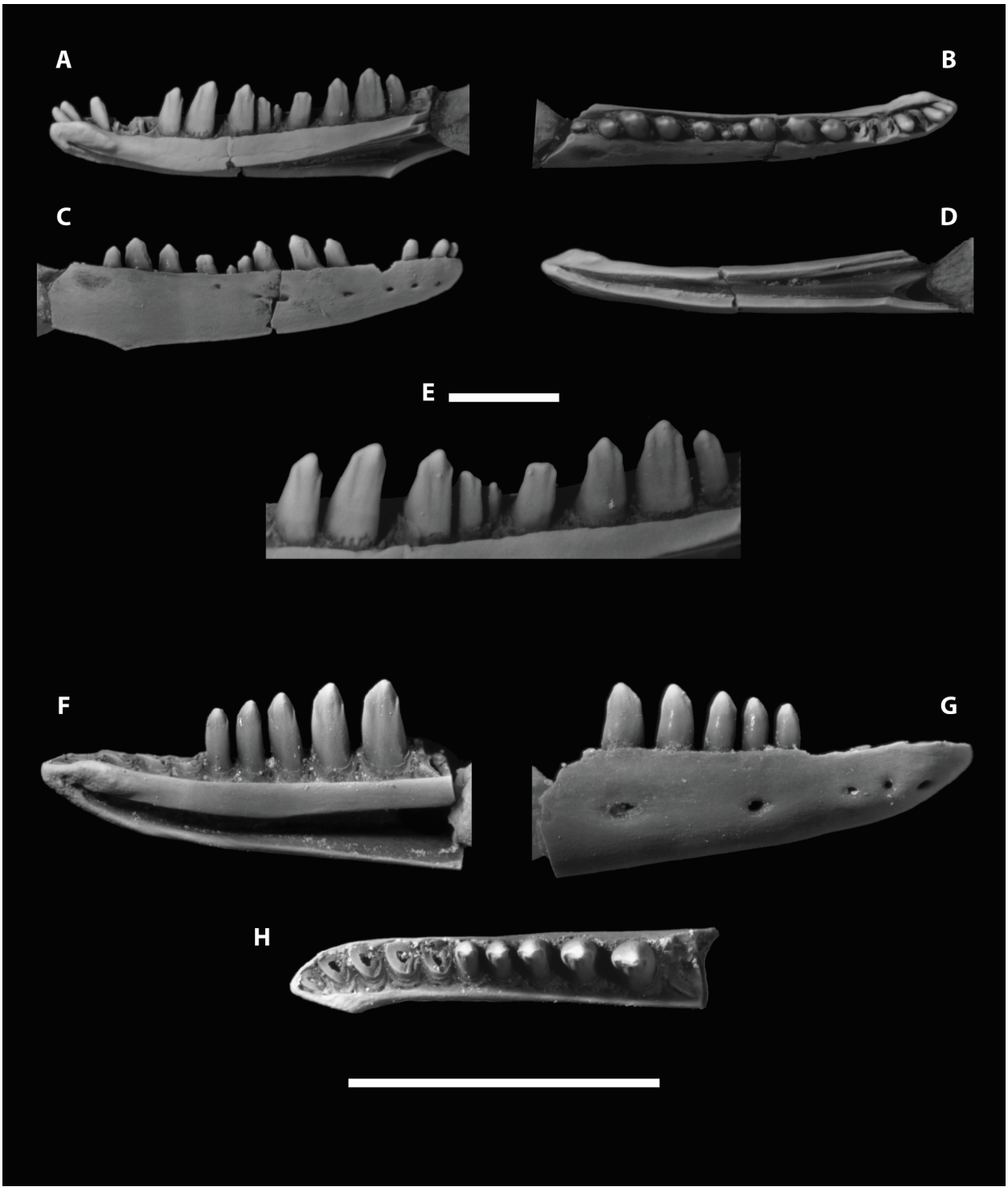

Figure A3.2. Chamopsiidae from the Hell Creek Formation, Garfield County, northeastern Montana. Genus and species undetermined A: proposed holotype partial right dentary (UWBM 104455) from MOR loc. HC-293 in lingual (**A**), dorsal (**B**), labial (**C**), and ventral (**D**) views;

close-up of distal teeth in lingual (**E**) view. Genus and species undetermined B: proposed holotype partial right dentary (UCMP 555268) from UCMP loc. V99230 in lingual (**F**), labial (**G**), and dorsal (**H**) views. Scale bar at E equals 1 mm. Scale bar for all others (**A**–**D**, **F**–**G**) equals 5 mm.

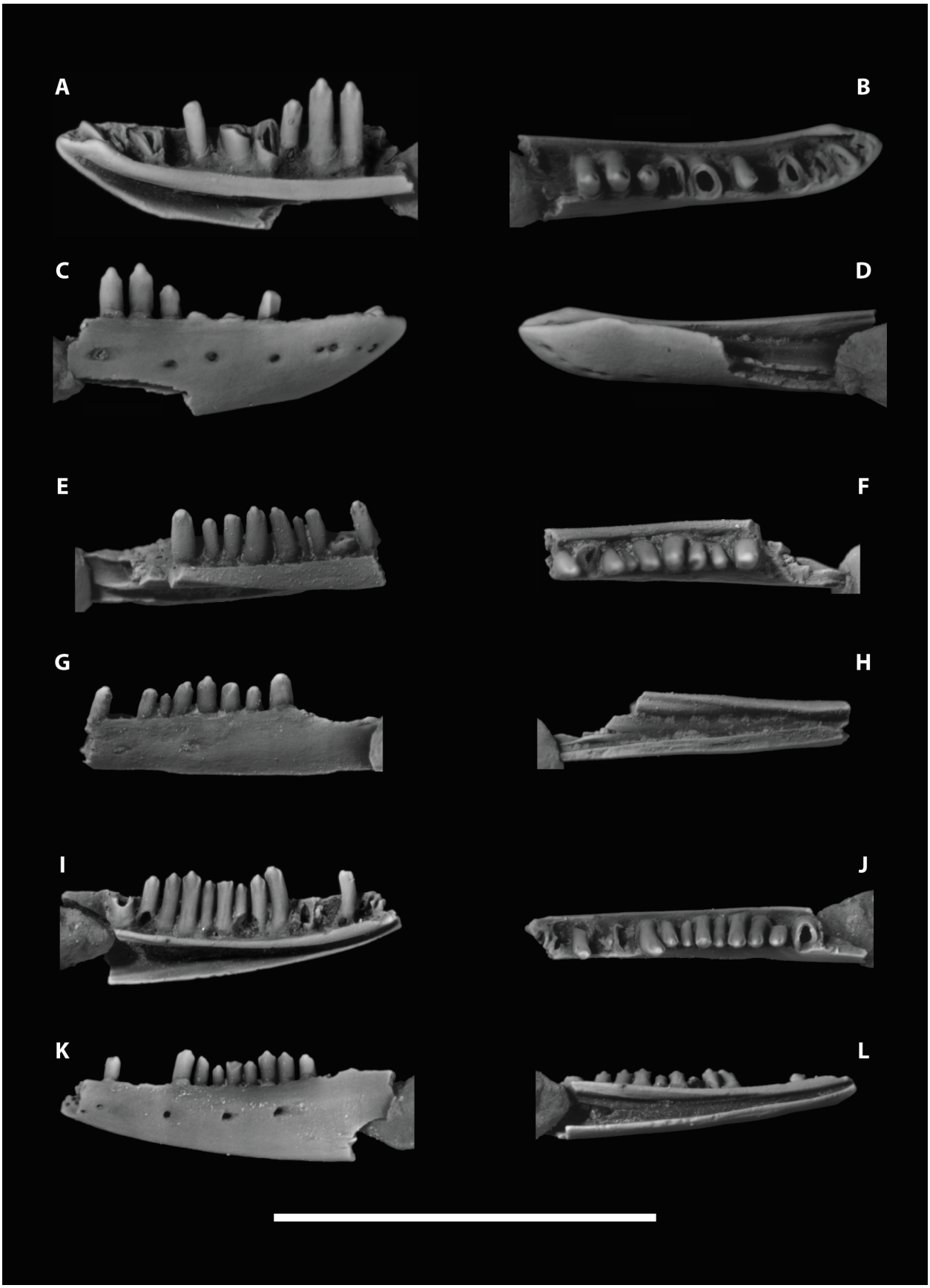
A
B
C
D
E
F
G
H
I
J
K
L

Figure A3.3. Chamopsiidae and ?Chamopsiidae from the Hell Creek Formation, Garfield County, northeastern Montana. Chamopsiidae genus and species undetermined C: proposed holotype partial right dentary (UCMP 235674) from UCMP loc. V99369 in lingual (**A**), dorsal (**B**), labial (**C**), and ventral (**D**) views. Chamopsiidae genus and species undetermined D: partial left dentary (UCMP 235669) from UCMP loc. V99220 in lingual (**E**), dorsal (**F**), labial (**G**), and ventral (**H**) views. ?Chamopsiidae genus and species undetermined: proposed holotype partial left dentary (UWBM 104470) from UWBM loc. C1529 in lingual (**I**), dorsal (**J**), labial (**K**), and ventral (**L**) views. Scale bar equals 5 mm.

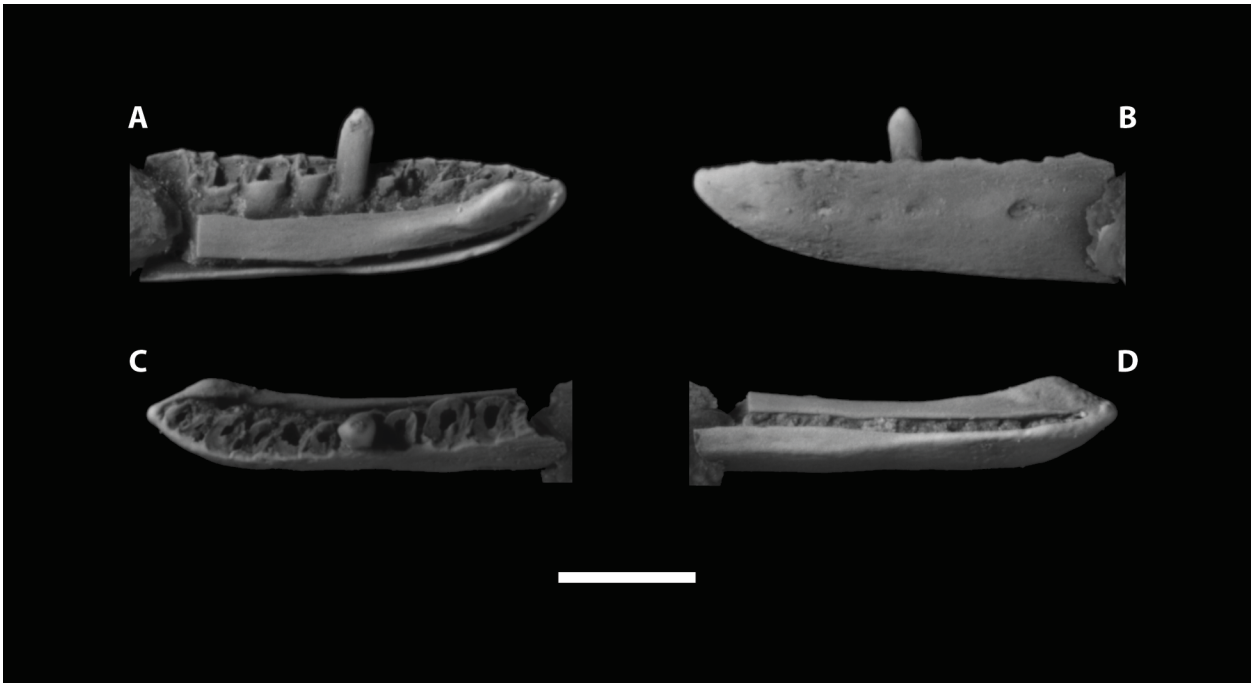

Figure A3.4. Scincomorpha family incertae sedis from the Hell Creek Formation, Garfield County, northeastern Montana. Proposed holotype partial left dentary (UCMP 235670) from UCMP loc. V99220 in lingual (**A**), labial (**B**), dorsal (**C**), and ventral (**D**) views. Scale bar equals 1 mm.

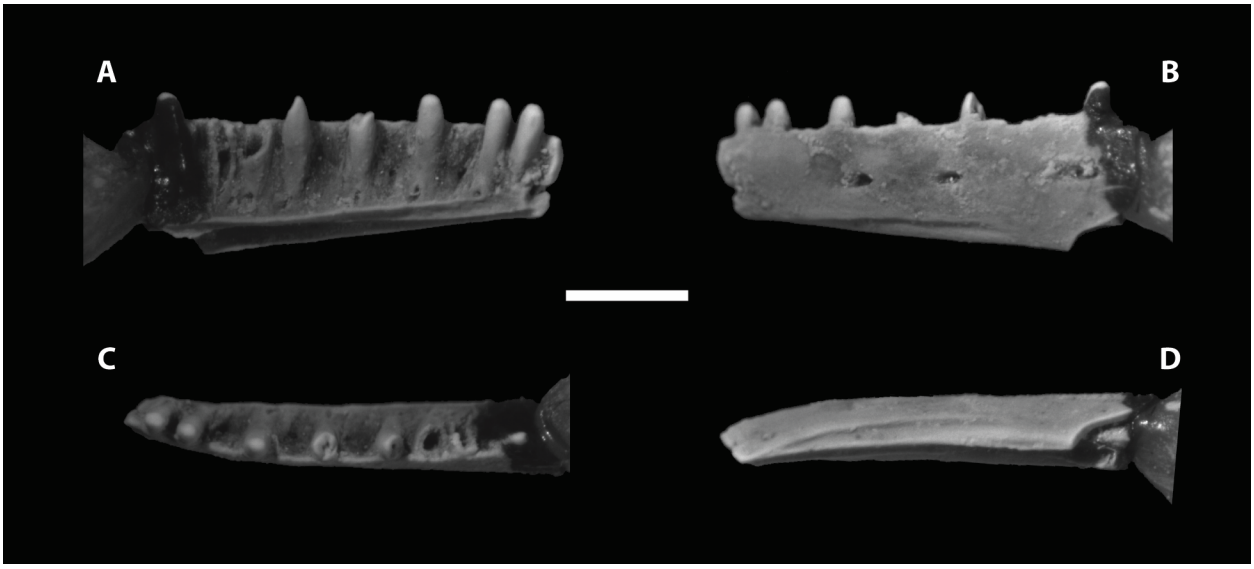

Figure A3.5. Anguidae genus and species undetermined from the Hell Creek Formation, Garfield County, northeastern Montana. Proposed holotype partial left dentary (UCMP 235684) from UCMP loc. V73087 in lingual (**A**), labial (**B**), dorsal (**C**), and ventral (**D**) views. Scale equals 1 mm.

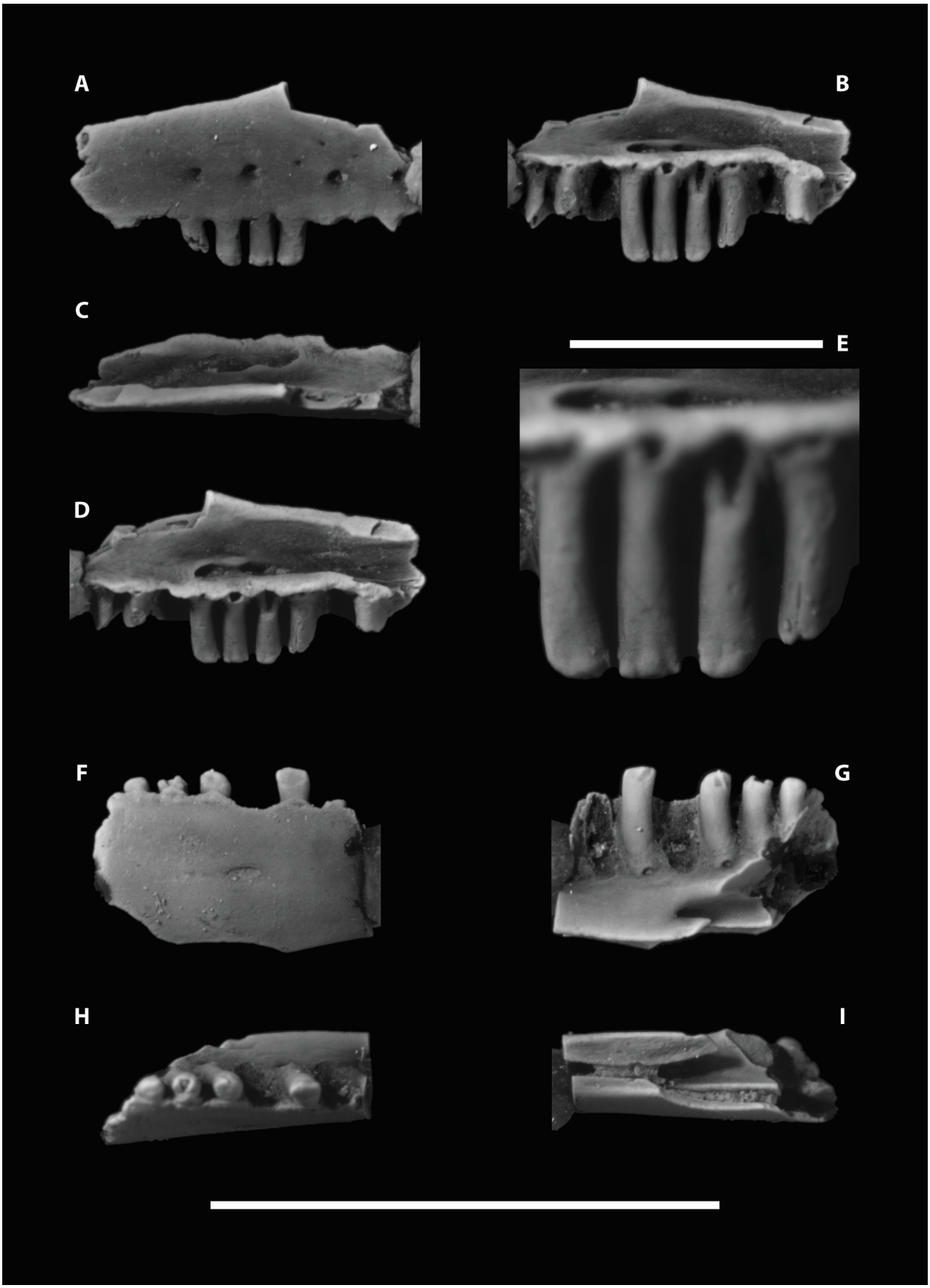
A
B
C
E
D
F
G
H
I

Figure A3.6. Gerrhonotinae genus and species undetermined from the Hell Creek Formation, Garfield County, northeastern Montana. Partial right maxilla (UCMP 235677) from UCMP loc. V99369 in labial (**A**), lingual (**B**), dorsal (**C**), and dorsolingual (**D**) views; close-up of teeth of same specimen in lingual (**E**) view; proposed holotype partial right dentary (UCMP 235676) from UCMP loc. V99369 in labial (**F**), lingual (**G**), dorsal (**H**), ventral (**I**) views. Scale bar equals 1 mm for E. Scale bar for all others (**A**–**D**, **F**–**I**) equals 5 mm.

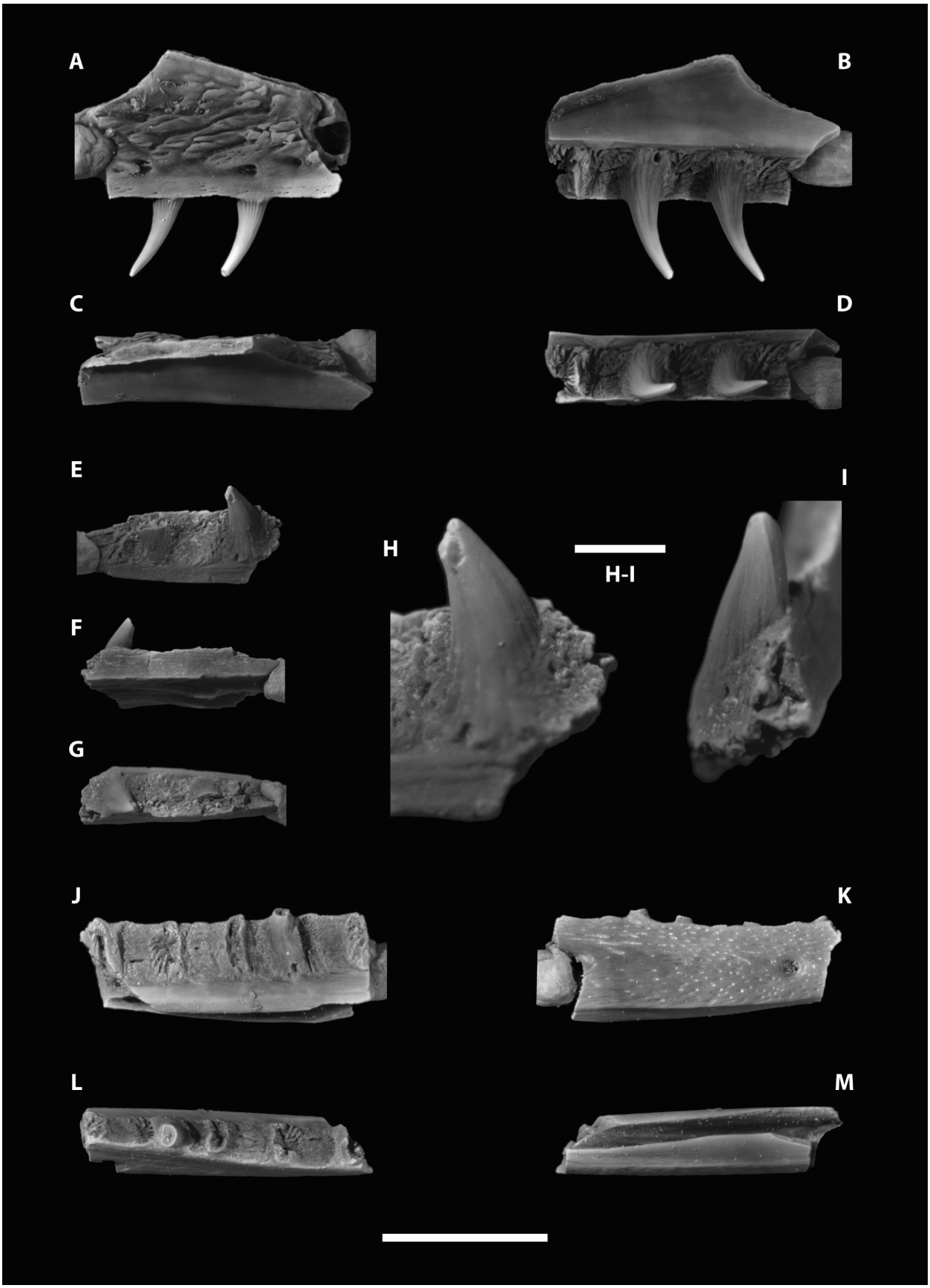
A
B
C
D
E
I
H
H-I
F
G
J
K
L
M

Figure A3.7. Platynota genus and species undetermined A and B from the Hell Creek Formation, Garfield County, northeastern Montana. Platynota genus and species undetermined A: proposed holotype partial right maxilla (MOR 4109) from MOR loc. HC-293 in labial (**A**), lingual (**B**), dorsal (**C**), and ventral (**D**) views; partial left dentary (UWBM 104469) from UWBM loc. C1153 in lingual (**E**), labial (**F**), and dorsal (**G**) views and close-up of its mesial most tooth in lingual (**H**) and mesiolabial (**I**) views. Platynota genus and species undetermined B: proposed holotype partial right dentary (MOR 3437) from MOR loc. HC-583 in lingual (**J**), labial (**K**), dorsal (**L**), and ventral (**M**) views. Scale bar for H–I equals 1 mm. Scale bar for all others (**A**–**G**, **J**–**M**) equals 5 mm.

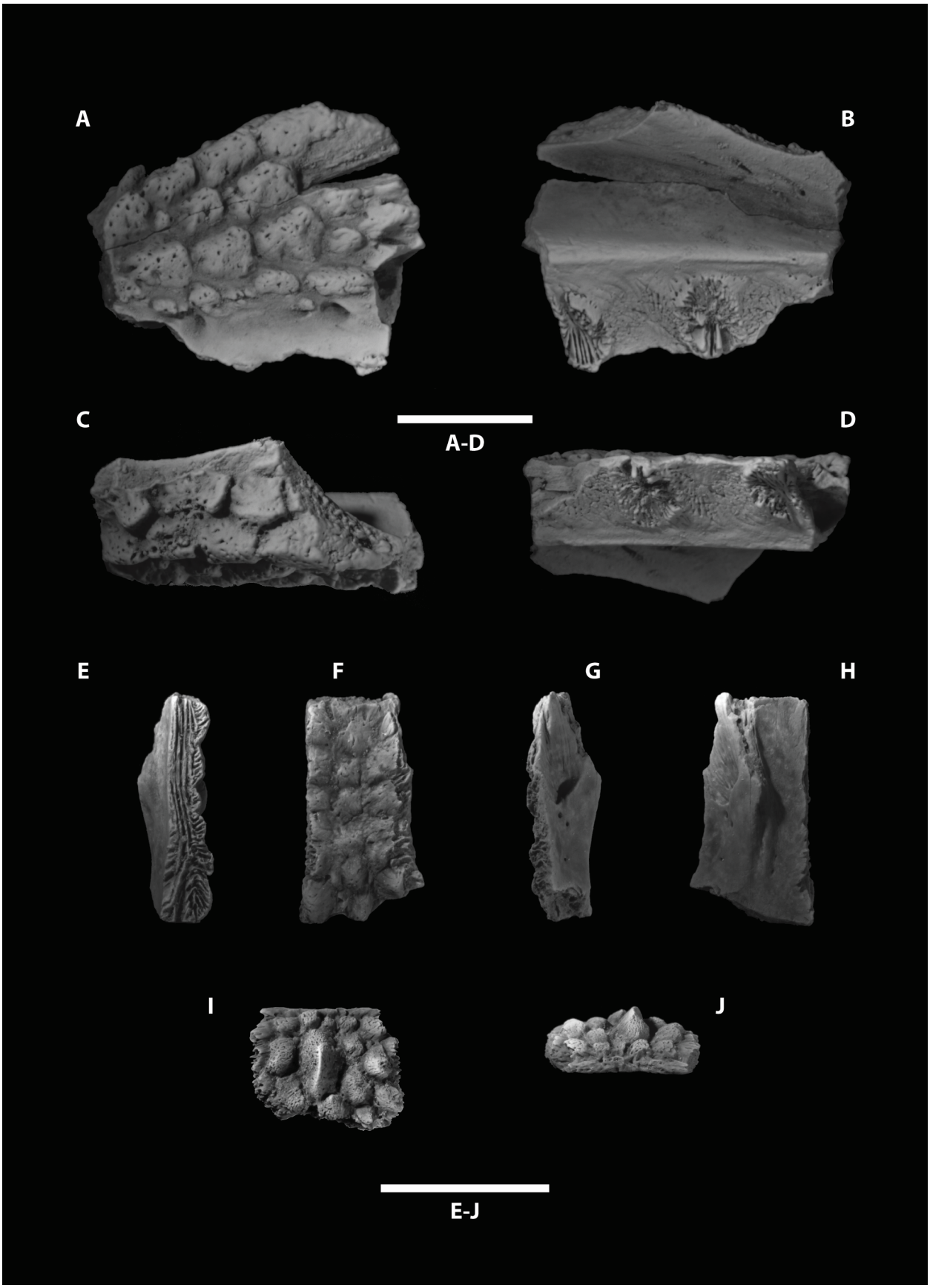
A
B
C
A-D
D
E
F
G
H
I
J
E-J

Figure A3.8. Platynota genus and species undetermined C from the Hell Creek Formation, Garfield County, northeastern Montana. Proposed holotype partial left maxilla (UWBM 104471) from UWBM loc. C1492 in labial (**A**), lingual (**B**), dorsal (**C**), and ventral (**D**) views; partial right frontal (MOR 9101) from MOR loc. HC-293 in medial (**E**), dorsal (**F**), lateral (**G**), and ventral (**H**) views; complete osteoderm (MOR 4874) from MOR loc. HC-293 in external (**I**) and side (**J**) views. Scale bars both equal 5 mm.

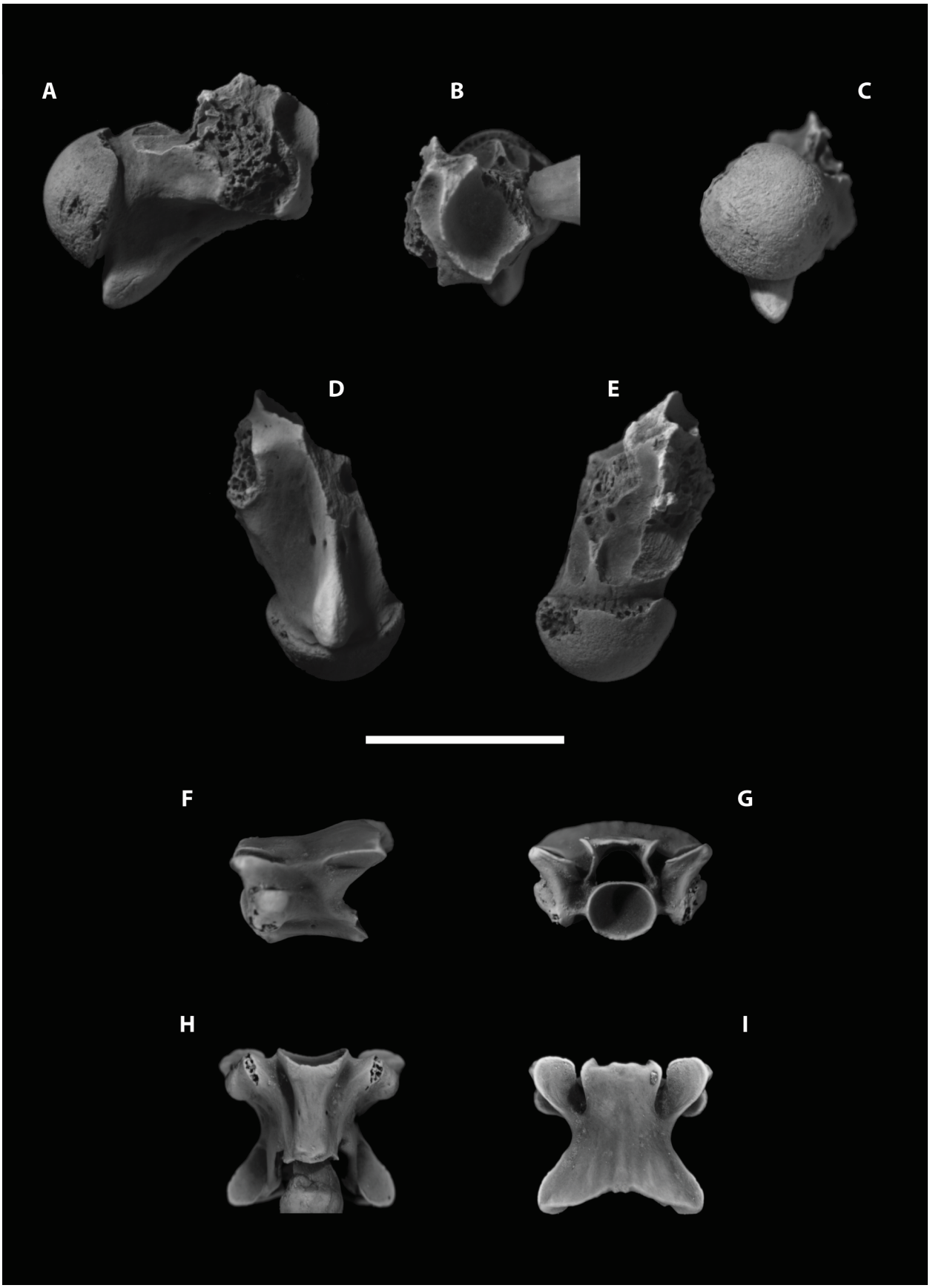
A
B
C
D
E
F
G
H
I

Figure A3.9. Serpentes from the Hell Creek Formation, Garfield County, northeastern Montana. *Cerberophis robustus* Longrich et al.: partial anterior precloacal (cervical) vertebra (UWBM 104198) from UWBM loc. C1151 in right lateral (**A**), anterior (**B**), posterior (**C**), ventral (**D**), and dorsal (**E**) views. *Coniophis precedens* Marsh: Precloacal vertebra (UWBM 104191) from UWBM loc. C1153 in left lateral (**F**), anterior (**G**), ventral (**H**), and dorsal (**I**) views. Scale bar equals 5 mm.

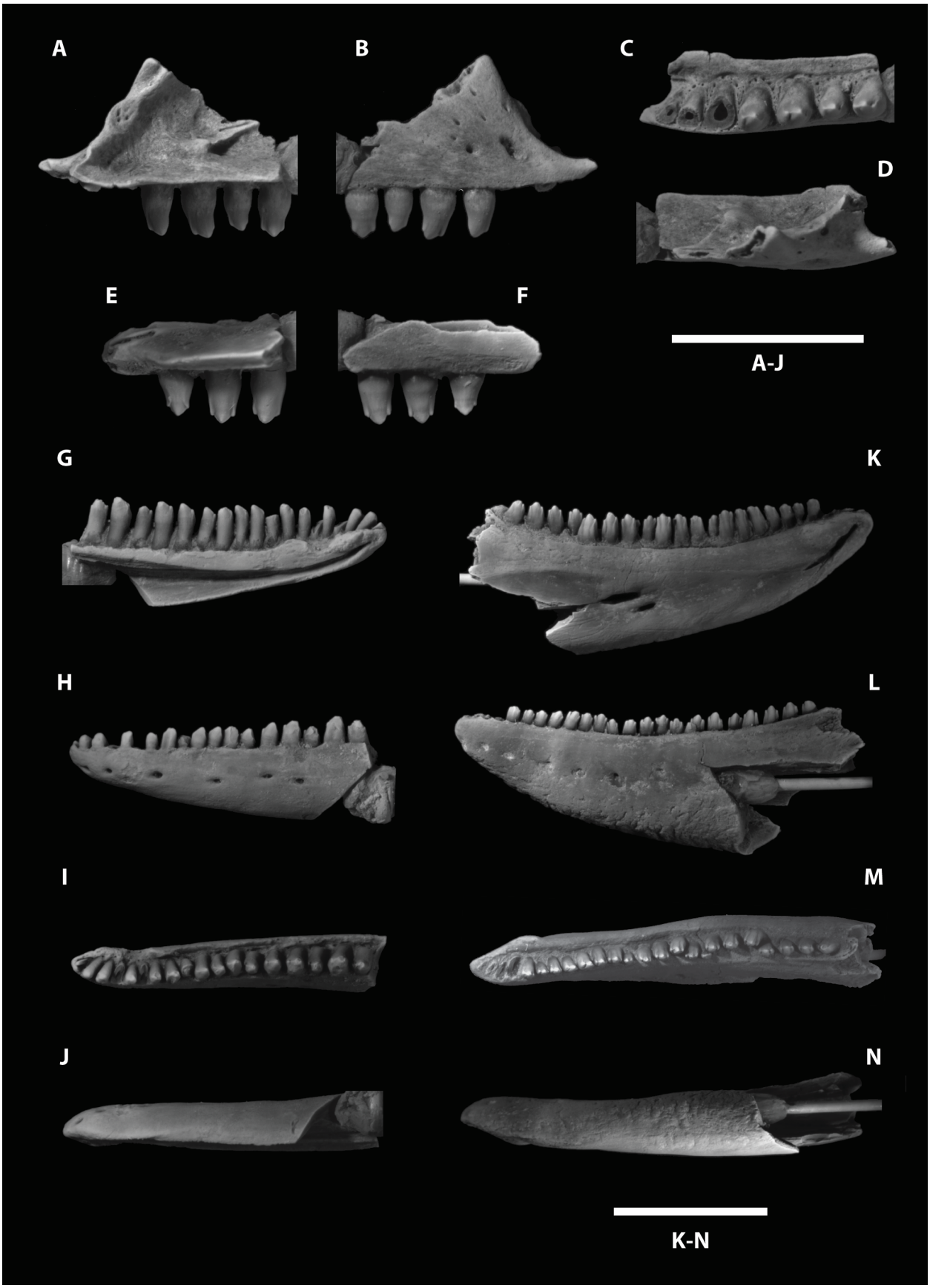
A
B
C
D
E
F
A-J
G
K
H
L
I
M
J
N
K-N

Figure A3.10. Chamopsiidae from the Hell Creek Formation, Garfield County, northeastern Montana. *Chamops segnis* Marsh: partial right maxilla (UCMP 235685) from UCMP loc. V80091 in lingual (**A**), labial (**B**), ventral (**C**), and dorsal (**D**) views; partial left maxilla (UWBM 104459) from UWBM loc. C1153 in lingual (**E**) and labial (**F**) views. *Meniscognathus altmani* Estes: partial left dentary (UCMP 555565) from UCMP loc. V99226 in lingual (**G**), labial (H), dorsal (**I**), and ventral (**J**) views. *Haptosphenus placodon* Estes: partial left mandible (UWBM 104460) preserving most of the dentary and splenial and the anteromedial corner of the coronoid from UWBM loc. C1153 in lingual (**K**), labial (**L**), dorsal (**M**), and ventral (**N**) views. Scale bars both equal 5 mm.

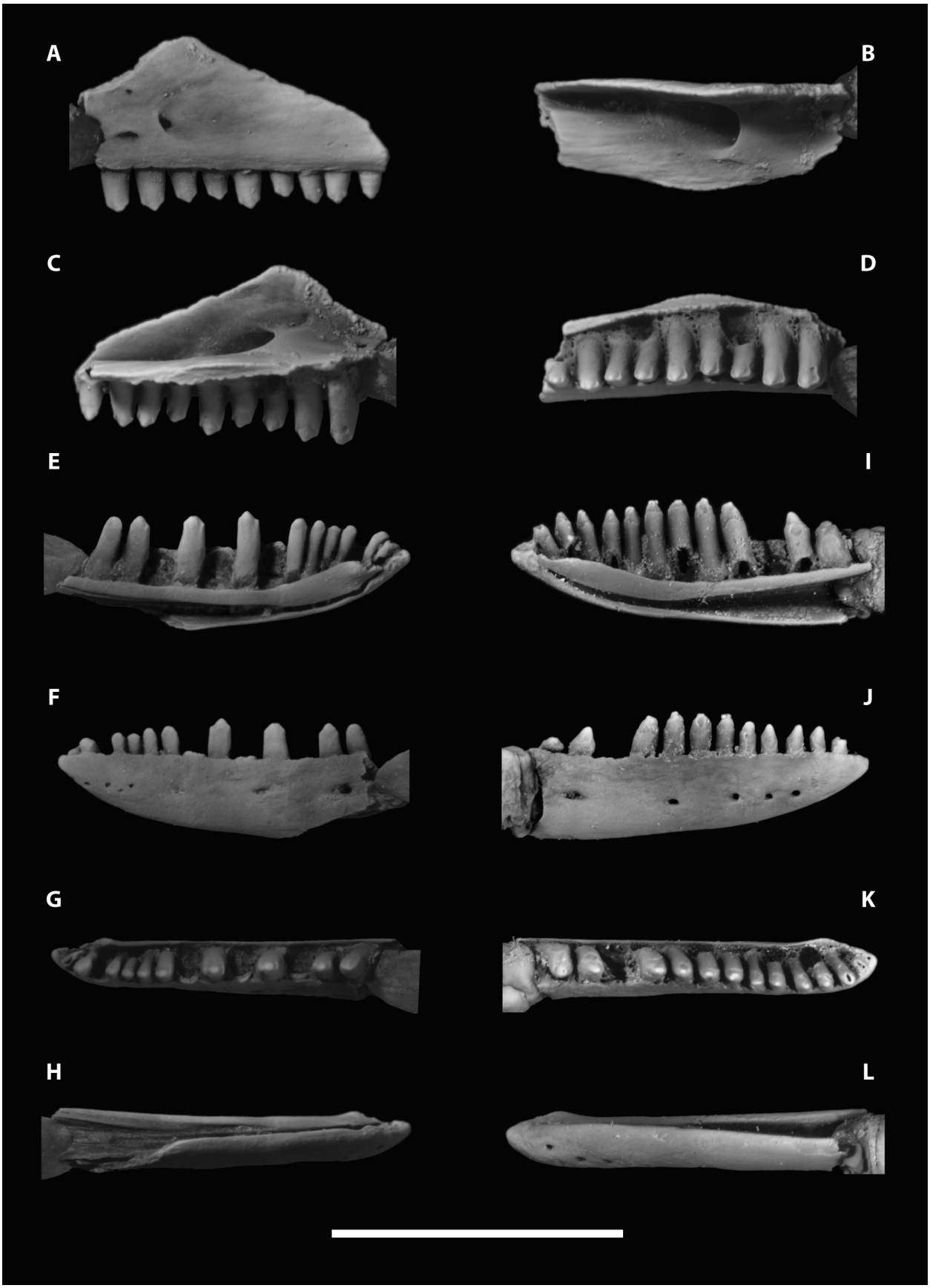
A
B
C
D
E
I
F
J
G
K
H
L

Figure A3.11. *Leptochamops denticulatus* Estes from the Hell Creek Formation, Garfield County, northeastern Montana. Partial left maxilla (UWBM 104464) from UWBM loc. C1153 in labial (**A**), dorsal (**B**), lingual (**C**), and ventral (**D**) views; partial left dentary (UWBM 104463) from UWBM loc. C1153 in lingual (**E**), labial (**F**), dorsal (**G**), and ventral (**H**) views; partial right dentary (UWBM 104462) from UWBM loc. C1153 in lingual (**I**), labial (**J**), dorsal (K), and ventral (L) views. Scale equals 5 mm.

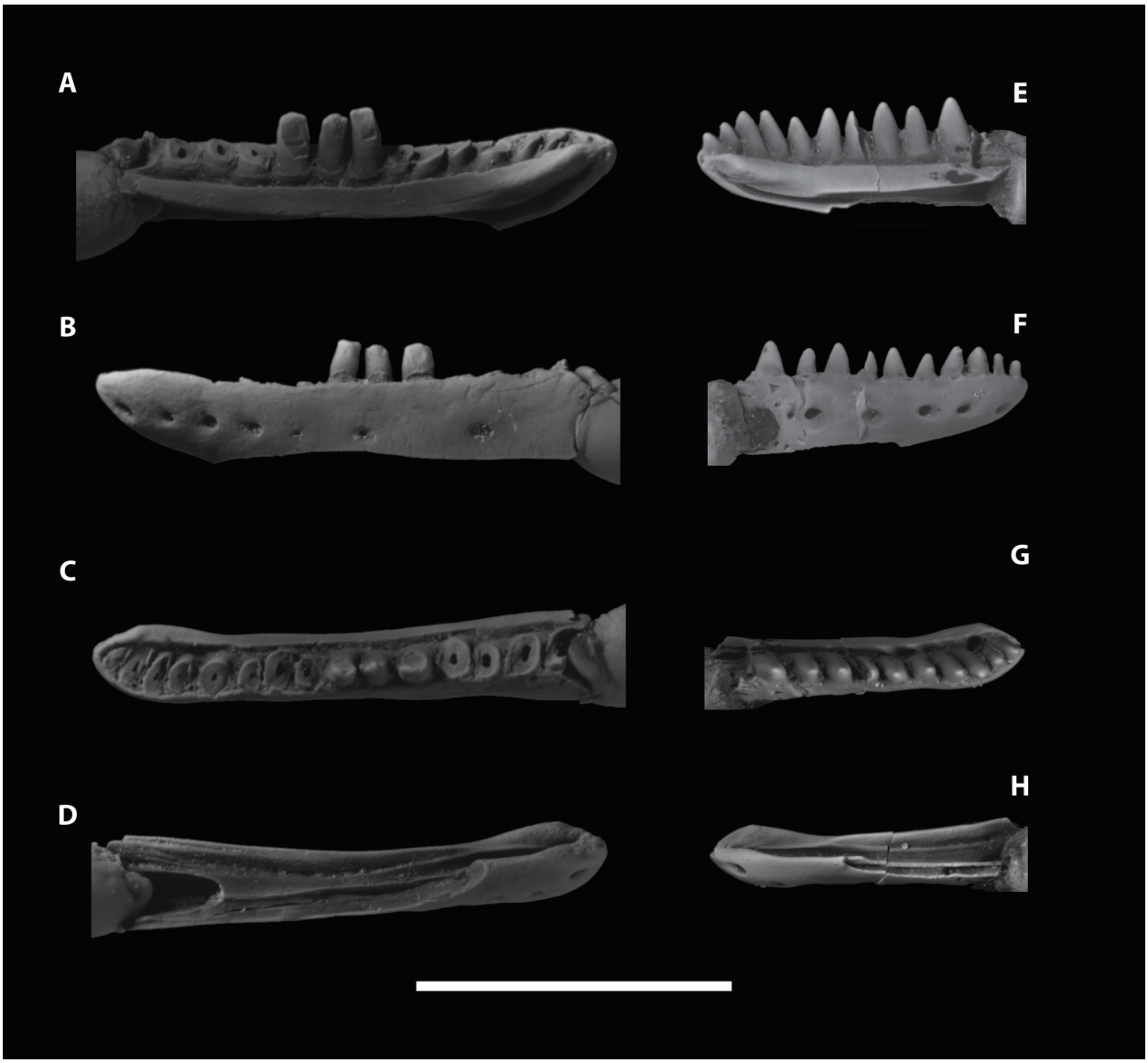

Figure A3.12. *Leptochamops thrinax* Gao and Fox from the Hell Creek Formation, Garfield County, northeastern Montana. Partial left dentary (MOR 9100) from MOR loc. HC-1105 in lingual (**A**), labial (**B**), dorsal (**C**), and ventral (**D**) views; partial right dentary (UCMP 235678) from UCMP loc. V99369 in lingual (**E**), labial (**F**), dorsal (**G**), and ventral (**H**) views. Scale bar equals 5 mm.

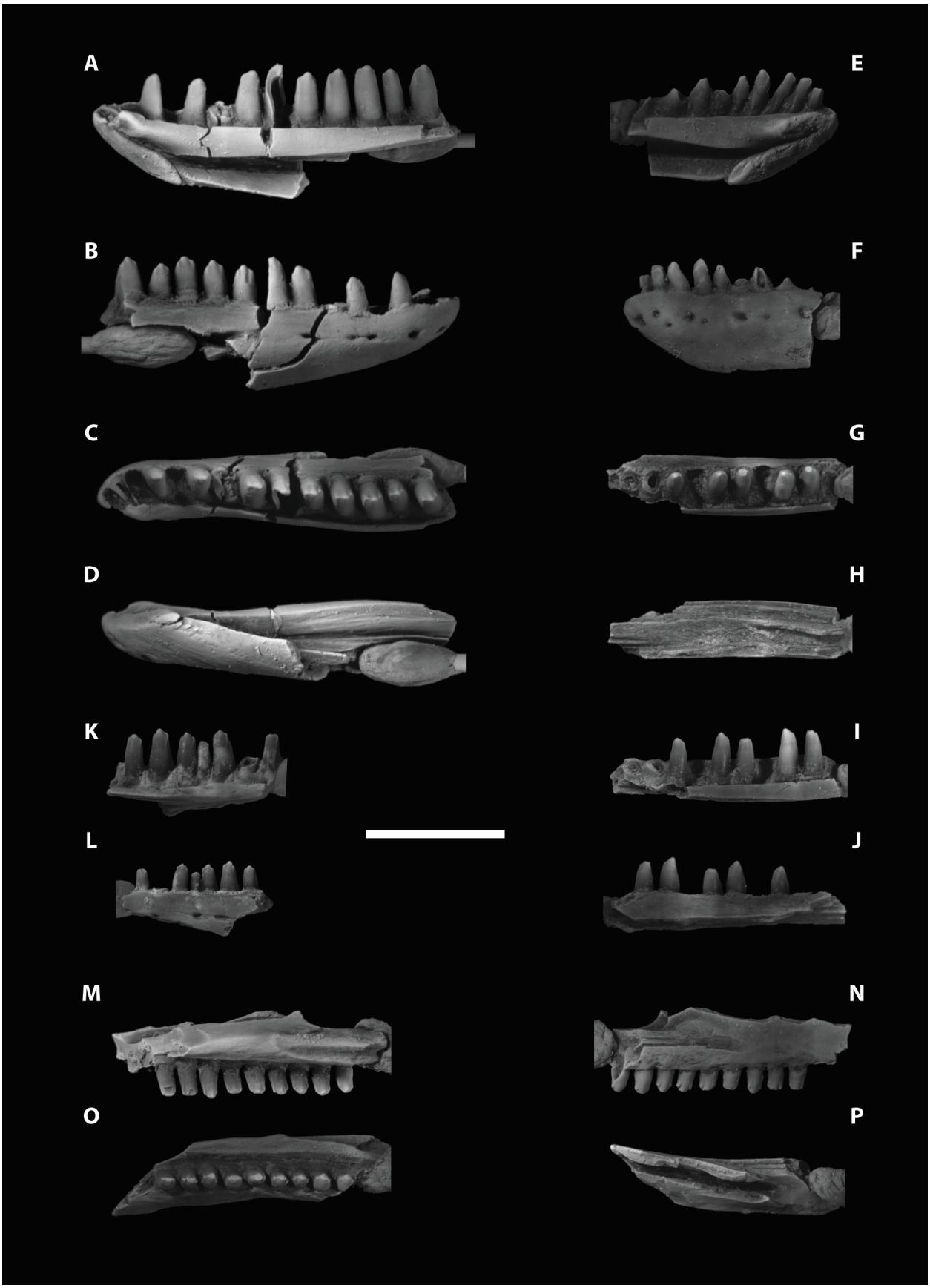
A
E
B
F
C
G
D
H
K
I
L
J
M
N
O
P

Figure A3.13. *Socognathus* spp. from the Hell Creek Formation, Garfield County, northeastern Montana. *Socognathus brachyodon* Longrich et al.: partial right dentary (UCMP 556403) from UCMP loc. V99369 in lingual (**A**), labial (**B**), dorsal (**C**), and ventral (**D**) views. *Socognathus* sp. indet.: partial left dentary (UCMP 235682) from UCMP loc. V99370 in lingual (**E**) and labial (**F**) views. *Socognathus unicuspis* Gao and Fox: partial left dentary (UCMP 235673) from UCMP loc. V99220 in dorsal (**G**), ventral (**H**), lingual (**I**), and labial (**J**) views; partial left dentary (UCMP 235680) from UCMP loc. V99369 in lingual (**K**) and labial (**L**) views. *Socognathus* sp. indet.: partial right maxilla (UWBM 91219) from UWBM loc. C1153 in lingual (**M**), labial (**N**), ventral (**O**), and dorsal (**P**) views. Scale bar equals 5 mm.

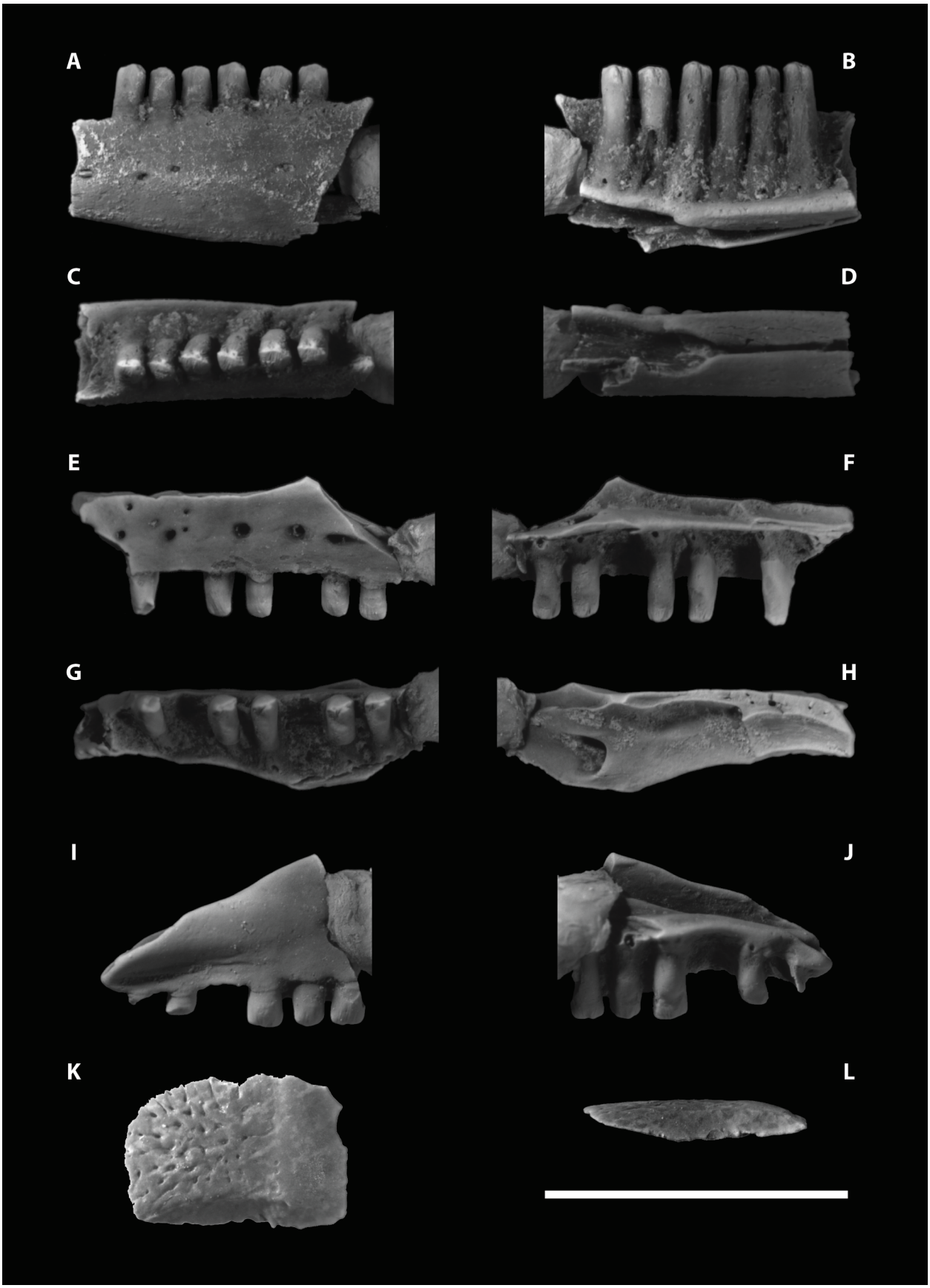
A
B
C
D
E
F
G
H
I
J
K
L

Figure A3.14. *Odaxosaurus piger* (Gilmore) from the Hell Creek and Tullock formations, Garfield County, northeastern Montana. Partial left dentary (UWBM 104467) from UWBM loc. C1153 in labial (**A**), lingual (**B**), dorsal (**C**), and ventral (**D**) views; partial left maxilla (UWBM 104466) from UWBM loc. C1153 in labial (**E**), lingual (**F**), ventral (**G**), and dorsal (**H**) views; partial right maxilla (UCMP 229335) from UCMP loc. V72129 in labial **(I**) and lingual (**J**) views. Nearly complete osteoderm (MOR 5838) commonly referred to *O. piger* from MOR loc. HC-293 in external (**K**) and side (**L**) views. Scale bar equals 5 mm.

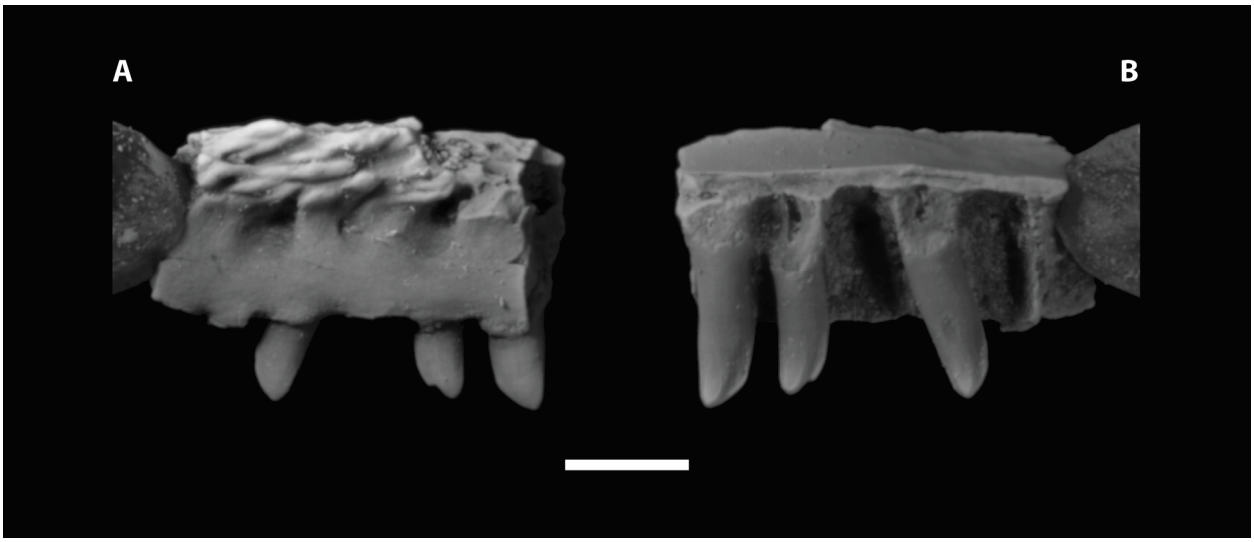

Figure A3.15. *Exostinus lancensis* Gilmore from the Hell Creek Formation, Garfield County, northeastern Montana. Partial left maxilla (UWBM 104456) from UWBM loc. C1115 in labial (**A**) and lingual (**B**) views. Scale bar equals 1 mm.

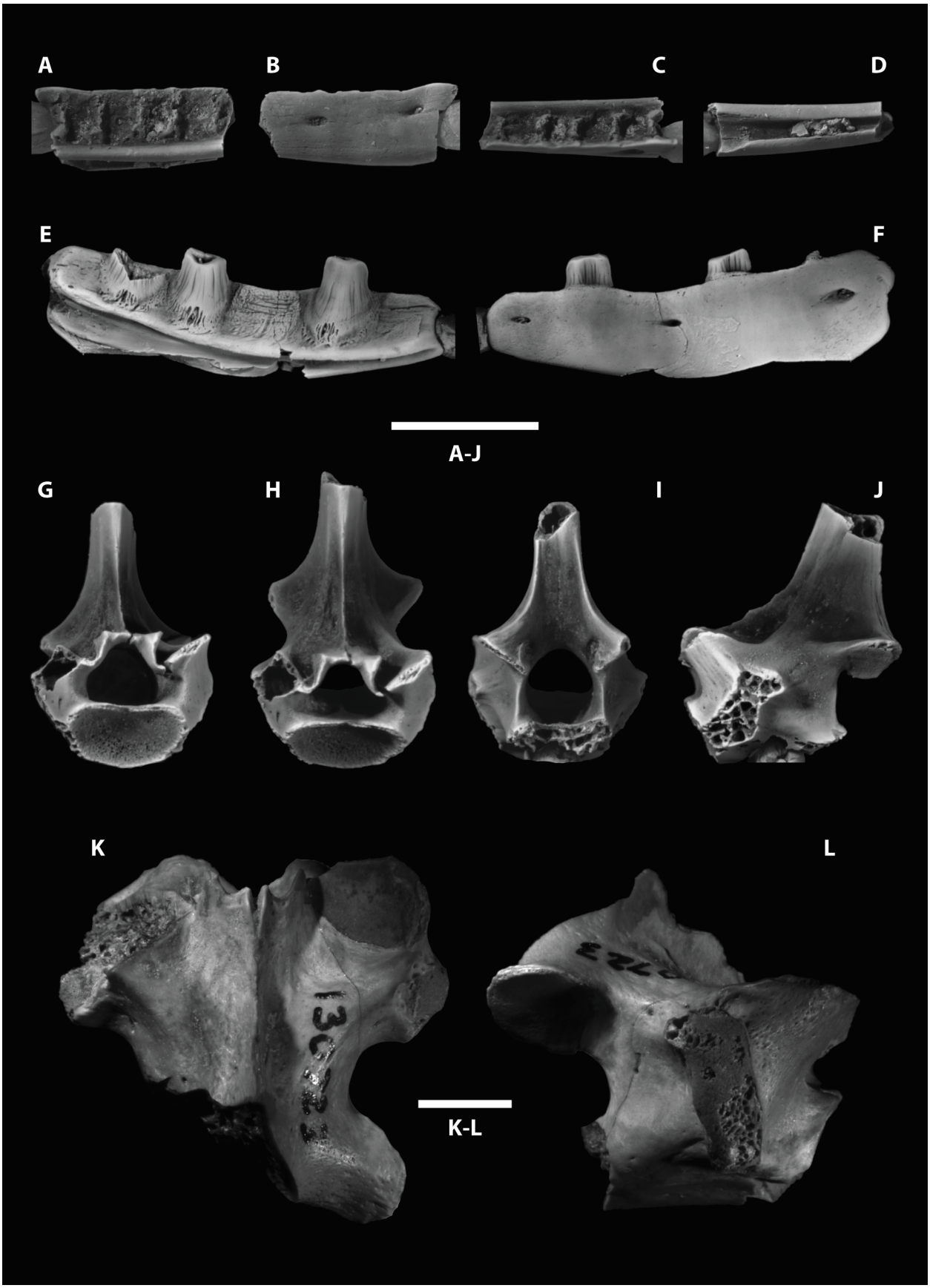
A
B
C
D
E
F
A-J
G
H
I
J
K
L
K-L

Figure A3.16. Anguimorpha incertae sedis and Platynota from the Hell Creek Formation, Garfield County, northeastern Montana. Anguimorpha incertae sedis–*Colpodontosaurus cracens* Estes: partial left dentary (UCMP 235683) from UCMP loc. V77130 in lingual (**A**), labial (**B**), dorsal (**C**), and ventral (**D**) views. Platynota–*Parasaniwa wyomingensis* Gilmore: partial left dentary (UCMP 130742) from UCMP loc. V77130 in lingual (**E**) and labial (**F**) views. *Paraderma bogerti* Estes: nearly complete dorsal vertebra (UWBM 104468) from UWBM loc. C1153 in anterior (**G**), dorsoanterior (**H**), posterior (**I**), and left lateral (**J**) views. *Palaeosaniwa* sp.: dorsal vertebra (UCMP 130723) from UCMP loc. V82022 in dorsal (**K**) and right lateral (**L**) views. Scale bars both equal 5 mm.

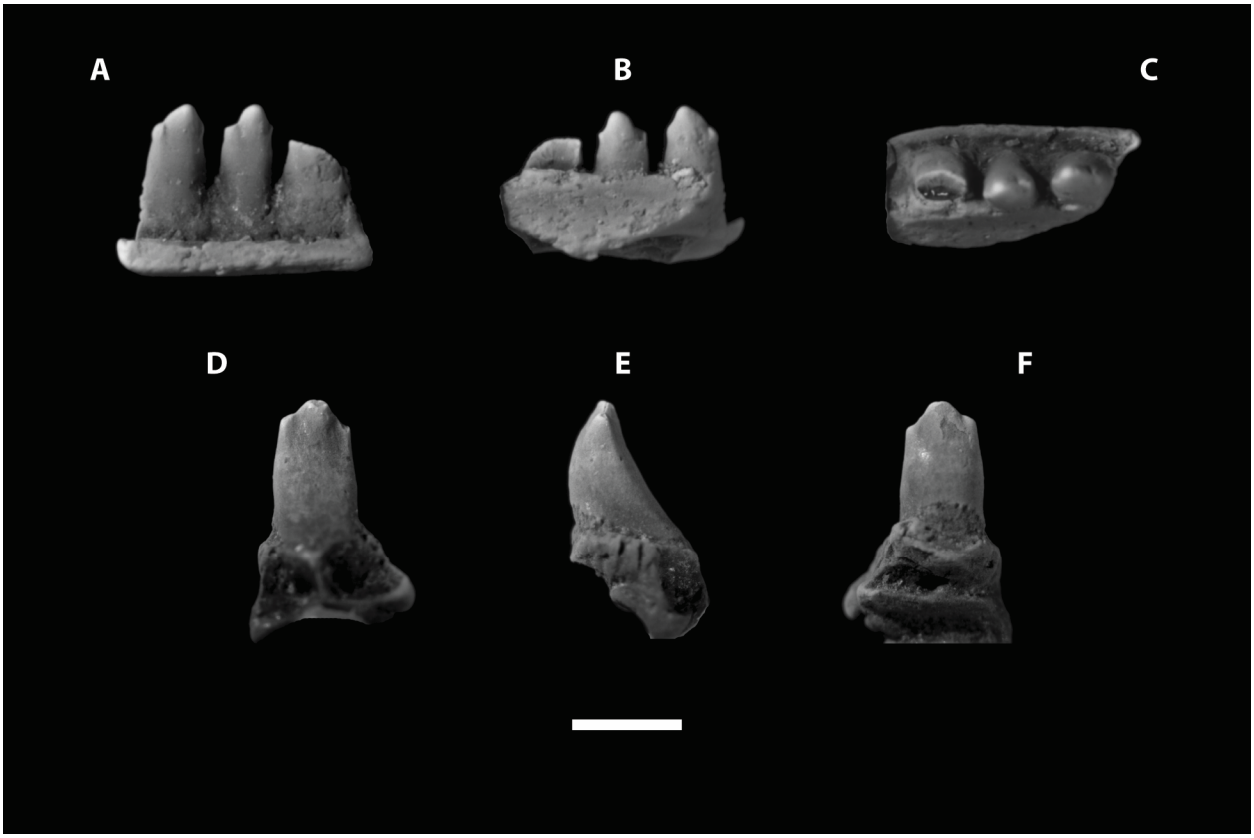

Figure A3.17. Chamopsiidae genus and species indeterminate from the Tullock Formation, Garfield County, northeastern Montana. "Harley's Point chamopsiid": partial dentary fragment (UWBM 104472) from UWBM loc. C1367 in lingual (**A**), labial (**B**), and dorsal (**C**) views. "Hell Hollow chamopsiid": isolated tooth attached to fragmentary jaw (UCMP 235686) from UCMP loc. V74110 in lingual (**D**), mesial or distal (**E**), and labial (**F**) views. Scale bar equals 1 mm.

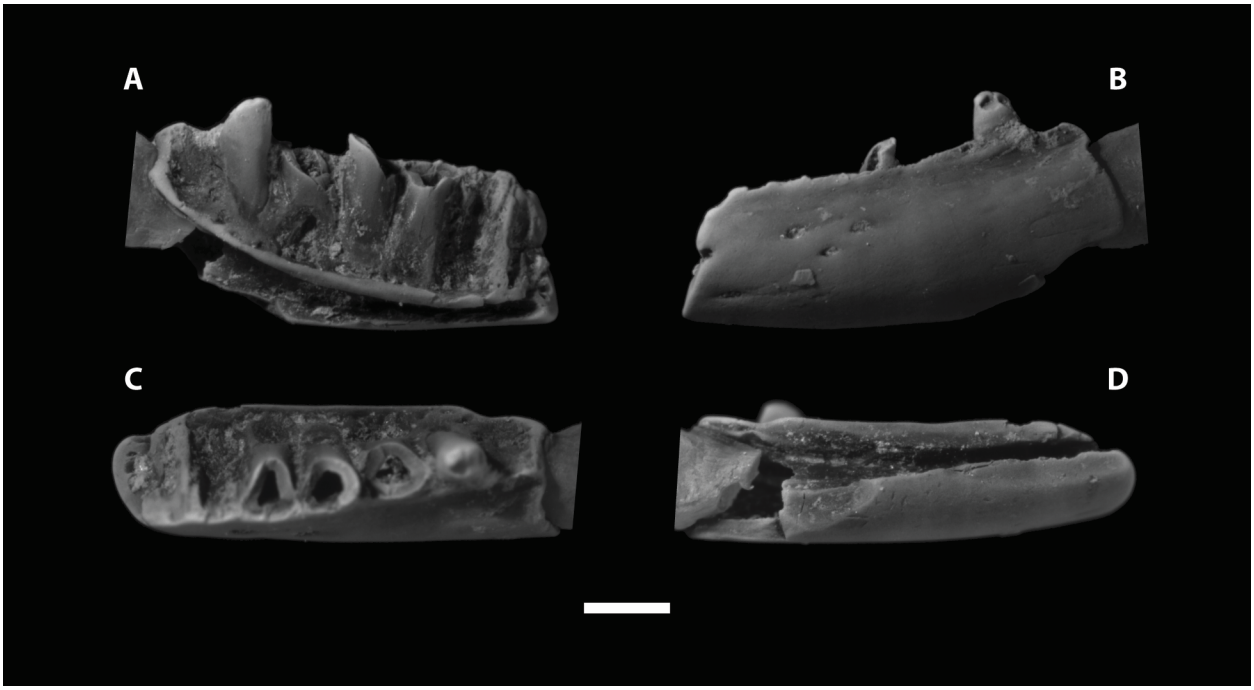

Figure A3.18. *Contogenys* sp. from the Tullock Formation, Garfield County, northeastern Montana. Partial left dentary (UCMP 235687) from UCMP loc. V74122 in lingual (**A**), labial (**B**), dorsal (**C**), and ventral (**D**) views. Scale bar equals 1 mm.

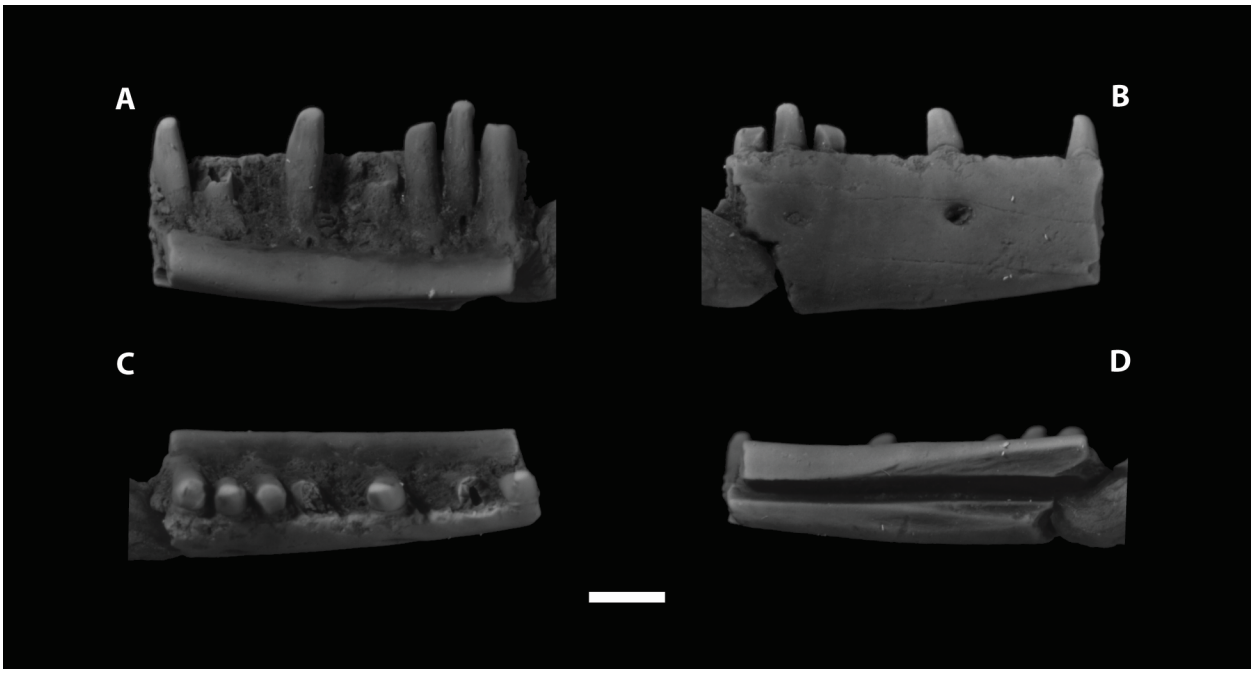

Figure A3.19. cf. *Machaerosaurus torrejonensis* from the Tullock Formation, Garfield County, northeastern Montana. Partial right dentary (UCMP 227950) from UCMP loc. V73080 in lingual (**A**), labial (**B**), dorsal (**C**), and ventral (**D**) views. Scale bar equals 1 mm.

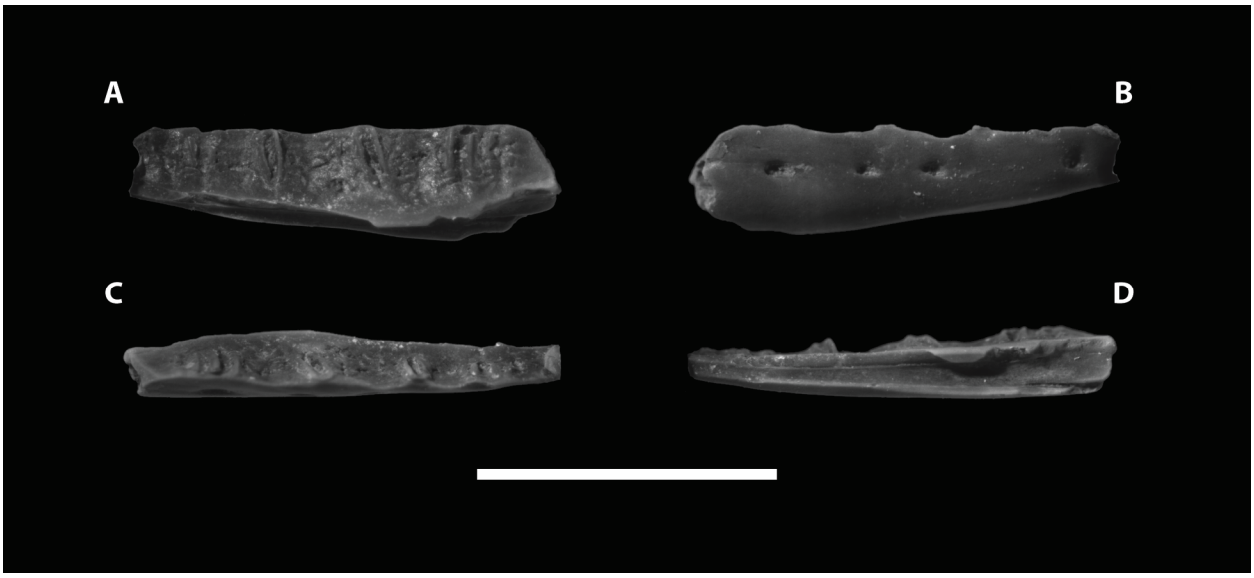

Figure A3.20. Platynota gen. et sp. indet. from the Tullock Formation, Garfield County, northeastern Montana. Partial right dentary (UCMP 235688) from UCMP loc. V74122 in lingual (**A**), labial (**B**), dorsal (**C**), and ventral (**D**) views. Scale bar equals 5 mm.

CHAPTER 4:

A NEW FOSSIL SALAMANDER (CAUDATA: PROTEIDAE) FROM THE UPPER CRETACEOUS (MAASTRICHTIAN) HELL CREEK FORMATION, MONTANA, USA[1]

[1]A version of this chapter has been published. The official citation is listed below.

DeMar, D. G., Jr. 2013. A new fossil salamander (Caudata, Proteidae) from the Upper Cretaceous (Maastrichtian) Hell Creek Formation, Montana, U.S.A. Journal of Vertebrate Paleontology 33(3):588–598. DOI: 10.1080/02724634.2013.734887

ABSTRACT

North American Late Cretaceous salamanders are principally known by isolated atlantes and trunk vertebrae. Here I describe a new genus and species of fossil salamander, *Paranecturus garbanii*, gen. et sp. nov., based on these elements from the lower portions of the Hell Creek Formation (Maastrichtian), Garfield County, northeastern Montana, USA. It is diagnosed by a unique combination of character states which include the presence of an alar-like process of the atlas and a groove on the posterior face of the neural arch and solid dorsal rib-bearers of the trunk vertebrae. My phylogenetic analysis of 13 caudate taxa and 23 atlantal and trunk vertebral characters recovered *P. garbanii* as a member of the Proteidae. *P. garbanii* represents the oldest fossil record of the Proteidae and demonstrates that this lineage was present before the Cretaceous-Paleogene mass extinction event.

INTRODUCTION

Fossil salamanders (Caudata) are common components of latest Cretaceous vertebrate microfossil assemblages of the Western Interior of North America (e.g., Estes 1964, 1981; Gardner 2000; Holman 2006; Wilson et al. 2014). Three currently recognized clades are represented: Batrachosauroididae, Scapherpetontidae, and Sirenidae (Estes 1981; Gardner 2000, 2005; Holman 2006). The Amphiumidae may have had a latest Cretaceous existence (Estes 1969); but see Gardner (2003a), DeMar (2011), and Wilson et al. (2014). The Proteidae are unequivocally known from the late Paleocene of southwestern Saskatchewan, Canada (*Necturus krausei*; Naylor 1978a), whereas reports of Cretaceous and earlier occurrences of the family are unsubstantiated (Estes 1981).

Caudates are well represented in the Upper Cretaceous (Maastrichtian) Hell Creek Formation of Montana (e.g., Estes and Berberian 1970; Bryant 1989; Gardner 2000) and recent work in these deposits has recognized a total of nine species (Wilson et al. 2014). Here I describe a new genus and species of caudate from Garfield County, northeastern Montana, USA (Fig. 4.1). *Paranecturus garbanii*, gen. et sp. nov., is based on isolated atlantes and trunk vertebrae from six distinct stratigraphic horizons in the lower three-quarters of the Hell Creek Formation. In addition to the description, I assessed the phylogenetic relationships of *P. garbanii* through a cladistic analysis of 13 caudate taxa and 23 vertebral characters. I find *P. garbanii* as the earliest member of Proteidae.

Institutional Abbreviations

DMNH, Denver Museum of Nature and Science (formerly the Denver Museum of Natural History), Denver, Colorado, USA; MOR, Museum of the Rockies, Bozeman, Montana, USA; UALVP, University of Alberta Laboratory for Vertebrate Paleontology, Edmonton, Alberta, Canada; UCMP, University of California Museum of Paleontology, Berkeley, California, USA; UWBM, University of Washington Burke Museum of Natural History and Culture, Seattle, Washington, USA

Anatomical Abbreviations

aco, anterior cotyle; alp, alar-like process; bpr, bony protuberance; cc, calcified cartilage; dor, dorsal ridge; lf, lateral fossa; na, neural arch; nc, neural canal; npt, notochordal pit; nsp, neural spine; opr, odontoid process; opr(b), broken odontoid process; pco, posterior cotyle; pnag, groove on posterior face of neural arch; popr, postzygapophyseal process; spfo, spinal foramen; sufo, subcentral foramen; ver, ventral ridge; vlf, anterior ventrolateral foramen; vlr, ventrolateral ridge.

Other Abbreviations

NALMA, North American Land-Mammal “Age”.

MATERIALS AND METHODS

Osteological terms primarily come from Gardner (2003a). Measurements were made using a microscope with an ocular micrometer and from images measured via ImageJ 1.44p (Abramoff et al. 2004). Published descriptions and figures (Estes 1964, 1965, 1975, 1981; Estes and Darevsky 1977; Naylor 1978a, b, 1983; Naylor and Krause 1981; Gardner 2000, 2012) and direct observation of specimens of most taxa facilitated taxonomic comparisons and scoring for cladistic analysis. Observations of the skeletal anatomy of *Necturus* were based on *N. maculosus*. The stratigraphic positions of fossil localities are relative to the Hell Creek-Tullock formational contact in Garfield County, northeastern Montana, USA and are based on measurements in Wilson (2004, 2005) and Wilson et al. (2014).

Systematic Paleontology

LISSAMPHIBIA Haeckel, 1866

CAUDATA Scopoli, 1777

PROTEIDAE Gray, 1825

PARANECTURUS, gen. nov.

Type Species—*Paranecturus garbanii*, sp. nov.

Etymology—From the Greek *Para* (beside) and *Necturus* (genus of the caudate family Proteidae), referring to the close phylogenetic relationship.

Diagnosis—As for the type and only species.

PARANECTURUS GARBANII, sp. nov.

(Figs. 4.2–4.6A)

Proteidae gen. et sp. nov.; Wilson et al., 2014, fig. 2G, H; *Chapter Two*, fig. 2.2G, H.

Etymology—Specific epithet after the late Harley J. Garbani for his enormous efforts in collecting and preserving vertebrate fossils from the study area of northeastern Montana, USA

Holotype—UWBM 93370 (Figs. 4.2, 4.3), incomplete atlas missing neural arch roof, crest, and spine, anterior portion of odontoid process, and portions of the anterior and posterior cotylar rims.

Type locality, Age, and Horizon—UWBM C1153 (= UCMP V82022), Garfield County, Montana, USA; late Maastrichtian, Lancian NALMA; within Hell Creek Formation, ~ 41.2 m below the Hell Creek-Tullock formational contact.

Referred Specimens—Fragmentary atlantes (N = 27): DMNH 52363, 52367, 55803, 55804, 55814, 56464, 56465, 56466, 56468, 56470; MOR 5375; UCMP 191301, 191538, 556483, 556509, 556586, 556611; UWBM 91059, 91771, 92730, 93364, 93368, 93372, 93377; fragmentary trunk vertebrae (N = 3): MOR 5344; UWBM 94095, 94999.

Referred Specimen Localities, Ages, and Horizons—MOR HC–377, HC–583 (= UCMP V99220); DMNH 3302, 3304, 3305; UCMP V99220 (= MOR HC–583), V99230, V99369; UWBM C1153 (= UCMP V82022); all in Garfield County, Montana, USA; late Maastrichtian, Lancian NALMA; within lower three-quarters of Hell Creek Formation from ~ 76.4 m to 19.5 m below the Hell Creek-Tullock formational contact.

Diagnosis—Differs from the Sirenidae in having articular surface of odontoid process of atlas not confluent with the anterior cotyles and in lacking transverse processes at the base of the neural arch walls; differs further in having trunk vertebrae lacking the Y-shaped configuration of the neural crest and paired aliform processes, single headed rib-bearers on all but the anterior most trunk vertebrae, anterior basapophyses, and spinal nerve foramina. Differs from the Amphiumidae in lacking a condyle on either side of the ventral midline of the odontoid process of the atlas; differs further in having trunk vertebrae lacking the paired postzygapophyseal crests and anterior basapophyses. Differs from the Batrachosauroididae in having anterior cotyles of atlas dorsoventrally compressed and shallowly concave and in having a prominent odontoid process; differs further in having trunk vertebrae amphicoelous (except from *Palaeoproteus*) and in lacking basapophyses (except from *Batrachosauroides* and *Peratosauroides*). Differs from the Scapherpetontidae in having atlas with an alar-like process along the ventrolateral aspect of centrum; differs further in having trunk vertebrae with a prominent groove on the posterior face of the neural arch and in having solid (i.e., lateral ends not hollow) dorsal rib-bearers. Differs from the proteids *Proteus anguinus*, *Mioproteus caucasicus*, and *Necturus maculosus* in having articular surface of odontoid process of atlas (atlas unknown for *N. krausei*) not confluent with the anterior cotyles; differs from *P. anguinus* (following atlantal character states uncertain for *M. caucasicus*), but similar to *N. maculosus*, in having an alar-like process along the ventrolateral aspect of centrum; differs from *P. anguinus* and *N. maculosus* in having odontoid process found approximately mid height of anterior cotyles (versus dorsal half), in having neural canal partly between anterior cotyles (versus above), and in lacking lateral flanges of the neural arch; differs further from *P. anguinus*, but similar to *N. maculosus*, in having a dorsally concave and perforated ventromedial surface of the centrum (versus ventrally convex and non-perforated);

trunk vertebrae differ from *P. anguinus*, *M. caucasicus*, *N. maculosus*, and *N. krausei* in having generally smaller subcentral foramina; differs from *P. anguinus* and *M. caucasicus*, but similar to *N. maculosus* and *N. krausei*, in having a unicipitate neural spine and divergent, bicipitate rib-bearers; differs from *M. caucasicus*, but similar to *P. anguinus*, *N. maculosus*, and *N. krausei*, in having a short neural crest and in lacking posterior basapophyses; differs further from *N. krausei*, but similar to *N. maculosus*, in having dorsal rib-bearer solid; differs from *N. maculosus*, but similar to *N. krausei*, in having anteroposteriorly-elongate postzygapophyses.

Justification of Association

Association of the atlas and trunk vertebrae of *Paranecturus garbanii* is based on their similar cotylar morphology and size and on co-occurrences within the Hell Creek Formation. The cotyles of the atlas and trunk vertebrae are subcircular to dorsoventrally compressed. They also have a thin layer of calcified cartilage internally and the moderate-sized open notochordal pit is slightly above the center. Dimensions of the cotyles are also similar. The width of the posterior cotyle of the holotype (UWBM 93370) is 0.81 mm. The average anterior and posterior cotylar width of the most nearly complete trunk vertebra (UWBM 94999) is 0.85 mm. Similarly, the approximate height of the posterior cotyle of the holotype is 0.72 mm versus an average height of 0.79 mm for the trunk vertebra. Finally, association of the vertebrae is made based on several co-occurrences at the same localities in the Hell Creek Formation. For example, both the holotype (UWBM 93370) and the most nearly complete trunk vertebra (UWBM 94999) come from the same locality (UWBM C1153).

Description

Atlas

Atlantes of *Paranecturus garbanii* (Figs. 4.2–4.4) range in intercotylar width from 1.6 mm to 2.5 mm and in centrum length (including odontoid process) from about 1.1 mm to 2.0 mm. The average dimensions are 2.0 mm (N=23) and 1.4 mm (N=20), respectively.

The odontoid process (= "intercotylar process" or "interglenoid tubercle" of some authors; e.g., Estes [1981] and Evans and Milner [1993], respectively) of the holotype (UWBM 93370) is damaged anteriorly and is bilaterally asymmetrical (Figs. 4.2A–C, E; 4.3A–C, E–G), but resembles referred specimens in most other respects. In the holotype, the process is moderately elongate and set between the medial edges of, and approximately in line with, the dorsoventral mid height of the anterior cotyles. The base of the odontoid process is expanded laterally on the left side, but slightly constricted on the right. In dorsal view, at approximately its mid length the process becomes restricted before broadening and becoming rounded anteriorly. In lateral view, the odontoid process is thick and extends near the horizontal. Anteriorly, the undamaged portion of the ventral and lateral surface is roughened. Specimens preserving a more nearly complete odontoid process indicate that the bilateral asymmetry seen in the holotype is atypical, because all referred specimens have bilaterally symmetrical expanded bases (e.g., DMNH 56465, UWBM 93372: Fig. 4.4C and 4.4J, respectively). A bilaterally symmetrical odontoid process is the normal condition among caudates.

The anterior cotyles are trapezoidal in anterior outline (Fig. 4.3A, B). The dorsal cotylar rim is inclined dorsolaterally along much of its width from the medial aspect of the cotyle and peaks well past the cotylar mid width. The surface of the anterior cotyles is roughened, slightly

concave top to bottom, and moderately concave side to side. Medially, the anterior cotyles are drawn forward onto the base of the odontoid process, and, in lateral view, they taper anteriorly (Fig. 4.3A–C, E). In dorsal and ventral views, the lateral three-fourths of the anterior cotyles face nearly perpendicular relative to the anteroposterior axis of the centrum (Fig. 4.3F, G).

The posterior cotyle of the holotype (UWBM 93370) was slightly damaged during examination but shows its original preservation in Figure 3A (see also Fig. 4.2A). In the undamaged DMNH 56465 (Fig. 4.4A–E), the posterior cotyle is subcircular, slightly dorsoventrally compressed, lined anteriorly with a thin layer of calcified cartilage, and has a moderate-sized open notochordal pit just above its center (Fig. 4.4B; see also Fig.4. 2D). In lateral view, the ventral margin of the anterior and posterior cotyles are approximately in line with each another (Fig. 4.4E).

The centrum of the holotype (UWBM 93370) is short anteroposteriorly and, in dorsal and ventral views, tapers posteriorly. Ventrally, the centrum is concave dorsally and relatively smooth at its center and is perforated by two medial subcentral foramina (Figs. 4.2E, 4.3G), one to either side of the mid line. A third foramen (Figs. 4.2B, E, 4.3C, G) is found posterior to the left anterior cotyle, whereas the right side lacks the same foramen. Along the ventrolateral margin of the centrum there is a moderately thick alar-like process or ridge that projects posteriorly from behind the anterior cotyles (Figs. 4.2B–E; 4.3B–G). An anterolaterally arcing ventrolateral ridge (Figs. 4.2E, 4.3G) bridges the posterior cotyle and the alar-like process. In lateral view, the centrum is excavated by a lateral fossa (Fig. 4.2B–D). The lateral fossa is found dorsal to the alar-like process which, in turn, is bordered medially by a deep groove. The left lateral fossa is open, whereas the right lateral fossa is partially covered roughly at its mid length by a thin webbing of bone that forms an anterior and posterior opening (Figs. 4.2B, 4.3C versus

4.2C, 4.3E; see also Fig. 4.2D). The right fossa is connected ventromedially to the right subcentral foramen as evidenced by passing a thin filament through the posterior opening (not figured). Posterior to the right alar-like process are two small openings (Fig. 4.2C–D). At the same level and position on the opposite side of the centrum the area is non-perforated and open to the left lateral fossa. The ventral margin of the centrum is concave dorsally (Figs. 4.2C, 4.3C, E). Immediately behind the anterior cotyle and ventral to the anterior region of the base of the neural arch is an ovoid spinal foramen (Figs. 4.2B–D, 4.3B–E). In some specimens, there are small and very low, rounded bony protuberances anterior to the spinal foramen (Fig. 4.2A and arrows in Fig. 4.4F)

None of the atlantes possess a complete neural arch. The holotype (UWBM 93370) is the most nearly complete atlas in the sample and it preserves most of the left and right neural arches. In lateral view, the base of the neural arch spans most of the distance between the anterior and posterior cotyles. The anterior margin is directed dorsally and slightly anteriorly and is offset posteriorly from the anterior cotylar rim. In general, the posterior border is sinuous (Figs. 4.2C, 4.3C, E). The lateral face of the neural arch wall is shallowly excavated and confluent ventrally with the lateral fossa of the centrum (Figs. 4.2B–D, 4.3B–E). The neural arches are widely divergent, forming a broad neural canal (Figs. 4.2A, D, 4.3A, D). In anterior view, the lateral edges of the neural arches are inclined at a slight angle medially.

Some notable individual morphological variation exists in the atlantes of *Paranecturus garbanii*. In dorsal view, the relatively complete odontoid process of UWBM 93372 (Fig. 4.4J) resembles the odontoid process of *Lisserpeton* in being slightly more arrowhead shaped anteriorly yet maintains the expanded base as in DMNH 56465 (Figs. 4.4J versus 4.4C, respectively). In lateral view, the odontoid process in the holotype (UWBM 93370) extends

approximately horizontal (Fig. 4.3C, E) versus slightly more ventral in DMNH 56465 (Fig. 4.4E). The relatively short and broadly rounded odontoid process of UCMP 191538 is atypical in having a dorsal surface that drops abruptly onto a short shelf-like projection anteriorly (see white arrow in Fig. 4.4I).

The anterior cotyles of *Paranecturus garbanii* are trapezoidal in outline but can vary in the degree of marginal curvature. For example, the ventral margin can be gently convex (UWBM 93370; Fig. 4.3A) to broadly rounded (UCMP 191538; Fig. 4.4I). Likewise, the lateral margin may be roughly straight (DMNH 56465, left anterior cotyle; Fig. 4.4A), broadly rounded (UCMP 191538; Fig. 4.4I), or more acutely rounded (UWBM 93370; Fig. 4.3A) as is the case for the medial margin. The degree of concavity also varies among the anterior cotyles. In dorsal and ventral views of most specimens, the lateral three-fourths or more of the anterior cotyles face nearly perpendicular to the anteroposterior axis of the centrum (e.g., UWBM 93370; Fig. 4.3F, G), whereas some face slightly more lateroposteriorly at their outermost edges (e.g., UCMP 191538; view not figured). The medial one-fourth or less of the cotyle is drawn forward onto or near the base of the odontoid process (e.g., see black arrow in Fig. 4.4J) and, in some specimens, this region of the anterior cotyle is oriented nearly perpendicular to the remainder of the cotyle (e.g., UWBM 93377; not figured). A few specimens (e.g., DMNH 55814, 56466; neither figured) have both medial and lateral edges drawn forward forming a posteriorly concave cotylar margin in dorsal view. No major differences in morphology occur in the posterior cotyle.

Ventrally, the centrum bears up to nine medially-placed subcentral foramina or pits (Figs. 4.3G; 4.4D, G). The alar-like process varies in dorsoventral thickness and length and in some specimens, it is only a round, knob-like protuberance (e.g., DMNH 56465:Fig. 4.4B, D, E; UCMP 556611:Fig. 4.4G, H). The lateral fossa may or may not be partially covered by a thin

webbing of bone (e.g., UWBM 93370 versus DMNH 56465; Fig. 4.3B–E versus Fig. 4.4B, E, respectively). The presence of the ventrolateral foramen can vary among the different atlantes as well as from side to side within the same specimen (e.g., UWBM 93370; Figs. 4.2E, 4.3G). The spinal nerve foramen is generally oval in outline, but the outline can vary from being anteroposteriorly to more dorsoventrally compressed (e.g., DMNH 56465 and UWBM 93370, respectively; Fig. 4.4E versus Fig. 4.3C, E).

In general, the neural arches of the referred specimens do not vary significantly from the holotype specimen (UWBM 93370). However, in several specimens the anterior face of the neural arch is flush with the anterior rim of the anterior cotyles (e.g., DMNH 56465; UCMP 556611; Fig. 4.4E and 4.4H, respectively) versus being offset posteriorly as in the holotype (Figs. 4.2C, 4.3C, E). In UCMP 556611, the anterior face of the base of the neural arch is flat and oriented transversely versus anterolaterally as in the holotype.

Trunk vertebrae

The sample of trunk vertebrae (Fig. 4.5) includes one nearly complete specimen (UWBM 94999) and two fragmentary specimens (UWBM 94095; MOR 5344). UWBM 94999 (Fig. 4.5A–H) is missing the anterior portion of the right prezygapophysis, the medial one half of the left prezygapophysis, and the lateral ends of most of the rib-bearers. UWBM 94095 (Fig. 4.5I–L) preserves the anterior portion of the centrum and most of the right side including both rib-bearers and the adjacent part of the neural arch. MOR 5344 (Fig. 4.5M–O) is the posterior half of a centrum.

The vertebra is moderately elongate and low (Fig. 4.5C, F). UWBM 94999 is 2.8 mm in length and 1.9 mm in height. The centrum is deeply amphicoelous and the cotyles are subcircular

(Fig. 4.5A, D, G, J) to moderately compressed dorsoventrally (Fig. 4.5M) in outline. In MOR 5344, the dorsal margin of the posterior cotyle is flattened relative to the ventral margin (Fig. 4.5M). An open and moderate-sized notochordal pit is found just above the center of the cotyle. A thin layer of calcified cartilage is present within the cotyles. The subcentral keel is concave dorsally. In ventral view, the subcentral keel varies from being relatively narrow (UWBM 94999; Fig. 4.5H) to moderately wide (UWBM 94095 and MOR 5344; Fig. 4.5K and N, respectively). In all three specimens the anterior and posterior extremities of the keel do not reach the cotylar rims. In UWBM 94095, a small foramen pierces the subcentral keel medially in the anterior half, whereas in MOR 5344 a small foramen pierces the keel in the posterior half (Fig. 4.5K versus N, respectively). In UWBM 94999, four small subcentral foramina are present: three on the left side and one on the right. The medial most left foramen is connected to a shallow and narrow groove that is oriented posteroventrally along the side of the subcentral keel (Fig. 4.5G, H). Two small subcentral foramina are present on the right side of UWBM 94095 (Fig. 4.5K). One relatively larger posterior subcentral foramen is found on either side of the subcentral keel in MOR 5344 (Fig. 4.5N). Basapophyses are lacking.

The transverse processes are bicipitate, divergent, and connected by a webbing of bone. Most of the rib-bearers of all three trunk vertebrae are broken laterally except for the left dorsal rib-bearer of UWBM 94999 (Fig. 4.5F, G), which is only slightly chipped, and the right dorsal rib-bearer of UWBM 94095 (Fig. 4.5I, L), which is intact. The base of the dorsal rib-bearer arises from the lateral edge of the neural arch roof. The ventral rib-bearer is at roughly the mid height of the centrum. The dorsal rib-bearers are solid (Fig. 4.5F, I). In UWBM 94999, the left dorsal rib-bearer is short and flattened side to side, whereas in UWBM 94095 the right dorsal rib-bearer is more elongate and oval in cross-section. Because the right dorsal rib-bearer of

UWBM 94999 is broken laterally it cannot be determined if it is solid or hollow. In UWBM 94999, the ventral rib-bearers are relatively larger and both right rib-bearers are more expanded than their left counterparts. The ventral rib-bearer in UWBM 94095 has a small hole at its tip suggesting that it may have been hollow laterally (Fig. 4.5K). The alar processes of the ventral rib bearers are thin and short. The right posterior alar process of UWBM 94999 is restricted to the base of the rib-bearer (Fig. 4.5H). A narrow vertebrarterial canal passes anteroposteriorly through the base of the transverse process.

The neural canal is vaulted but wider than tall (Fig. 4.5A, D). The roof of the neural arch is low and essentially flat. In UWBM 94999 a faint anteroposteriorly directed ridge is present along the lateral edge of the neural arch, whereas in UWBM 94095 the ridge is acutely rounded and prominent (Fig. 4.5B, C, F versus 4.5I, J, L). The neural crest is low, narrow, and extends posteriorly from the front of the neural arch to at least the level of the base of the neural spine. The neural spine in UWBM 94999 is unicipitate, low, and extends posteriorly well past the rim of the posterior cotyle. The neural spine is worn posteriorly and along the dorsal crest. The posterior face of the neural arch is indented by a prominent groove to either side of the neural spine (Figs. 4.5D, G, 4.6A). The groove is bounded dorsally and ventrally by a ridge (Fig. 4.6A). The ventral ridge is lamellar and forms an acutely V-shaped flange directly beneath the neural spine. No spinal foramina pierce the neural arch walls.

The preserved portions of the prezygapophyses indicate that they likely were oval in outline (Fig. 4.5E). The prezygapophyseal facets are tipped dorsally and medially at their lateral edges. The postzygapophyses are anteroposteriorly elongate and the facets are elliptical in outline (Fig. 4.5C, F, H). In UWBM 94999, the right postzygapophysis is larger and more rectangular in dorsal outline than the left (Fig. 4.5E). In posterior view, the postzygapophyses are

inclined laterally at ~35° from the horizontal (Fig. 4.5D). In lateral view, the left and right postzygapophyses range in posterior inclination from ~4° to ~12.5° from the horizontal, respectively. In UWBM 94999, the anterolateral margin of the postzygapophysis is nearly confluent with the base of the dorsal rib-bearer.

Remarks

Based on the unique combination of vertebral character states described above, it is apparent that *Paranecturus garbanii*, gen. et sp. nov., is a distinct caudate. *P. garbanii* possesses a suite of vertebral character states allying it with *Necturus*, *Proteus*, and *Mioproteus* (atlas with dorsoventrally compressed anterior cotyles, trunk vertebrae deeply amphicoelous with little calcified cartilage lining the cotylar walls, subcircular cotyles, low neural spine, and lack of spinal nerve foramina), with *Necturus* and *Proteus* (atlas with prominent odontoid process, trunk vertebrae with low neural crest, presence of a groove on the posterior face of the neural arch, and lack of basapophyses), and, more exclusively, with *Necturus* (atlas with shallowly concave anterior cotyles, presence of alar-like process of centrum, trunk vertebrae with unicipitate neural spines, divergent rib-bearers, and solid dorsal rib-bearers). Together, these features support assigning *P. garbanii* to the Proteidae. However, there are considerable differences in atlantal morphology between *Paranecturus*, *Necturus*, and *Proteus* (following atlantal character states uncertain for *Mioproteus*), such as the lack of a confluent articular surface between the odontoid process and the anterior cotyles, the odontoid process set at mid height of the anterior cotyles (versus upper half), and the neural arch partly between the anterior cotyles (versus above). These character states, in addition to having dorsoventrally compressed and shallowly concave anterior cotyles, are also seen in the Scapherpetontidae (e.g., *Scapherpeton*, *Lisserpeton*) which raises the

possibility that *P. garbanii* represents a small scapherpetontid. Nevertheless, the presence and configuration of the alar-like process along the ventrolateral margin of the centrum is inconsistent with known scapherpetontids. In contrast, it shares this feature with some atlantes (3 out of 5 examined) of *N. maculosus* and with some batrachosauroidids, which are thought to be closely related to proteids (e.g., Naylor 1978b, 1979; Estes 1981). Both *Opisthotriton kayi* and *Prodesmodon copei* have an alar-like process showing varying degrees of development (e.g., Estes 1964: figs. 38F and 42C, respectively; see also Estes 1975:fig. 2C, D and Gardner 2000).

Many features of the trunk vertebrae of *Paranecturus garbanii* are also shared among scapherpetontids (amphicoelous centra, unicipitate neural spines, divergent rib-bearers of the transverse process, lack of basapophyses and spinal nerve foramina). However, the presence of a well-developed groove on the posterior face of the neural arch is lacking in specimens of *Scapherpeton* and *Lisserpeton* available to me and in the two species of *Piceoerpeton* based on figured and described specimens in the literature (e.g., Estes 1981; Naylor and Krause 1981; Gardner, 2012). This feature is prominent in *N. maculosus* (Fig. 4.6B; see also Naylor 1978a:fig. 2), in the holotype of *N. krausei* (UALVP 14310; Naylor, 1978a:fig. 1A), and to a lesser extent, in *Proteus anguinus* (pers. obs.). In addition, the solid dorsal rib-bearer seen in the trunk vertebrae of *P. garbanii* is also found in some vertebrae of *N. maculosus*, but not in any known scapherpetontid.

PHYLOGENETIC ANALYSIS

Methods

I conducted a series of phylogenetic analyses in order to explore relationships of the new taxon among select caudates. The first set of analyses was conducted using TNT v. 1.1 (Goloboff et al. 2008). The data matrix was created using Mesquite v. 2.75 (Maddison and Maddison 2011). The matrix includes 13 taxa and 23 characters from the atlas and trunk vertebrae. The character matrix created by Denton and O'Neill (1998) and later revised by Gardner (2000) formed the basis of the analyses. Minor modifications and additions were made (list of characters, Appendix 4.1; character matrix, Appendix 4.2). All characters were unordered and were equally weighted. The first phylogenetic analysis includes all 13 taxa, whereas, the second analysis excludes the fossil proteid *Necturus krausei*, because more than half (57%) of the characters of *N. krausei* are not scorable (see Appendix 4.2). The extant cryptobranchid *Cryptobranchus alleganiensis* was chosen as the outgroup, because cryptobranchoids are widely considered to occupy a basal position among crown-group salamanders or Urodela (e.g., Gao and Shubin 2001; Roelants et al. 2007) and was used to polarize character states. The ingroup includes mostly Late Cretaceous to early Eocene caudates from the Western Interior of Canada and the USA Two extant and one late Paleocene proteid were also included. Members of the ingroup were chosen specifically to test the proteid versus scapherpetontid affinities of *P. garbanii*. The ingroup comprises: the amphiumid *Proamphiuma cretacea;* the batrachosauroidids *Opisthotriton kayi* and *Prodesmodon copei*; the proteids *N. krausei*, *N. maculosus*, and *Proteus anguinus*; the scapherpetontids *Scapherpeton tectum*, *Lisserpeton bairdi*, *Piceoerpeton willwoodense*, and *P.* sp; the sirenid *Habrosaurus dilatus*; and the new taxon, *Paranecturus*

garbanii (see Table 4.1 for the ages and biogeographic ranges of each taxon). Exhaustive searches (implicit enumeration) were performed to find the most parsimonious trees. Bremer and bootstrap values are reported. Bootstrap values are based on 10,000 replicates. The last set of phylogenetic analyses is based on the results (i.e., most parsimonious tree topology) from the second exhaustive search excluding *N. krausei*. I performed a heuristic search in PAUP* v. 4.0b10 (Swofford 2002) of two alternative topologies to determine the difference in tree length between the single most parsimonious tree and one in which monophyly was enforced between *P. garbanii* and the Scapherpetontidae.

Results

The first set of phylogenetic analyses using the exhaustive search method recovered similar topologies regardless of whether or not *Necturus krausei* was included (Fig. 4.7A versus 4.7B). Inclusion of *N. krausei* resulted in three most parsimonious trees (strict consensus shown in Fig. 4.7A; tree length = 49 steps; consistency index [CI] = 0.633; retention index [RI] = 0.640), whereas, only one most parsimonious tree (Fig. 4.7B; tree length = 49 steps; CI = 0.633; RI = 0.633) was recovered when *N. krausei* was excluded from the analysis. Both exhaustive searches recovered a monophyletic Batrachosauroididae (*Opisthrotriton kayi* + *Prodesmodon copei*; Fig. 4.7A, B, Node B) and Scapherpetontidae ((*Piceoerpeton willwoodense* + *P.* sp.) + (*Scapherpeton tectum* + *Lisserpeton bairdi*); Fig. 4.7A, B, Node S) and a sister-pair relationship between the amphiumid *Proamphiuma cretacea* and the sirenid *Habrosaurus dilatus* (Fig. 4.7A, B). The strict consensus including *N. krausei* places *Paranecturus garbanii* in an unresolved polytomy with the proteids *N. krausei*, *N. maculosus*, and *Proteus anguinus* (Fig. 4.7A, Node P). Exclusion of *N. krausei* resulted in *P. garbanii* being the sister taxon to the extant proteids (Fig.

4.7B, Node P). Both exhaustive searches recovered similar Bremer and bootstrap values (see values above and below branches, respectively, leading to the nodes in Fig. 4.7A and 4.7B). The batrachosauroidids, scapherpetontids, and the genus *Piceoerpeton* are moderately supported (i.e., decay index = 2; bootstrap ≥ 50%), whereas, all other nodes are weakly supported (i.e., decay index = 1; bootstrap < 50%). Results from the heuristic search indicate that removal of *P. garbanii* from the Proteidae (i.e., from the most parsimonious tree topology) and enforcing strict monophyly of *P. garbanii* with the Scapherpetontidae requires one additional step (tree length = 50 versus 51 steps, respectively).

Remarks

The phylogenetic relationships presented here are based on atlantal and trunk vertebral character states only, and thus, the higher-level relationships of the ingroup (i.e., Amphiumidae, Batrachosauroididae, Proteidae, Scapherpetontidae, Sirenidae) are tentative. Previous work based on qualitative assessments and on more nearly complete specimens or suites of elements than those used here suggested a sister taxon relationship between the Batrachosauroididae and Proteidae (Estes 1975, 1981; Estes and Darevsky 1978; Naylor 1978a, b, 1979, 1981). More complete sampling of taxa and characters might help resolve the higher-level relationships of these taxa.

DISCUSSION and CONCLUSIONS

Several character states observed in *Paranecturus garbanii*, gen. et sp. nov., provide evidence for assigning it to the Proteidae. Among these are characters states that are most notably present in *Necturus maculosus* such as the alar-like process of the atlas (character 10, state 1) and the solid dorsal rib-bearers (character 21, state 1) and neural arch groove (character 23, state 1) of the trunk vertebrae. In addition, the results of the phylogenetic analysis provide a testable hypothesis for the affinities of *P. garbanii* and indicate that *P. garbanii* is likely a basal proteid (Fig. 4.7A, B).

Paranecturus garbanii represents a latest Cretaceous proteid. Reports of pre-Cenozoic proteids such as the Late Jurassic *Comonecturoides* (Hecht and Estes 1960) and the Early Cretaceous *Hylaeobatrachus croyi* (Dollo 1884; Herre 1935) are better regarded as Caudata *incertae sedis* (Estes 1981). Owing to its relationship with the late Paleocene *Necturus krausei*, the presence of *P. garbanii* in the latest Cretaceous implies that the lineage survived the Cretaceous-Paleogene mass extinction. This hypothesis is consistent with molecular divergence estimates, which also support a pre-Cenozoic origin for the Proteidae (e.g., Roelants et al. 2007; Zhang and Wake 2009).

The fossil record of proteids is still poor (Naylor 1978a; Estes 1981). Thus, the discovery of the fossil proteid *Paranecturus garbanii* adds significantly to our understanding of the clade's evolution. Based on specimens of *P. garbanii*, it can be postulated when certain character states of the atlas and trunk vertebrae evolved in this lineage. For example, the lateral flanges of the atlas (character 11) had not yet evolved in the Proteidae by the end of the Cretaceous; whereas, the alar-like process (character 10) seen in *Necturus* had. Discovery of atlantes of *Necturus*

krausei may aid in determining more precisely when certain other atlantal features evolved in the *Necturus* lineage.

ACKNOWLEDGMENTS

I thank G. P. Wilson, C. Sidor, L. Tsuji, S. Nesbitt, J. Calede, J. Grummer (University of Washington, Seattle, Washington [UW]), and J. Gardner (Royal Tyrrell Museum of Palaeontology, Drumheller, Alberta) for helpful reviews, discussions, or technical support, on topics related to this project. Additional thanks to J. Gardner for providing relevant literature and SEM images of *Necturus krausei* for comparison. A. Leaché, K. Petersen (UW), and D. Wake (University of California, Berkeley, California) provided access to skeletonized specimens of *Cryptobranchus alleganiensis*, *Necturus maculosus*, and *Proteus anguinus*, respectively. Reviews by J. Gardner and P. Skutschas (Saint Petersburg State University, Saint Petersburg, Russia) and editorial comments by J. Anderson (University of Calgary, Alberta, Canada) were valuable in improving this manuscript. The Bureau of Land Management, Charles M. Russell Wildlife Refuge, and Montana Fish, Wildlife, and Parks have provided logistical support and special use permits for the collection of the vertebrate fossils studied here. This material, in part, is based upon work supported by the National Science Foundation Graduate Research Fellowship under Grant No. DGE-0718124.

REFERENCES CITED

Abramoff, M. D., P. J. Magalhaes, and S. J. Ram. 2004. Image Processing with ImageJ. Biophotonics International 11:36–42.

Bryant, L. J. 1989. Non-dinosaurian lower vertebrates across the Cretaceous-Tertiary boundary in northeastern Montana. University of California Publications in Geological Sciences 134:1–107.

DeMar, D. G., Jr. 2011. New taxonomic, paleobiogeographic, and biostratigraphic records of fossil salamanders (Caudata) from the Hell Creek and Tullock formations of Garfield County, Montana. Journal of Vertebrate Paleontology 31(3, Supplement):98A.

DeMar, D. G., Jr., and B. Breithaupt. 2006. The nonmammalian vertebrate microfossil assemblages of the Mesaverde Formation (Upper Cretaceous, Campanian) of the Wind River and Bighorn basins, Wyoming; pp. 33–54 in S. G. Lucas, and R. M. Sullivan (eds.), Late Cretaceous vertebrates from the Western Interior. New Mexico Museum of Natural History and Science Bulletin 35.

Denton, R. K., Jr., and R. C. O'Neill. 1998. *Parrisia neocesariensis*, a new batrachosauroidid salamander and other amphibians from the Campanian of eastern North America. Journal of Vertebrate Paleontology 18:484–494.

Dollo, L. 1884. Note sur le Batracien de Bernissart. Bulletin du Musée Royal d'Histoire Naturelle de Belgique 3:85-93.

Estes, R. 1964. Fossil vertebrates from the Late Cretaceous Lance Formation of eastern Wyoming. University of California Publications in Geological Sciences 49:1–187.

Estes, R. 1965. A new fossil salamander from Montana and Wyoming. Copeia 1965:90–95.

Estes, R. 1969. The fossil record of amphiumid salamanders. Breviora 322:1–11.

Estes, R. 1975. Lower vertebrates from the Fort Union Formation, late Paleocene, Big Horn Basin, Wyoming. Herpetologica 31:365–385.

Estes, R. 1981. Gymnophiona, Caudata; pp. 1–115 in P. Wellnhofer (ed.), Encyclopedia of Paleoherpetology, Part 2. Gustav Fischer Verlag, Stuttgart.

Estes, R., and P. Berberian. 1970. Paleoecology of a Late Cretaceous vertebrate community from Montana. Breviora 343:1–35.

Estes, R., and I. Darevsky. 1977. Fossil amphibians from the Miocene of the North Caucasus, U.S.S.R. Journal of the Palaeontological Society of India 20:164–169.

Evans, S. E., and A. R. Milner. 1993. Frogs and salamanders from the Upper Jurassic Morrison Formation (Quarry Nine, Como Bluff) of North America. Journal of Vertebrate Paleontology 13:24–30.

Gao, Ke-Qin, and N. H. Shubin. 2001. Late Jurassic salamanders from northern China. Nature 410:574–577.

Gardner, J. D. 2000. Systematics of albanerpetontids and other lissamphibians from the Late Cretaceous of western North America. Ph.D. dissertation. University of Alberta, Edmonton, 577 pp.

Gardner, J. D. 2003a. The fossil salamander *Proamphiuma cretacea* Estes (Caudata: Amphiumidae) and relationships within the Amphiumidae. Journal of Vertebrate Paleontology 23:769–782.

Gardner, J. D. 2003b. Revision of *Habrosaurus* Gilmore (Caudata; Sirenidae) and relationships among sirenid salamanders. Palaeontology 46:1089–1122.

Gardner, J. D. 2005. Lissamphibians; pp. 186–199 in P. J. Currie and E. B. Koppelhus (eds.), Dinosaur Provincial Park: A Spectacular Ancient Ecosystem Revealed. Indiana University Press, Bloomington, Indiana.

Gardner, J. D. 2012. Revision of *Piceoerpeton* Meszoely (Caudata: Scapherpetontidae) and description of a new species from the late Maastrichtian and ?early Paleocene of western North America. Bulletin de la Société Géologique de France 6:611–620.

Gardner, J. D., J. G. Eaton, and R. L. Cifelli. 2013. Preliminary report on salamanders (Lissamphibia; Caudata) from the Late Cretaceous (late Cenomanian–late Campanian) of southern Utah, U.S.A.; pp. 237–272 in A. L. Titus and M. A. Lowen (eds.), At the Top of the Grand Staircase: The Late Cretaceous of southern Utah. Indiana University Press, Bloomington, Indiana.

Goloboff, P. A., J. S. Farris, and K. C. Nixon. 2008. TNT, a free program for phylogenetic analysis. Cladistics 24:774–786.

Gray, J. E. 1825. A synopsis of the genera of reptiles and Amphibia, with a description of some new species. Annals of Philosophy (Series 2) 10:193-217.

Haeckel, E. 1866. Generelle Morphologie der Organismen, 2 volumes. Reimer, Berlin.

Hecht, M. K., and R. Estes. 1960. Fossil amphibians from Quarry Nine. Postilla 46:1–19.

Herre, W. 1935. Die Schwanzlurche der mitteleocänen (oberlutetischen) Braunkohle des Geiseltales und der Phylogenie der Urodelen unter Einschluss der fossilen Formen. Zoologica (Stuttgart) 33:1–85.

Holman, J. A. 2006. Fossil salamanders of North America. Indiana University Press, Bloomington, Indiana, 232 pp.

Maddison, W. P., and D. R. Maddison. 2011. Mesquite: a modular system for evolutionary analysis. Version 2.75. Available at http://mesquiteproject.org.

Naylor, B. G. 1978a. The earliest known *Necturus* (Amphibia, Urodela), from the Paleocene Ravenscrag Formation of Saskatchewan. Journal of Herpetology 12:565–569.

Naylor, B. G. 1978b. The systematics of fossil and recent salamanders (Amphibia: Caudata), with special reference to the vertebral column and trunk musculature. Ph.D. dissertation, University of Alberta, Edmonton, 857 pp.

Naylor, B. G. 1979. The Cretaceous salamander *Prodesmodon* (Amphibia: Caudata). Herpetologica 35:11–20.

Naylor, B. G. 1981. A new salamander of the family Batrachosauroididae from the late Miocene of North America, with notes on other batrachosauroidids. Paleobios 39:1–14.

Naylor, B. G. 1983. New salamander (Amphibia: Caudata) atlantes from the Upper Cretaceous of North America. Journal of Paleontology 57:48–52.

Naylor, B. G., and D. W. Krause. 1981. *Piceoerpeton*, a giant Early Tertiary salamander from western North America. Journal of Paleontology 55:507–523.

Roelants, K., D. J. Gower, M. Wilkinson, S. P. Loader, S. D. Biju, K. Guillaume, L. Moriau, and F. Bossuyt. 2007. Global patterns of diversification in the history of modern amphibians. Proceedings of the National Academy of Sciences of the USA 104:887–892.

Scopoli, G. A. 1777. Introductio ad Historiam Naturalem. Wolfgang Gerle, Prague.

Sket, B. 1997. Distribution of *Proteus* (Amphibia: Urodela: Proteidae) and its possible explanation. Journal of Biogeography 24:263–280.

Swofford, D. L. 2002. PAUP*. Phylogenetic Analysis Using Parsimony (*and Other Methods). Version 4. Sinauer Associates, Sunderland, Massachusetts.

Wilson, G. P. 2004. A quantitative assessment of mammalian change leading up to and across the Cretaceous-Tertiary boundary in northeastern Montana. Ph.D. dissertation, University of California, Berkeley, California, 412 pp.

Wilson, G. P. 2005. Mammalian faunal dynamics during the last 1.8 million years of the Cretaceous in Garfield County, Montana. Journal of Mammalian Evolution 12:53–75.

Wilson, G. P., D. G. DeMar, Jr., and G. Carter. 2014. Extinction and survival of salamander and salamander-like amphibians across the Cretaceous-Paleogene boundary in northeastern Montana; in G. P. Wilson, W. A. Clemens, J. R. Horner, and J. Hartman (eds.), Through the end of the Cretaceous in the type locality of the Hell Creek Formation in Montana and adjacent areas. Geological Society of America Special Paper, Boulder, Colorado.

Zhang, P., and D. B. Wake. 2009. Higher-level salamander relationships and divergence dates inferred from complete mitochondrial genomes. Molecular Phylogenetics and Evolution 53:492–508.

FIGURES for CHAPTER 4

Figure 4.1. Maps illustrating provenance of *Paranecturus garbanii*, gen. et sp. nov. **A**, North America with Montana darkened. **B**, state of Montana with Garfield County darkened (modified from Wilson 2004).

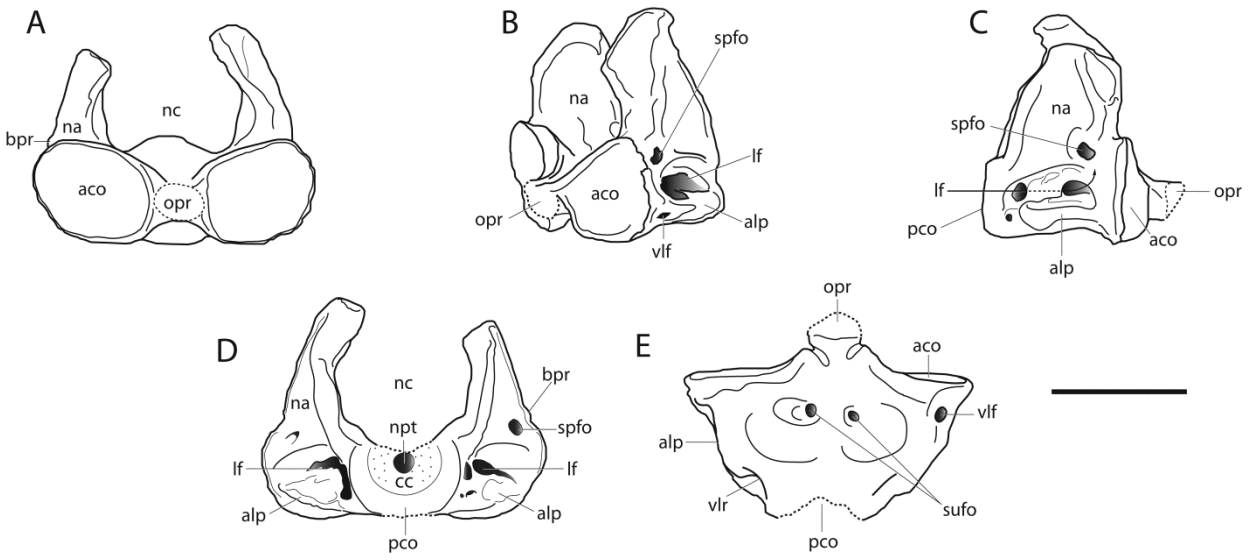

Figure 4.2. Holotype (UWBM 93370) of *Paranecturus garbanii*, gen. et sp. nov.., from the Hell Creek Formation, Montana. Labeled line drawings of the atlas in **A**, anterior, **B**, left lateral and anterior, **C**, right lateral, **D**, posterior, and **E**, ventral views. Arrow emphasizes the lateral fossa (lf) by passing behind thin webbing of bone in C. Dashed lines represent broken or worn areas. Scale bar equals 1 mm.

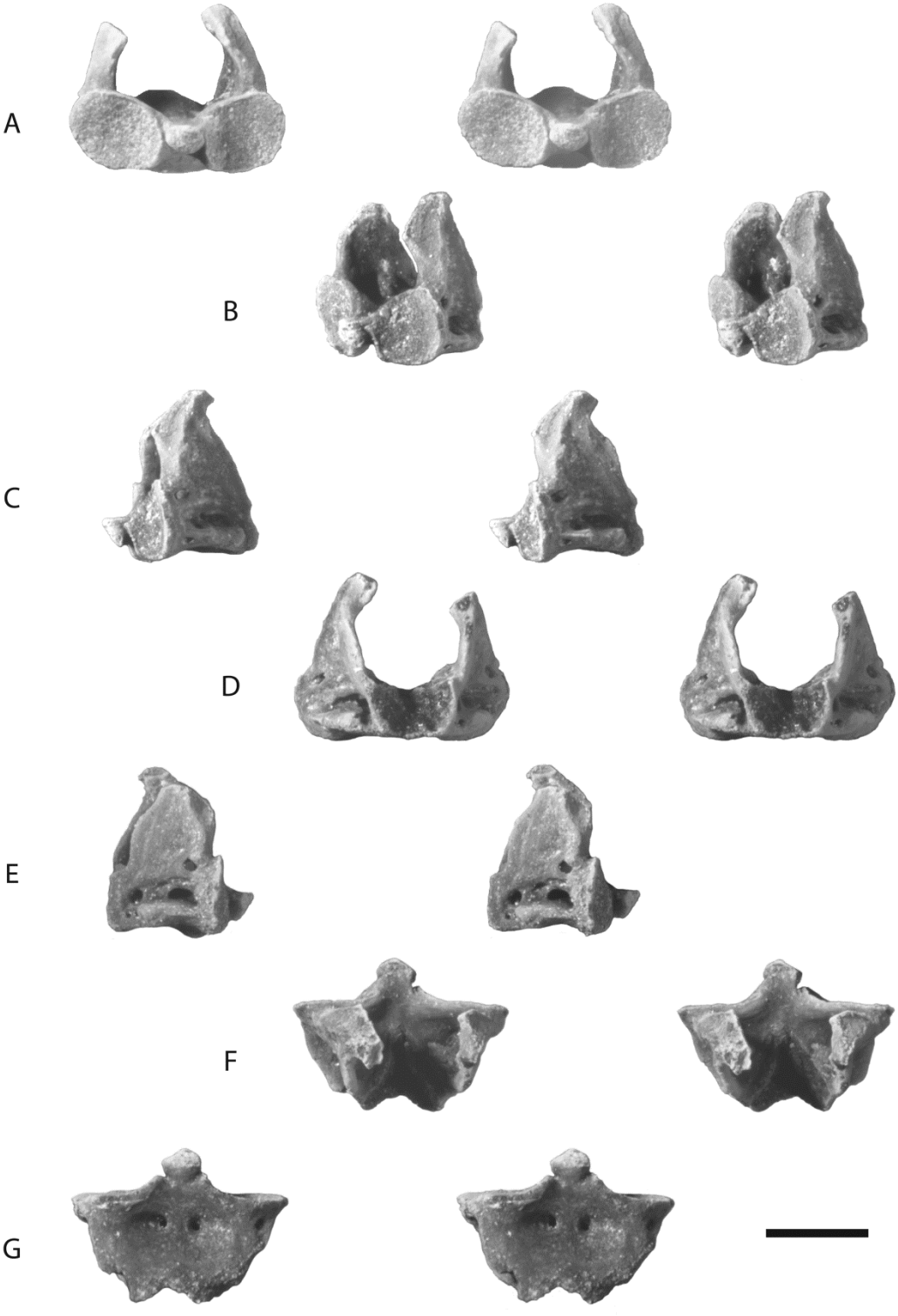

Figure 4.3. Holotype (UWBM 93370) of *Paranecturus garbanii*, gen. et sp. nov., from the Hell Creek Formation, Montana. Stereophotos of the atlas in **A**, anterior, **B**, left lateral and anterior,

C, left lateral, **D**, posterior, **E**, right lateral, **F**, dorsal, and, **G**, ventral views. Scale bar equals 1 mm. [stereo pair; print exact size]

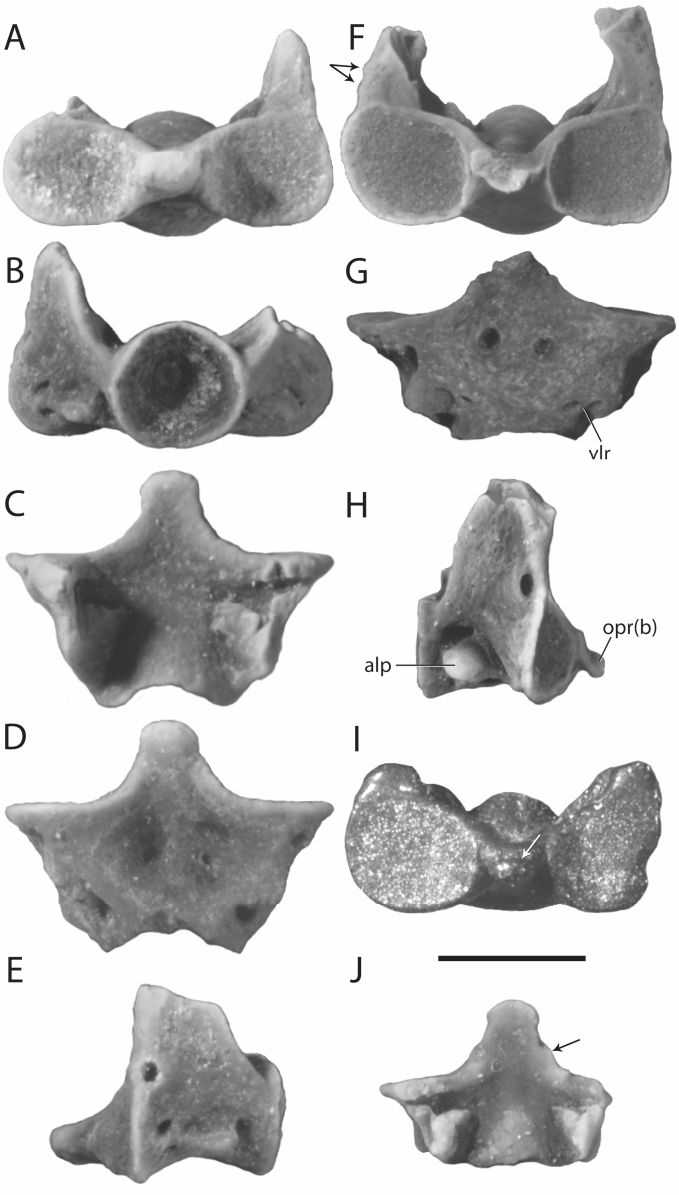

Figure 4.4. Referred atlantes of *Paranecturus garbanii*, gen. et sp. nov., from the Hell Creek Formation, Montana. DMNH 56465 in **A**, anterior, **B**, posterior, **C**, dorsal, **D**, ventral, and **E**, left lateral views. UCMP 556611 in **F**, anterior, **G**, ventral, and **H**, right lateral views. **I**, UCMP 191538 in anterior view. **J**, UWBM 93372 in dorsal view. Arrows in F point to low bony protuberances. See text for explanation of arrows in I and J. Scale bar equals 1 mm.

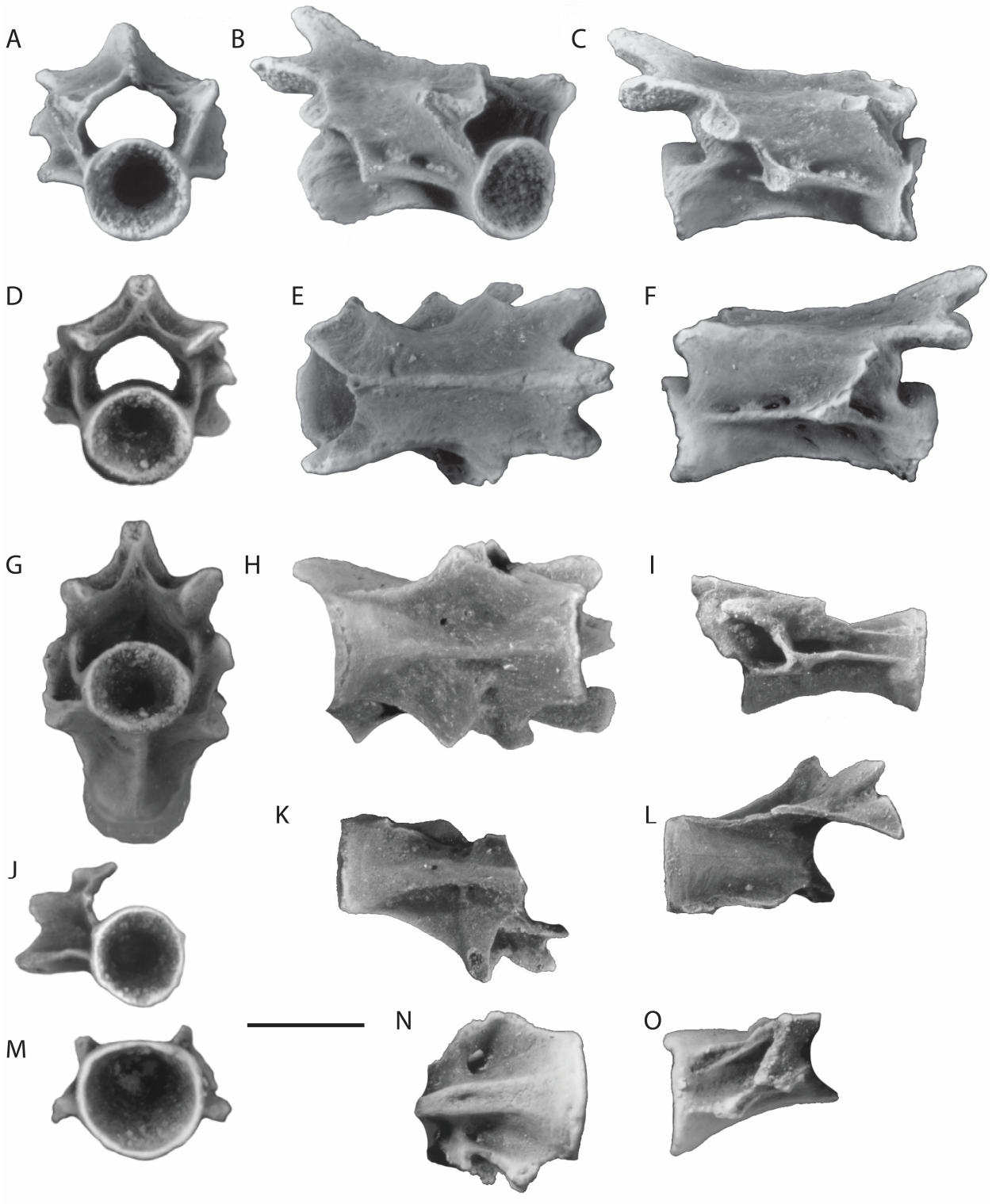

Figure 4.5. Referred trunk vertebrae of *Paranecturus garbanii*, gen. et sp. nov., from the Hell Creek Formation, Montana. UWBM 94999 in **A**, anterior, **B**, right lateral and anterior, **C**, right

lateral, **D**, posterior, **E**, dorsal, **F**, left lateral, **G**, posterior and ventral, and **H**, ventral views. UWBM 94095 in **I**, right lateral, **J**, anterior, **K**, ventral, and **L**, dorsal views. MOR 5344 in **M**, posterior, **N**, ventral, and **O**, right lateral views. Scale bar equals 1 mm.

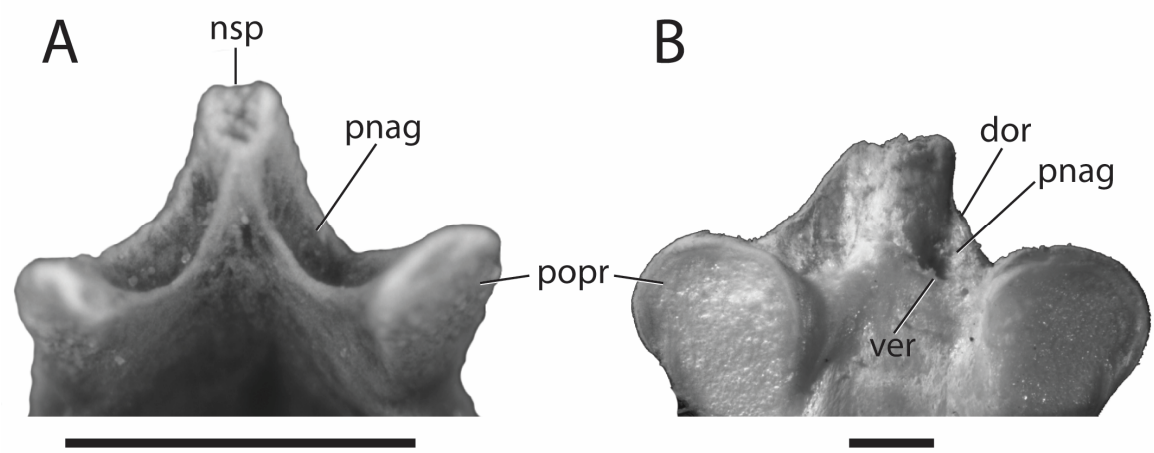

Figure 4.6. Configuration of the groove on the posterior face of the neural arch in **A**, *Paranecturus garbanii*, gen. et sp. nov. (UWBM 94999), and **B,** *Necturus maculosus* (uncatalogued specimen). Scale bars equal 1 mm.

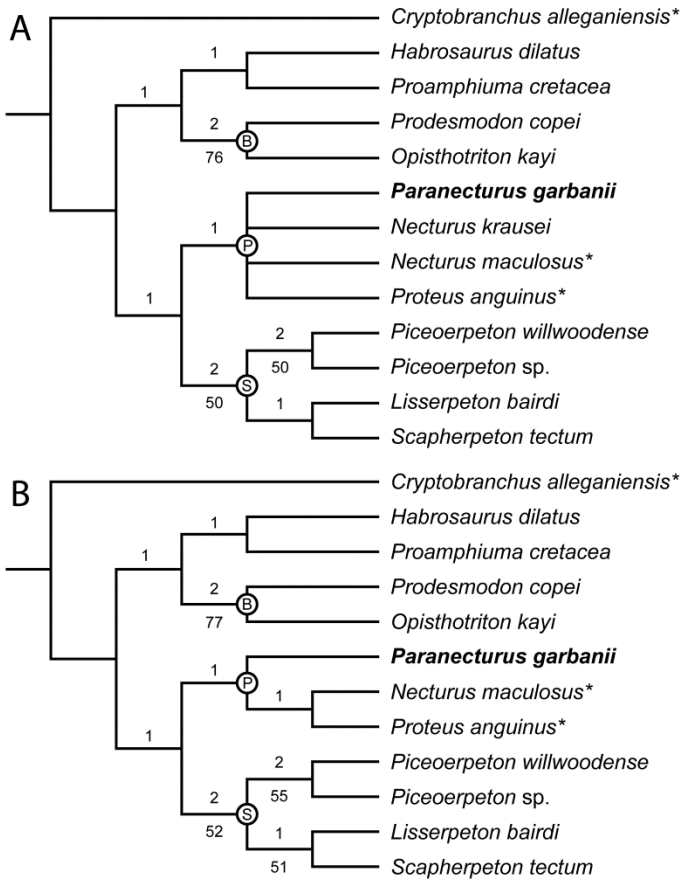

Figure 4.7. Phylogenetic hypotheses resulting from parsimony analysis. **A**, strict consensus of three most parsimonious trees (49 steps; CI = 0.633; RI = 0.640) including all 13 taxa based on an exhaustive search. **B**, single most parsimonious tree (49 steps; CI = 0.633; RI = 0.633) excluding *Necturus krausei* based on an exhaustive search. Node B = Batrachosauroididae, Node P = Proteidae, and Node S = Scapherpetontidae. Asterisks (*) indicate extant taxa. Values above branches leading to the nodes represent Bremer support, whereas, the values below the branches are the bootstrap values ≥ 50%.

TABLES for CHAPTER 4

Table 4.1. List of caudates used for the phylogenetic analyses and their temporal and biogeographic ranges.

Taxon	Age	Biogeography	References
Cryptobranchus alleganiensis	late Pleistocene–Recent	Eastern USA	11
Necturus maculosus	late Pleistocene–Recent	Southeastern Canada and eastern USA	11
Proteus anguinus	Recent	Southeastern Europe	16
Opisthotriton kayi	Santonian–late Paleocene	Western Interior of Canada and USA	5, 6, 10
Prodesmodon copei	late Campanian–early Paleocene	Western Interior of Canada and USA	1, 2, 5, 6, 10, 19
Scapherpeton tectum	Santonian–late Paleocene	Western Interior of Canada and USA	2, 5, 6, 10
Lisserpeton bairdi	late Campanian–middle Paleocene	Western Interior of Canada and	1, 3, 5, 6, 10

		USA	
Piceoerpeton willwoodense	late Paleocene–early Eocene	Western Interior of Canada and USA; Ellesmere Island, Canada	5, 9, 15
Piceoerpeton sp.	late Maastrichtian–?early Paleocene	Montana and Wyoming, USA	9, 12, 17
Proamphiuma cretacea	?late Maastrichtian–early Paleocene	Montana, USA	4, 5, 7, 17
Habrosaurus dilatus	late Maastrichtian–middle Paleocene	Western Interior of Canada and USA	2, 5, 8
Necturus krausei	late Paleocene	Saskatchewan, Canada	5, 13, 14
Paranecturus garbanii	late Maastrichtian	Montana, USA	17, 18

References: **1**, DeMar and Breithaupt (2006); **2**, Estes (1964); **3**, Estes (1965); **4**, Estes (1969); **5**, Estes (1981); **6**, Gardner (2000); **7**, Gardner (2003a); **8**, Gardner (2003b); **9**, Gardner (2012); **10**, Gardner et al. (2013); **11**, Holman (2006); **12**, Naylor (1983); **13**, Naylor (1978a); **14**, Naylor (1978b); **15**, Naylor and Krause (1981); **16**, Sket (1997); **17**, Wilson et al. (2014); **18**, this paper; **19**, personal observation.

APPENDIX to CHAPTER 4

Appendix 4.1. Description of characters used in the phylogenetic analyses. Some character descriptions are modified from previous studies and for those are formatted as: (author:character number). **Abbreviations**: **DO**, Denton and O'Neill (1998); **G**, Gardner (2000). Additional characters are polarized with respect to *Cryptobranchus alleganiensis*.

Atlas

(1) Relative depth of anterior cotyles: nearly flat to shallowly excavated (0); moderate to deeply excavated (1) (DO:6; G:4).

(2) Outline of anterior cotyles: subcircular (0); compressed dorsoventrally (1); compressed lateromedially (2) (DO:4; G:5).

(3) Form of odontoid process: anteriorly elongate knob (0); dorsoventrally flattened and reduced in length (1); dorsoventrally flattened and reduced further to a horizontal bar (2) (DO:7; G:6).

(4) Position of neural canal relative to anterior cotyles: above (0); partly between (1) (G:7).

(5) Dorsal outline of posterior margin of neural arch roof: truncate or pointed (0); forked (1) (DO:8; G:10).

(6) Dorsal outline of neural crest: broadens posteriorly (0); narrows posteriorly (1) (DO:9; G:11).

(7) Condition of anterior end of neural crest in dorsal view: not emarginated laterally (0); emarginated laterally (1) (G:12).

(8) Postzygapophyses: prominent and laterally divergent (0); smaller and directed more ventrolaterally (1); "…weakly developed and does not project ventrally or laterally any significant distance from the neural arch" (2; Gardner, 2003:774) (DO:10; G:13).

(9) Condition of articular surface of odontoid process: large (0); small (1); absent (2) (this paper).

(10) Alar-like process of centrum: absent (0); present (1) (this paper).

(11) Lateral flanges of neural arch: absent (0); present (1) (this paper).

(12) Condition of articular surface of odontoid process and anterior cotyles: not confluent (0); confluent (1) (this paper).

(13) Position of odontoid process relative to anterior cotyles: mid-height or lower (0); upper one half (1) (this paper).

Trunk vertebrae

(14) Form of centrum: amphicoelous (0); semi-opisthocoelous (1); fully opisthocoelous (2) (DO:11; G:16).

(15) Posterior basapophyses: absent (0); present (1) (DO:13,14; G:17).

(16) Anterior basapophyses: absent (0); present (1) (DO:13,14).

(17) Position of ventral margin of subcentral keel in lateral view of middle trunk vertebrae relative to ventral margin of anterior and posterior cotyles: above (0); approximately in line (1); below (2) (this paper).

(18) Height of neural spine: low (0); high (1) (DO:16; G:18).

(19) Height of neural crest of middle trunk vertebrae: low, gently rises posteriorly onto base of neural spine (0); moderate in height, rises at a more pronounced angle posteriorly relative to dorsal surface of neural arch roof (1); high, rises at a pronounced angle and is equal to or greater than the height of the neural spine (2) (this paper).

(20) Form of transverse process: bicipitate and appressed (0); bicipitate and divergent (1); unicipitate (2) (DO:17; G:19).

(21) Form of transverse process and condition of lateral ends of rib-bearer(s) of middle trunk vertebrae: bicipitate with dorsal and ventral rib-bearers hollow (0); bicipitate with dorsal rib-bearer solid and ventral rib-bearer hollow (1); unicipitate and solid (2) (this paper).

(22) Condition of neural spine: finished in cartilage (0); finished in bone (1) (DO:19; G:20).

(23) Mediolateral groove on the posterior face of the neural arch spanning between the neural spine and postzygapophyses: absent (0); present (1) (this paper).

Appendix 4.2. Character-taxon matrix used for phylogenetic analysis. Polymorphic states are identified as: **A**, (0,1); **B** (1,2).

	10	20	23
Cryptobranchus alleganiensis	0000000000	0000000000	000
Proteus anguinus	0100110000	1110001002	201
Necturus maculosus	010000000A	1110000001	A01
Necturus krausei	----------	---0000001	001
Paranecturus garbanii	0101----01	0000000001	1-1
Opisthotriton kayi	10B1A101BA	0001102000	010
Prodesmodon copei	1221010121	0002102002	210
Scapherpeton tectum	0101101000	0000002111	000
Lisserpeton bairdi	0101011000	0000001111	000
Piceoerpeton willwoodense	1111-00020	0000001111	000
Piceoerpeton sp.	1111----20	0000000-11	0-0
Habrosaurus dilatus	0100----00	0100010022	210
Proamphiuma cretacea	1001010200	0000010022	210

CHAPTER 5:

A NEW LATE CRETACEOUS (CAMPANIAN) STEM IGUANIAN FROM NORTHWESTERN MONTANA, USA

ABSTRACT and INTRODUCTION

Pre-Neogene iguanian lizards are poorly understood owing to their incomplete fossil record (Conrad and Norell 2007), particularly from North America (NA) where, prior to the Cretaceous-Paleogene boundary (K-Pg; ~66 million years ago), they are based solely on a few isolated jaw fragments (Gao and Fox 1996; Longrich et al. 2012). Here we describe a new fossil iguanomorph, *Magnuviator ovimonsensis* gen. et sp. nov., based on two nearly complete skeletons from Upper Cretaceous (Campanian) strata of Montana, USA. Our morphology-based phylogenetic analysis recovers *Magnuviator* as a stem iguanian (Iguanomorpha sensu Conrad 2008) and sister to Temujiniidae (Gauthier et al. 2012) a contemporaneous iguanomorph clade from the Gobi Desert of Mongolia. That relationship establishes the first phylogenetically informed paleobiogeographic link for Iguanomorpha between Asia and North America during the Cretaceous and sets a minimum estimate of iguanomorph occupation in North America of ~75.5 Ma (Varricchio et al. 2010). In light of this evidence and the equivocal phylogenetic position of the aforementioned fragmentary NA specimens, the occurrence of crown Iguania in NA prior to the K-Pg boundary is doubtful (contra Gao and Fox 1996 and Longrich et al. 2012). Geologic and fossil evidence at Egg Mountain (Rogers 1990; Varricchio et al. 2002) suggest *Magnuviator* inhabited a semi-arid environment; a similar environment interpreted for other Late Cretaceous iguanomorphs of Asia (Gao and Norell 2000) and South America (Simões et al. 2015). Comparative snout-vent length (SVL) and cranial measurements demonstrate that *Magnuviator* was a relatively large Late Cretaceous iguanomorph (e.g., nearly twice the SVL of its sister taxon *Saichangurvel davidsoni*). Based on dental similarities and diets of several extant

pleurodontan iguanians, *Magnuviator* likely preyed on wasps that are identified by their trace fossils at Egg Mountain.

MATERIALS and METHODS

Computed Tomography

Three dimensional volumetric renderings derived from CT scans of both specimens augmented our descriptions when possible. To enhance our understanding of the anatomy of *Magnuviator ovimonsensis* gen. et sp. nov. and to provide comparable visual data with that of Gauthier et al. (2012) for our cladistic analyses (see below) we subjected MOR 6627 and 7042 to computed and micro-computed tomography (CT and μCT, respectively). Voxel size resolution varied among each specimen scanned which was largely dependent on the physical size of each specimen block and CT scanner used. MOR 6627 was scanned at a voxel resolution of 67.7 microns (μm^3), MOR 7042a+c (skull and partial forelimb and pectoral girdle) at 58.6 μm^3, and the largest block of MOR 7042d containing the majority of the postcranial skeleton at 47.8 μm^3. Specimen blocks were scanned at the Microscopy and Imaging Facility at the American Museum of Natural History, New York, New York, USA using a GE phoenix Vtome x S 240 CT scanner. A fourth scan of a small block (MOR 7042b) containing portions of the premaxilla, nasals, prefrontals, and frontal was conducted using a SkyScan 1174 μCT scanner at a resolution of 30.7 μm^3 at the University of Washington (S. Santana Lab, Department of Biology), Seattle, Washington, USA. The quality and resolution of each scan varied considerably. The scans of MOR 6627, 7042b, and 7042d provided relatively poor resolution making segmentation and 3D rendering difficult and often impossible for most regions of those specimens. The scan of MOR 7042a+c provided quality resolution for processing. CT and μCT data was processed, segmented,

and visualized using the software programs Fiji (Schindelin et al. 2012), DataViewer (version 1.5.1.2, Bruker microCT, Belgium), and Mimics (version 17, Materialise, Belgium).

Phylogenetic analysis

To investigate the evolutionary relationships of *Magnuviator ovimonsensis* we conducted a series of cladistic analyses based on the phenotype. MOR 6627 and 7042 were scored based on direct observations of the specimens, CT images, and 3D reconstructions. We included *M. ovimonsensis* into the character/taxon data matrix assembled by Gauthier et al. (2012). We also added one North American Late Cretaceous (Maastrichtian) lizard, the putative iguanian *Pariguana lancensis* (Longrich et al. 2012), for further testing the iguanian affinities of that taxon. The data matrix was assembled in Mesquite version 3.02 (Maddison & Maddison 2015). Cladistic analyses were performed in the software program *Tree Analysis Using New Technology* (TNT; Goloboff et al. 2008). We used the New Technology search (sectorial, ratchet, drift, and tree fusing options activated) to search for 500 minimum tree length recoveries. Characters were ordered per Gauthier et al. (2012). MOR 6627 and 7042 were independently scored and cladistically analyzed initially as separate operational taxonomic units (OTUs) to test the assumption that they belong to the same taxon. Phylogenetic results demonstrated a sister pair relationship between those specimens. In subsequent analyses we treated MOR 6627 and 7042 as a single OTU by combining the non-overlapping characters and character states from each specimen. Our initial analyses excluded the poorly scored *Pariguana lancensis*, which is based exclusively on an isolated partial mandible. See Table 5.1 for character scores of *Magnuviator* and *Pariguana*. Minimum tree lengths, number of most parsimonious trees, and Consistency and

Retention indices (CI and RI, respectively) were recorded and provided in the accompanying figure captions. Strict consensus trees were constructed in PAUP* 4.0 (Swofford 2003) and visualized in FigTree (version 1.3.1). Bremer (1000 replicates) support values for nodes were determined based on a Traditional (TBR) Wagner Parsimony Analysis in TNT. A synapomorphy list including unambiguous character state optimizations for the strict consensus tree was created in PAUP* 4.0 to identify the key morphological features that diagnose *M. ovimonsensis* and the relevant taxonomic clades (Table 5.2).

RESULTS and DISCUSSION

Systematic Paleontology

Reptilia Linnaeus, 1758

Squamata Oppel, 1811

Iguanomorpha Sukhanov, 1961 (sensu Conrad, 2008)

Magnuviator ovimonsensis gen. et sp. nov.

Figures 5.1–5.6

Etymology. *Magnus*, mighty; *viator*, traveler, in reference to its relatively large body size and the North American occurrence of an otherwise Asian clade of iguanomorphs; *ovimonsensis,* from Egg Mountain.

Holotype. Museum of the Rockies (MOR) 6627, a nearly complete and mostly articulated skeleton (Fig. 5.1).

Locality and age. Egg Mountain locality (MOR loc. TM-006), Upper Cretaceous (Campanian; ~75.5 ± 0.40 Myr ago; Varricchio et al. 2010) Two Medicine Formation, Teton County, northwestern Montana, USA.

Paratype. MOR 7042, a nearly complete and mostly articulated skeleton (Figs. 5.2 and 5.3).

Diagnosis. The new taxon is a member of Iguanomorpha based on the following unambiguous character states: parietal foramen at the frontoparietal suture and presence of a prefrontal boss and prearticular angular process. It differs from its sister taxon Temujiniidae in possessing an ascending process of the squamosal and from other known iguanomorphs in possessing an astragalocalcaneal notch in the tibia.

Description. *Magnuviator* is relatively large for an iguanomorph being similar in size to extant *Basiliscus basiliscus* with an estimated snout-vent length (SVL) of up to ~216 mm (Table 5.3). *Magnuviator* is considerably larger than its sister taxon *Saichangurvel davidsoni* (SVL ~117 mm) and most extant iguanians (see Zug et al. 2001, pp. 469–477, and references therein) and, based on cranial dimensions, all other Late Cretaceous iguanomorphs from Mongolia except *Anchaurosaurus gilmorei* (Table 5.3).

Nearly all bones of the skull, hyoid, and sclerotic ring are preserved between the holotype and paratype of *Magnuviator* (Figs. 5.1–5.4). The azygous frontal is moderately rugose dorsally, has a narrow interorbital region and a transversely oriented posterior margin at the frontoparietal suture, and possesses the anterior margin of the pineal foramen. The parietal in both specimens is damaged anteriorly and, thus, the overall size of the pineal foramen or fontanelle is uncertain. The robust prefrontal possesses a lateral boss and an elongate frontal process. The jugal lacks a posteroventral process. A partial postfrontal may be preserved, but it is too fragmentary for positive identification. An ascending squamosal process is present as in most Iguania, but not in

Temujiniidae. The pyriform recess is closed anteriorly by the paired vomers. Anterolaterally, the palatine features an anteroventrally oriented foramen. The complete braincase lacks a prominent prootic alar process, contrasting the scleroglossan condition (Gauthier et al. 2012).

The elongate dentary possesses an open Meckel's canal (Fig. 5.4b), as in Chamaeleontiformes (sensu Conrad 2008), contrasting the condition in *Temujinia*, *Pariguana lancensis* (Longrich et al. 2012), and basal and most extant pleurodontans (Gauthier et al. 2012; Longrich et al. 2012; Smith 2009a). The splenial extends for about three-fourths the length of the dentary tooth row and houses the anterior mylohyoid foramen and the ventral margin of the anterior inferior alveolar foramen (Fig. 5.4b). The anterior mylohyoid foramen is positioned anteroventral to the anterior inferior alveolar foramen. The dentary is smooth externally, lacking the V-shaped wear facets diagnostic of Chamaeleontiformes. The prearticular possesses a well-developed angular process (Fig. 5.4b).

Marginal teeth are closely spaced, non-striated, columnar, and pleurodont (Fig. 5.4b). Most are straight and moderately tricuspid with a short primary central cusp and a small mesial and distal cusp. Maxillary tooth counts, including vacant tooth spaces in both specimens, range from 22–24, whereas, 30 tooth positions are present in each paratype dentary.

Twenty-nine procoelous vertebrae are preserved in the holotype (18 presacral, two sacral, nine proximal caudals) with approximately seven posterior presacrals missing; similar numbers are preserved in the paratype. Ventrolaterally oriented zygosphenes are present being similar to those of corytophanids, crotaphytids, and iguanids.

The pectoral and pelvic girdles and most elements of the fore- and hind limbs are preserved. The clavicle is expanded and notched medially. The interclavicle possesses an anterior interclavicular process (Fig. 5.5). A scapulocoracoid and primary coracoid fenestra of

the scapulocoracoid are present. The ilium, pubis, and ischium are fused at the acetabulum suggesting both specimens represent adult individuals. The symphyseal process of the pubis is thin, a feature uniting *Magnuviator* with Temujiniidae. *Magnuviator* possesses a distally notched tibia for articulation with a ridge on the fused astragalocalcaneum (Fig. 5.6).

Phylogenetic Results

Magnuviator ovimonsensis is a basal iguanomorph and sister to Temujiniidae (Fig. 5.7). This *Magnuviator* + Temujiniidae clade is variably recovered as the basalmost pleurodontan clade or as the sister taxon to all other iguanomorphs (Fig. 5.8). Bremer support is poor but favors the stem pleurodontan relationship (BS=1; Fig. 5.9). Previous phylogenetic analyses including one or both temujiniids similarly recovered them as either stem iguanians (Smith 2009a; Simões et al. 2015), stem pleurodontans (Reeder et al. 2015), or unresolved relative to those clades (Gauthier et al. 2012; Longrich et al. 2012) or as members of Gobiguania (Conrad and Norell 2007; Conrad 2015).

Magnuviator, like many Late Cretaceous iguanomorphs from Asia (Gao and Hou 1995, 1996; Gao and Norell 2000; Conrad and Norell 2007), provides important inferences on the ancestral characters of Iguanomorpha. The key features exhibited in these Cretaceous iguanomorphs, including those previously identified as scleroglossan synapomorphies, aid in polarizing character states throughout the iguanomorph and squamate tree. Several previously ascribed iguanian synapomorphies (e.g., presence of prefrontal boss, parietal foramen at frontoparietal suture; Estes et al. 1988) are present in all Late Cretaceous iguanomorphs including *Magnuviator*. Similarly, two unambiguous synapomorphies of crown Scleroglossa (Estes et al. 1988; Gauthier et al. 2012) absent in extant iguanians but present in Temujiniidae

and *Ctenomastix* (presence of medially and laterally forked postfrontals that clasp the frontoparietal suture and postorbital, respectively) and *Magnuviator* (distally notched tibia) also occur. Presence of an anterior interclavicular process is yet another proposed scleroglossan synapomorphy (Estes et al. 1988; Conrad 2008; Gauthier et al. 2012) found in *Magnuviator*, but it is homoplastic within crown Iguania (Gauthier et al. 2012). Currently, *Magnuviator* is the only fossil iguanomorph known to possess a distal tibial notch, which may represent a plesiomorphic character for Iguanomorpha.

Laurasian dispersal of Iguanomorpha during the Cretaceous

The sister taxon relationship of *Magnuviator* and Temujiniidae provides the first well-supported phylogenetic link among iguanomorphs between the Late Cretaceous of Asia and North America. Cretaceous biotic dispersal between these landmasses has been inferred for several other terrestrial vertebrate groups including non-iguanian lizards (Nydam 2002, 2013), dinosaurs (Evans et al. 2013), and mammals (Cifelli 2000). Extinct monstersaurian (platynotan) and polyglyphanodontian lizards are known to have closely related North American and East Asian representatives during the Late Cretaceous (Conrad et al. 2011; Gauthier et al. 2012) implying dispersal within those groups. The iguanomorph dispersal occurred prior to the late Campanian based on age estimates of the type locality of *Magnuviator* (~75.5 Ma; Varricchio et al. 2010), but may have happened as early as the Cenomanian (Nydam 2002, 2013).

Crown Iguania absent from North America prior to the K-Pg boundary

Magnuviator is the oldest unequivocal iguanomorph from North America and predates unambiguous crown pleurodontans on the continent by nearly 20 myr (Smith 2009b; Conrad et al. 2007; Conrad 2015). *Pariguana lancensis* (Longrich et al. 2012) from the Late Cretaceous (Maastrichtian) of Wyoming likely represents an iguanomorph, but not a member of the iguanian crown as the holotype mandible lacks unambiguous pleurodontan synapomorphies (see node 248 to 247 in Table 5.3) and its phylogenetic relationships among stem + crown Iguania are uncertain (Fig. 5.10). Similarly, the remaining putative iguanians from the late Santonian and Maastrichtian of Canada (Gao and Fox 1996) either lack diagnostic features of Pleurodonta, are too incomplete to make a confident referral to Iguanomorpha (based chiefly on tooth crown morphology), or are members of the stem scleroglossan clades Polyglyphanodontia or Chamopsiidae (Longrich et al. 2012; Nydam 2013).

Paleoecological inferences

Magnuviator inhabited a seasonal and semi-arid upland environment based on the geologic, taphonomic, and fossil evidence at Egg Mountain and from the parent Two Medicine Formation (Rogers 1990; Varricchio et al. 2002). The fine-grained sediments of Egg Mountain were heavily modified by pedogenesis and bioturbation under subaerial conditions (Varricchio et al. 2002) and have yielded body and trace fossils of mostly terrestrial taxa (e.g., lizards, dinosaurs, dinosaur egg clutches, mammals, terrestrial gastropods, insect pupae cases (Horner 1982, 1994; Varricchio et al. 1999; Montellano et al. 2000). These biotic and abiotic factors at Egg Mountain broadly resemble those from the Ukhaa Tolgod locality (Djadokhta), Mongolia, which preserves temujiniids and other iguanomorphs (Gao and Norell 2000; Conrad and Norell

2007). The dune-margin alluvial fan sediments at Ukhaa Tolgod represent deposition during rain storms within a predominantly arid to semi-arid environment and have yielded a similar well-preserved vertebrate fossil assemblage in addition to dinosaur egg clutches and insect traces (Gao and Norell 2000; Loope et al. 1998; Conrad and Norell 2007). The chamaeleontiform *Gueragama sulamericana* from the Late Cretaceous of Brazil also inhabited an arid environment (Simões et al. 2015). In contrast to these more xeric environments, most Late Cretaceous nonmarine squamate assemblages of North America were deposited within lowland freshwater meandering river systems of the Western Interior (Rocky Mountain region) and were predominated by non-iguanian lizards identified largely on the basis of fragmentary jaws collected from vertebrate microfossil assemblages (Gao and Fox 1996; Longrich et al. 2012; Nydam 2013). Combined, these observations suggest that stem iguanians likely favored and evolved in arid to semi-arid environments with younger crown lineages occupying more humid environments such as the polychrotids and corytophanids known from the Eocene of North America (Conrad et al. 2007; Conrad 2015) and Europe (Smith 2009a).

Diet inferences

Morphological comparisons with extant pleurodontan iguanians of known dietary habits and body size lead to our inference that *Magnuviator* was insectivorous and possibly carnivorous. The tricuspid tooth crowns of *Magnuviator* are present in a number of extant insectivorous pleurodontans (Hotton 1955) including phrynosomatids and the extant crotaphytid *Crotaphytus*, a morphological and, perhaps, ecological analog to *Saichangurvel* (Conrad and Norell 2007), other Gobi iguanians (Gao and Norell 2000), and *Magnuviator*. Some phrynosomatid species (*Callisaurus draconoides ventralis*, *Urosaurus ornatus levis*) are known

to feed heavily on wasps and bees (Hotton 1955). Wasp pupae cases are nearly ubiquitous at Egg Mountain (D. Varricchio and J. Moore, pers. commun. 2015) and are morphologically identical to those made by wasps identified from a neighboring fossil locality of the Two Medicine Formation (Martin and Varricchio 2011). The co-occurrence of wasp pupae cases and *Magnuviator* provides indirect evidence of probable predator-prey interactions at Egg Mountain (Fig. 5.11). Larger body size in extant *Gambelia wislizenii* (Crotaphytidae) is known to influence its prey selection with larger individuals (SVL 105–115 mm) preying on vertebrates in addition to larger insects (Pianka and Vitt 2003). The relatively large body size of *Magnuviator* (SVL ~216 mm) implies that it at least was capable of eating small vertebrates.

CONCLUSIONS

Globally, *Magnuviator ovimonsensis* represents one of only two Late Cretaceous iguanomorphs known from nearly complete remains–the other being *Saichangurvel*–and one of only two Late Cretaceous lizards from North America based on similarly complete skeletons and from multiple individuals (i.e., *Polyglyphanodon sternbergi*; Gilmore 1942). Our study of *Magnuviator* has provided a wealth of new morphological, phylogenetic, and paleoecological information crucial to understanding the early evolutionary history of Iguanomorpha. The study of additional well-preserved squamates at Egg Mountain has the potential to yield equally important information regarding the evolution of Squamata, such as that provided by the partial skeleton of the stem platynotan *Palaeosaniwa wyomingensis* present at that locality (Balsai 2001; Conrad et al. 2011).

REFERENCES CITED

Balsai, M. J. 2001. The phylogenetic position of *Palaeosaniwa* and the early evolution of the platynotan (varanoid) anguimorphs: In Earth and Environmental Sciences, Ph.D. dissertation, pp. 253. University of Pennsylvania, Philadelphia.

Cifelli, R. L. 2000. Cretaceous mammals of Asia and North America. Paleontological Society of Korea Special Publication 4:49–84.

Conrad, J. L. 2008. Phylogeny and systematics of Squamata (Reptilia) based on morphology. Bulletin of the American Museum of Natural History 310:1–182.

Conrad, J. L. 2015. A new Eocene casquehead lizard (Reptilia, Corytophanidae) from North America. PLoS ONE 10:e0127900.

Conrad, J. L., and M. A. Norell. 2007. A complete Late Cretaceous iguanian (Squamata, Reptilia) from the Gobi and identification of a new iguanian clade. American Museum Novitates 3584:1–47.

Conrad, J. L., O. Rieppel, and L. Grande. 2007. A Green River (Eocene) polychrotid (Squamata: Reptilia) and a re-examination of iguanian systematics. Journal of Paleontology 81:1365–1373.

Conrad, J. L., O. Rieppel, J. A. Gauthier, and M. A. Norell. 2011. Osteology of *Gobiderma pulchrum* (Monstersauria, Lepidosauria, Reptilia). Bulletin of the American Museum of Natural History 362:1–88.

Estes, R., K. de Queiroz, and J. A. Gauthier. 1988. Phylogenetic relationships within squamata; pp. 119–282 in R. Estes, and G. K. Pregill (eds.), Phylogenetic relationships of the lizard families. Stanford University Press, Stanford.

Evans, D., D. Larson, and P. J. Currie. 2013. A new dromaeosaurid (Dinosauria: Theropoda) with Asian affinities from the latest Cretaceous of North America. Naturwissenschaften 100:1041–1049.

Gao, K., and L. Hou. 1995. Iguanians from the Upper Cretaceous Djadokhta Formation, Gobi Desert, China. Journal of Vertebrate Paleontology 15:57–78.

Gao, K., and L. Hou. 1996. Systematics and taxonomic diversity of squamates from the Upper Cretaceous Djadokhta Formation, Bayan Mandahu, Gobi Desert, People's Republic of China. Canadian Journal of Earth Sciences 33:578–598.

Gao, K., and M. A. Norell. 2000. Taxonomic composition and systematics of Late Cretaceous lizard assemblages from Ukhaa Tolgod and adjacent localities, Mongolian Gobi Desert. Bulletin of the American Museum of Natural History 249:1–118.

Gao, K., and R. C. Fox. 1996. Taxonomy and evolution of Late Cretaceous lizards (Reptilia: Squamata) from western Canada. Bulletin of Carnegie Museum of Natural History 33:1–107.

Gauthier, J. A., M. Kearney, J. A. Maisano, O. Rieppel, and A. D. B. Behlke. 2012. Assembling the squamate tree of life: Perspectives from the phenotype and the fossil record. Bulletin of the Peabody Museum of Natural History 53:3–308.

Gilmore, C. W. 1942. Osteology of *Polyglyphanodon*, an Upper Cretaceous lizard from Utah. Proceedings of the United States National Museum 92:229–265.

Goloboff, P. A., J. S. Farris, and K. C. Nixon. 2008. TNT, a free program for phylogenetic analysis. Cladistics 24:774–786.

Horner, J. R. 1982. Evidence of colonial nesting and 'site fidelity' among ornithischian dinosaurs. Nature 297:675-676.

Horner, J. R. 1994. Comparative taphonomy of some nesting dinosaur and extant bird colonial nesting grounds; pp. 116–123 in K. Carpenter, K. E. Hirsch, and J. R. Horner (eds.), Dinosaur Eggs and Babies. Cambridge University Press, New York.

Hotton III, N. 1955. Survey of adaptive relationships of dentition to diet in the North American Iguanidae. American Midland Naturalist 53:88–114.

Linnaeus, C. V. 1758. Systema naturae per regna tria naturae, secundum classes, ordines, genera, species, cum characteribus, differentiis, synonymis, locis. 824 pp. Salvii Nat., Holmiae [Stockholm].

Longrich, N. R., B. A. S. Bhullar, and J. A. Gauthier. 2012. Mass extinction of lizards and snakes at the Cretaceous–Paleogene boundary. Proceedings of the National Academy of Sciences 109:21396–21401.

Loope, D. B., L. Dingus, C. C. Swisher, III, and C. Minjin. 1998. Life and death in a Late Cretaceous dune field, Nemegt Basin, Mongolia. Geology 26:27–30.

Maddison, W. P., and D. R. Maddison. 2015. Mesquite: a modular system for evolutionary analysis. Version 3.02 http://mesquiteproject.org

Martin, A. J., and D. J. Varricchio. 2011. Paleoecological utility of insect trace fossils in dinosaur nesting sites of the Two Medicine Formation (Campanian), Choteau, Montana. Historical Biology 23:15–25.

Montellano, M., A. Weil, and W. A. Clemens. 2000. An exceptional specimen of *Cimexomys judithae* (Mammalia: Multituberculata) from the Campanian Two Medicine Formation of Montana, and the phylogenetic status of *Cimexomys*. Journal of Vertebrate Paleontology 20:333–340.

Nydam, R. L. 2002. Lizards of the Mussentuchit local fauna (Albian–Cenomanian boundary) and comments on the evolution of the Cretaceous lizard fauna of North America. Journal of Vertebrate Paleontology 22:645–660.

Nydam, R. L. 2013. Squamates from the Jurassic and Cretaceous of North America. Palaeobiodiversity and Palaeoenvironments 93:535–565.

Oppel, M. 1811. Die Ordnungen, Familien, und Gattungen der Reptilien als Prodrom einer Naturgeschichte derselben. 86 pp. Joseph Lindauer, Munchen.

Pianka, E. R., and L. J. Vitt. 2003. Lizards: Windows to the evolution of diversity. 333 pp. University of California Press, Berkeley.

Reeder, T. W., T. M. Townsend, D. G. Mulcahy, B. P. Noonan, P. L. Wood, Jr., J. W. Sites, Jr., and J. J. Wiens. 2015. Integrated analyses resolve conflicts over squamate reptile phylogeny and reveal unexpected placements for fossil taxa. PLoS ONE: DOI:10.1371/journal.pone.0118199.

Rogers, R. R. 1990. Taphonomy of three dinosaur bone beds in the Upper Cretaceous Two Medicine Formation of northwestern Montana; evidence for drought-related mortality. Palaios 5:394–413.

Schindelin, J., I. Arganda-Carreras, E. Frise, V. Kaynig, M. Longair, T. Pietzsch, S. Preibisch, C. Rueden, S. Saalfeld, B. Schmid, J.-Y. Tinevez, D. J. White, V. Hartenstein, K. Eliceiri, P. Tomancak, and A. Cardona. 2012. Fiji: an open-source platform for biological-image analysis. Nature Methods 9:676-682.

Simões, T. R., E. Wilner, M. W. Caldwell, L. C. Weinschütz, and A. W. A. Kellner. 2015. A stem acrodontan lizard in the Cretaceous of Brazil revises early lizard evolution in Gondwana. Nature Communications 6:8149.

Smith, K. T. 2009a. Eocene Lizards of the Clade *Geiseltaliellus* from Messel and Geiseltal, Germany, and the Early Radiation of Iguanidae (Reptilia: Squamata). Bulletin of the Peabody Museum of Natural History 50:219–306.

Smith, K. T. 2009b. A new lizard assemblage from the earliest Eocene (zone Wa0) of the Bighorn Basin, Wyoming, U.S.A.: biogeography during the warmest interval of the Cenozoic. Journal of Systematic Palaeontology 7:299–358.

Sukhanov, V. B. 1961. Some problems of the phylogeny and systematics of Lacertilia (seu Sauria). Zoologicheskii Zhurnal 40:73–83.

Swofford, D. 2003. PAUP*. Phylogenetic Analysis Using Parsimony (*and Other Methods). Sinauer Associates, Sunderland, Massachusetts.

Varricchio, D. J., C. Koeberl, R. F. Raven, W. Wolbach, W. C. Elsik, and D. P. Miggins. 2010. Tracing the Manson impact event across the Western Interior Cretaceous Seaway; pp. 269–299 in W. U. Reimold, and R. L. Gibson (eds.), Proceedings of the Conference on Large Meteorite Impacts and Planetary Evolution 4. Geological Society of America Special Papers 465, Boulder.

Varricchio, D. J., F. D. Jackson, and C. N. Trueman. 1999. A Nesting Trace with Eggs for the Cretaceous Theropod Dinosaur *Troodon formosus*. Journal of Vertebrate Paleontology 19:91-100.

Varricchio, D. J., J. R. Horner, and F. D. Jackson. 2002. Embryos and eggs for the Cretaceous theropod dinosaur *Troodon formosus*. Journal of Vertebrate Paleontology 22:564–576.

Zug, G. R., L. J. Vitt, and J. P. Caldwell. 2001. Herpetology: An introductory biology of amphibians and reptiles. 630 pp. Academic Press, San Diego.

FIGURES for CHAPTER 5

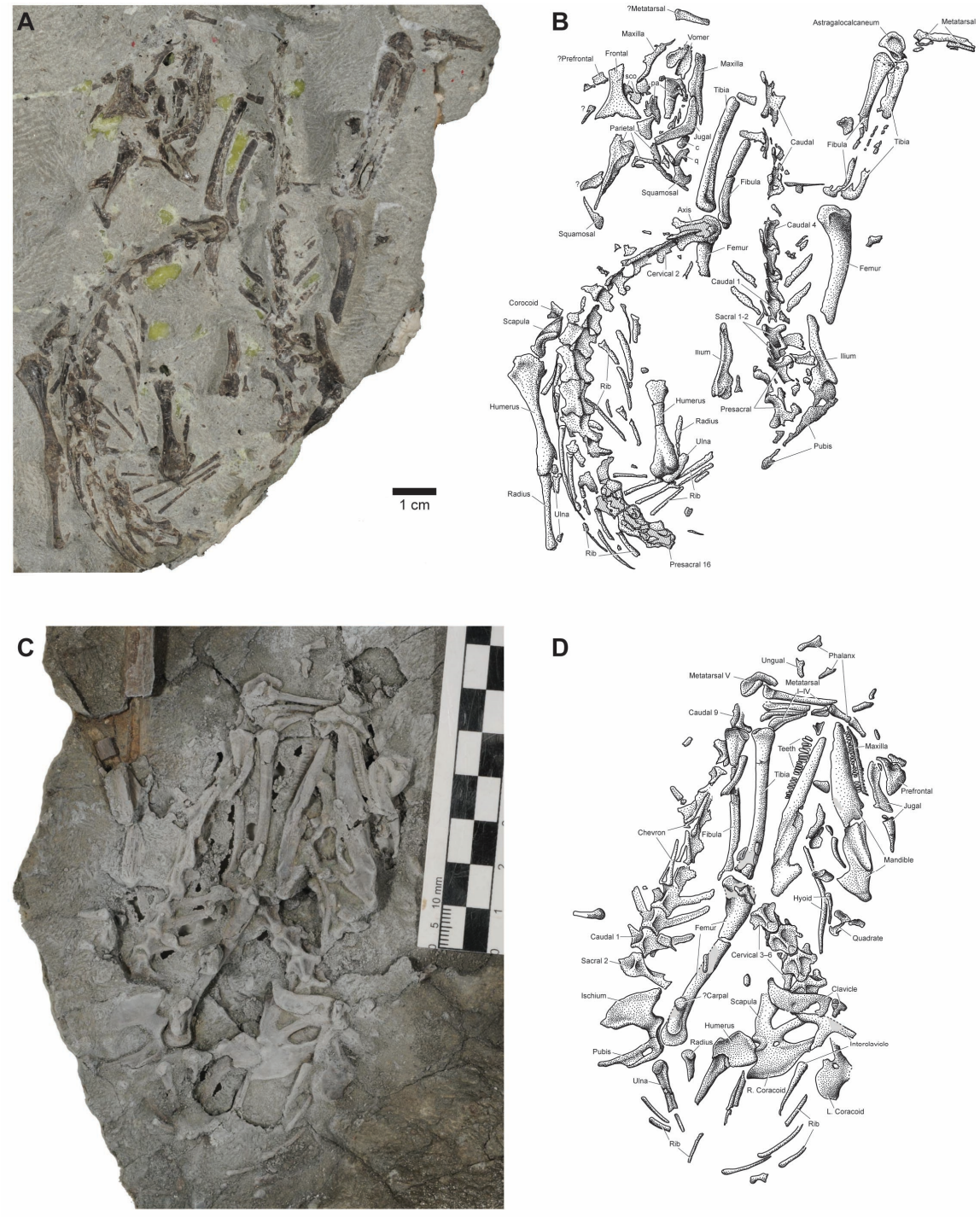

Figure 5.1. Holotype skeleton (MOR 6627) of *Magnuviator ovimonsensis* gen. et sp. nov. from the Egg Mountain locality (MOR loc. TM-006), Two Medicine Formation, Teton County,

northwestern Montana, USA. Photographs (**A** and **C**) and their corresponding stippled line drawings (**B** and **D**, respectively) are in dorsal (**A**, **B**) and ventral (**C**, **D**) views. The individual bones of the skeleton are labeled in the stippled line drawings. Stippling by Morgan Turner.

Figure 5.2. Paratype skeleton (MOR 7042) of *Magnuviator ovimonsensis* gen. et sp. nov. Specimen is in dorsal view. Scale bar equals 20 cm.

Figure 5.3. Anterior portion of paratype specimen (MOR 7042) of *Magnuviator ovimonsensis* gen. et sp. nov. Specimen is in ventral view. Scale bar equals 10 mm.

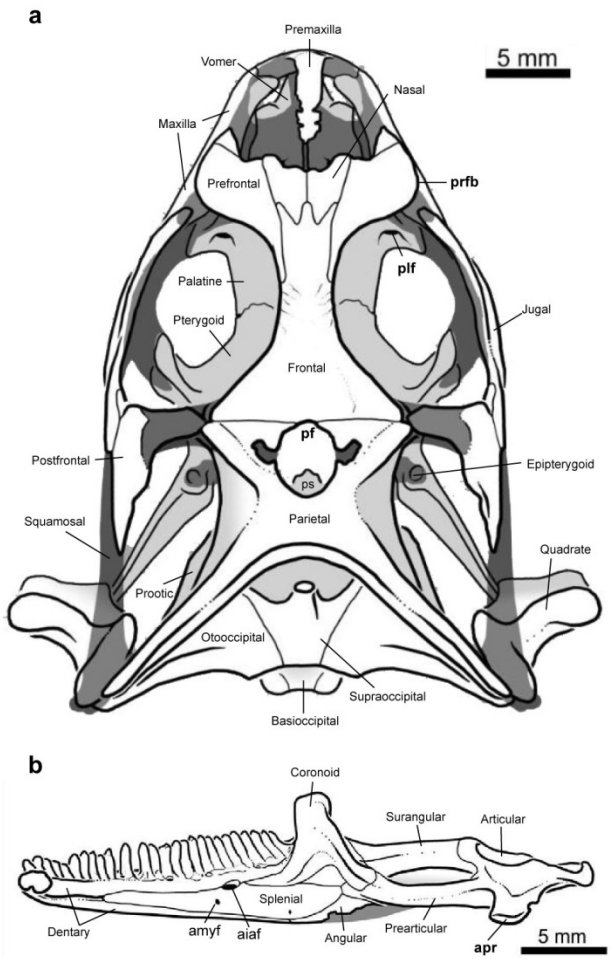

Figure 5.4. Two dimensional reconstructions of the skull and right mandible of *Magnuviator ovimonsensis* gen. et sp. nov. The skull (**a**) is in dorsal view. The right mandible (**b**) is in lingual view. The skull is a composite reconstruction based on raw observations of the holotype (MOR 6627) and paratype (MOR 7042) specimens and the three dimensional renderings of the paratype skull. The right mandible also is based on three dimensional renderings of the paratype. Anatomical abbreviations: aiaf, anterior inferior alveolar foramen; amyf, anterior mylohyoid foramen; apr, angular process of prearticular; pf, parietal foramen; plf, palatine foramen; prfb, prefrontal boss ; ps = parasphenoid process of basisphenoid. Skull and mandible reconstructions provided by Jack L. Conrad.

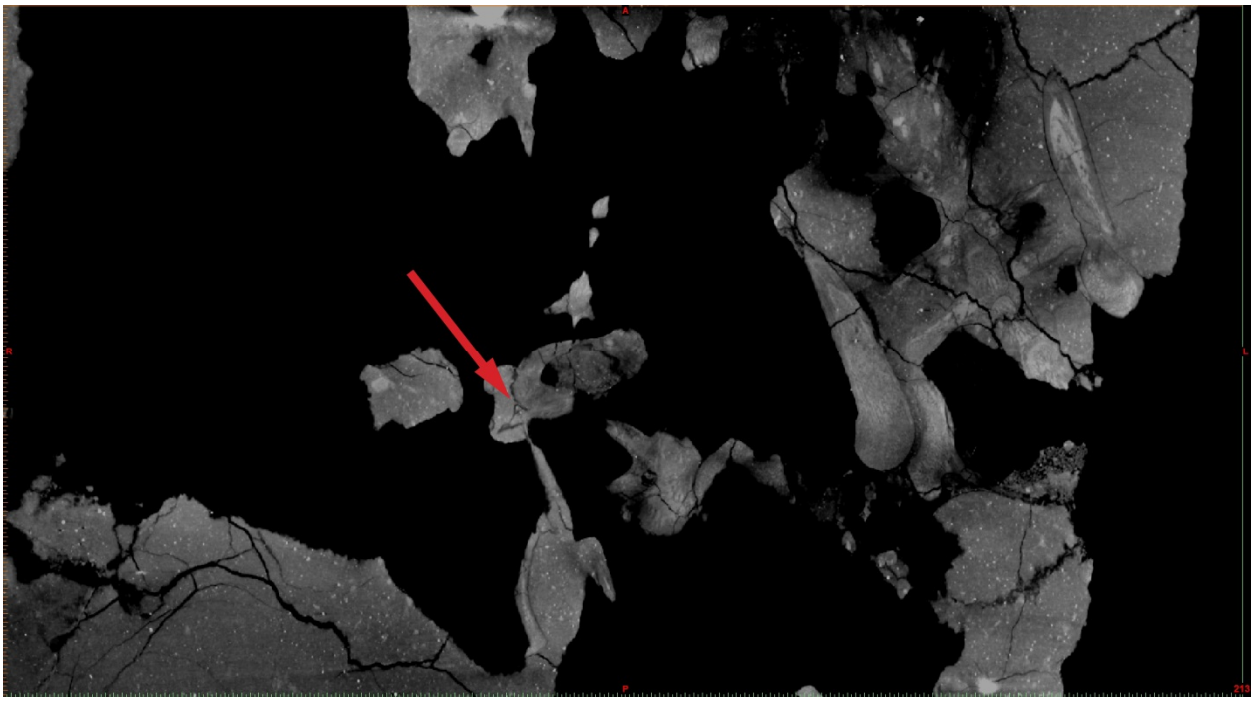

Figure 5.5. Anterior process of the interclavicle of *Magnuviator ovimonsensis* gen. et sp. nov. Frontal cross-section of the holotype (MOR 6627) specimen. Red arrow is pointing to the anterior process of the interclavicle. The pelvic girdle is visible to the right of the interclavicle.

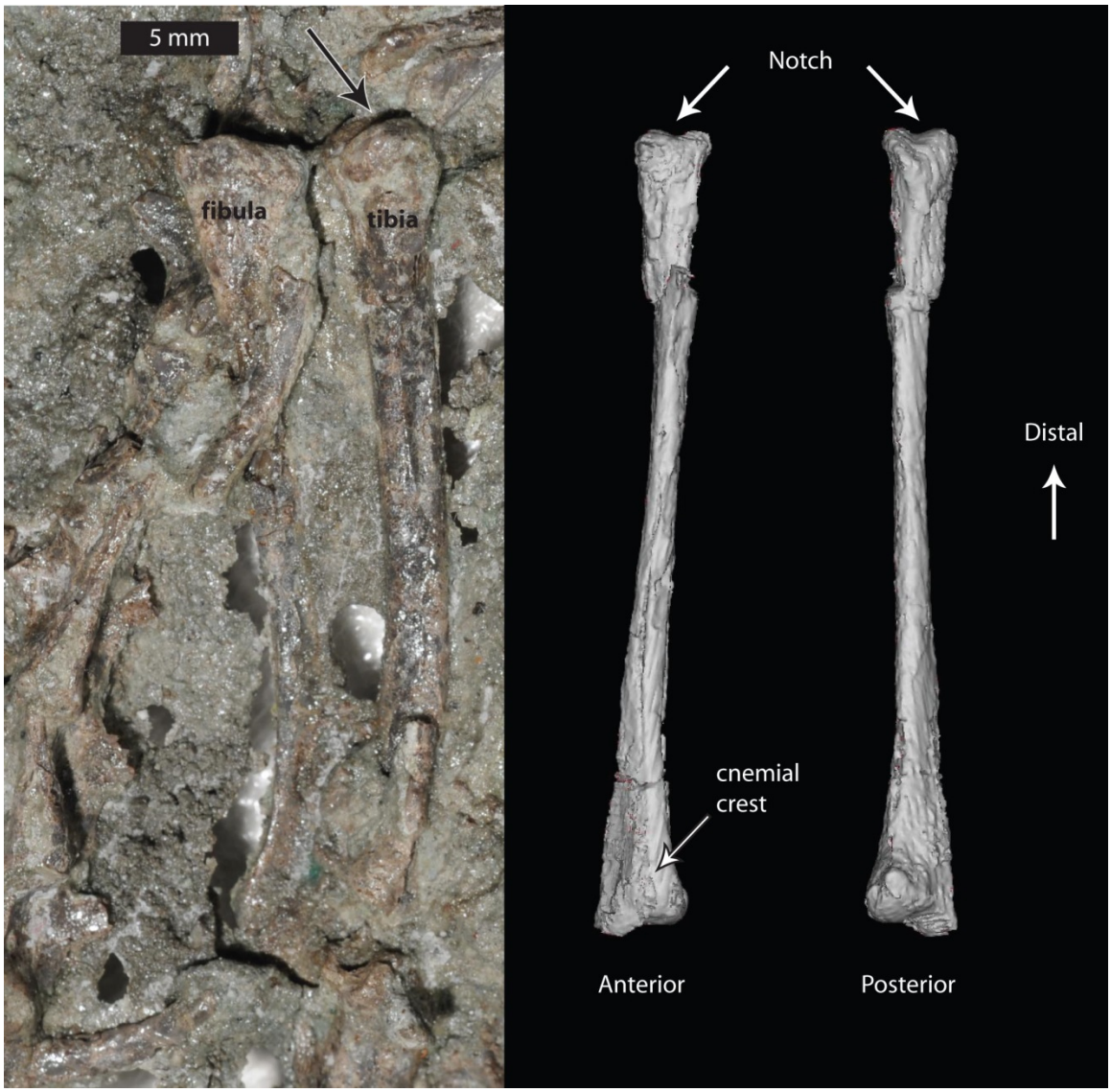

Figure 5.6. Photograph and 3D reconstruction of the right tibia of the holotype (MOR 6627) of *Magnuviator ovimonsensis* gen. et sp. nov. Black and white arrows are pointing to the distal tibial notch. The photograph on the left is in ventral view. The 3D reconstruction on the right is in anterior (left) and posterior (right) views. Distal is towards the top of the figure. Scale bar in photograph equals 5 mm.

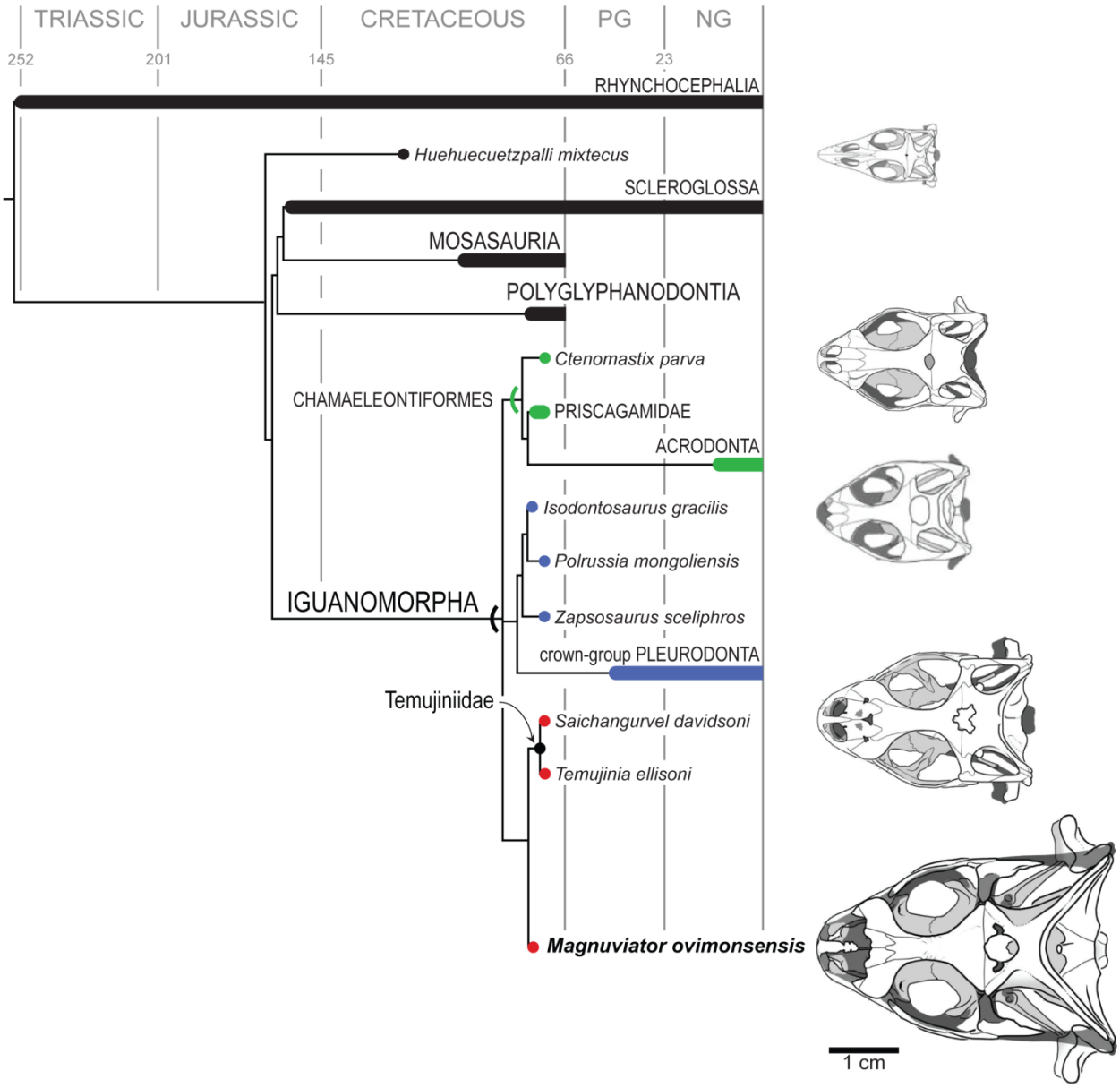

Figure 5.7. Time calibrated maximum parsimony strict consensus tree of 16 most parsimonious trees showing the phylogenetic relationships of *Magnuviator ovimonsensis* gen. et sp. nov. (tree length = 5301; Consistency Index = 0.1837; Retention Index = 0.7929). Thick lines represent the known temporal ranges of the taxa included in the phylogenetic analysis. The green, blue, and red dots represent the isolated occurrences of specific species. The black and green parentheses represent the stem clades Iguanomorpha and Chamaeleontiformes, respectively (sensu Conrad

2008). The “blue” clade represents stem + crown Pleurodonta. *Magnuviator ovimonsensis* and its sister taxa are shown in red. Skull reconstructions from top to bottom represent the stem squamate *Huehuecuetzpalli mixtecus*, the stem acrodontan *Ctenomastix parva*, the stem pleurodontan *Isodontosaurus gracilis*, the temujiniid *Saichangurvel davidsoni*, and *Magnuviator ovimonsensis*. Skulls are to scale for size comparisons. Skull reconstructions provided by Jack L. Conrad. PG = Paleogene; NG = Neogene.

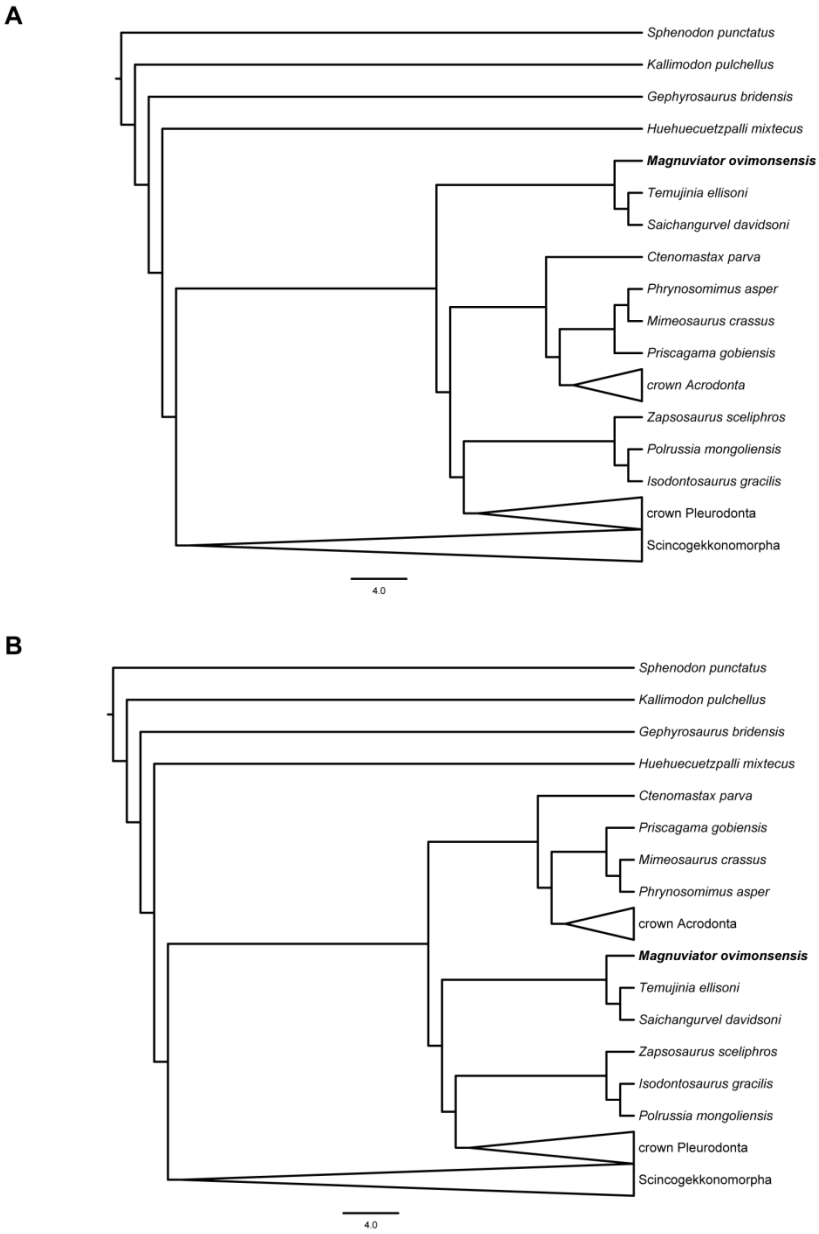

Figure 5.8. Two equally parsimonious and alternate phylogenetic hypotheses of *Magnuviator ovimonsensis* + Temujiniidae with Chamaeleontiformes and stem + crown Pleurodonta. The cladograms are based on the 16 most parsimonious trees recovered from the phylogenetic analysis. **A**) Hypothesis 1: sister taxon to all other iguanomorphs. **B**) Hypothesis 2: basalmost pleurodontan iguanian clade. The crown clades of Acrodonta and Pleurodonta and Scincogekkonomorpha (stem + crown Scleroglossa) are collapsed for brevity.

Figure 5.9. Maximum parsimony cladogram based on a Traditional (TBR) Wagner Parsimony Analysis. Bremer support (BS) values are listed at the base of each node. BS values greater than 5 are followed by a question mark (5?). Note the high BS value for the iguanomorph affinities of *Magnuviator* (BS >5), but the relatively low support for the basal pleurodontan relationship of *Magnuviator* + Temujiniidae (BS = 1). Scincogekkonomorpha collapsed for brevity (BS > 5).

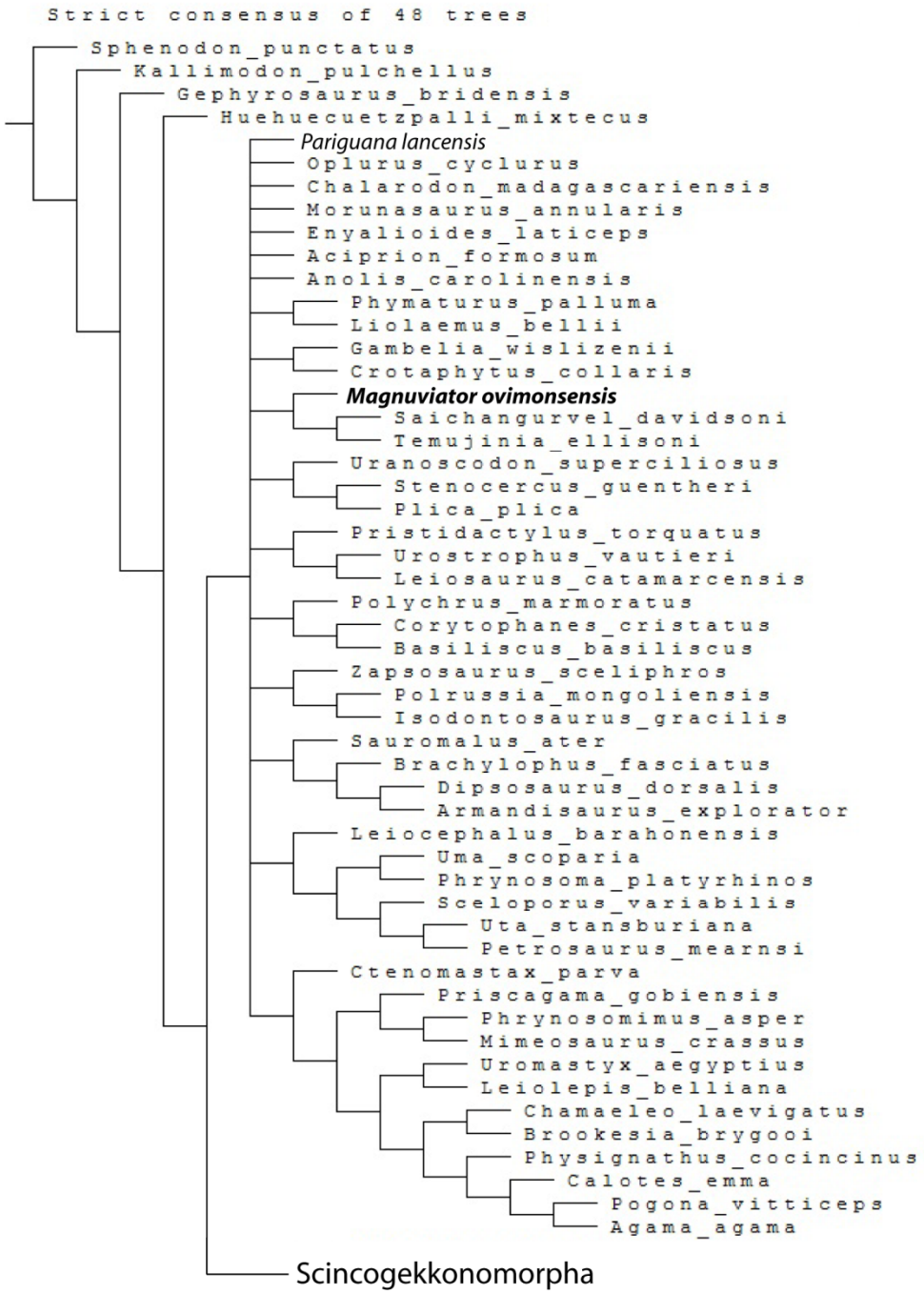

Figure 5.10. Maximum parsimony strict consensus tree of 48 most parsimonious trees. Note the unresolved phylogenetic placement of *Pariguana lancensis* relative to all other stem and crown iguanians. Scincogekkonomorpha collapsed for brevity.

Figure 5.11. Life reconstruction of *Magnuviator ovimonsensis* gen. et sp. nov. at Egg Mountain. The *Ephedra* plants, *Troodon* tooth, and wasps are based on fossil evidence at Egg Mountain (see text for details). Illustration by Misaki Ouchida (2015).

TABLES for CHAPTER 5

Table 5.1. Character scores of *Magnuviator ovimonsensis* gen. et sp. nov. and *Pariguana lancensis* used in the phylogenetic analyses. Character scorings for *Magnuviator* were individually scored for the holotype (MOR 6627) and paratype (MOR 7042) and later combined for the final phylogenetic analyses. Characters and character states from Gauthier et al. (2012).

*Magnuviator_ovimonsensis*_MOR_6627 (Holotype)
?????????? ?????????? ?????????? ?????1?0?0 000?0??200 0???011??? ??????????
?????????? ?????????0 ??00?????? 01?010???? ?????????? ?00?00???? ??????????
?00???00?0 000?2??00? 000?0????? ??????1?10 ?????0???? ?????????? ??????????
???0??0??0 ???0?????1 ??0??????? ?????1???? ?????????? ?????????? ??????????
?????????? ?????????? ?????????? ?????????? ?????????? ?????????? ??????????
??????0??? ?????????? ?????????0 ?????01?0? ????????00 0??000?00? 1?????0??3
?000000??0 ???20?0??? ?????????? ?????000?? 0???0?130? ?????0??0?? ????????00?
??1?10??01 1???001?10 011??00??0 0000??0010 ?0?1?????? ???????000 ????11????
0??0???0?? ?1???????? ?????????? ?????????? ??????????
*Magnuviator_ovimonsensis*_MOR_7042 (Paratype)
1????????? 0?000????? ?????????? ?????1?0?0 000?0????0 00??011??? ????????00?
????000??? ??0??????0 ??000?0?0? 011??0?0?? ????????0?? 000?00?0?1 0?00??????
?00??00020 000?2??0?? ?????????? ????????10 ?20??0???? ????0?????? ??????????
?0?0??0??0 ???0?????1 0?0??????? ???001?001 ??????121? 0?00?0???0 ??????????
??????????0 ??0?1??00? ??0?0?0?00 ?0????????? ???00????? ?001?????0 00????????0
??0?000??1 ????0????? 00003??110 ?????01?0? 0?1????000 ????0000000 1?????0??3
3000000000 00?2000??? ?????????? ??????00?? 0???0?130? ????????0?? ????????00?
??1?10??0? ??????????0 011??0???0 ?00???001? ?0???????? ???????000 ????1?????
0????????? ?1???????? ?????????? ?????????? ??????????
*Magnuviator_ovimonsensis*_MOR_6627_7042 (combined)
1????????? 0?000????? ?????????? ?????1?0?0 000?0??200 00??011??? ????????00?
????000??? ??0??????0 ??000?0?0? 011010?0?? ????????0?? 000?00?0?1 0?00??????
?00??00020 000?2??00? 000?0????? ??????1?10 ?20??0???? ????0?????? ??????????
?0?0??0??0 ???0?????1 0?0??????? ???001?001 ??????121? 0?00?0???0 ??????????
??????????0 ??0?1??00? ??0?0?0?00 ?0????????? ???00????? ?001?????0 00????????0
??0?000??1 ????0????? 00003??110 ?????01?0? 0?1????000 0??0000000 1?????0??3
3000000000 00?2000??? ?????????? ??????00?? 0???0?130? ????0??0?? ????????00?
??1?10??01 1???001?10 011??00??0 0000??0010 ?0?1?????? ???????000 ????11????
0??0???0?? ?1???????? ?????????? ?????????? ??????????
Pariguana_lancensis
?????????? ?????????? ?????????? ?????????? ?????????? ?????????? ??????????
?????????? ?????????? ?????????? ?????????? ?????????? ?????????? ??????????
?????????? ?????????? ?????????? ?????????? ?????????? ?????????? ??????????
?????????? ?????????? ?????????? ?????????? ?????????? ?????????? ??????????
?????????? ?????????? ?????????? ?????????? ?????????? ?????????? ??????????
??????0??0 ????0????? ?100??0000 ?????????? ?????????? ?????????? ??????????
??000000?? 00?2000??? ?????????? ?????????? ?????????? ?????????? ??????????
?????????? ?????????? ?????????? ?????????? ?????????? ?????????? ??????????
?????????? ?????????? ?????????? ?????????? ??????????

Table 5.2. Maximum parsimony strict consensus tree and apomorphy list created in PAUP* 4.0. *Magnuviator ovimonsensis* gen. et sp. nov. is listed as "EggMtn combined" in the tree and apomorphy list provided below.

```
P A U P *
Version 4.0b10 for Macintosh (PPC)
Thursday, January 22, 1970  7:03 PM

This copy registered to: Meng Chen
                         University of Washington
                         (serial number = B418094)

      -----------------------------NOTICE-----------------------------
        This is a beta-test version.  Please report any crashes,
        apparent calculation errors, or other anomalous results.
        There are no restrictions on publication of results obtained
        with this version, but you should check the WWW site
        frequently for bug announcements and/or updated versions.
        See the README file on the distribution media for details.
      ----------------------------------------------------------------

Strict consensus of 16 trees:

Consensus tree(s) written to treefile: strict.trees

Processing of file "strict.trees" begins...

>Consensus of 16 trees
>
>Source of trees from which consensus(es) calculated...
>Tree(s) input to PAUP* as user-defined tree(s)

1 tree read from TREES block
   Time used = 0.08 sec

Processing of file "strict.trees" completed.

Tree description:

  Unrooted tree(s) rooted using outgroup method
  Optimality criterion = parsimony
    Character-status summary:
      Of 610 total characters:
        149 characters are of type 'ord' (Wagner)
        461 characters are of type 'unord'
        All characters have equal weight
        4 characters are parsimony-uninformative
        Number of parsimony-informative characters = 606
    Multistate taxa interpreted as uncertainty
    Character-state optimization: Accelerated transformation (ACCTRAN)

Tree number 1 (rooted using default outgroup)

Tree length = 5301
Consistency index (CI) = 0.1837
Homoplasy index (HI) = 0.8163
CI excluding uninformative characters = 0.1831
HI excluding uninformative characters = 0.8169
Retention index (RI) = 0.7929
Rescaled consistency index (RC) = 0.1457
```

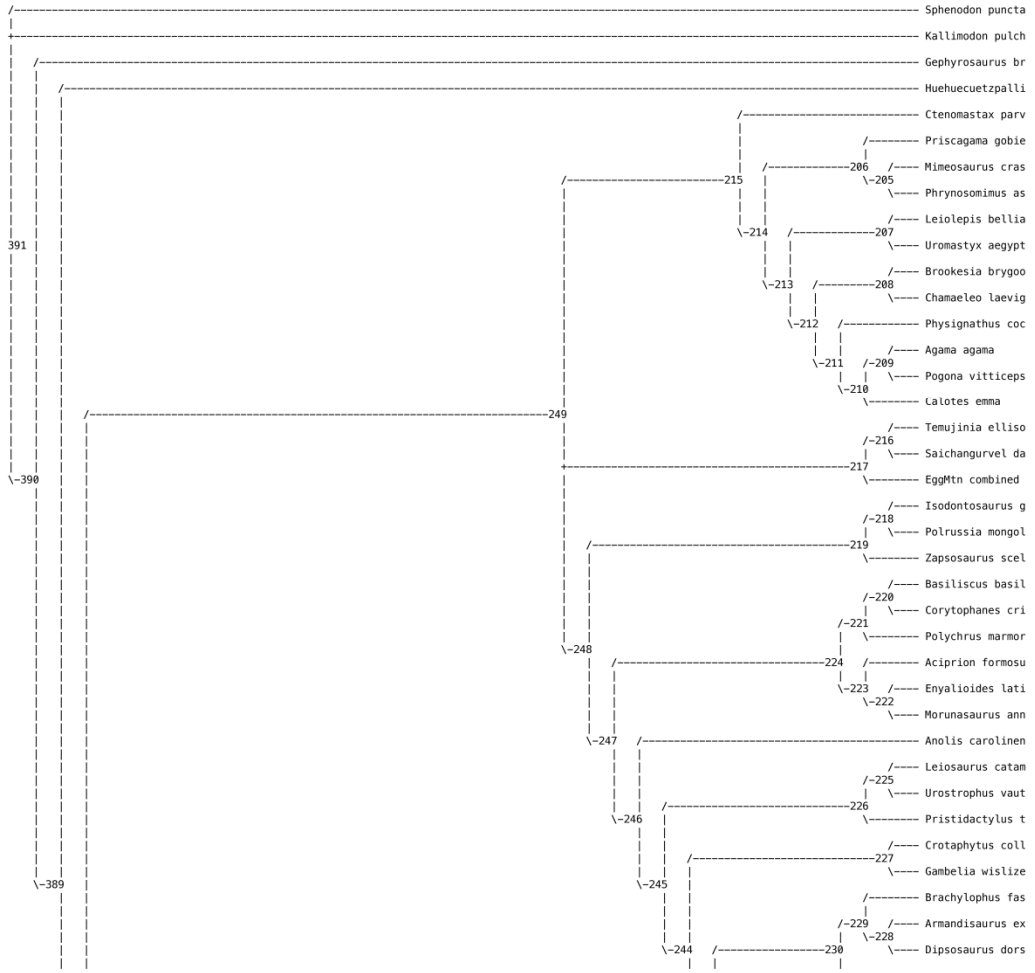

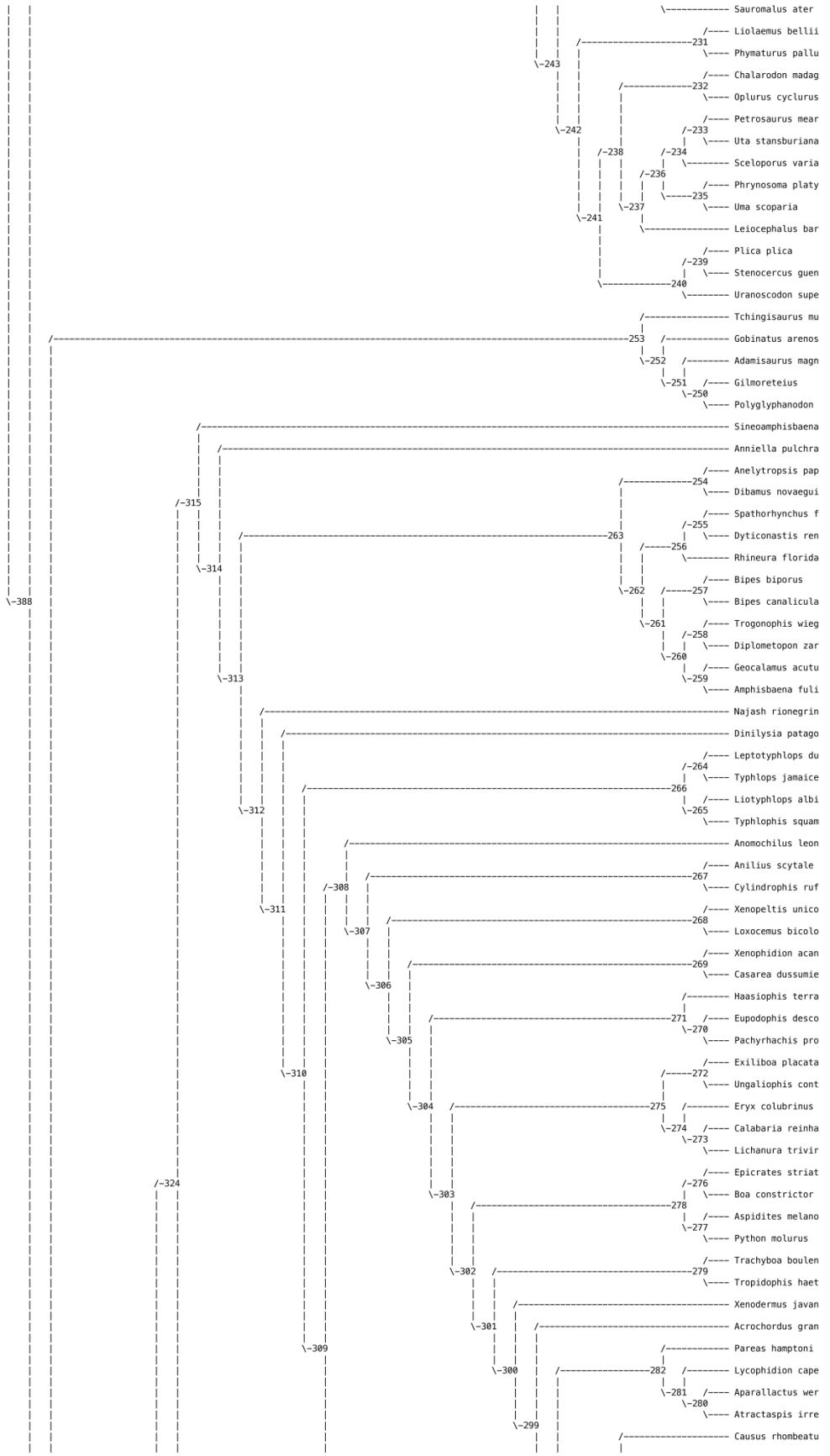
Sauromalus ater
Liolaemus bellii
Phymaturus pallu
Chalarodon madag
Oplurus cyclurus
Petrosaurus mear
Uta stansburiana
Sceloporus varia
Phrynosoma platy
Uma scoparia
Leiocephalus bar
Plica plica
Stenocercus guen
Uranoscodon supe
Tchingisaurus mu
Gobinatus arenos
Adamisaurus magn
Gilmoreteius
Polyglyphanodon
Sineoamphisbaena
Anniella pulchra
Anelytropsis pap
Dibamus novaegui
Spathorhynchus f
Dyticonastis ren
Rhineura florida
Bipes biporus
Bipes canalicula
Trogonophis wieg
Diplometopon zar
Geocalamus acutu
Amphisbaena fuli
Najash rionegrin
Dinilysia patago
Leptotyphlops du
Typhlops jamaice
Liotyphlops albi
Typhlophis squam
Anomochilus leon
Anilius scytale
Cylindrophis ruf
Xenopeltis unico
Loxocemus bicolo
Xenophidion acan
Casarea dussumie
Haasiophis terra
Eupodophis desco
Pachyrhachis pro
Exiliboa placata
Ungaliophis cont
Eryx colubrinus
Calabaria reinha
Lichanura trivir
Epicrates striat
Boa constrictor
Aspidites melano
Python molurus
Trachyboa boulen
Tropidophis haet
Xenodermus javan
Acrochordus gran
Pareas hamptoni
Lycophidion cape
Aparallactus wer
Atractaspis irre
Causus rhombeatu

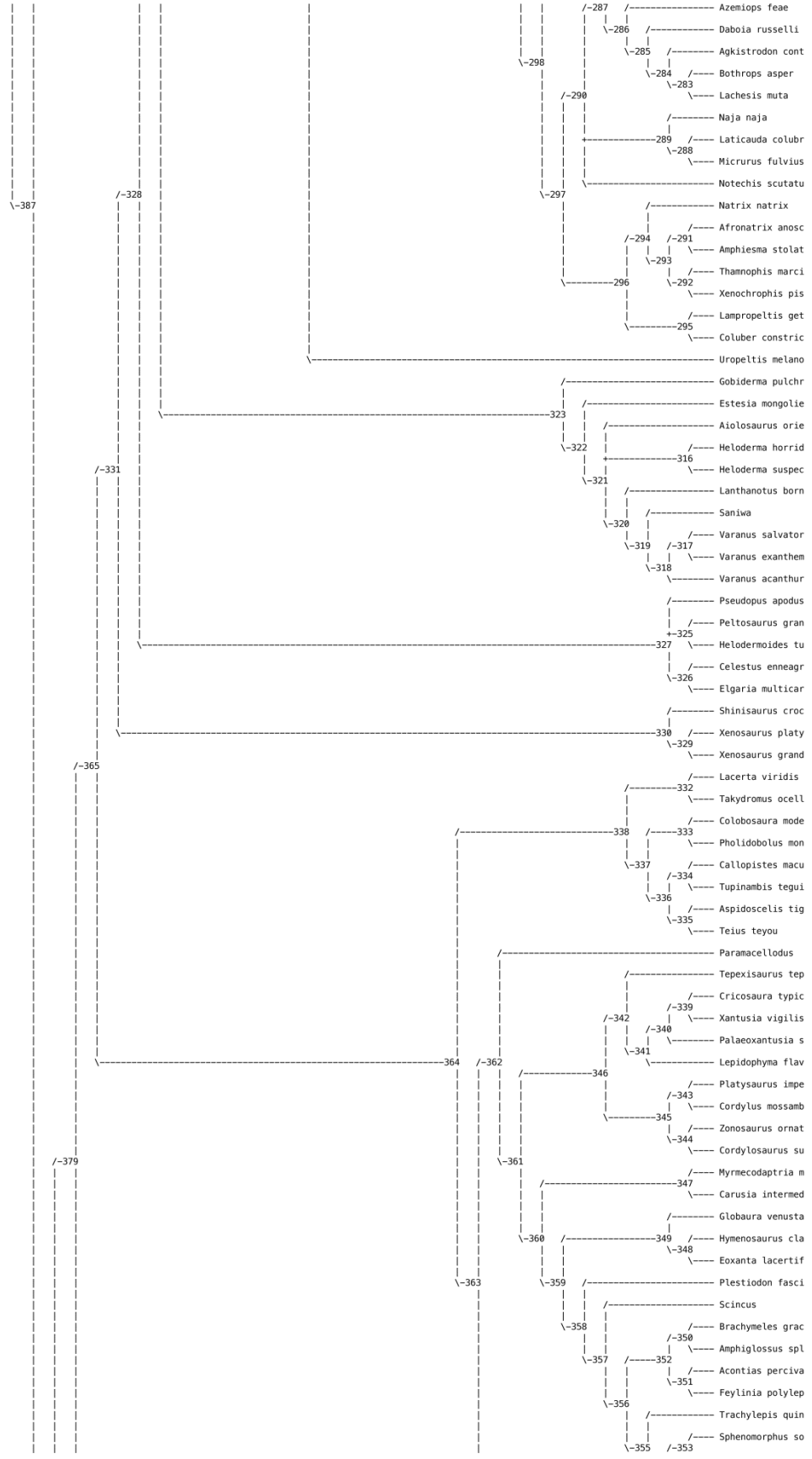
Azemiops feae
Daboia russelli
Agkistrodon cont
Bothrops asper
Lachesis muta
Naja naja
Laticauda colubr
Micrurus fulvius
Notechis scutatu
Natrix natrix
Afronatrix anosc
Amphiesma stolat
Thamnophis marci
Xenochrophis pis
Lampropeltis get
Coluber constric
Uropeltis melano
Gobiderma pulchr
Estesia mongolie
Aiolosaurus orie
Heloderma horrid
Heloderma suspec
Lanthanotus born
Saniwa
Varanus salvator
Varanus exanthem
Varanus acanthur
Pseudopus apodus
Peltosaurus gran
Helodermoides tu
Celestus enneagr
Elgaria multicar
Shinisaurus croc
Xenosaurus platy
Xenosaurus grand
Lacerta viridis
Takydromus ocell
Colobosaura mode
Pholidobolus mon
Callopistes macu
Tupinambis tegui
Aspidoscelis tig
Teius teyou
Paramacellodus
Tepexisaurus tep
Cricosaura typic
Xantusia vigilis
Palaeoxantusia s
Lepidophyma flav
Platysaurus impe
Cordylus mossamb
Zonosaurus ornat
Cordylosaurus su
Myrmecodaptria m
Carusia intermed
Globaura venusta
Hymenosaurus cla
Eoxanta lacertif
Plestiodon fasci
Scincus
Brachymeles grac
Amphiglossus spl
Acontias perciva
Feylinia polylep
Trachylepis quin
Sphenomorphus so

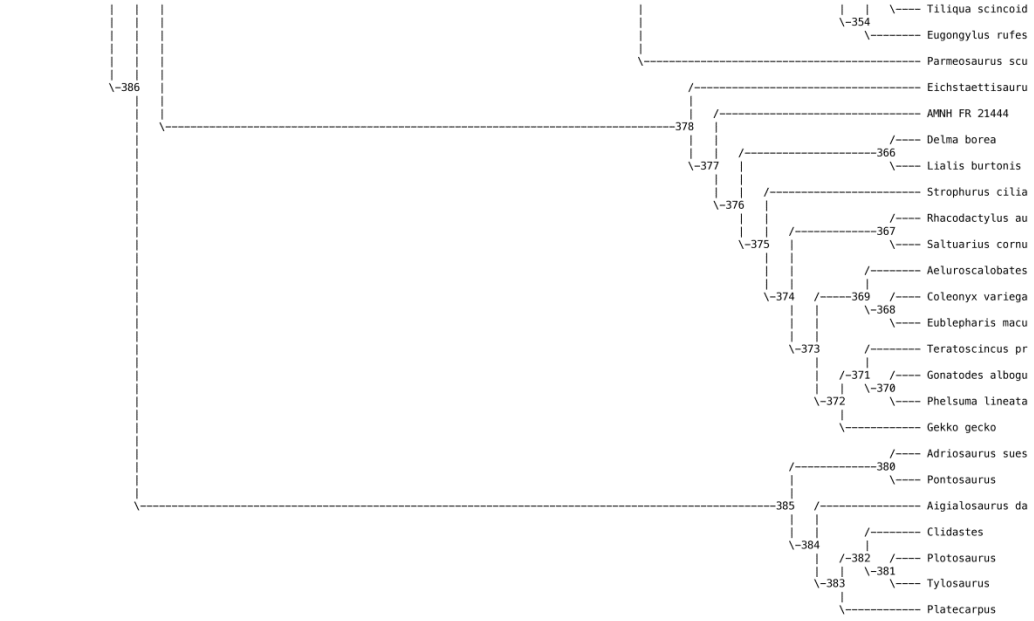

Apomorphy lists:

Branch	Character	Steps	CI	Change
node_391 --> Sphenodon puncta	8	1	0.182	0 ==> 2
	64	1	0.167	0 ==> 1
	120	1	0.130	1 --> 2
	123	1	0.125	0 --> 1
	137	1	0.077	0 --> 1
	154	1	0.077	0 --> 1
	180	1	0.250	0 --> 1
	193	1	0.100	0 --> 1
	213	1	0.048	0 --> 1
	307	1	0.125	0 --> 1
	351	1	0.375	0 --> 1
	382	1	0.333	0 --> 1
	387	1	0.222	0 --> 1
	397	1	0.333	0 --> 1
	455	1	0.148	0 ==> 1
	463	1	0.108	1 --> 2
	470	1	0.125	0 ==> 1
	561	1	0.154	1 ==> 0
node_391 --> Kallimodon pulch	328	1	0.054	0 ==> 1
	419	2	0.073	2 ==> 0
	488	1	0.133	0 ==> 1
	497	1	0.048	0 --> 1
node_391 --> node_390	29	1	0.083	0 --> 1
	36	1	0.062	0 ==> 1
	65	1	1.000	2 ==> 1
	85	1	0.500	1 ==> 0
	88	1	0.125	0 ==> 1
	93	1	0.111	1 ==> 0
	102	1	0.333	0 ==> 1
	116	1	0.300	0 ==> 1
	155	1	0.133	0 ==> 1
	187	1	0.500	0 --> 1
	209	1	1.000	0 --> 1
	254	1	0.182	2 ==> 0
	256	1	0.333	2 ==> 1
	267	1	0.038	1 --> 0
	297	1	0.100	0 --> 1
	316	1	0.200	0 --> 1
	334	1	0.167	0 --> 1
	346	1	1.000	0 --> 1
	360	1	0.125	0 --> 1
	364	1	0.105	2 ==> 1
	384	1	0.097	0 --> 1
	400	1	0.200	1 ==> 0
	404	1	0.100	1 ==> 0
	419	2	0.073	2 ==> 4
	420	1	0.085	2 ==> 3
	421	1	0.075	2 ==> 3
	423	1	0.100	1 ==> 0
	430	1	0.333	1 ==> 0
	521	1	0.067	1 ==> 0
	535	1	0.143	0 --> 1
	537	1	1.000	0 --> 1
	538	1	1.000	0 --> 1
	546	1	0.100	0 --> 1
	556	1	0.500	0 --> 1
	572	1	0.058	0 ==> 1
	584	1	0.188	0 --> 1
	590	1	0.308	0 --> 1
	605	1	1.000	0 --> 1
node_390 --> Gephyrosaurus br	153	1	0.100	0 ==> 1
	230	1	0.333	1 ==> 0
	278	1	0.500	0 ==> 1
	341	1	0.033	0 ==> 1
	401	1	0.077	0 ==> 1
	416	1	0.286	0 ==> 4
	420	1	0.085	3 ==> 4
	421	1	0.075	3 ==> 4
	463	1	0.108	1 ==> 0
	514	1	0.083	0 ==> 1
	529	1	0.286	1 ==> 0
node_390 --> node_389	9	1	0.250	1 ==> 0
	24	1	0.071	0 --> 1
	57	1	0.190	0 ==> 1
	63	1	0.286	0 --> 1
	65	1	1.000	1 ==> 0
	113	1	0.500	0 --> 1
	114	1	0.148	1 --> 2
	120	1	0.130	1 --> 0
	144	1	0.091	0 ==> 1

	149	2	0.087	0 ==> 2		364	1	0.105	1 ==> 2		451	1	0.333	0 --> 1
	155	1	0.133	1 ==> 2		366	1	0.500	0 ==> 2		454	1	0.400	1 ==> 2
	166	1	0.091	1 ==> 0		369	1	0.100	0 ==> 1		459	1	0.182	0 ==> 1
	177	1	1.000	0 ==> 1		375	1	0.065	1 ==> 0		463	1	0.108	3 --> 2
	179	1	0.143	0 ==> 1		385	1	0.067	0 --> 2		477	1	1.000	1 ==> 0
	181	1	1.000	0 ==> 1		388	1	0.105	1 ==> 0		481	1	0.083	1 ==> 0
	182	2	0.273	0 ==> 2		390	1	0.100	2 ==> 1		483	1	0.120	1 ==> 2
	187	1	0.500	1 --> 2		392	1	0.105	0 ==> 1		486	1	0.400	2 --> 3
	199	1	1.000	0 --> 1		401	1	0.077	0 ==> 1		487	2	0.222	0 ==> 2
	240	1	0.125	1 --> 0		419	1	0.073	2 --> 1		488	1	0.133	0 ==> 1
	241	1	0.667	0 --> 1		423	1	0.100	0 ==> 1		493	1	0.200	1 ==> 0
	250	1	0.273	0 --> 1		430	1	0.333	0 ==> 1		495	1	0.125	1 ==> 0
	255	1	0.077	0 --> 1	node_213 --> node_207	82	2	0.118	0 ==> 2		499	1	0.143	0 ==> 1
	256	1	0.333	1 --> 0		147	1	1.000	0 ==> 1		505	1	0.167	0 ==> 1
	257	1	0.500	0 --> 1		204	1	0.125	0 ==> 1		513	1	0.083	1 ==> 0
	259	1	0.250	0 --> 1		275	1	0.333	0 ==> 2		514	1	0.083	0 ==> 1
	285	1	0.333	0 --> 1		420	1	0.085	3 ==> 2		517	1	0.200	0 ==> 1
	295	1	1.000	0 ==> 1		424	1	0.500	0 ==> 1		518	2	0.100	0 ==> 2
	296	1	0.333	0 --> 2		439	1	0.118	0 ==> 1		521	1	0.067	0 ==> 1
	336	1	1.000	0 --> 1		447	1	0.083	1 --> 0		522	1	1.000	0 ==> 1
	352	1	0.500	0 --> 1		483	1	0.120	1 ==> 0		523	1	1.000	0 ==> 1
	354	1	1.000	0 --> 1		484	1	0.100	0 ==> 1		530	1	0.200	0 ==> 1
	364	1	0.105	1 ==> 0		494	1	0.133	1 ==> 0		531	1	0.125	0 ==> 1
	369	2	0.100	2 ==> 0		498	1	0.083	1 ==> 0		532	1	0.500	0 ==> 1
	374	1	0.250	1 ==> 0		512	1	0.091	0 --> 1		536	1	1.000	0 ==> 1
	381	1	0.500	0 ==> 1		572	1	0.058	1 ==> 0		539	1	0.500	1 ==> 0
	387	1	0.222	0 --> 1	node_207 --> Leiolepis bellia	94	1	0.062	2 --> 0		540	1	0.500	0 ==> 1
	388	1	0.105	0 --> 1		137	1	0.077	1 --> 0		542	1	0.273	0 --> 1
	390	2	0.100	0 ==> 2		148	1	0.091	0 ==> 1		545	1	1.000	0 ==> 1
	393	1	0.250	0 ==> 1		149	1	0.087	1 --> 2		546	1	0.100	1 ==> 0
	415	1	0.222	1 --> 0		154	1	0.077	0 ==> 2		547	1	0.250	0 ==> 1
	463	1	0.108	1 --> 2		182	1	0.273	2 ==> 1		549	1	0.250	0 ==> 1
	493	1	0.200	0 ==> 1		212	1	0.182	0 ==> 1		550	1	0.200	0 --> 1
	494	1	0.133	0 --> 1		294	1	0.091	0 ==> 1		554	1	0.167	0 --> 2
	495	1	0.125	0 ==> 1		385	1	0.067	2 --> 0		558	1	1.000	0 ==> 1
	503	1	0.286	0 --> 1		399	1	0.062	0 ==> 1		563	1	1.000	0 ==> 1
	504	1	0.125	0 --> 1		419	1	0.073	1 --> 2		566	1	0.444	0 --> 1
	507	1	0.167	0 --> 1		421	1	0.075	2 ==> 3		568	1	1.000	0 ==> 1
	509	1	0.158	0 --> 1		449	1	0.200	0 ==> 1		569	1	0.333	0 ==> 1
	513	1	0.083	0 ==> 1		500	1	0.133	0 ==> 2		584	1	0.188	2 --> 3
	557	1	0.125	0 --> 1		514	1	0.083	0 ==> 1	node_208 --> Brookesia brygoo	17	1	0.167	0 ==> 1
node_389 --> Huehuecuetzpalli	6	1	0.100	0 --> 1	node_207 --> Uromastyx aegypt	10	2	0.087	0 ==> 2		29	1	0.083	1 ==> 0
	7	2	0.069	0 ==> 2		19	1	0.167	0 ==> 1		132	3	0.176	0 ==> 3
	10	1	0.087	0 ==> 1		20	1	0.167	0 ==> 1		153	1	0.100	0 ==> 1
	63	1	0.286	1 ==> 2		48	1	0.103	3 ==> 4		154	1	0.077	0 ==> 1
	71	1	0.429	0 ==> 2		62	1	0.111	3 ==> 1		188	3	0.080	1 ==> 4
	191	1	0.167	0 ==> 1		120	1	0.130	1 ==> 0		306	1	0.286	1 ==> 0
	214	1	0.200	0 ==> 1		123	1	0.125	0 ==> 1		307	1	0.125	0 ==> 1
node_389 --> node_388	1	1	0.167	0 ==> 1		144	1	0.091	0 --> 1		312	1	0.222	0 ==> 1
	48	1	0.103	1 --> 2		153	1	0.100	0 ==> 1		484	1	0.100	0 ==> 1
	56	1	0.190	0 ==> 1		188	2	0.080	0 ==> 2		572	2	0.058	1 ==> 3
	58	1	0.222	0 ==> 1		213	1	0.048	0 ==> 1		588	2	0.167	0 ==> 2
	78	1	0.571	0 ==> 1		232	1	0.143	0 ==> 1	node_208 --> Chamaeleo laevig	93	1	0.111	0 ==> 1
	84	4	0.129	0 --> 4		240	1	0.125	0 ==> 2		101	2	0.105	0 ==> 2
	103	1	1.000	0 ==> 1		250	2	0.273	1 ==> 3		104	1	0.077	0 ==> 1
	111	1	0.222	0 --> 1		285	1	0.333	0 ==> 1		146	1	0.167	0 ==> 1
	413	1	0.033	0 --> 1		291	1	0.053	1 ==> 0		149	1	0.087	1 --> 2
	419	1	0.073	4 --> 3		340	1	0.095	0 ==> 1		317	1	0.250	0 ==> 1
	434	1	0.111	0 --> 2		344	1	0.048	0 ==> 1		341	1	0.033	0 ==> 1
	467	1	0.333	0 ==> 1		349	1	0.136	0 ==> 1		384	1	0.097	1 ==> 0
	468	1	0.120	1 ==> 2		360	1	0.125	1 ==> 0		411	1	0.333	1 ==> 0
	533	1	0.333	0 --> 1		367	1	0.125	0 ==> 1		419	1	0.073	1 ==> 0
	534	1	0.500	0 ==> 1		411	1	0.333	1 ==> 0		459	2	0.182	1 ==> 3
	560	1	1.000	0 ==> 1		415	1	0.222	1 ==> 0		483	1	0.120	2 ==> 3
	561	1	0.154	1 ==> 0		434	1	0.111	2 ==> 0		525	1	0.167	0 ==> 1
node_388 --> node_249	58	1	0.222	1 ==> 2		448	1	0.125	1 ==> 0		529	1	0.286	1 ==> 2
	79	1	0.500	0 --> 1		496	1	0.083	0 ==> 1		542	1	0.273	1 --> 2
	105	1	0.667	0 ==> 1		509	1	0.158	1 ==> 0		559	1	0.500	0 ==> 1
	112	1	0.167	0 --> 1		519	1	0.077	1 ==> 0		566	1	0.444	1 --> 2
	116	1	0.300	1 ==> 2		526	1	0.143	0 ==> 1	node_212 --> node_211	94	1	0.062	2 --> 1
	130	1	0.500	0 ==> 1		554	1	0.167	0 ==> 2		107	1	1.000	0 ==> 1
	258	1	0.081	0 ==> 1	node_213 --> node_212	8	1	0.182	0 ==> 2		154	1	0.077	0 ==> 2
	267	1	0.038	0 --> 1		78	1	0.571	1 ==> 4		193	1	0.100	0 --> 1
	291	1	0.053	0 ==> 1		79	1	0.500	1 --> 0		231	1	0.077	1 --> 2
	306	1	0.286	0 ==> 1		81	1	1.000	0 ==> 1		304	1	1.000	0 ==> 1
	411	1	0.333	0 ==> 1		114	1	0.148	2 ==> 1		340	1	0.095	0 --> 1
	447	1	0.083	0 --> 1		120	1	0.130	1 ==> 2		344	1	0.048	0 ==> 1
	448	1	0.125	0 ==> 1		139	1	1.000	0 ==> 1		390	1	0.100	1 ==> 0
	470	1	0.125	0 ==> 2		185	1	0.067	1 ==> 0		413	1	0.033	0 ==> 1
	481	1	0.083	0 ==> 1		231	1	0.077	0 ==> 1	node_211 --> Physignathus coc	29	1	0.083	1 ==> 0
	497	1	0.048	0 --> 1		240	1	0.125	0 --> 1		77	1	0.083	0 ==> 1
	519	1	0.077	0 --> 1		284	1	1.000	0 ==> 1		137	1	0.077	1 --> 0
	535	1	0.143	1 ==> 2		407	1	1.000	0 --> 1		155	1	0.133	2 ==> 1
	553	1	0.200	0 --> 1		412	1	0.111	0 ==> 1		341	1	0.033	0 ==> 1
	609	1	0.167	0 ==> 1		440	1	0.200	1 --> 2		349	1	0.136	0 ==> 1
node_249 --> node_215	62	1	0.111	0 ==> 2		442	1	0.143	1 ==> 0		388	1	0.105	0 ==> 1
	112	1	0.167	1 --> 0		454	1	0.400	0 --> 1		420	1	0.085	3 ==> 2
	348	1	0.111	0 --> 1		489	1	0.111	0 ==> 1		454	1	0.400	1 --> 0
	413	1	0.033	1 --> 0		491	1	0.143	0 --> 1		455	1	0.148	0 ==> 1
	417	1	0.400	0 ==> 1		503	1	0.286	1 --> 0		482	1	0.333	1 --> 0
	419	1	0.073	3 ==> 2		551	1	0.167	0 ==> 1		491	1	0.143	1 --> 0
	421	1	0.075	3 ==> 2	node_212 --> node_208	20	1	0.167	0 ==> 1		500	1	0.133	0 ==> 2
	436	1	0.500	0 ==> 1		50	1	0.167	0 ==> 1		572	1	0.058	1 ==> 0
	463	1	0.108	2 --> 3		56	1	0.190	1 ==> 2	node_211 --> node_210	7	1	0.069	3 ==> 4
	468	2	0.120	2 --> 0		57	1	0.190	1 ==> 3		18	1	0.053	0 --> 1
	470	1	0.125	2 --> 3		58	2	0.222	2 --> 0		120	1	0.130	2 ==> 3
	482	1	0.333	0 --> 1		98	1	1.000	0 ==> 1		153	1	0.100	0 ==> 1
	584	1	0.188	1 --> 2		99	1	0.250	0 ==> 1		240	1	0.125	1 --> 0
node_215 --> Ctenomastax parv	48	1	0.103	2 ==> 1		102	1	0.333	1 --> 0		246	1	0.167	0 ==> 1
	64	1	0.167	0 ==> 1		114	1	0.148	1 ==> 0		293	1	0.143	0 ==> 1
	361	1	0.160	4 ==> 3		116	1	0.300	2 ==> 0		306	1	0.286	1 --> 2
node_215 --> node_214	3	1	0.182	0 ==> 1		129	2	0.051	0 ==> 2		399	1	0.062	0 --> 1
	25	1	0.118	0 ==> 1		130	1	0.500	1 ==> 2		434	1	0.111	2 ==> 0
	48	1	0.103	2 --> 3		134	1	0.333	0 ==> 1		440	1	0.200	2 --> 1
	71	1	0.429	0 ==> 2		173	1	1.000	0 ==> 1		461	1	0.300	0 ==> 1
	120	1	0.130	0 ==> 1		177	1	1.000	1 ==> 2		562	1	0.111	1 ==> 0
	136	1	0.500	0 ==> 1		179	1	0.143	1 ==> 0	node_210 --> node_209	185	1	0.067	0 ==> 1
	285	1	0.333	1 --> 0		180	1	0.250	0 ==> 1		189	1	0.190	0 ==> 1
	364	1	0.105	0 ==> 1		182	1	0.273	2 ==> 3		193	1	0.100	1 --> 0
	415	1	0.222	0 ==> 1		183	1	0.500	0 ==> 1		231	2	0.077	2 ==> 0
node_214 --> node_206	30	1	0.167	0 --> 1		188	1	0.080	0 ==> 1		340	1	0.095	1 --> 0
	146	1	0.167	0 ==> 1		194	1	0.600	0 ==> 2		401	1	0.077	1 ==> 0
	156	1	0.333	0 ==> 1		196	1	1.000	0 ==> 1		504	1	0.125	1 ==> 0
	368	1	0.182	0 --> 1		212	1	0.182	0 ==> 1	node_209 --> Agama agama	137	1	0.077	1 --> 0
	375	2	0.065	1 ==> 3		290	1	0.333	0 ==> 1		155	1	0.133	2 ==> 1
	572	2	0.058	1 ==> 3		297	1	0.100	1 --> 0		306	1	0.286	2 --> 1
node_206 --> Priscagama gobie	301	1	0.333	0 ==> 1		301	2	0.333	0 ==> 2		361	1	0.160	4 ==> 3
node_206 --> node_205	48	1	0.103	3 --> 2		311	1	0.286	0 ==> 1		385	1	0.067	2 ==> 0
	151	1	1.000	0 ==> 1		328	2	0.054	0 ==> 2		399	1	0.062	1 --> 0
	399	1	0.062	0 --> 1		338	1	0.143	0 ==> 1		413	1	0.033	1 ==> 0
	420	1	0.085	3 --> 2		342	1	0.333	0 --> 1		419	1	0.073	1 ==> 0
node_214 --> node_213	3	1	0.182	1 ==> 2		350	1	0.333	0 ==> 1		445	1	0.300	1 ==> 0
	7	3	0.069	0 ==> 3		360	1	0.125	1 ==> 0		497	1	0.048	1 ==> 0
	23	1	0.158	0 ==> 1		361	1	0.160	4 ==> 3		509	1	0.158	1 ==> 0
	62	1	0.111	2 ==> 3		374	1	0.250	0 ==> 1		518	1	0.100	0 ==> 1
	63	1	0.286	1 ==> 2		383	1	0.080	0 ==> 1	node_209 --> Pogona vitticeps	18	1	0.053	1 --> 0
	94	1	0.062	0 --> 2		404	1	0.100	0 ==> 1		94	1	0.062	1 --> 0
	111	1	0.222	1 ==> 2		417	1	0.400	1 ==> 0		291	1	0.053	1 ==> 0
	137	1	0.077	0 --> 1		439	1	0.118	0 ==> 2		447	1	0.083	1 ==> 0
	144	1	0.091	1 --> 0		445	1	0.300	1 ==> 3		448	1	0.125	1 ==> 0
	149	1	0.087	2 --> 1		446	1	0.143	0 ==> 1		454	1	0.400	1 --> 0
	266	1	1.000	0 ==> 1		450	1	0.143	0 --> 1		455	1	0.148	0 ==> 1

	483	1	0.120	1 ==> 0		154	1	0.077	0 ==> 1		413	1	0.033	1 ==> 0
	491	1	0.143	1 --> 0		188	1	0.080	0 ==> 1		470	1	0.125	2 ==> 1
	515	1	0.250	0 ==> 1		250	2	0.273	1 ==> 3	node_226 --> Pristidactylus t	39	1	0.080	0 ==> 1
	551	1	0.167	1 ==> 0		344	1	0.048	1 --> 0		94	1	0.062	0 ==> 1
node_210 --> Calotes emma	114	1	0.148	1 ==> 2		375	1	0.065	1 ==> 0		388	1	0.105	2 ==> 1
	149	1	0.087	1 --> 2		378	1	0.091	0 ==> 1	node_245 --> node_244	10	2	0.087	2 --> 0
	212	1	0.182	0 ==> 2		383	1	0.080	0 ==> 1		364	1	0.105	2 --> 1
	258	1	0.081	1 ==> 0		384	1	0.097	1 ==> 2		392	1	0.105	0 ==> 1
	338	1	0.143	0 ==> 1		445	1	0.300	1 ==> 0		413	1	0.033	1 --> 0
	483	1	0.120	1 ==> 2		455	2	0.148	0 ==> 2		419	1	0.073	3 --> 2
	486	1	0.400	2 ==> 3		483	1	0.120	1 ==> 2		487	1	0.222	1 --> 0
	514	1	0.083	0 ==> 1		487	1	0.222	1 ==> 2		492	1	0.111	0 ==> 1
node_249 --> node_217	64	1	0.167	0 --> 1		494	1	0.133	1 ==> 0		588	1	0.167	1 --> 0
	114	1	0.148	2 --> 1		498	1	0.083	1 ==> 0	node_244 --> node_227	22	1	0.111	0 ==> 1
	160	1	0.143	0 --> 1		509	1	0.158	2 ==> 0		48	2	0.103	2 ==> 0
	258	1	0.081	1 --> 2		517	1	0.200	0 ==> 1		62	1	0.111	0 ==> 1
	375	1	0.065	1 --> 2		526	1	0.143	0 ==> 1		169	1	0.333	0 ==> 1
	378	1	0.091	0 ==> 1		588	1	0.167	0 ==> 1		372	1	0.058	3 ==> 2
	463	1	0.108	2 --> 1	node_224 --> node_223	80	1	0.333	0 ==> 1		375	1	0.065	0 ==> 1
	500	1	0.133	0 --> 1		114	1	0.148	2 ==> 1		422	1	0.182	0 ==> 2
	501	1	0.100	0 --> 1		178	1	0.286	0 --> 1	node_227 --> Crotaphytus coll	25	1	0.118	0 ==> 1
	512	1	0.091	0 ==> 1		246	1	0.167	0 ==> 1		114	1	0.148	2 ==> 1
	555	1	0.333	0 --> 1		254	1	0.182	0 --> 1		168	1	0.065	1 ==> 0
node_217 --> node_216	165	1	0.200	0 ==> 1		258	1	0.081	2 --> 3		294	1	0.091	0 ==> 1
	372	1	0.058	0 --> 1		294	1	0.091	0 --> 1		368	1	0.182	0 ==> 1
	421	1	0.075	3 --> 2		372	1	0.058	3 ==> 2		379	1	0.062	0 ==> 1
	489	1	0.111	0 --> 1		483	1	0.120	1 --> 0		421	1	0.075	3 ==> 2
	496	1	0.083	0 --> 1		553	1	0.200	1 --> 0		468	1	0.120	2 ==> 3
	511	1	0.143	0 --> 1		583	1	1.000	0 --> 1		470	1	0.125	2 ==> 3
node_216 --> Temujinia elliso	48	1	0.103	2 ==> 1	node_223 --> Aciprion formosu	11	1	0.105	2 --> 0		481	1	0.083	1 ==> 0
	94	1	0.062	0 ==> 1		48	1	0.103	2 ==> 3	node_227 --> Gambelia wislize	39	1	0.080	0 ==> 1
	301	1	0.333	0 ==> 1		62	1	0.111	0 ==> 1		168	1	0.065	1 ==> 2
node_216 --> Saichangurvel da	468	1	0.120	2 ==> 1		170	1	0.231	0 ==> 1		185	1	0.067	1 ==> 2
node_217 --> EggMtn combined	246	1	0.167	0 ==> 1		364	1	0.105	0 ==> 1		188	1	0.080	1 ==> 0
	375	1	0.065	2 ==> 3		368	1	0.182	0 ==> 1		255	1	0.077	1 ==> 0
	379	1	0.062	0 ==> 1		385	1	0.067	0 ==> 2		340	1	0.095	0 ==> 1
	468	1	0.120	2 ==> 3		572	1	0.058	2 ==> 1		383	1	0.080	0 ==> 1
node_249 --> node_248	63	1	0.286	1 --> 2	node_223 --> node_222	116	1	0.300	2 ==> 1		385	1	0.067	0 ==> 1
	71	1	0.429	0 ==> 2		188	2	0.080	0 ==> 2		413	1	0.033	0 --> 1
	94	1	0.062	0 --> 2		372	1	0.058	2 ==> 1		419	1	0.073	2 --> 3
	372	3	0.058	0 ==> 3		394	2	0.087	0 ==> 2		500	1	0.133	0 ==> 2
	462	1	0.071	0 --> 1	node_222 --> Enyalioides lati	13	1	0.067	0 ==> 1		501	1	0.100	0 ==> 1
	475	1	0.300	0 --> 1		419	1	0.073	3 ==> 4		518	1	0.100	0 ==> 1
	487	1	0.222	0 --> 1		497	1	0.048	1 ==> 0		572	2	0.058	2 ==> 0
	507	1	0.167	1 --> 0		575	1	0.167	0 ==> 1	node_244 --> node_243	80	1	0.333	0 ==> 1
	509	1	0.158	1 --> 2		577	1	0.167	0 ==> 1		146	1	0.167	1 ==> 0
node_248 --> node_219	48	1	0.103	2 --> 1		578	1	0.167	0 ==> 1		246	1	0.167	0 ==> 1
	59	1	0.200	0 ==> 1	node_222 --> Morunasaurus ann	22	1	0.111	0 ==> 1		394	2	0.087	0 --> 2
	62	1	0.111	0 ==> 1		37	1	0.059	0 ==> 1	node_243 --> node_230	7	1	0.069	0 --> 1
	245	1	0.167	0 --> 1		82	1	0.118	0 ==> 1		116	1	0.300	2 ==> 1
	399	1	0.062	0 ==> 1		231	1	0.077	0 ==> 1		168	1	0.065	1 ==> 0
	420	1	0.085	3 --> 2		273	1	0.062	0 ==> 1		176	1	1.000	0 ==> 1
	572	1	0.058	1 ==> 0		307	1	0.125	0 ==> 1		232	1	0.143	0 ==> 1
node_219 --> node_218	73	1	1.000	0 ==> 1		375	1	0.065	1 ==> 2		267	1	0.038	0 --> 1
	166	1	0.091	0 --> 1		383	1	0.080	0 ==> 1		268	1	0.250	0 --> 1
	421	1	0.075	3 ==> 2		413	1	0.033	1 ==> 0		369	1	0.100	1 ==> 0
node_218 --> Isodontosaurus g	48	1	0.103	1 --> 2		487	1	0.222	1 --> 0		388	1	0.105	2 ==> 1
	94	1	0.062	2 --> 0		492	1	0.111	0 ==> 1		399	1	0.062	0 --> 1
	129	1	0.051	0 ==> 1		496	1	0.083	0 ==> 1		401	1	0.077	0 --> 1
	154	1	0.077	0 ==> 2		509	1	0.158	2 --> 1		463	1	0.108	2 ==> 3
	366	1	0.500	0 ==> 2		512	1	0.091	0 ==> 1		468	1	0.120	2 ==> 3
	372	2	0.058	3 ==> 1		519	1	0.077	1 ==> 0		470	1	0.125	2 ==> 0
	375	1	0.065	1 ==> 2		526	1	0.143	0 ==> 1		471	1	0.250	0 ==> 2
	385	1	0.067	0 ==> 2	node_247 --> node_246	10	2	0.087	0 --> 2		554	1	0.167	0 --> 2
node_218 --> Polrussia mongol	48	1	0.103	1 ==> 0		146	1	0.167	0 ==> 1		609	1	0.167	1 ==> 0
	267	1	0.038	1 ==> 0		168	1	0.065	0 ==> 1	node_230 --> node_229	25	1	0.118	0 ==> 1
	333	0	0.333	0 ==> 1		364	2	0.105	0 ==> 2		136	1	0.500	0 ==> 1
	375	1	0.065	1 ==> 0		369	1	0.100	0 ==> 1		340	1	0.095	0 --> 1
	384	1	0.097	1 ==> 2		375	1	0.065	1 ==> 0		392	1	0.105	1 ==> 0
	406	1	0.143	0 ==> 1		378	1	0.091	0 --> 1		447	1	0.083	0 ==> 1
	434	1	0.111	2 ==> 0		588	1	0.167	0 --> 1		496	1	0.083	1 ==> 0
node_219 --> Zapsosaurus scel	94	1	0.062	2 ==> 1	node_246 --> Anolis carolinen	18	1	0.053	0 ==> 1		519	1	0.077	1 ==> 0
	360	1	0.125	1 ==> 0		37	1	0.059	0 ==> 1	node_229 --> Brachylophus fas	7	1	0.069	1 --> 0
node_248 --> node_247	267	1	0.038	1 --> 0		49	1	0.089	0 ==> 1		49	1	0.089	0 ==> 1
	344	1	0.048	0 --> 1		93	1	0.111	0 ==> 1		94	1	0.062	0 ==> 2
	388	1	0.105	1 ==> 2		114	1	0.148	2 ==> 3		114	1	0.148	2 ==> 3
	572	1	0.058	1 ==> 2		148	1	0.091	0 ==> 1		145	1	0.400	0 ==> 2
node_247 --> node_224	7	2	0.069	0 ==> 2		155	1	0.133	2 ==> 1		188	1	0.080	1 ==> 0
	11	1	0.105	0 --> 2		168	1	0.065	1 ==> 2		267	1	0.038	1 --> 0
	30	1	0.167	0 ==> 1		185	1	0.067	1 ==> 0		421	1	0.075	3 ==> 2
	258	1	0.081	1 ==> 2		204	1	0.125	0 ==> 1		470	1	0.125	0 ==> 3
node_224 --> node_221	62	1	0.111	0 ==> 2		254	1	0.182	0 ==> 2		487	1	0.222	0 ==> 1
	105	1	0.667	1 --> 2		258	1	0.081	1 ==> 0		497	1	0.048	0 ==> 1
	293	1	0.143	0 --> 1		267	1	0.038	0 --> 1		561	1	0.154	0 ==> 1
	307	1	0.125	0 --> 1		294	1	0.091	0 ==> 1	node_229 --> node_228	105	1	0.667	1 ==> 2
	442	1	0.143	1 ==> 0		349	1	0.136	0 ==> 1		185	1	0.067	1 --> 2
	463	1	0.108	2 --> 3		380	1	0.091	0 ==> 1		399	1	0.062	1 --> 0
	468	1	0.120	2 ==> 3		384	1	0.097	1 ==> 2		452	1	0.235	4 --> 0
	470	1	0.125	2 ==> 3		385	1	0.067	0 ==> 1		514	1	0.083	0 --> 1
	486	1	0.400	2 ==> 3		394	2	0.087	0 ==> 2		526	1	0.143	0 --> 1
	503	1	0.286	1 --> 0		463	1	0.108	2 ==> 3		572	1	0.058	2 ==> 1
	518	1	0.100	0 --> 1		489	1	0.111	0 ==> 1	node_228 --> Armandisaurus ex	231	1	0.077	1 ==> 0
node_221 --> node_220	93	2	0.111	0 ==> 2		504	1	0.125	1 ==> 0		413	1	0.033	0 ==> 1
	146	1	0.167	0 ==> 1		562	1	0.111	1 ==> 0		419	1	0.073	2 ==> 3
	231	1	0.077	0 ==> 1	node_246 --> node_245	94	1	0.062	2 --> 0	node_228 --> Dipsosaurus dors	11	1	0.105	0 ==> 1
	390	1	0.100	2 ==> 1		188	1	0.080	0 ==> 1		240	1	0.125	0 ==> 2
	487	1	0.222	1 --> 0		231	1	0.077	0 ==> 1		273	1	0.062	0 ==> 1
	500	1	0.133	0 ==> 2		344	1	0.048	1 --> 0		383	1	0.080	0 ==> 1
	501	1	0.100	0 ==> 1		447	1	0.083	1 --> 0		385	1	0.067	0 ==> 1
	551	1	0.167	0 --> 1		452	1	0.235	0 ==> 4	node_230 --> Sauromalus ater	48	1	0.103	2 ==> 3
	562	1	0.111	1 --> 0		483	1	0.120	1 ==> 0		82	1	0.118	0 ==> 1
node_220 --> Basiliscus basil	11	1	0.105	2 --> 0		496	1	0.083	0 ==> 1		112	1	0.167	1 ==> 0
	30	1	0.167	1 ==> 0		497	1	0.048	1 ==> 0		231	1	0.077	1 ==> 0
	48	1	0.103	2 ==> 3	node_245 --> node_226	48	1	0.103	2 ==> 3		306	1	0.286	1 ==> 2
	185	1	0.067	1 ==> 0		154	1	0.077	0 --> 1		341	1	0.033	0 ==> 1
	258	2	0.081	2 ==> 0		188	1	0.080	1 --> 2		344	1	0.048	0 ==> 1
	293	1	0.143	1 --> 0		378	1	0.091	1 --> 0		361	1	0.160	4 ==> 3
	306	1	0.286	1 ==> 2		421	1	0.075	3 ==> 2		364	1	0.105	1 ==> 0
	307	1	0.125	1 --> 0		509	1	0.158	2 --> 1		379	1	0.062	0 ==> 1
	390	1	0.100	1 ==> 0		588	1	0.167	1 ==> 2		385	1	0.067	0 ==> 2
	447	1	0.083	1 ==> 0	node_226 --> node_225	18	1	0.053	0 ==> 1		448	1	0.125	1 ==> 0
	463	1	0.108	3 --> 2		90	1	0.105	0 ==> 1		452	1	0.235	4 ==> 1
	488	1	0.133	0 ==> 1		340	1	0.095	0 ==> 1		481	1	0.083	1 ==> 0
	491	1	0.143	0 ==> 1		341	1	0.033	0 ==> 1		494	1	0.133	1 ==> 0
	503	1	0.286	0 --> 1		448	1	0.125	1 ==> 0		498	1	0.083	1 ==> 0
	509	1	0.158	2 --> 1	node_225 --> Leiosaurus catam	7	2	0.069	0 ==> 2		553	1	0.200	1 ==> 0
	572	1	0.058	2 ==> 1		114	1	0.148	2 ==> 1	node_243 --> node_242	258	1	0.081	1 ==> 2
node_220 --> Corytophanes cri	102	1	0.333	1 ==> 0		154	1	0.077	1 --> 0		364	1	0.105	1 --> 2
	153	1	0.100	0 ==> 1		185	1	0.067	1 ==> 0		383	1	0.080	0 --> 1
	154	1	0.077	0 ==> 2		188	1	0.080	2 --> 1		385	1	0.067	0 --> 1
	267	1	0.038	0 ==> 1		231	1	0.077	1 ==> 2		468	1	0.120	2 ==> 1
	291	1	0.053	1 ==> 0		268	1	0.250	0 ==> 1		497	1	0.048	0 ==> 1
	481	1	0.083	1 ==> 0		291	1	0.053	1 ==> 0		572	1	0.058	2 ==> 1
	489	1	0.111	0 ==> 1		344	1	0.048	0 ==> 1	node_242 --> node_231	25	1	0.118	0 ==> 1
	497	1	0.048	1 ==> 0		361	1	0.160	4 ==> 3		48	1	0.103	2 ==> 1
	518	1	0.100	1 --> 0		378	1	0.091	0 --> 1		59	1	0.200	0 ==> 1
node_221 --> Polychrus marmor	6	1	0.100	0 ==> 1		419	1	0.073	3 ==> 2		80	1	0.333	1 ==> 2
	49	1	0.089	0 ==> 1	node_225 --> Urostrophus vaut	48	1	0.103	3 ==> 4		258	1	0.081	2 ==> 3
	104	1	0.077	0 ==> 1		168	1	0.065	1 ==> 2		367	1	0.125	0 ==> 1
	112	1	0.167	1 ==> 0		317	1	0.250	0 ==> 1		383	1	0.080	1 --> 2
	138	1	0.500	0 ==> 2		328	2	0.054	0 ==> 2		448	1	0.125	1 ==> 0
	148	1	0.091	0 ==> 1		385	1	0.067	0 ==> 1		492	1	0.111	1 ==> 0

	512	1	0.091	0 --> 1		392	1	0.105	1 ==> 2		604	1	1.000	0 --> 1
	610	1	0.050	0 ==> 1		401	1	0.077	1 --> 0	node_387 --> node_253	13	1	0.067	0 --> 1
node_231 --> Liolaemus bellii	39	3	0.080	0 ==> 3		584	1	0.188	1 ==> 2		37	1	0.059	0 --> 1
	111	1	0.222	1 ==> 0	node_235 --> Phrynosoma platy	94	1	0.062	0 ==> 2		49	1	0.089	0 ==> 1
	128	1	0.167	0 ==> 1		99	1	0.250	0 ==> 1		56	1	0.190	1 ==> 2
	154	1	0.077	0 ==> 1		102	1	0.333	1 ==> 0		64	1	0.167	0 ==> 1
	169	1	0.333	0 ==> 1		114	1	0.148	2 ==> 1		87	1	0.200	0 --> 1
	188	1	0.080	1 ==> 2		124	1	0.077	0 ==> 1		96	1	0.222	0 --> 4
	254	1	0.182	0 ==> 1		144	1	0.091	1 ==> 0		116	1	0.300	1 --> 3
	297	1	0.100	1 ==> 0		153	1	0.100	0 ==> 1		145	1	0.400	0 --> 1
	328	2	0.054	0 ==> 2		154	1	0.077	1 ==> 2		150	1	0.200	0 ==> 1
	340	1	0.095	0 ==> 1		185	1	0.067	1 ==> 0		157	1	0.125	0 ==> 1
	361	1	0.160	4 ==> 3		188	2	0.080	2 ==> 4		167	1	0.125	0 --> 1
	392	1	0.105	1 ==> 0		254	1	0.182	0 ==> 2		213	1	0.048	0 --> 1
	421	1	0.075	3 ==> 2		291	1	0.053	1 ==> 0		271	1	0.167	0 --> 1
	518	1	0.100	0 ==> 1		293	1	0.143	0 ==> 1		273	1	0.062	0 --> 1
	519	1	0.077	1 ==> 0		297	1	0.100	1 ==> 0		285	1	0.333	1 --> 0
	541	1	0.100	0 ==> 1		340	1	0.095	0 ==> 1		375	1	0.065	2 ==> 3
	562	1	0.111	1 ==> 0		341	1	0.033	0 ==> 1		379	1	0.062	0 ==> 1
	572	1	0.058	1 ==> 0		364	1	0.105	1 ==> 0		437	1	1.000	0 ==> 1
node_231 --> Phymaturus pallu	7	2	0.069	0 ==> 2		369	1	0.100	1 ==> 0		500	1	0.133	0 --> 2
	82	2	0.118	0 ==> 2		372	1	0.058	2 ==> 1		509	1	0.158	1 --> 0
	170	1	0.231	0 ==> 1		375	1	0.065	0 ==> 1		511	1	0.143	0 --> 1
	306	1	0.286	1 ==> 0		383	1	0.080	0 --> 2		512	1	0.091	0 --> 1
	307	1	0.125	0 ==> 1		388	2	0.105	2 ==> 0		546	1	0.100	1 --> 0
	348	1	0.111	0 ==> 1		418	1	0.083	0 ==> 1	node_253 --> Tchingisaurus mu	39	1	0.080	2 --> 1
	349	1	0.136	0 ==> 1		420	1	0.085	3 ==> 2		230	1	0.333	1 ==> 0
	364	1	0.105	2 --> 1		421	1	0.075	3 ==> 2		245	1	0.167	0 ==> 1
	372	1	0.058	3 ==> 2		442	1	0.143	1 ==> 0		384	1	0.097	1 ==> 2
	378	1	0.091	1 ==> 0		448	1	0.125	1 ==> 0		572	1	0.058	1 ==> 2
	385	1	0.067	1 --> 0		452	1	0.235	4 ==> 0	node_253 --> node_252	39	2	0.080	2 --> 4
	413	1	0.033	0 --> 1		459	1	0.182	0 ==> 1		49	1	0.089	1 --> 2
	419	1	0.073	2 ==> 1		463	1	0.108	2 ==> 3		111	1	0.222	1 ==> 2
	462	1	0.071	1 ==> 0		470	1	0.125	2 ==> 3		122	1	0.500	0 ==> 1
	496	1	0.083	1 ==> 0		483	1	0.120	1 ==> 2		149	2	0.087	2 ==> 0
	504	1	0.125	1 ==> 0		492	1	0.111	1 ==> 0		175	1	0.333	0 ==> 1
	554	1	0.167	0 ==> 1		494	1	0.133	1 ==> 0		259	1	0.250	1 --> 0
node_242 --> node_241	344	1	0.048	0 ==> 1		497	1	0.048	1 ==> 0		399	1	0.062	0 ==> 1
	384	1	0.097	1 ==> 2		498	1	0.083	1 ==> 0		403	1	0.200	0 ==> 1
	394	2	0.087	2 --> 0		519	1	0.077	1 ==> 0		413	1	0.033	1 --> 0
	483	1	0.120	0 ==> 1		542	1	0.273	0 ==> 2		418	1	0.083	0 ==> 1
node_241 --> node_238	401	1	0.077	0 --> 1		543	1	0.500	0 ==> 1		420	1	0.085	3 --> 2
	413	1	0.033	0 --> 1		566	1	0.444	0 ==> 4	node_252 --> Gobinatus arenos	94	1	0.062	0 ==> 1
	419	1	0.073	2 --> 3		572	1	0.058	1 ==> 2	node_252 --> node_251	7	1	0.069	0 --> 1
	496	1	0.083	1 ==> 0	node_235 --> Uma scoparia	48	1	0.103	1 ==> 0		90	1	0.105	0 --> 1
	562	1	0.111	1 ==> 0		59	1	0.200	0 ==> 1		155	1	0.133	2 ==> 1
node_238 --> node_232	31	1	0.333	0 ==> 1		80	1	0.333	1 ==> 2		182	1	0.273	2 --> 1
	62	1	0.111	0 ==> 1		148	1	0.091	0 ==> 1		257	1	0.500	1 ==> 0
	80	1	0.333	1 ==> 2		188	1	0.080	2 --> 1		262	1	1.000	0 ==> 1
	111	1	0.222	1 ==> 0		372	1	0.058	2 --> 3		267	1	0.038	0 --> 1
	185	1	0.067	1 ==> 0		394	1	0.087	0 ==> 1		281	1	0.167	0 ==> 1
	188	1	0.080	1 ==> 0		413	1	0.033	1 ==> 0		360	1	0.125	1 ==> 0
	258	1	0.081	2 ==> 1		419	1	0.073	3 ==> 2	node_251 --> Adamisaurus magn	3	1	0.182	0 ==> 1
	340	1	0.095	0 ==> 1		447	1	0.083	0 ==> 1		49	1	0.089	2 --> 1
	378	1	0.091	1 ==> 0		462	1	0.071	1 ==> 0		71	1	0.429	0 ==> 1
	518	1	0.100	0 --> 1		546	1	0.100	1 ==> 0		85	1	0.500	0 ==> 1
	519	1	0.077	1 ==> 0		554	1	0.167	0 ==> 2		116	1	0.300	3 --> 1
	608	1	0.333	0 ==> 1		572	1	0.058	1 ==> 0		120	1	0.130	0 ==> 1
node_232 --> Chalarodon madag	7	1	0.069	0 ==> 1	node_237 --> Leiocephalus bar	25	1	0.118	1 ==> 2		357	1	0.083	0 ==> 1
	59	1	0.200	0 ==> 1		39	1	0.080	0 ==> 1		369	2	0.100	0 ==> 2
	168	1	0.065	1 ==> 0		254	1	0.182	0 ==> 1		375	1	0.065	3 ==> 2
	384	1	0.097	2 ==> 1		294	1	0.091	0 ==> 1		416	1	0.286	0 ==> 4
	442	1	0.143	1 ==> 0		369	1	0.100	1 ==> 2		419	1	0.073	3 ==> 2
	447	1	0.083	0 ==> 1		394	2	0.087	0 ==> 2		421	2	0.075	3 ==> 1
	452	1	0.235	4 ==> 0		447	1	0.083	0 ==> 1		434	1	0.111	2 ==> 0
	481	1	0.083	1 ==> 0		486	1	0.400	2 ==> 3		572	1	0.058	1 ==> 0
	486	2	0.400	2 ==> 4		507	1	0.167	0 ==> 1	node_251 --> node_250	13	1	0.067	1 --> 0
	497	1	0.048	1 ==> 0		526	1	0.143	0 ==> 1		110	1	1.000	0 ==> 1
node_232 --> Oplurus cyclurus	48	2	0.103	2 ==> 4	node_241 --> node_240	30	1	0.167	0 --> 1		166	1	0.091	0 ==> 1
	146	1	0.167	0 ==> 1		48	1	0.103	2 ==> 3		240	1	0.125	0 ==> 1
	168	1	0.065	1 ==> 2		170	1	0.231	0 --> 1		376	1	0.200	0 ==> 1
	255	1	0.077	1 ==> 0		246	1	0.167	1 ==> 0		420	1	0.085	2 --> 3
	372	2	0.058	3 ==> 1		452	1	0.235	4 --> 1	node_250 --> Gilmoreteius	37	1	0.059	1 ==> 0
	375	1	0.065	0 ==> 1		462	1	0.071	1 ==> 0		49	1	0.089	2 ==> 3
	385	1	0.067	1 ==> 0	node_240 --> node_239	7	1	0.069	0 ==> 1		90	1	0.105	1 --> 0
	419	1	0.073	3 --> 2		254	1	0.182	0 ==> 1		501	1	0.100	0 ==> 1
	421	1	0.075	3 ==> 2		369	1	0.100	1 ==> 2	node_250 --> Polyglyphanodon	231	2	0.077	0 ==> 2
	483	1	0.120	1 ==> 0		388	1	0.105	2 ==> 1		259	1	0.250	0 --> 1
	529	1	0.286	1 ==> 0		609	1	0.167	1 --> 0		508	1	0.143	1 --> 0
	572	1	0.058	1 ==> 2	node_239 --> Plica plica	3	1	0.182	0 ==> 1		561	1	0.154	0 ==> 1
node_238 --> node_237	25	1	0.118	0 --> 1		11	1	0.105	0 ==> 2	node_387 --> node_386	22	1	0.111	0 --> 1
	154	1	0.077	0 ==> 1		170	1	0.231	1 --> 0		24	1	0.071	1 --> 0
	267	1	0.038	0 ==> 1		232	1	0.143	0 ==> 1		83	1	1.000	1 ==> 2
	509	1	0.158	2 ==> 0		380	1	0.091	0 ==> 1		111	1	0.222	1 --> 0
	609	1	0.167	1 ==> 0		388	1	0.105	1 ==> 0		154	1	0.077	0 --> 1
node_237 --> node_236	30	1	0.167	0 ==> 1		413	1	0.033	0 --> 1		165	1	0.200	0 --> 1
	48	1	0.103	2 ==> 1		447	1	0.083	0 ==> 1		208	1	0.091	0 --> 1
	168	1	0.065	1 ==> 0		483	1	0.120	1 ==> 0		283	1	0.133	0 --> 1
	170	1	0.231	0 ==> 1		513	1	0.083	1 ==> 0		285	1	0.333	1 ==> 2
	188	1	0.080	1 --> 2		551	1	0.167	0 ==> 1		360	1	0.125	1 ==> 2
	231	1	0.077	1 --> 0	node_239 --> Stenocercus guen	18	1	0.053	0 ==> 1		388	1	0.105	1 --> 0
	372	1	0.058	3 --> 2		30	1	0.167	1 --> 0		394	1	0.087	0 ==> 1
	454	1	0.400	0 ==> 1		112	1	0.167	1 ==> 0		401	1	0.077	0 --> 1
node_236 --> node_234	25	1	0.118	1 --> 0		154	1	0.077	0 ==> 1		434	1	0.111	2 --> 0
	344	1	0.048	1 ==> 0		185	1	0.067	1 ==> 0		455	2	0.148	2 ==> 4
	392	1	0.105	1 ==> 0		258	2	0.081	2 ==> 0		470	1	0.125	0 --> 3
node_234 --> node_233	48	1	0.103	1 ==> 0		421	1	0.075	3 ==> 2		521	1	0.067	0 ==> 1
	59	1	0.200	0 ==> 1		452	1	0.235	1 --> 4		572	1	0.058	1 --> 0
	185	1	0.067	1 ==> 2		507	1	0.167	0 ==> 1	node_386 --> node_379	82	1	0.118	0 ==> 1
	307	1	0.125	0 ==> 1		509	1	0.158	2 ==> 1		90	2	0.105	0 ==> 2
	462	1	0.071	1 ==> 0		562	1	0.111	1 ==> 0		128	1	0.167	0 ==> 1
	492	1	0.111	1 ==> 0	node_240 --> Uranoscodon supe	144	1	0.091	1 ==> 0		162	1	0.333	0 ==> 1
node_233 --> Petrosaurus mear	7	1	0.069	0 ==> 1		168	1	0.065	1 ==> 0		178	1	0.286	0 --> 1
	18	1	0.053	0 ==> 1		328	2	0.054	0 ==> 2		188	2	0.080	0 ==> 2
	22	1	0.111	0 ==> 1		340	1	0.095	0 ==> 1		200	1	1.000	0 ==> 1
	82	1	0.118	0 ==> 1		470	1	0.125	2 ==> 3		220	1	0.375	0 --> 1
	154	1	0.077	1 ==> 0		519	1	0.077	1 ==> 0		241	1	0.667	1 ==> 2
	349	1	0.136	0 ==> 1		572	1	0.058	1 ==> 0		258	3	0.081	0 ==> 3
	372	1	0.058	2 --> 3	node_388 --> node_387	29	1	0.083	1 --> 0		272	1	0.500	0 ==> 1
	443	1	0.167	0 ==> 1		36	1	0.062	1 --> 0		328	1	0.054	0 --> 1
	483	1	0.120	1 ==> 0		39	2	0.080	0 ==> 2		463	1	0.108	1 --> 2
	497	1	0.048	1 ==> 0		48	1	0.103	2 --> 3		468	1	0.120	2 ==> 1
	509	1	0.158	0 ==> 2		63	1	0.286	1 --> 0		502	1	0.091	0 ==> 1
node_233 --> Uta stansburiana	80	1	0.333	1 ==> 2		83	1	1.000	0 ==> 1	node_379 --> node_365	7	1	0.069	0 ==> 1
	364	1	0.105	2 ==> 1		114	1	0.148	2 ==> 3		117	1	0.333	0 ==> 1
	401	1	0.077	1 --> 0		201	1	0.250	0 --> 1		145	1	0.400	0 ==> 2
	413	1	0.033	1 ==> 0		205	1	0.333	0 ==> 1		155	1	0.133	2 ==> 1
	419	1	0.073	3 ==> 2		250	1	0.273	1 ==> 2		157	1	0.125	0 --> 1
	448	1	0.125	1 ==> 0		305	1	0.333	0 ==> 1		182	1	0.273	2 --> 1
	572	1	0.058	1 ==> 0		315	1	0.071	0 --> 1		208	1	0.091	1 ==> 2
node_234 --> Sceloporus varia	94	1	0.062	0 ==> 1		317	1	0.250	0 --> 1		213	1	0.048	0 --> 1
	231	1	0.077	0 --> 1		375	1	0.065	1 --> 2		215	1	0.091	0 ==> 1
	258	1	0.081	2 ==> 3		439	1	0.118	0 --> 1		217	1	0.600	0 ==> 1
	486	1	0.400	2 ==> 3		455	2	0.148	0 ==> 2		245	1	0.167	0 ==> 1
	606	1	1.000	0 ==> 2		463	1	0.108	2 --> 1		275	1	0.333	0 ==> 2
node_236 --> node_235	7	1	0.069	0 ==> 1		475	1	0.300	0 --> 1		383	1	0.080	0 --> 1
	62	1	0.111	0 ==> 1		508	1	0.143	0 --> 1		388	1	0.105	0 --> 1
	137	1	0.077	0 ==> 1		555	1	0.333	0 ==> 1		512	1	0.091	0 --> 1
	167	1	0.125	0 ==> 1		557	1	0.125	1 --> 0		570	1	0.500	0 --> 1
	364	1	0.105	2 ==> 1		585	1	0.250	0 --> 1		572	2	0.058	0 ==> 2
	383	1	0.080	1 --> 0		593	1	0.231	0 --> 1		573	1	0.083	0 --> 1
	384	1	0.097	2 --> 1		600	1	1.000	0 --> 1		579	1	0.182	0 --> 1

	585	1	0.250	1 --> 0		564	1	0.500	0 --> 1		258	1	0.081	2 ==> 1
	590	1	0.308	1 --> 2		575	1	0.167	1 ==> 0		261	1	0.200	0 ==> 1
	607	1	0.250	0 ==> 1		577	1	0.167	1 ==> 0		271	1	0.167	0 ==> 1
node_365 --> node_331	56	1	0.190	1 ==> 2		578	1	0.167	1 --> 0		278	1	0.500	0 --> 1
	58	1	0.222	1 ==> 2		579	1	0.182	1 --> 0		311	1	0.286	1 ==> 2
	138	1	0.500	0 ==> 1		584	1	0.188	2 --> 3		320	1	1.000	1 --> 2
	160	1	0.143	0 --> 1		586	1	0.333	0 --> 1		337	2	0.136	1 ==> 3
	222	1	0.500	0 ==> 1	node_315 --> Sineoamphisbaena	66	1	0.286	1 ==> 0		340	1	0.095	0 --> 1
	232	1	0.143	0 ==> 1		76	1	0.333	0 ==> 1		341	1	0.033	0 ==> 1
	234	1	0.600	0 ==> 2		88	1	0.125	1 ==> 0		350	1	0.333	1 ==> 2
	337	1	0.136	0 --> 1		95	1	0.083	0 ==> 1		351	1	0.375	0 --> 3
	340	1	0.095	0 ==> 1		96	1	0.222	0 ==> 4		358	1	0.250	1 --> 0
	368	1	0.182	0 --> 1		101	1	0.105	0 ==> 1		360	2	0.125	0 ==> 2
	371	1	0.250	0 --> 1		102	1	0.333	1 ==> 0		369	1	0.100	0 ==> 1
	420	1	0.085	3 --> 2		122	1	0.500	0 ==> 1		372	3	0.058	0 --> 3
	421	1	0.075	3 --> 2		149	2	0.087	2 ==> 0		374	1	0.250	0 --> 1
	428	1	0.200	0 --> 1		150	1	0.200	0 ==> 1		380	1	0.091	0 --> 1
	446	1	0.143	0 ==> 1		155	1	0.133	2 --> 1		399	1	0.062	0 ==> 1
	461	1	0.300	0 ==> 2		166	1	0.091	0 ==> 1		412	1	0.111	1 --> 0
	475	1	0.300	1 ==> 2		179	1	0.143	1 ==> 0		419	1	0.073	1 --> 2
	575	1	0.167	0 ==> 1		240	1	0.125	0 ==> 2		420	1	0.085	2 --> 1
	577	1	0.167	0 ==> 1		261	1	0.200	0 ==> 1		470	1	0.125	3 --> 1
	589	1	0.500	0 ==> 1		271	2	0.167	0 ==> 2		561	1	0.154	1 --> 0
	593	1	0.231	1 --> 0		283	1	0.133	1 ==> 0		589	1	0.500	1 ==> 0
	603	1	0.500	0 ==> 1		311	1	0.286	1 ==> 2	node_263 --> node_254	8	1	0.182	0 ==> 2
node_331 --> node_328	39	2	0.080	2 --> 4		341	1	0.033	0 ==> 1		18	1	0.053	1 ==> 2
	48	1	0.103	3 --> 4		350	1	0.333	1 ==> 2		23	1	0.158	0 ==> 2
	66	1	0.286	0 ==> 1		358	1	0.250	1 --> 0		38	2	0.143	2 ==> 0
	77	1	0.083	0 --> 1		412	1	0.111	1 --> 0		54	1	0.333	0 ==> 1
	94	1	0.062	0 --> 1		419	1	0.073	3 ==> 4		93	1	0.111	1 ==> 0
	157	1	0.125	1 --> 0		422	1	0.182	1 --> 0		95	1	0.083	0 ==> 1
	255	1	0.077	1 --> 0		423	1	0.100	0 ==> 1		101	1	0.105	0 ==> 1
	360	1	0.125	2 ==> 1		427	1	0.100	1 --> 0		128	1	0.167	2 --> 1
	388	1	0.105	1 --> 0		497	1	0.048	1 --> 0		185	2	0.067	0 ==> 2
	456	1	0.190	0 ==> 1	node_315 --> node_314	28	1	0.143	3 ==> 1		190	1	0.250	0 ==> 1
	468	1	0.120	1 ==> 0		37	1	0.059	0 --> 1		216	1	0.222	1 ==> 2
	483	1	0.120	1 --> 2		38	1	0.143	1 --> 2		249	1	0.231	1 --> 3
	484	1	0.100	0 --> 1		75	1	1.000	0 ==> 1		251	2	0.333	0 --> 2
	531	1	0.125	0 --> 1		90	2	0.105	2 ==> 0		319	1	1.000	0 ==> 1
	578	1	0.167	0 --> 1		93	1	0.111	0 ==> 1		328	1	0.054	1 ==> 2
node_328 --> node_324	38	1	0.143	0 ==> 1		152	1	0.400	0 --> 1		345	1	0.250	0 ==> 1
	82	1	0.118	1 --> 2		159	1	0.333	0 ==> 1		352	1	0.500	1 ==> 0
	104	1	0.077	0 --> 1		258	1	0.081	3 --> 2		361	1	0.160	3 ==> 4
	129	1	0.051	0 ==> 1		276	2	0.118	0 --> 2		369	1	0.100	1 ==> 2
	155	1	0.133	1 --> 2		283	1	0.133	1 --> 2		384	1	0.097	1 ==> 2
	216	1	0.222	0 --> 1		340	1	0.095	1 --> 0		385	1	0.067	0 ==> 1
	273	1	0.062	0 ==> 1		349	1	0.136	3 --> 2		391	1	0.500	0 ==> 1
	291	1	0.053	0 --> 1		367	1	0.125	0 --> 1		459	1	0.182	3 ==> 2
	294	1	0.091	0 ==> 1		419	2	0.073	3 ==> 1		463	1	0.108	1 ==> 0
	316	1	0.200	1 --> 0		465	1	0.250	0 --> 1		480	1	0.200	1 --> 0
	349	3	0.136	0 ==> 3		488	1	0.133	0 ==> 1		487	4	0.222	0 --> 4
	358	1	0.250	0 --> 1		493	1	0.200	1 --> 0		524	1	0.200	1 --> 0
	360	1	0.125	1 ==> 0		495	1	0.125	1 --> 0		548	1	0.100	1 --> 0
	375	1	0.065	2 ==> 1		505	1	0.167	0 ==> 1		586	1	0.333	1 --> 0
	379	1	0.062	0 --> 1		528	1	0.200	0 ==> 1		590	4	0.308	4 ==> 0
	412	1	0.111	0 --> 1	node_314 --> Anniella pulchra	22	1	0.111	1 ==> 0		593	3	0.231	0 ==> 3
	418	1	0.083	0 ==> 1		96	1	0.222	0 ==> 2		607	1	0.250	1 --> 0
	422	1	0.182	0 --> 1		129	1	0.051	1 ==> 2	node_254 --> Anelytropsis pap	7	1	0.069	2 --> 1
	427	1	0.100	0 --> 1		170	1	0.231	0 ==> 1		47	1	0.188	1 --> 0
	450	1	0.143	0 --> 1		220	1	0.375	1 ==> 0		62	1	0.111	1 --> 0
	486	1	0.400	2 ==> 1		249	1	0.231	1 ==> 2		188	1	0.080	4 ==> 3
	497	1	0.048	0 --> 1		280	1	0.500	0 ==> 1		290	1	0.333	1 ==> 0
	504	1	0.125	1 ==> 0		337	1	0.136	1 --> 0		421	1	0.075	1 ==> 2
	509	1	0.158	1 --> 2		351	1	0.375	0 ==> 1		439	1	0.118	1 ==> 0
	535	1	0.143	1 --> 2		365	1	0.333	0 ==> 1		440	1	0.200	1 ==> 0
	561	1	0.154	0 --> 1		366	1	0.500	0 ==> 1	node_254 --> Dibamus novaegui	13	1	0.067	0 ==> 1
	573	1	0.083	1 --> 0		371	1	0.250	0 --> 1		25	2	0.118	0 ==> 2
	584	1	0.188	1 --> 2		378	1	0.091	0 ==> 1		96	1	0.222	0 ==> 1
	590	1	0.308	2 --> 3		379	1	0.062	1 --> 0		106	1	0.182	0 ==> 1
node_324 --> node_315	56	1	0.190	2 ==> 1		384	1	0.097	1 ==> 2		128	1	0.167	1 ==> 0
	87	1	0.200	0 --> 1		406	1	0.143	0 ==> 1		217	1	0.600	1 ==> 2
	109	1	0.750	0 --> 2		410	1	0.091	0 ==> 1		220	1	0.375	1 ==> 2
	154	1	0.077	1 --> 0		463	1	0.108	2 ==> 3		286	1	0.111	0 ==> 1
	180	1	0.250	0 ==> 1		470	1	0.125	3 --> 0		355	1	0.059	1 --> 0
	191	1	0.167	0 ==> 1		471	1	0.250	0 ==> 1		402	1	0.167	0 ==> 1
	192	1	0.250	0 ==> 1		510	1	0.143	0 ==> 1		419	1	0.073	2 ==> 3
	193	1	0.100	0 --> 1		516	1	0.143	0 ==> 1		420	1	0.085	1 --> 2
	194	1	0.600	0 --> 1		573	1	0.083	0 ==> 1		444	1	0.500	0 ==> 1
	249	1	0.231	0 --> 1		578	1	0.167	0 --> 1		591	1	0.250	1 --> 0
	250	1	0.273	2 --> 3		579	1	0.182	0 --> 1	node_263 --> node_262	2	1	0.083	0 --> 1
	255	1	0.077	0 --> 1		580	1	0.333	0 ==> 1		10	1	0.087	0 --> 1
	256	1	0.333	0 --> 1		582	1	0.250	0 ==> 1		11	1	0.105	1 --> 0
	267	1	0.038	0 ==> 1		587	1	0.100	1 ==> 0		22	1	0.111	1 ==> 0
	268	1	0.250	0 --> 1		590	1	0.308	3 --> 2		28	1	0.143	1 ==> 0
	281	1	0.167	0 --> 1		610	1	0.050	0 ==> 1		40	1	0.500	0 ==> 1
	290	1	0.333	0 --> 1	node_314 --> node_313	7	1	0.069	1 --> 2		56	2	0.190	1 ==> 3
	293	1	0.143	0 --> 1		11	1	0.105	0 --> 1		129	2	0.051	0 ==> 2
	307	1	0.125	0 ==> 2		18	1	0.053	0 ==> 1		221	1	1.000	0 ==> 1
	311	1	0.286	0 ==> 1		24	1	0.071	0 --> 1		264	1	1.000	0 ==> 1
	312	2	0.222	0 ==> 2		47	1	0.188	0 --> 1		271	1	0.167	1 ==> 2
	324	1	0.300	0 --> 1		62	1	0.111	0 --> 1		297	1	0.100	0 --> 1
	333	1	0.333	0 ==> 1		68	1	0.077	0 --> 1		299	1	0.600	0 ==> 3
	334	1	0.167	1 ==> 0		71	1	0.429	0 --> 3		305	1	0.333	0 --> 1
	344	1	0.048	0 --> 1		128	1	0.167	1 --> 2		312	1	0.222	2 --> 1
	350	1	0.333	0 ==> 1		129	1	0.051	1 --> 0		316	2	0.200	0 ==> 2
	361	1	0.160	4 --> 3		137	1	0.077	0 ==> 1		321	1	0.231	0 ==> 2
	371	1	0.250	1 --> 0		142	1	0.250	0 ==> 1		340	1	0.095	1 ==> 2
	375	1	0.065	1 --> 0		143	1	0.200	0 --> 1		349	1	0.136	2 ==> 3
	421	1	0.075	2 --> 1		154	1	0.077	0 --> 1		370	1	0.333	0 --> 1
	442	1	0.143	1 --> 0		157	1	0.125	0 --> 1		396	1	0.095	0 ==> 1
	445	1	0.300	1 --> 0		182	1	0.273	1 ==> 2		414	1	1.000	1 ==> 2
	451	1	0.333	0 --> 1		185	1	0.067	1 --> 0		422	1	0.182	1 ==> 0
	456	2	0.190	1 --> 3		188	2	0.080	2 ==> 4		445	1	0.300	0 ==> 1
	459	3	0.182	0 --> 3		194	1	0.600	1 --> 2		449	1	0.200	0 --> 1
	462	1	0.071	0 --> 1		232	1	0.143	1 --> 0		470	1	0.125	1 --> 2
	480	1	0.200	0 --> 1		234	1	0.600	2 ==> 0		510	1	0.143	0 --> 1
	483	1	0.120	2 --> 3		281	1	0.167	1 --> 0		550	1	0.200	0 --> 1
	486	1	0.400	1 --> 0		297	1	0.100	1 --> 0	node_262 --> node_256	6	1	0.100	0 --> 1
	491	1	0.143	0 --> 1		305	1	0.333	1 --> 0		18	1	0.053	1 ==> 0
	499	1	0.143	0 --> 1		320	1	1.000	0 --> 1		23	1	0.158	0 ==> 3
	502	1	0.091	1 --> 0		348	1	0.111	0 ==> 1		24	1	0.071	1 --> 0
	517	1	0.200	0 --> 1		355	1	0.059	0 --> 1		25	1	0.118	0 --> 1
	518	2	0.100	0 --> 2		368	1	0.182	1 --> 0		142	1	0.250	1 ==> 0
	524	1	0.200	0 --> 1		383	1	0.080	1 --> 0		161	1	0.125	0 ==> 1
	529	1	0.286	1 --> 0		392	1	0.105	0 ==> 1		216	1	0.222	1 --> 0
	530	1	0.200	0 --> 1		394	1	0.087	1 ==> 0		259	1	0.250	1 ==> 0
	531	1	0.125	1 --> 0		414	1	1.000	0 --> 1		283	1	0.133	2 --> 1
	533	1	0.333	1 --> 0		456	1	0.190	3 ==> 4		328	1	0.054	1 --> 0
	534	1	0.500	1 --> 0		457	1	0.174	0 ==> 1		355	1	0.059	1 --> 0
	542	1	0.273	0 --> 1		463	1	0.108	2 ==> 1		367	1	0.125	1 --> 0
	544	1	1.000	0 --> 2		572	2	0.058	2 ==> 0		374	1	0.250	1 --> 0
	546	1	0.100	1 --> 0		590	1	0.308	3 --> 4		380	1	0.091	1 --> 0
	547	1	0.250	0 --> 1		591	1	0.250	0 --> 1		388	1	0.105	0 ==> 1
	548	1	0.100	0 --> 1		592	1	0.667	0 --> 2		394	1	0.087	0 --> 1
	549	1	0.250	0 --> 1		595	1	0.333	0 --> 1		406	1	0.143	0 ==> 1
	551	1	0.167	0 --> 1		596	1	0.333	0 --> 1		412	1	0.111	0 --> 1
	552	1	0.500	0 --> 1		603	1	0.500	1 --> 0		418	1	0.083	1 ==> 2
	553	1	0.200	0 --> 1	node_313 --> node_263	114	1	0.148	3 ==> 4		419	1	0.073	2 --> 1
	554	1	0.167	0 --> 2		124	1	0.077	0 --> 1		488	1	0.133	1 --> 2
	555	1	0.333	1 --> 0		222	1	0.500	1 ==> 0		572	2	0.058	0 ==> 2
	557	1	0.125	0 --> 1		240	1	0.125	0 ==> 2	node_256 --> node_255	62	1	0.111	1 --> 0
	559	1	0.500	0 --> 1		245	1	0.167	1 ==> 0		152	1	0.400	1 --> 0

	258	1	0.081	1 ==> 0		25	1	0.118	0 ==> 1		277	1	0.333	0 --> 1
	297	1	0.100	1 --> 0		28	1	0.143	0 ==> 1		289	1	0.200	0 --> 1
	312	1	0.222	1 --> 2		37	1	0.059	1 ==> 0		300	1	0.250	1 ==> 0
	364	1	0.105	0 ==> 1		124	1	0.077	0 ==> 1		328	1	0.054	0 --> 1
	394	1	0.087	1 ==> 2		126	1	0.667	1 --> 0		344	1	0.048	0 --> 1
	410	1	0.091	0 --> 1		206	1	0.091	0 ==> 1		374	1	0.250	0 --> 1
	420	1	0.085	1 --> 2		215	1	0.091	0 --> 1		420	1	0.085	2 ==> 1
node_255 --> Spathorhynchus f	6	1	0.100	1 --> 0		276	1	0.118	1 ==> 2		426	1	0.333	1 --> 0
	10	1	0.087	1 ==> 2		297	1	0.100	1 --> 0		439	1	0.118	1 --> 2
	25	1	0.118	1 --> 0		361	1	0.160	3 ==> 4		458	1	0.100	0 --> 1
	332	1	0.222	0 ==> 2		388	1	0.105	0 ==> 1	node_266 --> node_264	16	1	0.500	0 ==> 1
	379	1	0.062	1 ==> 0		418	1	0.083	1 ==> 2		51	1	0.200	1 ==> 0
node_255 --> Dyticonastis ren	216	1	0.222	0 --> 1		587	1	0.100	1 ==> 0		185	4	0.067	0 ==> 4
	328	1	0.054	0 --> 1	node_313 --> node_312	8	1	0.182	0 --> 1		270	1	1.000	0 ==> 1
	369	1	0.100	1 ==> 2		9	1	0.250	0 --> 1		298	1	1.000	0 ==> 1
	383	1	0.080	0 ==> 1		20	1	0.167	0 --> 1		299	1	0.600	1 ==> 0
	385	1	0.067	0 ==> 1		21	1	0.500	0 --> 1		390	1	0.100	0 --> 1
	399	1	0.062	1 ==> 0		32	1	1.000	0 --> 1		459	1	0.182	3 --> 4
node_256 --> Rhineura florida	10	1	0.087	1 --> 0		37	1	0.059	1 --> 0	node_264 --> Leptotyphlops du	179	1	0.143	1 ==> 0
	99	1	0.250	0 ==> 1		39	1	0.080	4 --> 3		247	1	0.333	1 --> 0
	143	1	0.200	1 ==> 2		51	1	0.200	0 --> 1		328	1	0.054	1 --> 0
	206	1	0.091	0 ==> 1		57	1	0.190	1 --> 2		341	1	0.033	0 ==> 1
	208	2	0.091	2 ==> 0		96	1	0.222	0 ==> 1		361	1	0.160	2 ==> 1
	286	1	0.111	0 ==> 1		113	1	0.500	1 --> 0		374	1	0.250	1 --> 0
	360	2	0.125	2 ==> 0		114	2	0.148	3 --> 1		392	1	0.105	1 ==> 2
node_262 --> node_261	4	1	0.143	0 --> 1		115	1	0.600	0 --> 1		420	1	0.085	1 ==> 0
	10	1	0.087	1 ==> 2		119	1	0.800	0 --> 1		440	1	0.200	0 --> 1
	56	1	0.190	3 --> 4		120	3	0.130	0 --> 3		458	1	0.100	1 --> 0
	102	1	0.333	1 ==> 2		133	1	0.500	0 --> 1		548	1	0.100	1 --> 0
	124	1	0.077	1 --> 0		135	1	0.600	0 --> 2	node_264 --> Typhlops jamaice	6	1	0.100	1 --> 0
	127	1	1.000	0 ==> 1		141	1	0.250	0 --> 1		7	1	0.069	2 --> 1
	215	1	0.091	1 --> 0		168	2	0.065	0 ==> 2		17	1	0.167	1 --> 0
	275	1	0.333	2 ==> 4		182	1	0.273	2 ==> 3		28	1	0.143	1 ==> 0
	276	1	0.118	2 --> 1		195	1	1.000	0 --> 1		31	1	0.333	1 --> 0
	281	1	0.167	0 ==> 1		201	1	0.250	1 --> 0		50	1	0.167	0 ==> 1
	318	1	1.000	0 ==> 1		204	2	0.125	0 --> 2		101	1	0.105	2 --> 1
	372	3	0.058	3 --> 0		211	1	1.000	0 --> 1		192	1	0.250	0 --> 1
	375	1	0.065	0 --> 1		215	1	0.091	1 --> 0		197	1	1.000	1 --> 3
	381	1	0.500	1 --> 0		216	1	0.222	1 --> 0		208	1	0.091	2 ==> 1
	390	1	0.100	2 ==> 1		217	1	0.600	1 --> 2		349	1	0.136	2 ==> 3
	396	1	0.095	1 ==> 2		220	1	0.375	1 --> 2		351	1	0.375	0 ==> 1
	400	1	0.200	0 ==> 1		249	1	0.231	1 --> 0		361	2	0.160	2 ==> 4
	427	1	0.100	1 ==> 0		258	1	0.081	2 --> 3		367	1	0.125	0 ==> 1
	446	1	0.143	1 ==> 0		273	1	0.062	1 --> 0		372	2	0.058	0 ==> 2
	457	1	0.174	1 --> 0		276	2	0.118	2 --> 0		377	1	0.333	3 --> 0
	463	1	0.108	1 ==> 2		296	1	0.333	2 ==> 0		382	1	0.333	1 ==> 0
	475	1	0.300	2 ==> 3		299	1	0.600	0 ==> 1		384	1	0.097	1 ==> 0
node_261 --> node_257	2	1	0.083	1 --> 0		300	1	0.250	0 ==> 1		402	1	0.167	0 ==> 1
	36	1	0.062	0 ==> 1		321	1	0.231	0 ==> 1		421	1	0.075	1 ==> 0
	38	1	0.143	2 ==> 3		328	1	0.054	1 ==> 0		510	1	0.143	0 ==> 1
	55	1	1.000	0 ==> 1		331	1	1.000	0 --> 1		520	1	0.250	0 ==> 1
	99	1	0.250	0 ==> 1		332	1	0.222	0 ==> 1	node_266 --> node_265	14	1	0.200	0 ==> 1
	101	1	0.105	0 ==> 1		344	1	0.048	1 --> 0		68	1	0.077	1 --> 0
	114	1	0.148	4 ==> 3		346	1	1.000	1 --> 2		119	1	0.800	1 ==> 3
	212	1	0.182	0 ==> 1		357	1	0.083	0 --> 1		129	2	0.051	0 ==> 2
	258	1	0.081	1 ==> 2		359	1	1.000	0 --> 1		135	1	0.600	2 ==> 3
	300	1	0.250	0 ==> 1		361	1	0.160	3 ==> 2		197	1	1.000	1 --> 2
	419	1	0.073	2 ==> 3		367	1	0.125	1 --> 0		208	1	0.091	2 ==> 3
	480	1	0.200	1 ==> 0		373	1	0.500	0 --> 1		296	1	0.333	0 ==> 1
	484	1	0.100	1 ==> 0		376	1	0.200	0 --> 1		303	1	1.000	0 ==> 1
	489	1	0.111	0 ==> 1		377	1	0.333	0 --> 3		431	1	0.250	1 --> 0
	491	1	0.143	1 --> 0		382	1	0.333	0 --> 1		516	1	0.143	0 --> 1
	499	1	0.143	1 ==> 0		385	1	0.067	0 --> 2		587	1	0.100	1 ==> 0
	528	1	0.200	1 ==> 0		413	1	0.033	1 --> 0	node_265 --> Liotyphlops albi	207	1	0.200	0 ==> 1
	548	1	0.100	1 --> 0		415	1	0.222	0 --> 1	node_265 --> Typhlophis squam	106	1	0.182	1 ==> 0
node_257 --> Bipes biporus	457	1	0.174	0 --> 1		418	1	0.083	1 --> 0		303	1	1.000	1 ==> 2
	481	1	0.083	0 ==> 1		419	1	0.073	1 --> 0		337	1	0.136	1 ==> 0
	503	1	0.286	1 ==> 2		423	1	0.100	0 --> 1	node_310 --> node_309	7	1	0.069	2 --> 1
	587	1	0.100	1 ==> 0		426	1	0.333	0 --> 1		12	1	0.500	0 ==> 1
node_257 --> Bipes canalicula	543	1	0.500	0 ==> 1		431	1	0.250	0 --> 1		41	1	0.182	0 ==> 1
node_261 --> node_260	126	1	0.667	0 --> 1		440	1	0.200	1 --> 0		45	1	0.333	0 ==> 1
	166	1	0.091	0 --> 1		457	3	0.174	1 --> 4		57	1	0.190	2 ==> 3
	167	2	0.125	0 --> 2		468	3	0.120	0 ==> 3		84	1	0.129	4 --> 3
	369	2	0.100	1 ==> 3		488	1	0.133	1 --> 2		106	1	0.182	1 ==> 2
	370	1	0.333	1 --> 0		589	1	0.500	1 --> 2		119	1	0.800	1 ==> 2
	387	1	0.222	1 ==> 0		599	1	0.500	0 --> 1		206	1	0.091	0 ==> 1
	398	1	0.500	0 ==> 2		602	4	0.267	0 --> 4		207	1	0.200	0 ==> 1
	404	1	0.100	0 ==> 1	node_312 --> Najash rionegrin	421	1	0.075	1 ==> 2		208	1	0.091	2 ==> 1
	456	1	0.190	4 --> 3		548	1	0.100	1 --> 0		218	1	0.333	0 --> 1
	470	1	0.125	2 --> 3	node_312 --> node_311	302	1	0.400	0 ==> 1		219	1	0.250	0 ==> 1
	516	1	0.143	0 --> 1		353	1	0.333	0 ==> 1		224	1	1.000	0 ==> 1
node_260 --> node_258	231	1	0.077	0 ==> 1		356	1	1.000	0 --> 1		242	1	0.667	0 ==> 1
	276	1	0.118	1 ==> 0		550	1	0.200	0 --> 1		315	1	0.071	1 --> 0
	328	1	0.054	1 ==> 0	node_311 --> Dinilysia patago	18	1	0.053	1 ==> 2		323	1	1.000	0 ==> 1
	360	2	0.125	2 ==> 0		38	1	0.143	2 --> 1		351	1	0.375	0 ==> 2
	367	1	0.125	1 ==> 2		39	1	0.080	3 ==> 2		361	1	0.160	2 ==> 1
	391	1	0.500	0 ==> 1		52	1	0.333	0 ==> 1		377	1	0.333	3 --> 1
	393	1	0.250	1 ==> 0		56	1	0.190	1 ==> 2		387	1	0.222	1 ==> 0
	423	1	0.100	0 ==> 1		62	1	0.111	1 --> 0		389	1	0.200	0 ==> 1
	424	1	0.500	0 ==> 1		68	1	0.077	1 --> 0		392	1	0.105	1 ==> 2
	430	1	0.333	0 ==> 1		118	1	0.143	0 ==> 1		393	1	0.250	1 ==> 0
	447	1	0.083	0 ==> 1		255	1	0.077	1 ==> 0		397	1	0.333	0 ==> 1
node_258 --> Trogonophis wieg	166	1	0.091	1 --> 0		267	1	0.038	1 ==> 0		400	1	0.200	0 ==> 1
	185	2	0.067	0 ==> 2		283	1	0.133	2 --> 1		429	1	0.500	0 ==> 1
	208	1	0.091	2 ==> 1		285	1	0.333	2 ==> 1		438	1	0.100	0 --> 1
	297	1	0.100	1 --> 0		287	1	0.083	0 ==> 1	node_309 --> node_308	2	1	0.083	0 ==> 1
	488	1	0.133	1 ==> 2		337	1	0.136	1 ==> 0		7	1	0.069	1 ==> 0
	610	1	0.050	0 ==> 1		387	1	0.222	1 ==> 2		47	1	0.188	2 --> 1
node_258 --> Diplometopon zar	101	1	0.105	0 ==> 1		404	1	0.100	0 ==> 1		101	1	0.105	2 --> 1
	126	1	0.667	1 ==> 2		415	1	0.222	1 ==> 2		188	2	0.080	4 ==> 2
	215	1	0.091	0 --> 1	node_311 --> node_310	40	1	0.500	0 ==> 1		213	1	0.048	0 --> 1
	220	1	0.375	1 ==> 0		47	1	0.188	1 --> 2		396	2	0.095	0 ==> 2
	300	1	0.250	0 ==> 1		53	1	1.000	0 ==> 1		416	1	0.286	0 ==> 2
	355	1	0.059	1 --> 0		72	1	1.000	0 --> 1	node_308 --> Anomochilus leon	93	1	0.111	1 ==> 0
	392	1	0.105	1 ==> 2		101	2	0.105	0 ==> 2		120	3	0.130	3 ==> 0
	419	1	0.073	2 --> 1		106	1	0.182	0 ==> 1		124	1	0.077	0 ==> 1
	434	1	0.111	0 ==> 2		166	1	0.091	0 ==> 1		322	1	0.167	0 ==> 1
	436	1	0.500	0 ==> 1		213	1	0.048	1 --> 0		328	1	0.054	0 ==> 1
	456	1	0.190	3 --> 4		241	1	0.667	2 --> 4		341	1	0.033	0 ==> 1
	463	1	0.108	2 ==> 1		275	1	0.333	2 ==> 0		377	1	0.333	1 --> 3
	480	1	0.200	1 ==> 0		310	1	1.000	0 ==> 1		415	1	0.222	1 ==> 0
node_260 --> node_259	4	1	0.143	1 --> 0		332	1	0.222	1 ==> 2		420	1	0.085	2 ==> 1
	21	1	0.500	0 ==> 1		390	2	0.100	2 ==> 0		431	1	0.250	1 --> 0
	128	1	0.167	2 --> 1		423	1	0.100	1 --> 0	node_308 --> node_307	45	1	0.333	1 --> 2
	179	1	0.143	1 ==> 0		433	1	0.100	0 --> 1		68	1	0.077	1 --> 0
	222	1	0.500	0 ==> 2		461	1	0.300	2 ==> 3		118	1	0.143	0 --> 1
	332	1	0.222	0 ==> 2		476	1	0.333	0 --> 1		166	1	0.091	1 ==> 0
	380	1	0.091	1 --> 0	node_310 --> node_266	6	1	0.100	0 --> 1		188	2	0.080	2 ==> 0
	456	1	0.190	3 --> 2		13	1	0.067	0 --> 1		198	1	0.500	0 ==> 1
	490	1	0.500	0 --> 1		17	1	0.167	0 --> 1		218	1	0.333	1 --> 0
node_259 --> Geocalamus acutu	116	1	0.300	1 ==> 0		31	1	0.333	0 --> 1		234	1	0.600	0 ==> 3
	234	1	0.600	0 ==> 2		39	1	0.080	3 --> 4		242	1	0.667	1 ==> 2
	258	2	0.081	1 ==> 3		60	1	0.111	0 ==> 1		255	1	0.077	1 ==> 0
	355	1	0.059	1 --> 0		93	1	0.111	1 ==> 0		267	1	0.038	1 --> 0
	361	1	0.160	3 ==> 2		120	1	0.130	3 --> 2		276	1	0.118	0 --> 1
	384	1	0.097	1 ==> 0		192	1	0.250	1 --> 0		277	1	0.333	0 --> 1
	419	1	0.073	2 --> 1		197	1	1.000	0 --> 1		279	1	0.125	0 ==> 1
	427	1	0.100	0 ==> 1		198	1	0.500	0 ==> 1		326	1	0.200	0 ==> 1
	440	1	0.200	1 ==> 0		236	1	1.000	0 --> 1		398	1	0.500	0 ==> 1
	445	1	0.300	1 ==> 0		247	1	0.333	0 --> 1		415	1	0.222	1 ==> 2
node_259 --> Amphisbaena fuli	2	1	0.083	1 --> 0		248	1	0.222	0 ==> 1		421	1	0.075	1 ==> 2
	10	1	0.087	2 ==> 1		276	2	0.118	0 --> 2		548	1	0.100	1 --> 0

node_307 --> node_267	56	1	0.190	1 --> 2		326	1	0.200	1 ==> 0		93	1	0.111	1 ==> 0					
	84	2	0.129	3 --> 1		337	1	0.136	0 ==> 1		106	1	0.182	1 ==> 0					
	101	1	0.105	1 ==> 0		344	1	0.048	0 ==> 1		185	2	0.067	3 ==> 1					
	208	2	0.091	1 ==> 3		384	1	0.097	1 ==> 0		203	1	0.500	1 ==> 0					
	355	1	0.059	1 ==> 0		389	1	0.200	1 ==> 2		207	1	0.200	0 --> 1					
	367	1	0.125	0 --> 1		398	1	0.500	1 ==> 0		242	1	0.667	2 ==> 1					
	404	1	0.100	0 ==> 1	node_269 --> Casarea dussumie	33	2	0.154	0 ==> 2		255	1	0.077	0 ==> 1					
	610	1	0.050	0 ==> 1		34	1	0.231	1 --> 2		267	1	0.038	0 ==> 1					
node_267 --> Anilius scytale	45	1	0.333	2 ==> 3		41	1	0.182	1 ==> 0		315	1	0.071	0 ==> 1					
	46	1	0.167	2 ==> 0		46	1	0.167	2 ==> 1		341	1	0.033	0 ==> 1					
	68	1	0.077	0 --> 1		60	1	0.111	0 ==> 1		343	1	0.250	0 ==> 1					
	141	1	0.250	1 ==> 2		168	1	0.065	2 ==> 1		355	1	0.059	0 --> 1					
	168	2	0.065	2 ==> 0		191	1	0.167	0 --> 1		377	1	0.333	1 ==> 3					
	188	1	0.080	0 --> 1		203	1	0.500	1 ==> 2		396	1	0.095	1 ==> 0					
	219	1	0.250	1 ==> 0		213	1	0.048	0 --> 1		472	1	0.500	1 --> 0					
	275	1	0.333	0 ==> 1		238	1	0.133	1 ==> 0		474	1	0.500	1 --> 0					
	276	1	0.118	1 --> 0		256	1	0.333	2 ==> 1		476	1	0.333	1 ==> 0					
	277	1	0.333	1 --> 0		386	1	0.333	0 ==> 1		574	1	0.333	0 ==> 1					
	315	1	0.071	0 --> 1		466	1	0.250	0 ==> 1		610	1	0.050	1 ==> 0					
	322	1	0.167	0 ==> 1	node_305 --> node_304	12	1	0.500	1 --> 2		node_273 --> Lichanura trivir	14	1	0.200	1 --> 0				
	327	1	0.500	0 ==> 1		15	1	0.167	0 --> 1			33	1	0.154	1 ==> 2				
	341	1	0.033	0 ==> 1		47	1	0.188	1 --> 2			34	1	0.231	0 --> 2				
	367	1	0.125	1 --> 2		106	1	0.182	1 --> 0			46	1	0.167	0 --> 2				
	369	1	0.100	0 ==> 1		185	2	0.067	2 ==> 4			84	3	0.129	4 ==> 1				
	374	1	0.250	0 ==> 1		239	1	0.500	0 ==> 1			287	1	0.083	1 ==> 0				
	380	1	0.091	0 ==> 1		287	1	0.083	0 ==> 1			302	1	0.400	1 ==> 0				
	384	1	0.097	1 ==> 0		332	1	0.222	2 --> 1			330	1	0.333	1 --> 0				
	419	2	0.073	0 ==> 2		404	1	0.100	0 ==> 1			332	1	0.222	1 --> 2				
	438	1	0.100	1 --> 0		610	1	0.050	0 --> 1			353	1	0.333	1 ==> 0				
	458	2	0.100	0 ==> 2	node_304 --> node_271	3	2	0.182	0 --> 2			389	1	0.200	1 ==> 2				
node_267 --> Cylindrophis ruf	45	1	0.333	2 --> 1		19	1	0.167	0 ==> 1		node_303 --> node_302	33	1	0.154	1 --> 2				
	132	1	0.176	0 ==> 1		45	1	0.333	2 --> 1			34	1	0.231	1 --> 2				
	170	1	0.231	0 ==> 1		56	1	0.190	1 --> 2			74	1	0.200	0 --> 1				
	189	1	0.190	0 ==> 1		101	1	0.105	1 ==> 0			86	1	0.167	0 ==> 1				
	342	1	0.333	0 ==> 1		115	1	0.600	2 ==> 1			96	1	0.222	1 --> 2				
	343	1	0.250	0 ==> 1		189	1	0.190	1 --> 0			189	1	0.190	1 --> 2				
	389	1	0.200	1 ==> 0		219	1	0.250	1 --> 0			238	1	0.133	1 --> 0				
	433	1	0.100	1 --> 0		265	1	0.500	1 ==> 0			263	1	0.286	1 ==> 2				
node_307 --> node_306	18	1	0.053	1 ==> 2		299	1	0.600	2 --> 1			288	1	0.167	1 --> 2				
	115	1	0.600	1 ==> 2		300	1	0.250	2 --> 1			343	1	0.250	0 ==> 1				
	170	1	0.231	0 ==> 3		302	1	0.400	1 --> 0		node_302 --> node_278	39	1	0.080	3 --> 2				
	174	1	0.333	0 ==> 1		341	1	0.033	0 --> 1			100	1	0.333	0 --> 1				
	185	2	0.067	0 ==> 2		353	1	0.333	1 --> 0			132	3	0.176	0 ==> 3				
	194	1	0.600	2 ==> 3		379	1	0.062	1 --> 0			248	1	0.222	1 --> 2				
	203	1	0.500	0 ==> 1		387	1	0.222	2 ==> 1			302	1	0.400	1 ==> 2				
	208	1	0.091	1 ==> 0		390	2	0.100	0 --> 2			315	1	0.071	0 ==> 1				
	210	1	0.250	0 ==> 1		457	1	0.174	3 ==> 2			325	1	0.091	1 --> 0				
	224	1	1.000	1 ==> 2		463	2	0.108	1 ==> 3			387	1	0.222	2 ==> 0				
	247	1	0.333	0 ==> 1		469	1	1.000	0 ==> 1			458	2	0.100	0 ==> 2				
	248	1	0.222	0 ==> 1		478	1	0.250	0 --> 1		node_278 --> node_276	8	1	0.182	1 ==> 0				
	256	1	0.333	1 ==> 2	node_271 --> Haasiophis terra	174	1	0.333	1 ==> 0			46	1	0.167	2 ==> 1				
	260	1	0.667	0 ==> 1		421	1	0.075	2 ==> 3			74	1	0.200	1 --> 0				
	265	1	0.500	0 ==> 1	node_271 --> node_270	86	1	0.167	0 ==> 1			96	1	0.222	2 --> 1				
	268	1	0.250	1 ==> 2		129	2	0.051	0 --> 2			243	1	0.250	0 ==> 1				
	274	1	1.000	0 ==> 1		171	1	0.250	0 --> 1			253	1	0.333	0 ==> 1				
	288	1	0.167	0 --> 1		263	1	0.286	1 --> 2			288	2	0.167	2 --> 0				
	299	1	0.600	1 ==> 2		279	1	0.125	1 ==> 0			322	1	0.167	0 ==> 1				
	300	1	0.250	1 ==> 2		361	1	0.160	1 --> 2			330	1	0.333	0 ==> 1				
	324	1	0.300	1 ==> 2	node_270 --> Eupodophis desco	478	1	0.250	1 --> 0		node_276 --> Epicrates striat	12	1	0.500	2 ==> 3				
	325	1	0.091	0 --> 1	node_270 --> Pachyrhachis pro	420	1	0.085	3 ==> 2			84	1	0.129	4 ==> 3				
	337	1	0.136	1 ==> 0	node_304 --> node_303	33	1	0.154	0 ==> 1			189	1	0.190	2 --> 1				
	351	1	0.375	2 ==> 0		118	1	0.143	1 --> 0			223	1	0.333	0 ==> 1				
	387	1	0.222	0 ==> 2		184	1	0.286	0 ==> 1			238	1	0.133	0 --> 1				
	420	1	0.085	2 ==> 3		327	1	0.500	0 ==> 1			248	1	0.222	2 --> 1				
	423	1	0.100	0 --> 1		363	1	0.333	0 ==> 1			341	1	0.033	0 ==> 1				
node_306 --> node_268	74	1	0.200	0 --> 1		457	1	0.174	3 --> 4		node_276 --> Boa constrictor	47	1	0.188	2 ==> 3				
	86	1	0.167	0 --> 1		524	1	0.200	1 --> 0			185	2	0.067	4 ==> 2				
	184	1	0.286	0 ==> 1	node_303 --> node_275	45	1	0.333	2 ==> 3			189	1	0.190	2 ==> 3				
	289	1	0.200	0 ==> 1		46	1	0.167	2 --> 0			342	1	0.333	0 ==> 1				
	315	1	0.071	0 --> 1		60	1	0.111	0 ==> 1			357	1	0.083	1 ==> 0				
	419	1	0.073	0 ==> 1		106	1	0.182	0 --> 1		node_278 --> node_277	12	1	0.500	2 ==> 1				
node_268 --> Xenopeltis unico	33	1	0.154	0 ==> 1		210	1	0.250	1 ==> 0			15	1	0.167	1 ==> 0				
	41	1	0.182	1 ==> 0		276	1	0.118	1 ==> 0			33	1	0.154	2 --> 1				
	68	1	0.077	0 --> 1		288	1	0.167	1 --> 0			34	1	0.231	2 --> 1				
	132	2	0.176	0 ==> 2		322	1	0.167	0 ==> 1			47	1	0.188	2 ==> 1				
	287	1	0.083	0 ==> 1	node_275 --> node_272	2	1	0.083	1 ==> 0			141	1	0.250	1 ==> 2				
	355	1	0.059	1 ==> 0		12	1	0.500	2 ==> 3			289	1	0.200	0 ==> 1				
	377	1	0.333	1 ==> 0		41	1	0.182	1 ==> 0			321	1	0.231	1 ==> 3				
	382	1	0.333	1 ==> 0		84	2	0.129	4 ==> 2			329	1	0.250	0 ==> 1				
	384	1	0.097	1 ==> 0		332	1	0.222	1 --> 2			574	1	0.333	0 ==> 1				
	386	1	0.333	0 ==> 1		344	1	0.048	0 ==> 1			610	1	0.050	1 --> 0				
	389	1	0.200	1 ==> 2		389	1	0.200	1 ==> 2		node_277 --> Aspidites melano	39	1	0.080	2 --> 3				
	412	1	0.111	1 --> 0		416	1	0.286	3 ==> 0			100	1	0.333	1 --> 0				
	416	1	0.286	2 ==> 0	node_272 --> Exiliboa placata	7	1	0.069	0 ==> 1			171	1	0.250	0 ==> 1				
	419	3	0.073	1 ==> 4		18	1	0.053	2 ==> 1			287	1	0.083	1 ==> 0				
	420	1	0.085	3 ==> 4		39	1	0.080	3 ==> 2			326	1	0.200	1 ==> 0				
	421	2	0.075	2 ==> 4		84	1	0.129	2 ==> 1			337	1	0.136	0 ==> 1				
	427	1	0.100	1 ==> 0		92	1	0.250	0 ==> 1			341	1	0.033	0 ==> 1				
	438	1	0.100	1 --> 0		185	2	0.067	4 ==> 2			384	1	0.097	1 ==> 0				
	510	1	0.143	0 ==> 1		253	1	0.333	0 ==> 1			420	1	0.085	3 ==> 2				
	516	1	0.143	0 ==> 1		287	1	0.083	1 ==> 0		node_277 --> Python molurus	51	1	0.200	1 ==> 2				
	520	1	0.250	0 ==> 1		363	1	0.333	1 ==> 2			189	1	0.190	2 --> 1				
	548	1	0.100	0 --> 1		421	1	0.075	2 ==> 3			210	1	0.250	1 ==> 0				
node_268 --> Loxocemus bicolo	46	1	0.167	2 ==> 1	node_272 --> Ungaliophis cont	33	1	0.154	1 ==> 0			213	1	0.048	0 ==> 1				
	96	1	0.222	1 ==> 2		46	1	0.167	0 --> 2			419	1	0.073	0 ==> 1				
	185	2	0.067	2 ==> 4		47	1	0.188	2 ==> 1		node_302 --> node_301	12	1	0.500	2 ==> 3				
	288	1	0.167	1 ==> 2		120	2	0.130	3 ==> 1			91	1	0.333	0 ==> 1				
	332	1	0.222	2 ==> 1		132	1	0.176	0 ==> 1			101	1	0.105	1 ==> 2				
	341	1	0.033	0 ==> 1		206	1	0.091	1 ==> 0			121	1	1.000	0 ==> 1				
	343	1	0.250	0 ==> 1		315	1	0.071	0 ==> 1			248	1	0.222	1 --> 0				
	458	2	0.100	0 ==> 2		337	1	0.136	0 ==> 1			287	1	0.083	1 --> 0				
	574	1	0.333	0 ==> 1		384	1	0.097	1 ==> 0			332	1	0.222	1 --> 2				
node_306 --> node_305	34	1	0.231	0 --> 1		420	1	0.085	3 ==> 2			344	1	0.048	0 --> 1				
	57	1	0.190	3 ==> 2	node_275 --> node_274	14	1	0.200	0 --> 1			363	1	0.333	1 ==> 2				
	84	1	0.129	3 --> 4		34	1	0.231	1 --> 0			389	1	0.200	1 ==> 2				
	106	1	0.182	2 ==> 1		207	1	0.200	1 --> 0			398	1	0.500	1 ==> 3				
	179	1	0.143	1 ==> 0		277	1	0.333	1 ==> 0			404	1	0.100	1 ==> 0				
	189	1	0.190	0 --> 1		279	1	0.125	1 ==> 0			421	1	0.075	2 --> 3				
	191	1	0.167	1 --> 0		330	1	0.333	0 --> 1			438	1	0.100	1 --> 0				
	213	1	0.048	1 --> 0		355	1	0.059	1 --> 0			466	1	0.250	0 ==> 1				
	263	1	0.286	0 ==> 1		387	1	0.222	2 ==> 0		node_301 --> node_279	41	1	0.182	1 ==> 0				
	392	1	0.105	2 ==> 1		472	1	0.500	0 --> 1			51	1	0.200	1 ==> 2				
	416	1	0.286	2 ==> 3		473	1	1.000	0 ==> 1			92	1	0.250	0 ==> 1				
	457	1	0.174	4 --> 3		474	1	0.500	0 --> 1			120	2	0.130	3 ==> 1				
node_305 --> node_269	8	1	0.182	1 ==> 0	node_274 --> Eryx colubrinus	47	1	0.188	2 ==> 3			208	3	0.091	0 ==> 3				
	45	1	0.333	2 ==> 3		100	1	0.333	0 ==> 1			210	1	0.250	1 ==> 0				
	91	1	0.333	0 --> 1		238	1	0.133	1 ==> 2			219	1	0.250	1 ==> 0				
	125	1	1.000	0 ==> 1		263	1	0.286	1 ==> 2			223	1	0.333	0 ==> 1				
	325	1	0.091	1 --> 0		302	1	0.400	1 ==> 2			235	1	1.000	0 ==> 1				
	343	1	0.250	0 ==> 1		325	1	0.091	1 --> 0			238	1	0.133	0 --> 1				
	438	1	0.100	1 --> 0		420	1	0.085	3 ==> 2			279	1	0.125	1 ==> 0				
	510	1	0.143	0 ==> 1	node_274 --> node_273	16	1	0.500	0 ==> 1			321	1	0.231	1 ==> 3				
	516	1	0.143	0 ==> 1		92	1	0.250	0 ==> 1			337	1	0.136	0 ==> 1				
	520	1	0.250	0 ==> 1		185	1	0.067	4 ==> 3			415	1	0.222	2 ==> 1				
	548	1	0.100	0 --> 1		189	1	0.190	1 ==> 0		node_279 --> Trachyboa boulen	384	1	0.097	1 ==> 0				
node_269 --> Xenophidion acan	68	1	0.077	0 --> 1		243	1	0.250	0 --> 1			420	1	0.085	3 ==> 2				
	96	1	0.222	1 ==> 2		392	1	0.105	1 --> 2			457	3	0.174	4 ==> 1				
	101	1	0.105	1 ==> 2		396	1	0.095	2 ==> 1		node_279 --> Tropidophis haet	57	1	0.190	2 ==> 1				
	172	1	0.200	0 ==> 1		458	2	0.100	0 ==> 2			168	1	0.065	2 ==> 1				
	208	2	0.091	0 ==> 2	node_273 --> Calabaria reinha	7	2	0.069	0 ==> 2			288	1	0.167	2 --> 1				
	288	1	0.167	1 --> 0		33	1	0.154	1 ==> 0			344	1	0.048	1 --> 0				
	324	1	0.300	2 ==> 1		60	1	0.111	1 ==> 0			458	1	0.100	0 ==> 1				

node_301 --> node_300	19	1	0.167	0 ==> 1		417	1	0.400	0 --> 2		47	1	0.188	3 ==> 2					
	34	1	0.231	2 --> 3		435	1	0.333	0 ==> 1		355	1	0.059	1 ==> 0					
	45	1	0.333	2 ==> 3		439	1	0.118	1 --> 2		439	1	0.118	1 --> 2					
	60	1	0.111	0 ==> 1	node_280 --> Aparallactus wer	2	1	0.083	1 ==> 0		457	1	0.174	3 ==> 4					
	131	1	0.167	0 --> 1		19	1	0.167	1 ==> 0		458	1	0.100	0 ==> 1					
	141	1	0.250	1 ==> 2		39	1	0.080	3 ==> 2	node_283 --> Bothrops asper	60	1	0.111	1 ==> 0					
	171	1	0.250	0 ==> 1		57	1	0.190	2 ==> 3		189	1	0.190	3 ==> 4					
	172	1	0.200	0 --> 1		167	2	0.125	0 ==> 2		438	1	0.100	0 ==> 1					
	203	1	0.500	1 ==> 2		168	1	0.065	1 ==> 0		587	1	0.100	1 ==> 0					
	213	1	0.048	0 --> 1		185	3	0.067	4 ==> 1	node_283 --> Lachesis muta	7	1	0.069	1 ==> 0					
	218	1	0.333	0 ==> 1		188	1	0.080	0 ==> 1		15	1	0.167	1 ==> 0					
	220	1	0.375	2 ==> 3		189	3	0.190	3 ==> 0		34	1	0.231	2 ==> 3					
	260	1	0.667	1 ==> 2		263	2	0.286	2 ==> 0		131	1	0.167	1 ==> 0					
	276	1	0.118	1 ==> 2		296	1	0.333	0 ==> 2		372	3	0.058	3 ==> 0					
	289	1	0.200	0 --> 1		324	1	0.300	2 ==> 1		458	1	0.100	1 ==> 2					
	326	1	0.200	1 ==> 0		329	1	0.250	0 ==> 1		610	1	0.050	1 ==> 0					
	327	1	0.500	1 ==> 0		357	1	0.083	1 ==> 0	node_290 --> node_289	132	2	0.176	0 ==> 2					
	386	1	0.333	0 ==> 1		377	1	0.333	1 ==> 3		238	1	0.133	1 --> 0					
	463	1	0.108	1 --> 2		457	2	0.174	4 ==> 2		279	1	0.125	1 ==> 0					
	510	1	0.143	0 ==> 1		458	1	0.100	1 --> 0		457	1	0.174	3 ==> 4					
	516	1	0.143	0 ==> 1	node_280 --> Atractaspis irre	7	2	0.069	0 ==> 2		458	1	0.100	0 ==> 1					
	520	1	0.250	0 ==> 1		14	1	0.200	0 ==> 1		463	1	0.108	1 --> 2					
	548	1	0.100	0 ==> 1		46	1	0.167	0 ==> 2	node_289 --> Naja naja	2	1	0.083	1 ==> 0					
	606	1	1.000	0 --> 3		51	1	0.200	1 ==> 0		12	1	0.500	4 ==> 3					
	610	1	0.050	1 --> 0		68	1	0.077	0 ==> 1		15	1	0.167	0 ==> 1					
node_300 --> Xenodermus javan	3	1	0.182	0 ==> 1		96	1	0.222	1 --> 2		28	1	0.143	0 ==> 1					
	18	1	0.053	2 ==> 1		119	1	0.800	2 ==> 4		41	1	0.182	1 ==> 2					
	46	1	0.167	2 ==> 0		131	1	0.167	1 ==> 0		93	1	0.111	1 --> 0					
	47	1	0.188	2 ==> 1		189	1	0.190	3 ==> 4		213	1	0.048	1 ==> 0					
	269	1	0.500	0 ==> 1		267	1	0.038	0 ==> 1		248	1	0.222	1 ==> 2					
	287	1	0.083	0 --> 1		288	1	0.167	1 --> 2		337	2	0.136	0 ==> 2					
	324	1	0.300	2 ==> 1		300	1	0.250	2 ==> 1		384	1	0.097	0 ==> 1					
	325	1	0.091	1 --> 0		341	1	0.033	0 ==> 1		587	1	0.100	1 ==> 0					
	341	1	0.033	0 ==> 1		343	1	0.250	1 ==> 0	node_289 --> node_288	44	1	0.333	1 ==> 0					
	396	1	0.095	2 ==> 1		361	1	0.160	1 ==> 0		47	1	0.188	3 ==> 1					
	416	1	0.286	3 ==> 0		396	2	0.095	2 ==> 0		60	1	0.111	1 ==> 0					
	433	1	0.100	1 ==> 0		404	1	0.100	0 ==> 1		86	1	0.167	0 --> 1					
	457	1	0.174	4 ==> 3		420	1	0.085	2 ==> 1		91	1	0.333	1 ==> 0					
node_300 --> node_299	8	1	0.182	1 --> 0		421	3	0.075	3 ==> 0		106	1	0.182	0 ==> 1					
	12	1	0.500	3 --> 4		435	1	0.333	1 ==> 2		132	1	0.176	2 ==> 3					
	15	1	0.167	1 --> 0		458	1	0.100	1 ==> 2		184	1	0.286	2 ==> 1					
	28	1	0.143	1 ==> 0	node_298 --> node_297	34	1	0.231	3 --> 2		189	1	0.190	3 ==> 2					
	84	2	0.129	4 ==> 2		39	1	0.080	3 ==> 2		224	1	1.000	2 ==> 4					
	93	1	0.111	1 --> 0		44	1	0.333	0 ==> 1		277	1	0.333	1 ==> 0					
	134	1	0.333	0 ==> 1		47	1	0.188	2 ==> 3		324	1	0.300	2 ==> 1					
	184	1	0.286	1 --> 2		84	1	0.129	2 --> 3		325	1	0.091	1 ==> 0					
	189	1	0.190	2 ==> 3		93	1	0.111	0 --> 1		341	1	0.033	0 ==> 1					
	207	1	0.200	1 ==> 0		133	1	0.500	1 ==> 2		433	1	0.100	0 ==> 1					
	217	1	0.600	2 ==> 3		238	1	0.133	0 ==> 1		458	1	0.100	1 ==> 2					
	239	1	0.500	1 ==> 0		372	1	0.058	2 ==> 3	node_288 --> Laticauda colubr	34	1	0.231	2 ==> 3					
	421	1	0.075	3 --> 2		433	1	0.100	1 --> 0		46	1	0.167	2 ==> 0					
node_299 --> Acrochordus gran	2	1	0.083	1 ==> 0		457	1	0.174	4 ==> 3		52	1	0.333	0 ==> 1					
	8	1	0.182	0 --> 2	node_297 --> node_290	96	1	0.222	2 ==> 1		131	1	0.167	1 ==> 0					
	14	1	0.200	0 ==> 1		223	1	0.333	2 --> 1		184	1	0.286	1 ==> 0					
	57	1	0.190	2 ==> 1		253	1	0.333	0 ==> 1		204	2	0.125	2 ==> 0					
	84	1	0.129	2 ==> 1		276	1	0.118	2 --> 1		238	2	0.133	0 ==> 2					
	92	1	0.250	0 ==> 1		384	1	0.097	1 ==> 0		276	1	0.118	1 ==> 0					
	131	1	0.167	1 --> 0		398	1	0.500	3 --> 1		287	1	0.083	0 ==> 1					
	213	1	0.048	1 --> 0		417	1	0.400	0 ==> 1		357	1	0.083	1 ==> 0					
	279	1	0.125	1 ==> 0		420	1	0.085	2 --> 1		363	1	0.333	2 ==> 1					
	289	1	0.200	1 --> 0		435	2	0.333	0 ==> 2		377	1	0.333	1 ==> 3					
	320	1	1.000	1 ==> 3	node_290 --> node_287	35	1	0.500	0 --> 1		396	2	0.095	2 ==> 0					
	321	1	0.231	1 ==> 3		39	1	0.080	2 --> 3	node_288 --> Micrurus fulvius	4	1	0.143	0 ==> 1					
	322	1	0.167	0 ==> 1		51	1	0.200	1 --> 2		57	1	0.190	2 ==> 3					
	343	1	0.250	1 ==> 0		57	1	0.190	2 --> 1		68	1	0.077	0 ==> 1					
	351	1	0.375	0 ==> 1		84	1	0.129	3 --> 4		106	1	0.182	1 ==> 2					
	357	1	0.083	1 ==> 0		93	1	0.111	1 --> 0		133	1	0.500	2 ==> 1					
	363	1	0.333	2 ==> 1		119	1	0.800	2 ==> 4		288	1	0.167	2 ==> 1					
	384	1	0.097	1 ==> 0		260	1	0.667	2 ==> 1		321	1	0.231	1 ==> 3					
	404	1	0.100	0 ==> 1		273	1	0.062	0 ==> 1		322	1	0.167	0 ==> 1					
	459	3	0.182	3 ==> 0		276	1	0.118	1 --> 2		329	1	0.250	0 ==> 1					
	463	2	0.108	2 ==> 4		327	1	0.500	0 --> 3		355	1	0.059	1 ==> 0					
	610	1	0.050	0 --> 1		372	1	0.058	3 ==> 2	node_290 --> Notechis scutatu	84	1	0.129	3 --> 2					
node_299 --> node_298	61	1	0.500	0 ==> 2		398	1	0.500	1 --> 3		238	1	0.133	1 ==> 2					
	74	1	0.200	1 ==> 0		405	1	0.250	0 ==> 1		337	2	0.136	0 ==> 2					
	86	1	0.167	1 ==> 0	node_287 --> Causus rhombeatu	41	1	0.182	1 ==> 2		341	1	0.033	0 ==> 1					
	172	1	0.200	1 --> 0		45	1	0.333	3 ==> 2		420	1	0.085	1 --> 2					
	223	2	0.333	0 ==> 2		131	1	0.167	1 ==> 0		421	1	0.075	2 --> 3					
	248	1	0.222	0 --> 1		189	1	0.190	3 ==> 4		438	1	0.100	0 ==> 1					
	372	2	0.058	0 --> 2		208	3	0.091	0 ==> 3		610	1	0.050	0 ==> 1					
	382	1	0.333	1 ==> 2		238	1	0.133	1 ==> 2	node_297 --> node_296	41	1	0.182	1 ==> 2					
	416	1	0.286	3 --> 4		300	1	0.250	2 ==> 1		51	1	0.200	1 ==> 2					
	420	1	0.085	3 ==> 2		361	1	0.160	1 ==> 0		172	1	0.200	0 --> 1					
	463	1	0.108	2 --> 1		421	1	0.075	2 --> 3		203	1	0.500	2 ==> 3					
node_298 --> node_282	18	1	0.053	2 ==> 1		457	1	0.174	3 ==> 2		269	1	0.500	0 ==> 1					
	33	1	0.154	2 --> 1	node_287 --> node_286	7	1	0.069	0 ==> 1		321	1	0.231	1 ==> 3					
	46	1	0.167	2 ==> 0		15	1	0.167	0 ==> 1		326	1	0.200	0 --> 1					
	129	2	0.051	0 --> 2		44	1	0.333	1 ==> 0		329	1	0.250	0 ==> 1					
	168	1	0.065	2 --> 1		61	1	0.500	2 --> 0		439	1	0.118	1 --> 2					
	466	1	0.250	1 ==> 0		243	1	0.250	0 ==> 1		463	1	0.108	1 --> 2					
node_282 --> Pareas hamptoni	57	1	0.190	2 ==> 1		279	1	0.125	1 ==> 0	node_296 --> node_294	27	1	1.000	0 ==> 1					
	120	2	0.130	3 ==> 1		315	1	0.071	0 ==> 1		34	1	0.231	2 --> 3					
	171	1	0.250	1 ==> 0	node_286 --> Azemiops feae	33	1	0.154	2 ==> 1		84	1	0.129	3 --> 2					
	174	1	0.333	1 ==> 0		35	1	0.500	1 --> 0		277	1	0.333	1 ==> 2					
	243	1	0.250	0 ==> 1		47	1	0.188	3 ==> 2		287	1	0.083	0 ==> 1					
	287	1	0.083	0 ==> 1		51	1	0.200	2 --> 1		327	1	0.500	0 ==> 2					
	361	1	0.160	1 ==> 2		57	1	0.190	1 --> 2		417	1	0.400	0 ==> 2					
	372	2	0.058	2 --> 0		74	1	0.200	0 ==> 1		420	1	0.085	2 ==> 3					
	415	1	0.222	2 ==> 1		86	1	0.167	0 ==> 1		421	1	0.075	2 --> 3					
	459	1	0.182	3 ==> 4		96	1	0.222	1 ==> 2	node_294 --> Natrix natrix	56	1	0.190	1 ==> 2					
node_282 --> node_281	47	1	0.188	2 ==> 1		129	1	0.051	0 ==> 1		189	1	0.190	3 ==> 4					
	96	1	0.222	2 --> 1		189	1	0.190	3 ==> 2		587	1	0.100	1 ==> 0					
	106	1	0.182	0 ==> 1		327	1	0.500	3 --> 0	node_294 --> node_293	438	1	0.100	0 ==> 1					
	115	1	0.600	2 ==> 3		355	1	0.059	1 ==> 0		457	1	0.174	3 ==> 2					
	224	1	1.000	2 ==> 3		372	2	0.058	2 ==> 0	node_293 --> node_291	227	1	1.000	0 ==> 1					
	279	1	0.125	1 ==> 0		433	1	0.100	0 ==> 1	node_291 --> Afronatrix anosc	41	1	0.182	2 ==> 1					
	288	1	0.167	2 --> 1	node_286 --> node_285	52	1	0.333	0 ==> 1		47	1	0.188	3 ==> 2					
	315	1	0.071	0 ==> 1		61	1	0.500	0 --> 1		84	1	0.129	2 ==> 3					
	421	1	0.075	2 --> 3		84	2	0.129	4 --> 2		287	1	0.083	1 ==> 0					
	458	1	0.100	0 --> 1		133	1	0.500	2 --> 1		357	1	0.083	1 ==> 0					
node_281 --> Lycophidion cape	33	1	0.154	1 --> 2		248	1	0.222	1 --> 2		463	1	0.108	2 ==> 1					
	60	1	0.111	1 ==> 0		326	2	0.200	0 ==> 2	node_291 --> Amphiesma stolat	7	1	0.069	0 ==> 1					
	93	1	0.111	0 --> 1		343	1	0.250	1 ==> 2		93	1	0.111	1 ==> 0					
	168	1	0.065	1 --> 2		357	1	0.083	1 ==> 0		172	1	0.200	1 ==> 0					
	203	1	0.500	2 ==> 1		610	1	0.050	0 ==> 1		184	1	0.286	2 ==> 1					
	206	1	0.091	1 ==> 0	node_285 --> Daboia russelli	34	1	0.231	2 ==> 3		315	1	0.071	0 ==> 1					
	213	1	0.048	1 ==> 0		41	1	0.182	1 ==> 2		435	1	0.333	0 ==> 1					
	363	1	0.333	2 ==> 0		132	3	0.176	0 ==> 3	node_293 --> node_292	337	1	0.136	0 ==> 1					
	372	1	0.058	2 ==> 3		189	1	0.190	3 ==> 4		341	1	0.033	0 ==> 1					
	416	1	0.286	4 --> 3		223	1	0.333	1 ==> 2	node_292 --> Thamnophis marci	60	1	0.111	1 ==> 0					
	420	1	0.085	2 ==> 3		238	1	0.133	1 ==> 2		184	1	0.286	2 ==> 1					
	433	1	0.100	1 ==> 0		341	1	0.033	0 ==> 1		189	1	0.190	3 ==> 4					
node_281 --> node_280	33	1	0.154	1 ==> 0		438	1	0.100	0 ==> 1		610	1	0.050	0 ==> 1					
	34	1	0.231	3 ==> 0	node_285 --> node_284	46	1	0.167	2 --> 0	node_292 --> Xenochrophis pis	84	2	0.129	2 ==> 0					
	61	1	0.500	2 --> 0		84	2	0.129	2 ==> 0		213	1	0.048	1 ==> 0					
	84	2	0.129	2 --> 0		238	1	0.133	1 ==> 0		433	1	0.100	0 ==> 1					
	129	2	0.051	2 --> 0		372	1	0.058	2 --> 3	node_296 --> node_295	57	1	0.190	2 ==> 4					
	191	1	0.167	0 ==> 1		463	1	0.108	1 ==> 2		315	1	0.071	0 ==> 1					
	238	1	0.133	0 ==> 1	node_284 --> Agkistrodon cont	2	1	0.083	1 ==> 0		433	1	0.100	0 --> 1					
	321	1	0.231	1 --> 3		288	1	0.167	2 ==> 1		466	1	0.250	1 ==> 0					
	325	1	0.091	1 --> 0		457	1	0.174	3 ==> 2	node_295 --> Lampropeltis get	438	1	0.100	0 ==> 1					
	337	1	0.136	0 ==> 1	node_284 --> node_283	41	1	0.182	1 ==> 0		457	1	0.174	3 ==> 4					

	458	2	0.100	0 ==> 2		19	1	0.167	0 ==> 1		10	1	0.087	1 ==> 2					
node_295 --> Coluber constric	56	1	0.190	1 ==> 2		90	2	0.105	2 ==> 0		48	1	0.103	4 ==> 3					
	132	1	0.176	0 ==> 1		129	1	0.051	2 --> 1		56	1	0.190	2 ==> 1					
	238	1	0.133	1 ==> 0		140	1	1.000	0 ==> 1		145	1	0.400	2 ==> 0					
	248	1	0.222	1 ==> 0		143	1	0.200	1 ==> 2		168	1	0.065	0 ==> 1					
	326	1	0.200	1 --> 0		148	1	0.091	0 --> 1		185	1	0.067	3 ==> 4					
	349	1	0.136	2 ==> 3		185	1	0.067	1 ==> 2		208	3	0.091	0 ==> 3					
node_309 --> Uropeltis melano	9	1	0.250	1 ==> 0		291	1	0.053	1 --> 0		326	1	0.200	0 ==> 1					
	25	1	0.118	0 ==> 1		313	1	0.500	0 ==> 1		419	1	0.073	3 ==> 2					
	96	1	0.222	1 ==> 2		339	1	1.000	0 ==> 1		445	1	0.300	1 ==> 0					
	134	1	0.333	0 ==> 1		348	1	0.111	0 ==> 1		513	1	0.083	0 --> 1					
	208	1	0.091	1 ==> 0		453	1	0.250	0 ==> 1		572	1	0.058	1 ==> 0					
	222	1	0.500	1 ==> 0		463	1	0.108	2 --> 3	node_328 --> node_327	49	2	0.089	0 ==> 2					
	249	1	0.231	0 ==> 3		475	1	0.300	2 ==> 3		66	1	0.286	1 ==> 2					
	275	1	0.333	0 ==> 1		476	1	0.333	0 ==> 1		161	1	0.125	0 ==> 1					
	296	1	0.333	0 ==> 2		477	1	1.000	1 ==> 2		170	1	0.231	0 ==> 1					
	337	1	0.136	1 ==> 2		573	1	0.083	0 ==> 1		188	1	0.080	2 ==> 3					
	367	1	0.125	0 ==> 1		590	1	0.308	3 ==> 4		258	1	0.081	3 --> 2					
	404	1	0.100	0 ==> 1		599	1	0.500	0 ==> 1		328	1	0.054	1 --> 0					
	423	1	0.100	0 --> 1		602	1	0.267	0 ==> 1		338	1	0.143	0 --> 1					
	457	1	0.174	4 --> 3		608	1	0.333	0 ==> 1		366	1	0.500	0 ==> 1					
node_324 --> node_323	29	1	0.083	0 ==> 1	node_320 --> Lanthanotus born	56	1	0.190	2 ==> 1		368	1	0.182	1 --> 2					
	39	2	0.080	4 --> 2		68	1	0.077	0 ==> 1		378	1	0.091	0 ==> 1					
	77	1	0.083	1 --> 0		94	1	0.062	0 --> 1		396	2	0.095	0 --> 2					
	94	1	0.062	1 --> 0		96	1	0.222	0 ==> 3		405	1	0.250	0 ==> 1					
	124	1	0.077	0 ==> 1		128	2	0.167	1 ==> 3		406	1	0.143	0 ==> 1					
	156	1	0.333	0 --> 1		150	1	0.200	0 ==> 1		410	1	0.091	0 ==> 1					
	167	1	0.125	0 --> 1		204	1	0.125	1 ==> 2		453	1	0.250	0 ==> 1					
	204	1	0.125	0 ==> 1		206	1	0.091	0 ==> 1		471	1	0.250	0 --> 1					
	214	1	0.200	0 ==> 1		208	1	0.091	2 ==> 3		482	1	0.333	0 --> 1					
	215	1	0.091	1 --> 0		214	1	0.200	1 ==> 0		511	1	0.143	0 --> 1					
	325	1	0.091	0 ==> 1		256	1	0.333	0 ==> 1		515	1	0.250	0 --> 1					
	328	1	0.054	1 --> 2		268	1	0.250	0 ==> 1		576	1	1.000	0 ==> 1					
	357	1	0.083	0 ==> 1		326	1	0.200	0 ==> 1		580	1	0.333	0 ==> 1					
	373	1	0.500	0 ==> 1		375	1	0.065	1 ==> 0		582	1	0.250	0 ==> 1					
	376	1	0.200	0 ==> 1		392	1	0.105	0 ==> 1	node_327 --> Pseudopus apodus	5	1	0.167	0 ==> 1					
	385	1	0.067	0 ==> 2		419	1	0.073	3 ==> 2		7	1	0.069	1 ==> 0					
	395	1	0.500	0 ==> 1		509	1	0.158	2 --> 1		23	1	0.158	0 ==> 1					
	401	1	0.077	1 ==> 0		519	1	0.077	0 ==> 1		39	3	0.080	4 ==> 1					
	425	1	1.000	0 ==> 1		521	1	0.067	0 --> 1		49	2	0.089	2 ==> 4					
	426	1	0.333	0 ==> 1		542	1	0.273	0 ==> 2		67	1	0.300	0 ==> 1					
	431	1	0.250	0 ==> 1		546	1	0.100	1 ==> 0		69	1	0.333	0 ==> 1					
	460	1	0.600	0 --> 1		566	1	0.444	0 ==> 2		76	1	0.333	0 ==> 1					
	464	1	1.000	0 --> 1		572	1	0.058	1 ==> 0		114	1	0.148	3 ==> 4					
	512	1	0.091	1 --> 0		584	1	0.188	2 ==> 3		149	1	0.087	2 ==> 1					
	513	1	0.083	1 --> 0	node_320 --> node_319	39	1	0.080	3 --> 2		155	1	0.133	1 ==> 2					
	570	1	0.500	1 --> 0		62	1	0.111	0 ==> 2		188	1	0.080	3 ==> 4					
	594	1	0.333	0 --> 1		104	1	0.077	1 ==> 0		204	1	0.125	0 ==> 1					
node_323 --> Gobiderma pulchr	99	1	0.250	0 ==> 1		160	1	0.143	0 --> 1		213	1	0.048	1 ==> 0					
	104	1	0.077	1 --> 0		185	1	0.067	2 --> 3		214	1	0.200	0 ==> 1					
	168	2	0.065	0 ==> 2		208	2	0.091	2 --> 0		215	1	0.091	1 ==> 0					
	341	1	0.033	0 ==> 1		216	1	0.222	0 --> 1		230	1	0.333	1 ==> 0					
node_323 --> node_322	18	2	0.053	0 ==> 2		250	2	0.273	3 ==> 1		283	1	0.133	1 ==> 2					
	20	1	0.167	0 ==> 1		294	1	0.091	1 --> 0		349	1	0.136	0 ==> 1					
	24	1	0.071	0 --> 1		315	1	0.071	1 --> 0		360	1	0.125	1 ==> 0					
	118	1	0.143	0 ==> 1		316	1	0.200	0 --> 1		365	1	0.333	0 ==> 1					
	129	1	0.051	1 --> 2		328	2	0.054	2 --> 0		367	1	0.125	0 ==> 1					
	280	1	0.500	0 ==> 1		439	1	0.118	1 --> 2		379	1	0.062	0 ==> 1					
	416	1	0.286	0 ==> 2		442	1	0.143	1 --> 0		396	2	0.095	2 --> 0					
	418	1	0.083	1 ==> 2		444	1	0.500	0 --> 1		419	1	0.073	3 ==> 2					
	465	1	0.250	0 --> 1		449	1	0.200	0 --> 1		456	1	0.190	1 ==> 2					
	521	1	0.067	1 --> 0		452	1	0.235	0 --> 4		459	3	0.182	0 ==> 3					
	572	1	0.058	2 --> 1		456	1	0.190	1 ==> 0		462	1	0.071	0 ==> 1					
node_322 --> Estesia mongolie	62	1	0.111	0 ==> 2		496	1	0.083	0 --> 1		463	1	0.108	2 ==> 3					
	94	1	0.062	0 --> 1		503	1	0.286	1 --> 0		483	1	0.120	2 ==> 3					
	150	1	0.200	0 ==> 1		507	1	0.167	1 --> 0		488	1	0.133	0 ==> 1					
	311	1	0.286	0 ==> 1		517	1	0.200	0 --> 1		494	1	0.133	1 ==> 0					
	337	1	0.136	1 --> 0		518	1	0.100	0 --> 1		495	1	0.125	1 ==> 0					
	575	1	0.167	1 ==> 0		575	1	0.167	1 ==> 0		498	1	0.083	1 ==> 0					
	577	1	0.167	1 ==> 0		577	1	0.167	1 ==> 0		502	1	0.091	1 ==> 0					
	578	1	0.167	1 --> 0		578	1	0.167	1 --> 0		504	1	0.125	1 ==> 0					
node_322 --> node_321	2	1	0.083	0 --> 1		579	1	0.182	1 ==> 0		507	1	0.167	1 ==> 0					
	39	1	0.080	2 --> 3		584	1	0.188	2 --> 1		509	1	0.158	1 ==> 3					
	143	1	0.200	0 ==> 1		589	1	0.500	1 --> 2		528	1	0.200	0 ==> 1					
	160	1	0.143	1 --> 0		602	3	0.267	1 --> 4	node_327 --> node_325	7	1	0.069	1 ==> 2					
	167	1	0.125	1 --> 0	node_319 --> Saniwa	5	1	0.167	0 ==> 1		62	1	0.111	0 ==> 2					
	216	1	0.222	1 --> 0		7	1	0.069	2 --> 1		108	1	0.125	0 ==> 1					
	250	1	0.273	2 --> 3		117	1	0.333	1 ==> 0		154	1	0.077	1 ==> 0					
	252	1	0.200	0 ==> 1		213	1	0.048	1 ==> 0		258	1	0.081	2 --> 3					
	281	1	0.167	0 ==> 1		416	1	0.286	2 ==> 0		291	1	0.053	0 --> 1					
	307	1	0.125	0 ==> 1		418	1	0.083	2 ==> 1		294	1	0.091	0 --> 1					
	362	1	0.333	0 --> 1		420	1	0.085	2 ==> 3		328	2	0.054	0 --> 2					
node_321 --> Aiolosaurus orie	5	1	0.167	0 ==> 1		463	1	0.108	3 --> 2		368	2	0.182	2 --> 0					
	167	1	0.125	0 --> 1		484	1	0.100	1 ==> 0		383	1	0.080	1 --> 0					
	179	1	0.143	1 ==> 0	node_319 --> node_318	10	1	0.087	0 ==> 1		388	1	0.105	0 ==> 1					
	362	1	0.333	1 --> 0		11	1	0.105	0 ==> 1		420	1	0.085	2 --> 3					
	375	1	0.065	1 ==> 0		18	1	0.053	1 --> 2		421	1	0.075	2 --> 3					
	389	1	0.200	0 ==> 1		38	1	0.143	1 ==> 2		463	1	0.108	2 --> 1					
	396	1	0.095	0 ==> 1		129	1	0.051	1 --> 0		468	1	0.120	0 --> 1					
	419	1	0.073	3 ==> 2		140	1	1.000	1 ==> 2		570	1	0.500	1 ==> 2					
node_321 --> node_316	2	1	0.083	1 --> 0		148	1	0.091	1 --> 0		571	1	1.000	0 ==> 1					
	7	1	0.069	1 ==> 0		152	1	0.400	0 ==> 1	node_325 --> Peltosaurus gran	11	1	0.105	0 ==> 2					
	13	1	0.067	0 ==> 1		204	1	0.125	1 --> 0		18	1	0.053	0 ==> 1					
	24	1	0.071	1 ==> 0		222	1	0.500	1 ==> 3		36	1	0.062	0 ==> 1					
	29	1	0.083	1 ==> 0		255	1	0.077	0 ==> 1		49	1	0.089	2 --> 1					
	38	1	0.143	1 ==> 2		267	1	0.038	0 ==> 1		217	1	0.600	1 ==> 0					
	39	1	0.080	3 ==> 4		460	1	0.600	1 ==> 2	node_325 --> Helodermoides tu	13	1	0.067	0 ==> 1					
	58	1	0.222	2 ==> 1		561	1	0.154	1 --> 0		24	1	0.071	0 ==> 1					
	68	1	0.077	0 ==> 1	node_318 --> node_317	25	1	0.118	0 ==> 1		49	2	0.089	2 ==> 4					
	118	1	0.143	1 ==> 0		307	1	0.125	1 ==> 0		108	1	0.125	1 ==> 2					
	168	2	0.065	0 ==> 2		462	1	0.071	0 ==> 1		129	1	0.051	0 ==> 1					
	169	1	0.333	0 ==> 1		463	1	0.108	3 ==> 4		148	1	0.091	0 ==> 1					
	240	1	0.125	0 ==> 1		494	1	0.133	1 ==> 0		150	1	0.200	0 ==> 1					
	241	1	0.667	2 ==> 3		514	1	0.083	0 ==> 1		161	1	0.125	1 ==> 0					
	255	1	0.077	0 ==> 1		578	1	0.167	0 --> 1		168	1	0.065	0 ==> 1					
	267	1	0.038	0 ==> 1	node_317 --> Varanus salvator	5	1	0.167	0 ==> 1		170	1	0.231	1 ==> 0					
	383	1	0.080	1 --> 0		7	1	0.069	2 --> 1		175	1	0.333	0 ==> 1					
	413	1	0.033	1 ==> 0		49	1	0.089	0 ==> 1		378	1	0.091	1 ==> 0					
	421	1	0.075	2 ==> 1		94	1	0.062	0 ==> 2		385	1	0.067	0 ==> 2					
	428	1	0.200	1 --> 0		129	1	0.051	0 --> 1	node_327 --> node_326	228	1	0.500	0 ==> 1					
	435	1	0.333	0 ==> 1		502	1	0.091	1 ==> 0		232	1	0.143	1 ==> 0					
	450	1	0.143	1 --> 0		575	1	0.167	0 ==> 1		249	1	0.231	0 ==> 1					
	462	1	0.071	0 ==> 1		577	1	0.167	0 ==> 1		255	1	0.077	0 --> 1					
	483	1	0.120	2 --> 1		579	1	0.182	0 ==> 1		258	1	0.081	2 ==> 1					
	488	1	0.133	0 ==> 1		580	1	0.333	0 ==> 1		338	1	0.143	1 --> 0					
	495	1	0.125	1 ==> 0		587	1	0.100	1 ==> 0		375	1	0.065	2 ==> 3					
	506	1	0.250	0 ==> 1	node_317 --> Varanus exanthem	90	1	0.105	0 ==> 1		383	1	0.080	1 ==> 2					
	535	1	0.143	2 --> 1		117	1	0.333	1 ==> 0		434	1	0.111	0 ==> 1					
	572	1	0.058	1 --> 2		148	1	0.091	0 --> 1		470	1	0.125	3 --> 0					
	609	1	0.167	0 ==> 1		185	1	0.067	3 --> 2		483	1	0.120	2 --> 1					
node_316 --> Heloderma horrid	316	1	0.200	0 --> 1		204	1	0.125	0 --> 1		484	1	0.100	1 --> 0					
	513	1	0.083	0 --> 1		315	1	0.071	0 --> 1	node_326 --> Celestus enneagr	5	1	0.167	0 ==> 1					
	532	1	0.500	0 ==> 1		337	1	0.136	1 ==> 0		8	1	0.182	0 ==> 1					
	535	1	0.143	1 ==> 0		375	1	0.065	1 ==> 2		11	1	0.105	0 ==> 2					
	561	1	0.154	1 --> 0		416	1	0.286	2 ==> 0		13	1	0.067	0 ==> 1					
	584	1	0.188	2 --> 1		422	1	0.182	1 ==> 0		37	1	0.059	0 ==> 1					
node_316 --> Heloderma suspec	155	1	0.133	2 ==> 1		427	1	0.100	1 ==> 0		66	2	0.286	2 ==> 0					
	188	1	0.080	2 ==> 3		453	1	0.250	1 ==> 0		94	1	0.062	1 ==> 0					
	465	1	0.250	1 --> 0		484	1	0.100	1 ==> 0		95	1	0.083	0 ==> 1					
node_321 --> node_320	7	1	0.069	1 --> 2		561	1	0.154	0 --> 1		108	1	0.125	0 ==> 1					
	17	1	0.167	0 ==> 1		566	1	0.444	0 ==> 4		167	1	0.125	0 ==> 1					
	18	1	0.053	2 --> 1	node_318 --> Varanus acanthur	3	1	0.182	0 ==> 1		367	1	0.125	0 ==> 1					

	452	1	0.235	0 ==> 1		501	1	0.100	0 ==> 1		76	1	0.333	0 ==> 1
	470	1	0.125	0 --> 1		511	1	0.143	0 ==> 1		90	1	0.105	1 --> 2
	471	1	0.250	1 --> 0		515	1	0.250	0 ==> 1		161	1	0.125	0 ==> 1
	481	1	0.083	0 ==> 1		591	1	0.250	0 ==> 1		252	1	0.200	0 ==> 1
	492	1	0.111	0 ==> 1		592	1	0.667	0 ==> 2		283	1	0.133	1 ==> 2
	542	1	0.273	0 ==> 2		593	1	0.231	1 --> 2		291	1	0.053	1 ==> 0
	566	1	0.444	0 ==> 2		595	1	0.333	0 ==> 1		328	1	0.054	0 ==> 1
	587	1	0.100	1 ==> 0		596	1	0.333	0 --> 1		388	1	0.105	1 ==> 0
	607	1	0.250	1 ==> 0	node_364 --> node_338	13	1	0.067	0 --> 1		439	1	0.118	1 ==> 2
	610	1	0.050	0 ==> 1		24	1	0.071	0 --> 1		593	1	0.231	2 ==> 3
node_326 --> Elgaria multicar	36	1	0.062	0 ==> 1		58	1	0.222	1 --> 0	node_333 --> Pholidobolus mon	24	1	0.071	1 --> 0
	49	1	0.089	2 --> 1		66	1	0.286	0 ==> 1		29	1	0.083	1 --> 0
	77	1	0.083	1 ==> 0		89	1	0.500	0 ==> 1		38	3	0.143	0 ==> 3
	128	2	0.167	1 ==> 3		128	1	0.167	1 --> 2		39	1	0.080	2 ==> 3
	231	1	0.077	0 ==> 1		144	1	0.091	1 ==> 0		67	1	0.300	0 ==> 1
	365	1	0.333	0 ==> 1		145	1	0.400	2 ==> 1		82	1	0.118	1 ==> 2
	385	1	0.067	0 ==> 2		222	1	0.500	0 ==> 2		123	1	0.125	0 ==> 1
	399	1	0.062	0 ==> 1		258	2	0.081	3 --> 1		129	1	0.051	0 ==> 1
	420	1	0.085	2 --> 3		328	1	0.054	1 --> 0		149	1	0.087	1 ==> 0
	421	1	0.075	2 --> 3		369	1	0.100	0 --> 1		204	1	0.125	0 ==> 1
	428	1	0.200	1 ==> 0		379	1	0.062	0 --> 1		267	1	0.038	0 ==> 1
	456	1	0.190	1 ==> 0		394	1	0.087	1 ==> 2		335	1	0.333	1 --> 0
	461	1	0.300	2 ==> 0		475	1	0.300	1 --> 0		372	3	0.058	0 ==> 3
	519	1	0.077	0 ==> 1		481	1	0.083	0 ==> 1		375	2	0.065	2 ==> 0
	521	1	0.067	1 ==> 0		521	1	0.067	1 --> 0		379	1	0.062	1 --> 0
node_331 --> node_330	7	1	0.069	1 ==> 2		579	1	0.182	1 --> 0		416	1	0.286	0 ==> 1
	24	1	0.071	0 --> 1		590	1	0.308	2 ==> 3		420	1	0.085	3 ==> 2
	36	1	0.062	0 ==> 1		602	2	0.267	0 ==> 2		421	1	0.075	3 ==> 2
	42	1	0.500	0 ==> 1	node_338 --> node_332	18	1	0.053	1 ==> 2		455	1	0.148	2 ==> 1
	62	1	0.111	0 --> 2		49	1	0.089	0 ==> 1		572	2	0.058	2 ==> 0
	101	1	0.105	0 ==> 1		67	3	0.300	0 ==> 3	node_337 --> node_336	7	1	0.069	1 ==> 0
	153	1	0.100	0 ==> 1		77	1	0.083	0 ==> 1		23	1	0.158	2 ==> 0
	213	1	0.048	1 --> 0		82	1	0.118	1 ==> 0		37	1	0.059	1 --> 0
	268	1	0.250	0 --> 1		101	1	0.105	0 ==> 1		39	1	0.080	1 ==> 0
	375	1	0.065	2 ==> 3		123	1	0.125	0 ==> 1		56	1	0.190	1 ==> 2
	442	1	0.143	1 --> 0		170	1	0.231	0 ==> 1		58	1	0.222	0 --> 1
	494	1	0.133	1 ==> 0		206	1	0.091	0 ==> 1		78	1	0.571	1 ==> 2
	498	1	0.083	1 ==> 0		283	1	0.133	1 ==> 0		87	1	0.200	0 --> 1
	508	1	0.143	1 ==> 0		399	1	0.062	1 --> 0		90	1	0.105	1 ==> 0
	512	1	0.091	1 --> 0		401	1	0.077	1 --> 0		109	1	0.750	0 --> 1
	541	1	0.100	0 --> 1		452	1	0.235	0 ==> 3		114	1	0.148	3 --> 4
	565	1	0.125	0 --> 1		575	1	0.167	0 ==> 1		155	1	0.133	1 ==> 2
	570	1	0.500	1 --> 0		577	1	0.167	0 ==> 1		233	1	1.000	0 ==> 1
	572	1	0.058	2 ==> 3	node_332 --> Lacerta viridis	7	1	0.069	1 ==> 0		258	1	0.081	1 ==> 0
	610	1	0.050	0 ==> 1		23	1	0.158	2 ==> 1		261	1	0.200	0 ==> 1
node_330 --> Shinisaurus croc	20	1	0.167	0 ==> 1		39	3	0.080	1 ==> 4		271	1	0.167	0 --> 1
	25	1	0.118	0 ==> 1		56	1	0.190	1 ==> 2		273	1	0.062	0 ==> 1
	39	1	0.080	2 --> 1		114	1	0.148	3 ==> 4		281	1	0.167	0 ==> 1
	90	2	0.105	2 ==> 0		128	1	0.167	2 --> 1		294	1	0.091	0 ==> 1
	94	1	0.062	0 ==> 2		244	1	0.333	0 ==> 1		317	1	0.250	1 ==> 0
	116	1	0.300	1 ==> 0		273	1	0.062	0 ==> 1		360	1	0.125	2 ==> 1
	129	1	0.051	0 ==> 1		375	1	0.065	2 ==> 3		368	1	0.182	0 --> 1
	130	1	0.500	0 ==> 1		385	1	0.067	1 --> 0		369	1	0.100	1 --> 0
	144	1	0.091	1 ==> 0		439	1	0.118	1 ==> 0		375	1	0.065	2 --> 3
	148	1	0.091	0 ==> 1		455	2	0.148	2 ==> 4		385	1	0.067	1 --> 0
	160	1	0.143	1 --> 0		489	1	0.111	0 ==> 1		412	1	0.111	0 ==> 1
	208	1	0.091	2 ==> 1		513	1	0.083	1 ==> 0		462	1	0.071	0 ==> 1
	258	1	0.081	3 --> 2		562	1	0.111	1 ==> 0		502	1	0.091	1 --> 0
	307	1	0.125	0 ==> 1		572	1	0.058	2 ==> 3		508	1	0.143	1 ==> 0
	328	1	0.054	1 ==> 2	node_332 --> Takydromus ocell	13	1	0.067	1 --> 0		512	1	0.091	1 ==> 0
	344	1	0.048	0 ==> 1		57	1	0.190	1 ==> 4		514	1	0.083	0 ==> 1
	348	1	0.111	0 ==> 1		62	1	0.111	0 ==> 2		519	1	0.077	0 --> 1
	349	1	0.136	0 ==> 1		138	1	0.500	0 ==> 3		526	1	0.143	0 --> 1
	357	1	0.083	0 ==> 1		185	1	0.067	1 ==> 2		554	1	0.167	0 ==> 1
	367	1	0.125	0 ==> 1		188	1	0.080	2 ==> 3		593	2	0.231	2 ==> 0
	371	1	0.250	1 --> 0		213	1	0.048	1 --> 0	node_336 --> node_334	13	1	0.067	1 --> 0
	383	1	0.080	1 --> 0		258	1	0.081	1 --> 2		71	1	0.429	0 --> 1
	412	1	0.111	0 ==> 1		413	1	0.033	1 ==> 0		93	1	0.111	0 ==> 1
	427	1	0.100	0 ==> 1		419	1	0.073	3 ==> 4		94	1	0.062	0 ==> 2
	455	2	0.148	4 ==> 2		443	1	0.167	0 ==> 1		193	1	0.100	0 ==> 1
	463	1	0.108	2 ==> 3		445	1	0.300	1 ==> 2		344	1	0.048	0 ==> 1
	470	1	0.125	3 --> 0		470	1	0.125	0 ==> 2		379	1	0.062	1 --> 0
	471	1	0.250	0 ==> 1		572	1	0.058	2 ==> 1		383	1	0.080	2 --> 1
	496	1	0.083	0 ==> 1		593	1	0.231	2 ==> 3		416	1	0.286	0 ==> 1
	502	1	0.091	1 ==> 0	node_338 --> node_337	29	1	0.083	0 --> 1		455	1	0.148	2 ==> 1
	521	1	0.067	1 ==> 0		36	1	0.062	0 ==> 1		500	1	0.133	2 --> 0
	530	1	0.200	0 ==> 1		90	1	0.105	2 --> 1		535	1	0.143	1 ==> 2
	535	1	0.143	1 ==> 2		104	1	0.077	0 ==> 1	node_334 --> Callopistes macu	18	1	0.053	1 ==> 0
	561	1	0.154	0 ==> 1		128	1	0.167	2 ==> 3		109	1	0.750	1 --> 0
node_330 --> node_329	6	1	0.100	0 ==> 1		178	1	0.286	0 --> 1		114	1	0.148	4 --> 3
	10	2	0.087	0 ==> 2		188	1	0.080	2 --> 1		185	1	0.067	1 ==> 2
	11	1	0.105	0 ==> 2		208	2	0.091	2 ==> 0		271	1	0.167	1 --> 0
	48	1	0.103	3 ==> 2		231	1	0.077	0 ==> 1		340	1	0.095	0 ==> 1
	76	1	0.333	0 ==> 1		245	1	0.167	1 ==> 0		394	1	0.087	2 ==> 1
	82	1	0.118	1 ==> 2		268	1	0.250	0 --> 1		418	1	0.083	0 ==> 1
	99	1	0.250	0 ==> 1		314	1	1.000	0 ==> 1		420	1	0.085	3 ==> 2
	154	1	0.077	1 ==> 0		335	1	0.333	0 --> 1		485	1	0.250	0 ==> 1
	162	1	0.333	1 ==> 0		383	1	0.080	1 --> 2		501	1	0.100	1 ==> 0
	163	1	0.500	0 ==> 1		403	1	0.200	0 ==> 1		504	1	0.125	1 ==> 0
	164	1	0.333	0 ==> 1		441	1	1.000	0 ==> 1		509	1	0.158	1 ==> 0
	165	1	0.200	1 ==> 0		449	1	0.200	0 ==> 1		519	1	0.077	1 --> 0
	185	1	0.067	1 ==> 2		450	1	0.143	0 ==> 1		572	2	0.058	2 ==> 0
	228	1	0.500	0 ==> 1		451	1	0.333	0 ==> 1	node_334 --> Tupinambis tegui	23	1	0.158	0 ==> 1
	267	1	0.038	0 ==> 1		468	2	0.120	1 ==> 3		37	1	0.059	0 --> 1
	328	1	0.054	1 --> 0		471	1	0.250	0 ==> 2		57	1	0.190	1 ==> 4
	337	1	0.136	1 --> 0		494	1	0.133	1 ==> 0		71	1	0.429	1 --> 2
	368	1	0.182	1 --> 0		496	1	0.083	0 ==> 1		188	1	0.080	1 ==> 0
	378	1	0.091	0 ==> 1		498	1	0.083	1 --> 0		231	1	0.077	1 ==> 0
	379	1	0.062	0 ==> 1		530	1	0.200	0 ==> 1		267	1	0.038	0 ==> 1
	385	1	0.067	0 ==> 1		531	1	0.125	0 ==> 1		291	1	0.053	1 ==> 0
	396	1	0.095	0 ==> 1		573	1	0.083	1 --> 0		348	1	0.111	0 ==> 1
	406	1	0.143	0 ==> 1		590	1	0.308	3 ==> 4		349	1	0.136	0 ==> 1
	420	1	0.085	2 --> 3		594	1	0.333	0 ==> 1		357	1	0.083	0 ==> 1
	421	1	0.075	2 --> 3		608	1	0.333	0 ==> 1		368	1	0.182	1 --> 0
	428	1	0.200	1 --> 0		609	1	0.167	0 ==> 1		369	1	0.100	0 --> 1
	434	1	0.111	0 --> 1	node_337 --> node_333	4	1	0.143	0 ==> 1		419	1	0.073	3 ==> 4
	439	1	0.118	1 ==> 0		5	1	0.167	0 ==> 1		421	1	0.075	3 ==> 2
	535	1	0.143	1 --> 0		10	1	0.087	0 ==> 1		422	1	0.182	0 ==> 2
node_329 --> Xenosaurus platy	48	1	0.103	2 ==> 1		11	1	0.105	0 ==> 2		434	1	0.111	1 ==> 2
	62	1	0.111	2 --> 0		39	1	0.080	1 --> 2		439	1	0.118	1 ==> 2
	232	1	0.143	1 ==> 0		56	1	0.190	1 ==> 0		440	1	0.200	1 ==> 2
	340	1	0.095	1 ==> 0		69	1	0.333	0 ==> 1		446	1	0.143	0 ==> 1
	578	1	0.167	0 ==> 1		94	1	0.062	0 ==> 1		481	1	0.083	1 ==> 0
node_329 --> Xenosaurus grand	182	1	0.273	1 ==> 2		108	2	0.125	0 ==> 2		500	1	0.133	0 --> 1
	291	1	0.053	0 ==> 1		135	1	0.600	0 ==> 1		502	1	0.091	0 --> 1
	396	1	0.095	1 ==> 2		138	1	0.500	0 ==> 3		526	1	0.143	1 --> 0
	413	1	0.033	1 ==> 0		149	1	0.087	2 ==> 1	node_336 --> node_335	24	1	0.071	1 --> 0
	483	1	0.120	1 ==> 0		168	1	0.065	0 ==> 1		64	1	0.167	0 --> 1
node_365 --> node_364	18	1	0.053	0 ==> 1		226	1	1.000	0 ==> 1		96	1	0.222	0 ==> 3
	23	1	0.158	0 ==> 2		249	1	0.231	0 ==> 1		130	1	0.500	0 ==> 1
	37	1	0.059	0 ==> 1		338	1	0.143	0 ==> 1		162	1	0.333	1 ==> 0
	39	1	0.080	2 --> 1		364	1	0.105	0 ==> 1		165	1	0.200	1 ==> 0
	178	1	0.286	1 --> 0		384	1	0.097	1 ==> 3		188	1	0.080	1 --> 2
	250	1	0.273	2 ==> 3		419	1	0.073	3 ==> 4		498	1	0.083	0 --> 1
	254	1	0.182	0 ==> 1		445	1	0.300	1 ==> 2		511	1	0.143	1 ==> 0
	291	1	0.053	0 --> 1		461	1	0.300	0 ==> 1		591	1	0.250	1 ==> 0
	385	1	0.067	0 --> 1		487	1	0.222	0 --> 1		595	1	0.333	1 ==> 0
	399	1	0.062	0 --> 1		497	1	0.048	0 --> 1		602	1	0.267	2 ==> 3
	434	1	0.111	0 --> 1		521	1	0.067	0 --> 1	node_335 --> Aspidoscelis tig	62	1	0.111	0 ==> 2
	455	2	0.148	4 ==> 2		606	1	1.000	0 ==> 1		87	1	0.200	1 --> 0
	470	1	0.125	3 --> 0	node_333 --> Colobosaura mode	18	1	0.053	1 ==> 0		148	1	0.091	0 ==> 1
	500	1	0.133	0 ==> 2		49	2	0.089	0 ==> 2		216	1	0.222	0 ==> 1

	375	2	0.065	3 ==> 1		244	1	0.333	0 ==> 1		334	1	0.167	1 ==> 0					
	418	1	0.083	0 ==> 1		316	1	0.200	1 --> 0		375	1	0.065	1 --> 2					
	443	1	0.167	0 ==> 1		341	1	0.033	0 ==> 1		396	1	0.095	1 ==> 0					
	492	1	0.111	0 ==> 1		418	2	0.083	0 ==> 2		434	1	0.111	0 --> 2					
node_335 --> Teius teyou	18	1	0.053	1 ==> 0		513	1	0.083	1 --> 0		535	1	0.143	1 ==> 2					
	48	1	0.103	3 ==> 4	node_340 --> node_339	78	1	0.571	2 --> 1		580	1	0.333	0 ==> 1					
	128	1	0.167	3 ==> 2		82	1	0.118	0 --> 1		610	1	0.050	0 ==> 1					
	154	1	0.077	1 ==> 0		95	1	0.083	1 ==> 0	node_345 --> node_344	94	1	0.062	0 ==> 1					
	212	1	0.182	0 ==> 1		123	1	0.125	1 ==> 0		99	1	0.250	1 ==> 2					
	231	1	0.077	1 ==> 2		153	1	0.100	1 --> 0		185	1	0.067	2 --> 1					
	341	1	0.033	0 ==> 1		155	1	0.133	1 ==> 2		267	1	0.038	1 --> 0					
	348	1	0.111	0 ==> 1		163	1	0.500	2 --> 0		325	1	0.091	0 ==> 1					
	355	1	0.059	0 ==> 1		240	1	0.125	2 ==> 1		394	1	0.087	0 ==> 1					
	401	1	0.077	1 ==> 0		324	1	0.300	0 ==> 1		446	1	0.143	0 --> 1					
	413	1	0.033	1 ==> 0		334	1	0.167	1 ==> 0		455	2	0.148	2 ==> 4					
	419	1	0.073	3 ==> 2		385	1	0.067	0 ==> 1		485	1	0.250	0 --> 1					
	420	1	0.085	3 ==> 2		403	1	0.200	1 ==> 0		508	1	0.143	0 --> 1					
	421	1	0.075	3 ==> 2		434	1	0.111	2 ==> 0		519	1	0.077	0 --> 1					
	450	1	0.143	1 ==> 0	node_339 --> Cricosaura typic	10	2	0.087	0 ==> 2		542	1	0.273	0 --> 2					
	494	1	0.133	0 ==> 1		11	1	0.105	1 --> 0		573	1	0.083	0 ==> 1					
	572	1	0.058	2 ==> 1		18	1	0.053	1 ==> 2		577	1	0.167	1 --> 2					
node_364 --> node_363	138	1	0.500	0 --> 2		29	1	0.083	0 ==> 1		580	1	0.333	0 ==> 2					
	167	2	0.125	0 --> 2		36	1	0.062	0 ==> 1	node_344 --> Zonosaurus ornat	13	1	0.067	0 ==> 1					
	170	1	0.231	0 --> 2		38	3	0.143	0 ==> 3		49	3	0.089	0 ==> 3					
	182	1	0.273	1 --> 2		77	1	0.083	0 ==> 1		104	1	0.077	1 --> 0					
	188	1	0.080	2 --> 3		88	1	0.125	0 ==> 1		193	1	0.100	0 ==> 1					
	255	1	0.077	1 --> 0		129	1	0.051	0 ==> 1		231	1	0.077	0 ==> 1					
	345	1	0.250	0 --> 1		141	1	0.250	1 ==> 2		291	1	0.053	1 --> 0					
	367	1	0.125	0 ==> 1		161	1	0.125	1 ==> 0		375	1	0.065	1 --> 2					
	383	1	0.080	1 --> 0		164	1	0.333	1 ==> 0		384	1	0.097	1 ==> 2					
	394	1	0.087	1 ==> 0		202	1	0.500	1 --> 0		385	1	0.067	1 ==> 0					
	410	1	0.091	0 --> 1		229	1	0.500	1 --> 0		421	1	0.075	3 ==> 2					
	434	1	0.111	1 --> 2		301	1	0.333	1 ==> 0		434	1	0.111	0 --> 1					
	518	2	0.100	0 --> 2		390	1	0.100	2 ==> 1	node_344 --> Cordylosaurus su	57	1	0.190	1 ==> 0					
	541	1	0.100	0 --> 1		413	1	0.033	1 ==> 0		108	1	0.125	1 ==> 0					
	565	1	0.125	0 --> 1		418	1	0.083	2 --> 1		123	1	0.125	1 ==> 0					
	582	1	0.250	0 ==> 1		421	1	0.075	2 ==> 3		124	1	0.077	0 ==> 1					
	590	1	0.308	2 --> 1		484	1	0.100	1 --> 0		128	2	0.167	1 ==> 3					
node_363 --> node_362	95	1	0.083	0 ==> 1		500	1	0.133	2 ==> 1		252	1	0.200	0 ==> 1					
	149	2	0.087	2 ==> 0		531	1	0.125	1 ==> 0		283	1	0.133	1 ==> 2					
	157	1	0.125	1 --> 0		542	1	0.273	0 ==> 2		286	1	0.111	0 ==> 1					
	573	1	0.083	1 --> 0		610	1	0.050	1 --> 0		340	1	0.095	0 ==> 1					
node_362 --> Paramacellodus	7	1	0.069	1 ==> 2	node_339 --> Xantusia vigilis	8	1	0.182	0 ==> 2		392	1	0.105	0 ==> 1					
	56	1	0.190	1 ==> 0		49	1	0.089	3 ==> 2		396	1	0.095	1 ==> 2					
	57	1	0.190	1 ==> 0		57	1	0.190	1 ==> 0		413	1	0.033	1 ==> 0					
	246	1	0.167	0 ==> 1		82	1	0.118	1 ==> 2		418	1	0.083	0 ==> 1					
	421	1	0.075	3 ==> 2		104	1	0.077	1 ==> 0		440	1	0.200	1 ==> 2					
node_362 --> node_361	108	2	0.125	0 ==> 2		185	2	0.067	2 ==> 4		452	1	0.235	0 ==> 1					
	123	1	0.125	0 ==> 1		452	1	0.235	3 ==> 2		470	1	0.125	1 --> 0					
	255	1	0.077	0 --> 1		497	1	0.048	0 ==> 1		471	1	0.250	0 ==> 2					
	267	1	0.038	0 --> 1		541	1	0.100	1 --> 0		579	1	0.182	1 --> 2					
	369	1	0.100	0 ==> 1		565	1	0.125	1 --> 0		587	1	0.100	1 ==> 0					
	375	1	0.065	2 --> 1		588	1	0.167	0 ==> 1	node_361 --> node_360	1	1	0.167	1 ==> 0					
	434	1	0.111	2 --> 0	node_340 --> Palaeoxantusia s	185	2	0.067	2 ==> 0		66	1	0.286	0 --> 1					
node_361 --> node_346	39	2	0.080	1 ==> 3		212	1	0.182	2 ==> 1		67	1	0.300	0 ==> 1					
	48	1	0.103	3 --> 4		572	1	0.058	2 ==> 3		82	1	0.118	1 ==> 2					
	76	1	0.333	0 ==> 2	node_341 --> Lepidophyma flav	18	1	0.053	1 ==> 2		154	1	0.077	1 --> 0					
	99	1	0.250	0 ==> 1		23	1	0.158	2 ==> 0		160	1	0.143	0 ==> 1					
	101	1	0.105	0 ==> 1		25	1	0.118	1 ==> 2		228	1	0.500	0 --> 2					
	104	1	0.077	0 --> 1		39	1	0.080	3 ==> 4		275	1	0.333	2 ==> 1					
	144	1	0.091	1 ==> 0		50	1	0.167	0 ==> 1		340	1	0.095	0 --> 1					
	161	1	0.125	0 ==> 1		51	1	0.200	0 ==> 1		413	1	0.033	1 --> 0					
	163	1	0.500	0 --> 2		56	1	0.190	1 ==> 2		452	1	0.235	0 --> 1					
	185	1	0.067	1 --> 2		89	1	0.500	0 ==> 1		475	1	0.300	1 --> 2					
	273	1	0.062	0 ==> 1		116	1	0.300	1 ==> 0		487	1	0.222	0 --> 1					
	301	1	0.333	0 ==> 1		120	2	0.130	1 ==> 2		513	1	0.083	1 --> 0					
	383	1	0.080	0 --> 1		182	1	0.273	2 ==> 1		525	1	0.167	0 --> 1					
	388	1	0.105	1 --> 0		188	1	0.080	3 ==> 4		579	1	0.182	1 --> 2					
	396	1	0.095	0 ==> 1		204	1	0.125	0 ==> 1		580	1	0.333	0 --> 2					
	508	1	0.143	1 --> 0		258	1	0.081	3 ==> 2		593	1	0.231	2 --> 1					
node_346 --> node_342	7	1	0.069	1 --> 0		271	1	0.167	1 ==> 2		596	1	0.333	1 --> 0					
	24	1	0.071	0 --> 1		291	1	0.053	1 --> 0		601	1	1.000	0 --> 1					
	25	1	0.118	0 --> 1		324	1	0.300	0 ==> 3		607	1	0.250	1 --> 0					
	49	3	0.089	0 ==> 3		325	1	0.091	0 ==> 1	node_360 --> node_347	6	1	0.100	0 ==> 1					
	62	1	0.111	0 ==> 2		338	1	0.143	0 ==> 1		7	1	0.069	1 ==> 2					
	82	1	0.118	1 --> 0		379	1	0.062	0 ==> 1		22	1	0.111	1 --> 0					
	88	1	0.125	1 --> 0		502	1	0.091	1 ==> 0		23	1	0.158	2 ==> 0					
	135	1	0.600	0 --> 1		562	1	0.111	1 ==> 0		36	1	0.062	0 ==> 1					
	137	1	0.077	0 --> 1		572	2	0.058	2 ==> 0		42	1	0.500	0 ==> 1					
	141	1	0.250	0 --> 1	node_346 --> node_345	37	1	0.059	1 --> 0		62	1	0.111	0 ==> 2					
	164	1	0.333	0 --> 1		77	1	0.083	0 ==> 1		95	1	0.083	1 ==> 0					
	212	1	0.182	0 --> 2		97	2	0.250	0 ==> 2		137	1	0.077	0 ==> 1					
	213	1	0.048	1 --> 0		108	1	0.125	2 --> 1		167	2	0.125	2 --> 0					
	220	1	0.375	1 --> 0		114	1	0.148	3 ==> 4		168	1	0.065	0 --> 1					
	229	1	0.500	0 --> 1		157	1	0.125	0 ==> 1		254	1	0.182	1 --> 2					
	231	1	0.077	0 --> 1		328	1	0.054	1 --> 0		399	1	0.062	1 ==> 0					
	245	1	0.167	1 --> 0		344	1	0.048	0 --> 1		410	1	0.091	1 --> 0					
	271	1	0.167	0 --> 1		470	1	0.125	0 --> 1		419	1	0.073	3 --> 4					
	282	1	1.000	0 ==> 1		518	1	0.100	2 --> 1	node_347 --> Myrmecodaptria m	155	1	0.133	1 ==> 2					
	283	1	0.133	1 ==> 0		541	1	0.100	1 --> 0		357	1	0.083	0 ==> 1					
	307	1	0.125	0 --> 1		554	1	0.167	0 --> 1	node_347 --> Carusia intermed	48	2	0.103	3 ==> 1					
	308	1	0.250	0 ==> 1		565	1	0.125	1 --> 0		94	1	0.062	0 ==> 2					
	328	1	0.054	1 --> 2		575	1	0.167	0 ==> 1		375	1	0.065	1 --> 2					
	372	2	0.058	0 ==> 2		577	1	0.167	0 --> 1		383	1	0.080	0 ==> 1					
	375	1	0.065	1 ==> 0		578	1	0.167	0 ==> 2		403	1	0.200	0 ==> 1					
	385	1	0.067	1 ==> 0	node_345 --> node_343	6	1	0.100	0 ==> 1		572	1	0.058	2 ==> 3					
	403	1	0.200	0 ==> 1		7	1	0.069	1 ==> 2	node_360 --> node_359	67	1	0.300	1 ==> 2					
	410	1	0.091	1 --> 0		78	1	0.571	1 ==> 2		76	1	0.333	0 ==> 1					
	434	1	0.111	0 --> 2		82	1	0.118	1 ==> 2		94	1	0.062	0 ==> 1					
	443	1	0.167	0 --> 1		204	1	0.125	0 ==> 1		97	1	0.250	0 ==> 1					
	447	1	0.083	0 --> 1		208	1	0.091	2 ==> 1		128	1	0.167	1 ==> 2					
	452	1	0.235	0 --> 3		241	1	0.667	2 ==> 3		249	1	0.231	0 --> 1					
	468	1	0.120	1 --> 0		244	1	0.333	0 ==> 1		267	1	0.038	1 --> 0					
	484	1	0.100	0 --> 1		369	1	0.100	1 ==> 2		418	1	0.083	0 --> 1					
	531	1	0.125	0 ==> 1		399	1	0.062	1 ==> 0		581	1	1.000	0 --> 1					
	579	1	0.182	1 --> 0		405	1	0.250	0 ==> 1	node_359 --> node_349	29	1	0.083	0 ==> 1					
	582	1	0.250	1 ==> 0		406	1	0.143	0 ==> 1		56	1	0.190	1 ==> 2					
	598	1	0.500	0 --> 1		453	1	0.250	0 --> 1		108	2	0.125	2 ==> 0					
	610	1	0.050	0 --> 1		483	1	0.120	1 ==> 0		124	1	0.077	0 ==> 1					
node_342 --> Tepexisaurus tep	49	1	0.089	3 ==> 4		500	1	0.133	2 ==> 0		156	1	0.333	0 ==> 1					
	163	1	0.500	2 --> 0		501	1	0.100	1 ==> 0		185	1	0.067	1 --> 0					
	369	1	0.100	1 ==> 0		592	1	0.667	2 ==> 1		312	1	0.222	0 --> 1					
	383	1	0.080	1 --> 0	node_343 --> Platysaurus impe	8	1	0.182	0 ==> 2		341	1	0.033	0 --> 1					
	419	1	0.073	3 ==> 4		23	1	0.158	2 ==> 0		369	1	0.100	1 ==> 0					
	420	1	0.085	3 ==> 4		37	1	0.059	0 --> 1		379	1	0.062	0 ==> 1					
	557	1	0.125	0 ==> 1		48	1	0.103	4 --> 3		408	1	0.500	0 --> 1					
node_342 --> node_341	78	1	0.571	1 --> 2		104	1	0.077	1 --> 0		419	1	0.073	3 ==> 2					
	153	1	0.100	0 --> 1		461	1	0.300	0 ==> 1		421	1	0.075	3 --> 2					
	183	1	0.500	0 ==> 1		511	1	0.143	1 ==> 0		434	1	0.111	0 --> 2					
	240	1	0.125	0 ==> 2		513	1	0.083	1 ==> 0	node_349 --> Globaura venusta	7	1	0.069	1 ==> 2					
	275	1	0.333	2 ==> 3		521	1	0.067	1 ==> 0		36	1	0.062	0 ==> 1					
	369	1	0.100	1 ==> 2		579	1	0.182	1 --> 0		375	1	0.065	1 --> 2					
	372	1	0.058	2 ==> 3	node_343 --> Cordylus mossamb	11	1	0.105	0 ==> 2		385	1	0.067	1 ==> 0					
	374	1	0.250	0 ==> 2		18	1	0.053	1 ==> 2	node_349 --> node_348	7	1	0.069	1 --> 0					
	376	1	0.200	0 ==> 1		36	1	0.062	0 ==> 1		24	1	0.071	0 --> 1					
	380	1	0.091	0 ==> 1		63	2	0.286	0 ==> 2		49	2	0.089	0 ==> 2					
	392	1	0.105	0 ==> 1		108	1	0.125	1 --> 2		240	1	0.125	0 --> 1					
	420	1	0.085	3 ==> 2		111	1	0.222	0 ==> 1		420	1	0.085	3 --> 2					
	421	1	0.075	3 ==> 2		188	1	0.080	3 ==> 2	node_348 --> Hymenosaurus cla	49	2	0.089	2 ==> 4					
node_341 --> node_340	11	1	0.105	0 --> 1		206	1	0.091	0 ==> 1		129	1	0.051	0 ==> 1					
	143	2	0.200	0 ==> 2		283	1	0.133	1 ==> 0		383	1	0.080	0 ==> 1					
	202	1	0.500	0 --> 1		291	1	0.053	1 --> 0		384	1	0.097	1 ==> 2					

	390	2	0.100	2 ==> 0		273	1	0.062	0 ==> 1		610	1	0.050	0 --> 1
node_348 --> Eoxanta lacertif	38	1	0.143	0 ==> 1		291	1	0.053	0 ==> 1	node_353 --> Sphenomorphus so	38	1	0.143	0 ==> 1
	94	1	0.062	1 ==> 0		307	1	0.125	0 --> 1		49	3	0.089	0 ==> 3
	95	1	0.083	1 ==> 0		311	1	0.286	0 ==> 1		62	1	0.111	2 ==> 0
	97	1	0.250	1 ==> 0		312	1	0.222	0 ==> 1		77	1	0.083	1 ==> 0
	267	1	0.038	0 ==> 1		316	1	0.200	1 ==> 0		97	1	0.250	0 --> 1
	273	1	0.062	0 ==> 1		324	1	0.300	0 ==> 1		178	1	0.286	1 ==> 0
	408	1	0.500	1 --> 0		350	1	0.333	0 ==> 1		335	1	0.333	0 ==> 1
node_359 --> node_358	18	1	0.053	1 ==> 2		388	1	0.105	1 ==> 0		383	1	0.080	0 ==> 1
	39	1	0.080	1 ==> 2		419	1	0.073	3 ==> 2		418	1	0.083	0 ==> 1
	48	1	0.103	3 --> 4		420	1	0.085	3 ==> 2		440	1	0.200	1 ==> 2
	67	1	0.300	2 --> 3		421	1	0.075	3 ==> 2		455	2	0.148	4 ==> 2
	69	1	0.333	0 ==> 1		445	1	0.300	1 ==> 0		481	1	0.083	0 ==> 1
	154	1	0.077	0 --> 1		446	1	0.143	0 ==> 1		488	1	0.133	0 ==> 1
	157	1	0.125	0 ==> 1		456	2	0.190	1 ==> 3		497	1	0.048	0 ==> 1
	161	1	0.125	0 ==> 1		462	1	0.071	0 ==> 1		531	1	0.125	0 ==> 1
	178	1	0.286	0 --> 1		463	1	0.108	2 ==> 1		535	1	0.143	2 ==> 1
	231	1	0.077	0 ==> 1		480	1	0.200	0 ==> 1		593	1	0.231	0 ==> 1
	249	1	0.231	1 --> 2		490	1	0.500	0 --> 1	node_353 --> Tiliqua scincoid	4	1	0.143	0 ==> 1
	278	1	0.500	0 ==> 1		495	1	0.125	1 --> 0		18	1	0.053	1 ==> 0
	291	1	0.053	1 --> 0		500	1	0.133	2 --> 0		94	1	0.062	1 ==> 0
	402	1	0.167	0 --> 1		501	1	0.100	1 --> 0		120	1	0.130	0 ==> 1
	573	1	0.083	0 ==> 1		502	1	0.091	1 --> 0		137	1	0.077	0 ==> 1
	575	1	0.167	0 ==> 2		503	1	0.286	1 --> 2		153	1	0.100	0 ==> 1
	577	1	0.167	0 ==> 2		504	1	0.125	1 --> 0		154	1	0.077	1 --> 0
	578	1	0.167	0 ==> 2		505	1	0.167	0 ==> 1		175	1	0.333	0 ==> 1
node_358 --> Plestiodon fasci	7	1	0.069	1 ==> 0		528	1	0.200	0 ==> 1		193	1	0.100	0 ==> 1
	49	2	0.089	0 ==> 2		548	1	0.100	0 ==> 1		258	2	0.081	2 ==> 0
	77	1	0.083	0 ==> 1		572	1	0.058	2 ==> 1		261	1	0.200	0 ==> 1
	308	1	0.250	0 ==> 1		573	1	0.083	1 ==> 0		271	1	0.167	0 ==> 1
	375	1	0.065	1 --> 2		586	1	0.333	0 --> 1		338	1	0.143	0 ==> 1
	413	1	0.033	0 --> 1		594	1	0.333	0 --> 1		361	4	0.160	4 ==> 0
	418	1	0.083	1 --> 0	node_351 --> Acontias perciva	4	1	0.143	0 ==> 1		364	1	0.105	0 ==> 1
	481	1	0.083	0 ==> 1		18	1	0.053	2 ==> 1		367	1	0.125	1 ==> 2
	497	1	0.048	0 ==> 1		38	2	0.143	0 ==> 2		384	1	0.097	1 ==> 2
node_358 --> node_357	23	1	0.158	2 --> 0		50	1	0.167	0 ==> 1		390	1	0.100	2 ==> 1
	62	1	0.111	0 --> 2		94	1	0.062	1 ==> 2		410	1	0.091	1 ==> 0
	129	1	0.051	0 ==> 1		97	1	0.250	1 ==> 0		420	1	0.085	3 ==> 2
	188	1	0.080	3 --> 2		101	1	0.105	0 ==> 1		421	1	0.075	3 ==> 2
	240	1	0.125	0 ==> 2		114	1	0.148	4 --> 3		456	1	0.190	0 ==> 1
	455	1	0.148	2 ==> 3		160	1	0.143	1 ==> 0		566	1	0.444	0 ==> 2
	461	1	0.300	0 ==> 1		185	1	0.067	1 ==> 0		573	1	0.083	1 ==> 0
	485	1	0.250	0 ==> 1		206	1	0.091	0 ==> 1		602	1	0.267	1 --> 0
	535	1	0.143	1 ==> 2		286	1	0.111	0 ==> 1	node_354 --> Eugongylus rufes	1	1	0.167	0 ==> 1
	593	1	0.231	1 ==> 0		294	1	0.091	0 ==> 1		95	1	0.083	1 ==> 0
node_357 --> Scincus	3	2	0.182	0 ==> 2		307	1	0.125	1 --> 2		206	1	0.091	0 ==> 1
	24	1	0.071	0 ==> 1		312	1	0.222	1 ==> 2		240	1	0.125	2 ==> 0
	67	1	0.300	3 --> 2		328	1	0.054	1 ==> 2		344	1	0.048	0 ==> 1
	149	1	0.087	0 ==> 1		333	1	0.333	0 ==> 1		349	1	0.136	2 --> 1
	154	1	0.077	1 --> 0		341	1	0.033	0 ==> 1		419	1	0.073	3 ==> 4
	188	1	0.080	2 ==> 1		372	3	0.058	0 ==> 3		492	1	0.111	1 --> 0
	228	1	0.500	2 ==> 0		375	1	0.065	1 ==> 0		554	1	0.167	1 --> 0
	254	1	0.182	1 ==> 0		390	2	0.100	2 ==> 0	node_363 --> Parmeosaurus scu	49	3	0.089	0 ==> 3
	355	1	0.059	0 ==> 1		440	1	0.200	1 ==> 0		64	1	0.167	0 ==> 1
	390	2	0.100	2 ==> 0		459	3	0.182	0 ==> 3		90	2	0.105	2 ==> 0
	402	1	0.167	1 --> 0		487	1	0.222	1 ==> 0		97	1	0.250	0 ==> 1
	412	1	0.111	0 ==> 1		488	1	0.133	1 ==> 2		361	1	0.160	4 ==> 3
	419	1	0.073	3 ==> 2		499	1	0.143	0 ==> 1		375	1	0.065	2 ==> 3
	421	1	0.075	3 ==> 2		572	1	0.058	1 ==> 0		401	1	0.077	1 ==> 0
	502	1	0.091	1 ==> 0	node_351 --> Feylinia polylep	1	1	0.167	0 ==> 1		575	1	0.167	0 ==> 2
	521	1	0.067	1 ==> 0		17	1	0.167	0 ==> 1		577	1	0.167	0 ==> 2
	543	1	0.500	0 ==> 2		28	1	0.143	0 ==> 1		578	1	0.167	0 ==> 2
	544	1	1.000	0 ==> 3		39	1	0.080	3 --> 2	node_379 --> node_378	38	1	0.143	0 ==> 1
	546	1	0.100	1 ==> 0		54	1	0.333	0 ==> 1		39	1	0.080	2 --> 3
	567	1	1.000	0 ==> 2		90	1	0.105	1 ==> 0		88	1	0.125	1 ==> 0
node_357 --> node_356	128	1	0.167	2 ==> 3		104	1	0.077	1 ==> 1		128	1	0.167	1 --> 2
	144	1	0.091	1 ==> 0		124	1	0.077	0 ==> 1		135	1	0.600	0 --> 1
	251	1	0.333	0 ==> 1		137	1	0.077	0 ==> 1		154	1	0.077	1 --> 0
	267	1	0.038	0 ==> 1		142	1	0.250	0 ==> 1		161	1	0.125	0 ==> 1
	283	1	0.133	1 ==> 2		188	1	0.080	2 ==> 3		178	1	0.286	1 --> 2
	340	1	0.095	1 --> 0		193	1	0.100	0 ==> 1		185	3	0.067	1 --> 4
	369	1	0.100	1 --> 2		212	1	0.182	0 ==> 1		187	1	0.500	2 --> 1
	452	1	0.235	1 --> 3		249	1	0.231	2 ==> 3		201	1	0.250	1 --> 0
	455	1	0.148	3 --> 4		261	1	0.200	0 ==> 1		204	1	0.125	0 --> 1
	525	1	0.167	1 --> 0		271	1	0.167	0 ==> 1		206	1	0.091	0 --> 1
node_356 --> node_352	39	1	0.080	2 --> 3		276	1	0.118	0 ==> 1		208	1	0.091	1 --> 0
	62	1	0.111	2 --> 0		293	1	0.143	0 ==> 1		234	1	0.600	0 --> 1
	90	1	0.105	2 ==> 1		345	1	0.250	1 ==> 0		267	1	0.038	0 --> 1
	114	1	0.148	3 --> 4		383	1	0.000	0 ==> 1		297	1	0.100	1 --> 0
	129	1	0.051	1 ==> 2		392	1	0.105	0 ==> 1		308	1	0.250	0 --> 1
	157	1	0.125	1 --> 0		418	1	0.083	1 ==> 2		309	1	0.333	0 --> 1
	456	1	0.190	0 --> 1		422	1	0.182	0 ==> 1		315	1	0.071	1 --> 0
	468	1	0.120	1 ==> 0		427	1	0.100	0 ==> 1		316	1	0.200	1 --> 0
	488	1	0.133	0 --> 1		461	1	0.300	1 ==> 2		321	1	0.231	0 --> 3
	497	1	0.048	0 --> 1		471	1	0.250	0 ==> 1		328	1	0.054	1 --> 2
	541	1	0.100	1 --> 0		487	2	0.222	1 ==> 3		347	1	0.500	0 --> 1
	542	1	0.273	0 --> 1		510	1	0.143	0 ==> 1		419	1	0.073	3 ==> 4
	565	1	0.125	1 --> 0		516	1	0.143	0 ==> 1		420	1	0.085	3 ==> 4
	610	1	0.050	0 --> 1	node_356 --> node_355	7	1	0.069	1 ==> 0		421	1	0.075	3 --> 4
node_352 --> node_350	23	1	0.158	0 --> 2		36	1	0.062	0 ==> 1		470	1	0.125	3 ==> 2
	240	1	0.125	2 ==> 1		39	1	0.080	2 ==> 1		475	1	0.300	1 --> 0
	384	1	0.097	1 ==> 2		77	1	0.083	0 ==> 1		479	1	0.250	0 --> 1
	413	1	0.033	0 ==> 1		185	1	0.067	1 --> 2		514	1	0.083	0 --> 1
node_350 --> Brachymeles grac	7	1	0.069	1 ==> 0		212	1	0.182	0 ==> 2		518	1	0.100	0 --> 1
	62	1	0.111	0 --> 2		249	1	0.231	2 ==> 3		525	1	0.167	0 --> 1
	67	1	0.300	3 --> 2		251	1	0.333	1 ==> 2		562	1	0.111	1 --> 0
	104	1	0.077	0 ==> 1		328	1	0.054	1 --> 0		584	1	0.188	1 --> 0
	128	1	0.167	3 ==> 2		349	2	0.136	0 ==> 2		588	1	0.167	0 --> 1
	185	1	0.067	1 ==> 2		372	3	0.058	0 ==> 3		597	1	1.000	0 --> 1
	345	1	0.250	1 ==> 0		418	1	0.083	1 --> 0		598	1	0.500	0 --> 1
	348	1	0.111	0 ==> 1		492	1	0.111	0 --> 1	node_378 --> Eichstaettisauru	1	1	0.167	1 ==> 0
	452	1	0.235	3 --> 1		554	1	0.167	0 --> 1		18	1	0.053	0 ==> 1
	456	1	0.190	1 --> 0	node_355 --> Trachylepis quin	48	1	0.103	4 ==> 3		48	2	0.103	3 ==> 1
	470	1	0.125	0 ==> 1		129	1	0.051	1 ==> 0		168	1	0.065	0 ==> 1
	485	1	0.250	1 ==> 0		154	1	0.077	1 --> 0		375	1	0.065	2 ==> 3
	525	1	0.167	0 --> 1		240	1	0.125	2 ==> 1		413	1	0.033	1 --> 0
	529	1	0.286	1 ==> 0		291	1	0.053	0 ==> 1		521	1	0.067	1 ==> 0
	543	1	0.500	0 ==> 1		355	1	0.059	0 ==> 1		557	1	0.125	0 ==> 1
	546	1	0.100	1 ==> 0		369	1	0.100	2 --> 1	node_378 --> node_377	95	1	0.083	0 ==> 1
	566	1	0.444	0 ==> 2		384	1	0.097	1 ==> 2		137	1	0.077	0 --> 1
	584	1	0.188	1 ==> 2		385	1	0.067	1 ==> 0		138	1	0.500	0 --> 2
node_350 --> Amphiglossus spl	212	1	0.182	0 ==> 1		443	1	0.167	0 ==> 1		158	1	0.333	0 ==> 1
	231	1	0.077	1 ==> 0		455	2	0.148	4 ==> 2		159	1	0.333	0 --> 1
	328	1	0.054	1 --> 0		487	1	0.222	1 ==> 0		241	1	0.667	2 --> 3
	340	1	0.095	0 ==> 1		561	1	0.154	0 ==> 1		369	1	0.100	0 --> 1
	349	1	0.136	0 ==> 1		573	1	0.083	1 ==> 0		489	1	0.111	0 --> 1
	488	1	0.133	1 --> 0	node_355 --> node_354	23	1	0.158	0 --> 2		535	1	0.143	1 --> 2
	494	1	0.133	1 ==> 0		97	1	0.250	1 --> 0	node_377 --> AMNH FR 21444	57	1	0.190	1 ==> 0
	498	1	0.083	1 ==> 0		258	1	0.081	3 ==> 2		112	1	0.167	0 ==> 1
	513	1	0.083	0 ==> 1		375	1	0.065	1 ==> 0	node_377 --> node_376	36	1	0.062	0 ==> 1
	535	1	0.143	2 ==> 1		402	1	0.167	1 --> 0		38	2	0.143	1 ==> 3
	542	1	0.273	1 --> 3		461	1	0.300	1 ==> 2		43	1	0.375	0 --> 1
node_352 --> node_351	68	1	0.077	0 --> 1		513	1	0.083	0 ==> 1		68	1	0.077	0 ==> 1
	123	1	0.125	1 --> 0		602	1	0.267	0 --> 1		70	1	0.667	0 --> 1
	143	2	0.200	0 --> 2	node_354 --> node_353	18	1	0.053	2 ==> 1		104	1	0.077	0 ==> 1
	155	1	0.133	1 --> 2		114	1	0.148	3 ==> 4		128	1	0.167	2 ==> 3
	180	1	0.250	0 ==> 1		129	1	0.051	1 ==> 2		129	1	0.051	0 --> 1
	191	1	0.167	0 ==> 1		231	1	0.077	1 ==> 2		141	1	0.250	0 ==> 1
	192	1	0.250	0 ==> 1		328	1	0.054	0 --> 1		149	1	0.087	2 --> 1
	194	1	0.600	0 ==> 2		341	1	0.033	0 ==> 1		152	2	0.400	0 ==> 2
	216	1	0.222	0 ==> 1		413	1	0.033	0 ==> 1		273	1	0.062	0 --> 1
	231	1	0.077	1 ==> 2		542	1	0.273	0 ==> 2		283	1	0.133	1 ==> 2

	286	1	0.111	0 --> 1		193	1	0.100	0 ==> 1		286	1	0.111	1 --> 0
	347	1	0.500	1 ==> 2		468	1	0.120	1 --> 0		379	1	0.062	0 ==> 1
	372	3	0.058	0 ==> 3	node_367 --> Rhacodactylus au	18	1	0.053	0 ==> 1		380	1	0.091	1 ==> 0
	375	2	0.065	2 ==> 0		49	1	0.089	0 ==> 1		401	1	0.077	1 ==> 0
	380	1	0.091	0 ==> 1		149	1	0.087	1 ==> 0		446	1	0.143	0 ==> 1
	384	1	0.097	1 --> 0		185	2	0.067	4 ==> 2		449	1	0.200	0 ==> 1
	385	1	0.067	0 --> 1		215	1	0.091	1 --> 0		450	1	0.143	0 ==> 1
node_376 --> node_366	10	1	0.087	0 ==> 1		275	1	0.333	0 ==> 1		517	1	0.200	0 ==> 1
	23	1	0.158	0 --> 1		375	1	0.065	0 --> 1		529	1	0.286	1 ==> 2
	49	2	0.089	0 --> 2		413	1	0.033	1 ==> 0		557	1	0.125	0 ==> 1
	54	1	0.333	0 ==> 1		419	1	0.073	4 ==> 3		561	1	0.154	0 ==> 1
	94	1	0.062	0 ==> 2		420	1	0.085	4 ==> 3		572	2	0.058	0 ==> 2
	129	1	0.051	1 ==> 2		421	1	0.075	4 ==> 3	node_371 --> node_370	39	1	0.080	1 ==> 2
	143	1	0.200	0 --> 1		509	1	0.158	1 ==> 2		48	1	0.103	3 --> 4
	144	1	0.091	1 --> 0		521	1	0.067	1 ==> 0		190	1	0.250	0 ==> 1
	166	1	0.091	0 ==> 1		541	1	0.100	0 ==> 1		213	1	0.048	1 ==> 0
	237	1	1.000	0 ==> 1		557	1	0.125	0 ==> 1		215	1	0.091	1 --> 0
	258	1	0.081	3 ==> 2	node_367 --> Saltuarius cornu	1	1	0.167	1 ==> 0		249	1	0.231	0 ==> 1
	275	1	0.333	0 --> 3		7	2	0.069	0 ==> 2		292	1	0.500	1 ==> 0
	307	1	0.125	0 ==> 1		11	1	0.105	0 ==> 2		309	1	0.333	1 ==> 0
	308	1	0.250	1 --> 0		23	1	0.158	0 ==> 1		418	1	0.083	0 ==> 1
	309	1	0.333	1 --> 0		37	1	0.059	1 --> 0		575	1	0.167	1 --> 0
	321	1	0.231	3 --> 0		39	1	0.080	2 --> 3		585	1	0.250	1 --> 0
	328	2	0.054	2 --> 0		148	1	0.091	0 ==> 1	node_370 --> Gonatodes albogu	10	1	0.087	0 ==> 1
	334	1	0.167	1 ==> 0		149	1	0.087	1 --> 2		96	1	0.222	0 ==> 1
	364	2	0.105	0 ==> 2		158	1	0.333	1 ==> 0		124	1	0.077	0 ==> 1
	369	1	0.100	1 ==> 2		286	1	0.111	1 --> 0		141	1	0.250	1 ==> 0
	422	1	0.182	0 ==> 1		384	1	0.097	3 ==> 0		225	1	0.500	1 ==> 0
	427	1	0.100	0 ==> 1		394	1	0.087	1 ==> 2		271	1	0.167	0 ==> 1
	456	2	0.190	0 --> 2		483	1	0.120	1 ==> 2		316	1	0.200	0 ==> 1
	459	3	0.182	0 --> 3		486	1	0.400	2 ==> 3		347	1	0.500	2 ==> 1
	462	1	0.071	0 --> 1		496	1	0.083	0 ==> 1		367	1	0.125	0 ==> 1
	463	1	0.108	2 --> 1		506	1	0.250	0 ==> 1		369	1	0.100	1 ==> 2
	468	1	0.120	1 --> 0		514	1	0.083	1 --> 0		439	1	0.118	0 ==> 1
	483	2	0.120	1 --> 3		547	1	0.250	0 ==> 1		500	1	0.133	2 --> 0
	484	1	0.100	0 --> 1		569	1	0.333	0 ==> 1		501	1	0.100	1 ==> 0
	488	1	0.133	0 --> 1		572	2	0.058	0 ==> 2		518	1	0.100	1 ==> 2
	493	1	0.200	1 --> 0	node_374 --> node_373	39	1	0.080	2 ==> 1		541	1	0.100	0 ==> 1
	495	1	0.125	1 --> 0		43	1	0.375	3 --> 2		565	1	0.125	0 ==> 1
	505	1	0.167	0 ==> 1		88	1	0.125	0 ==> 1		588	2	0.167	0 ==> 2
	518	1	0.100	1 --> 2		111	1	0.222	1 --> 0	node_370 --> Phelsuma lineata	11	1	0.105	1 --> 0
	524	1	0.200	0 --> 1		205	1	0.333	0 --> 1		17	1	0.167	0 ==> 1
	528	1	0.200	0 --> 1		208	1	0.091	0 ==> 1		18	1	0.053	1 ==> 2
	549	1	0.250	0 --> 1		213	1	0.048	0 ==> 1		23	1	0.158	0 ==> 2
	550	1	0.200	0 --> 1		225	1	0.500	0 ==> 1		43	1	0.375	2 ==> 1
	551	1	0.167	0 --> 1		321	1	0.231	3 --> 0		49	1	0.089	0 ==> 1
	552	1	0.500	0 --> 1	node_373 --> node_369	22	1	0.111	1 ==> 0		114	1	0.148	3 ==> 4
	553	1	0.200	0 --> 1		43	1	0.375	2 ==> 1		128	2	0.167	3 ==> 1
	554	1	0.167	0 --> 2		95	1	0.083	1 --> 0		129	2	0.051	0 ==> 2
	602	2	0.267	0 --> 2		128	1	0.167	3 ==> 4		149	1	0.087	1 ==> 0
node_366 --> Delma borea	7	1	0.069	0 ==> 1		159	1	0.333	1 ==> 0		208	1	0.091	1 ==> 0
	13	1	0.067	0 ==> 1		167	2	0.125	0 ==> 2		369	1	0.100	1 ==> 0
	23	1	0.158	1 --> 2		170	1	0.231	0 ==> 2		394	1	0.087	1 ==> 2
	43	1	0.375	1 --> 0		190	1	0.250	0 ==> 1		410	1	0.091	0 ==> 1
	57	1	0.190	1 ==> 4		251	2	0.333	0 --> 2		494	1	0.133	0 ==> 1
	101	1	0.105	0 ==> 1		286	1	0.111	1 --> 0		496	1	0.083	0 ==> 1
	108	2	0.125	0 ==> 2		380	1	0.091	1 --> 0		498	1	0.083	0 ==> 1
	124	1	0.077	0 ==> 1		409	1	0.333	1 --> 0		506	1	0.250	0 ==> 1
	188	1	0.080	2 ==> 3		450	1	0.143	0 ==> 1		511	1	0.143	0 ==> 1
	294	1	0.091	0 ==> 1		467	1	0.333	0 ==> 1		514	1	0.083	1 ==> 0
	312	1	0.222	0 ==> 1		489	1	0.111	0 --> 1		521	1	0.067	1 ==> 0
	361	1	0.160	4 ==> 3		494	1	0.133	0 --> 2		525	1	0.167	1 ==> 0
	413	1	0.033	1 --> 0		497	1	0.048	0 --> 1		546	1	0.100	1 ==> 0
	418	1	0.083	0 ==> 1		514	1	0.083	1 --> 0		547	1	0.250	0 ==> 1
	420	1	0.085	4 ==> 3		515	1	0.250	0 ==> 1		569	1	0.333	0 ==> 1
	584	1	0.188	0 --> 1	node_369 --> Aeluroscalobates	7	2	0.069	0 ==> 2	node_372 --> Gekko gecko	18	1	0.053	1 ==> 2
node_366 --> Lialis burtonis	4	1	0.143	0 ==> 1		118	1	0.143	0 ==> 1		129	2	0.051	0 ==> 2
	18	2	0.053	0 ==> 2		149	1	0.087	1 ==> 0		149	1	0.087	1 --> 2
	37	1	0.059	0 ==> 1		188	1	0.080	3 --> 2		168	1	0.065	0 ==> 1
	70	1	0.667	1 --> 0		201	1	0.250	0 ==> 1		185	1	0.067	3 ==> 2
	88	1	0.125	0 ==> 1		341	1	0.033	1 ==> 0		188	1	0.080	3 --> 2
	114	1	0.148	3 ==> 4		347	1	0.500	2 ==> 1		193	1	0.100	0 ==> 1
	142	1	0.250	0 ==> 1		351	1	0.375	0 ==> 1		212	1	0.182	0 ==> 2
	188	1	0.080	2 ==> 1		402	1	0.167	0 ==> 1		275	1	0.333	0 ==> 2
	249	1	0.231	0 ==> 1		462	1	0.071	0 ==> 1		394	1	0.087	1 ==> 2
	273	1	0.062	1 --> 0		479	1	0.250	1 --> 0		410	1	0.091	0 ==> 1
	286	1	0.111	1 --> 0		483	1	0.120	1 ==> 2		518	1	0.100	1 ==> 0
	324	1	0.300	0 ==> 1		500	1	0.133	2 ==> 0		521	1	0.067	1 ==> 0
	325	1	0.091	0 ==> 1		508	1	0.143	1 ==> 0		577	1	0.167	0 ==> 1
	355	1	0.059	0 ==> 1		509	1	0.158	1 ==> 2		578	1	0.167	0 ==> 1
	399	1	0.062	0 ==> 1	node_369 --> node_368	43	1	0.375	1 ==> 0		579	1	0.182	0 ==> 1
node_376 --> node_375	43	2	0.375	1 ==> 3		137	1	0.077	1 ==> 0	node_386 --> node_385	3	1	0.182	0 ==> 1
	111	1	0.222	0 --> 1		215	1	0.091	1 --> 0		6	1	0.100	0 --> 1
	205	1	0.333	1 --> 0		273	1	0.062	1 ==> 0		10	1	0.087	0 ==> 1
	220	1	0.375	1 --> 0		309	1	0.333	2 --> 1		11	1	0.105	0 ==> 1
	292	1	0.500	0 ==> 1		418	1	0.083	0 ==> 1		19	1	0.167	0 ==> 1
	341	1	0.033	0 ==> 1		557	1	0.125	0 ==> 1		20	1	0.167	0 ==> 1
	384	1	0.097	0 --> 3		585	1	0.250	1 --> 0		36	1	0.062	0 --> 1
	443	1	0.167	0 ==> 1		588	1	0.167	1 ==> 0		48	1	0.103	3 ==> 4
	452	1	0.235	0 ==> 2	node_368 --> Coleonyx variega	29	1	0.083	0 ==> 1		62	1	0.111	0 ==> 2
	455	2	0.148	4 ==> 2		95	1	0.083	0 --> 1		109	1	0.750	0 --> 3
	467	1	0.333	1 ==> 0		124	1	0.077	0 ==> 1		118	1	0.143	0 ==> 1
	500	1	0.133	0 ==> 2		166	1	0.091	0 ==> 1		186	1	1.000	0 ==> 1
	501	1	0.100	0 ==> 1		188	1	0.080	3 ==> 4		214	1	0.200	0 --> 1
	502	1	0.091	1 ==> 0		380	1	0.091	0 --> 1		231	1	0.077	0 --> 1
node_375 --> Strophurus cilia	22	1	0.111	1 ==> 0		409	1	0.333	0 --> 1		263	1	0.286	0 --> 1
	29	1	0.083	0 ==> 1		439	1	0.118	1 ==> 0		268	1	0.250	0 --> 1
	57	1	0.190	1 ==> 0		518	1	0.100	1 ==> 2		278	1	0.500	0 --> 2
	58	1	0.222	1 ==> 2		541	1	0.100	0 ==> 1		296	1	0.333	2 ==> 0
	108	2	0.125	0 ==> 2		565	1	0.125	0 ==> 1		311	1	0.286	0 --> 1
	149	1	0.087	1 --> 2	node_368 --> Eublepharis macu	23	1	0.158	0 ==> 1		334	1	0.167	1 --> 0
	190	1	0.250	0 ==> 1		321	1	0.231	0 --> 3		340	1	0.095	0 --> 1
	275	1	0.333	0 ==> 2		410	1	0.091	0 ==> 1		344	1	0.048	0 --> 1
	375	1	0.065	0 --> 1		494	1	0.133	2 --> 0		348	1	0.111	0 --> 1
	394	1	0.087	1 ==> 2		497	1	0.048	1 --> 0		349	3	0.136	0 --> 3
	439	1	0.118	1 ==> 0		498	1	0.083	0 ==> 1		350	1	0.333	0 --> 1
	479	1	0.250	1 --> 0		509	1	0.158	1 ==> 0		358	1	0.250	0 --> 1
	506	1	0.250	0 ==> 1		512	1	0.091	0 ==> 1		359	1	1.000	0 --> 2
	512	1	0.091	0 ==> 1		514	1	0.083	0 --> 1		362	1	0.333	0 --> 1
	518	1	0.100	1 --> 0	node_373 --> node_372	18	1	0.053	0 ==> 1		375	1	0.065	2 --> 1
	541	1	0.100	0 ==> 1		185	1	0.067	4 ==> 3		376	1	0.200	0 ==> 1
	554	1	0.167	0 ==> 1		254	1	0.182	0 ==> 2		377	1	0.333	0 ==> 2
	565	1	0.125	0 ==> 1		439	1	0.118	1 ==> 0		385	1	0.067	0 ==> 2
node_375 --> node_374	13	1	0.067	0 ==> 1		575	1	0.167	0 --> 1		392	2	0.105	0 --> 2
	37	1	0.059	0 --> 1		584	1	0.188	0 ==> 1		395	1	0.500	0 ==> 1
	39	1	0.080	3 --> 2	node_372 --> node_371	11	1	0.105	0 --> 1		410	1	0.091	0 ==> 1
	129	1	0.051	1 --> 0		13	1	0.067	1 ==> 0		413	1	0.033	1 --> 0
	187	1	0.500	1 --> 2		144	1	0.091	1 ==> 0		418	1	0.083	0 --> 1
	188	1	0.080	2 --> 3		309	1	0.333	2 --> 1		419	1	0.073	3 ==> 2
	215	1	0.091	0 --> 1		321	1	0.231	0 --> 3		420	1	0.085	3 --> 2
	252	1	0.200	0 ==> 1		420	1	0.085	4 ==> 3		422	1	0.182	0 ==> 1
	309	1	0.333	1 --> 2		421	1	0.075	4 ==> 3		427	1	0.100	0 ==> 1
	409	1	0.333	0 --> 1		479	1	0.250	1 --> 0		428	1	0.200	0 --> 1
	489	1	0.111	1 --> 0		588	1	0.167	1 --> 0		432	1	1.000	0 --> 1
	494	1	0.133	1 ==> 0	node_371 --> Teratoscincus pr	36	1	0.062	1 ==> 0		433	1	0.100	0 --> 1
	498	1	0.083	1 ==> 0		37	1	0.059	1 ==> 0		461	1	0.300	0 ==> 2
	539	1	0.500	1 ==> 0		88	1	0.125	1 ==> 0		462	1	0.071	0 ==> 1
node_374 --> node_367	50	1	0.167	0 ==> 1		95	1	0.083	1 ==> 0		465	1	0.250	0 ==> 1
	70	1	0.667	1 ==> 2		166	1	0.091	0 ==> 1		468	1	0.120	2 ==> 3
	94	1	0.062	0 --> 2		204	1	0.125	1 ==> 0		475	1	0.300	1 ==> 2
	114	1	0.148	3 ==> 4		252	1	0.200	1 ==> 0		478	1	0.250	0 ==> 1
	168	2	0.065	0 ==> 2		273	1	0.062	1 ==> 0		483	1	0.120	1 --> 2

	488	1	0.133	0 ==> 1
	491	1	0.143	0 --> 1
	497	1	0.048	0 --> 1
	499	1	0.143	0 --> 1
	530	1	0.200	0 --> 1
	533	1	0.333	1 --> 0
	535	1	0.143	1 --> 0
	549	1	0.250	0 ==> 1
	550	1	0.200	0 ==> 1
	556	1	0.500	1 --> 0
	561	1	0.154	0 ==> 2
	566	1	0.444	0 --> 3
node_385 --> node_380	9	1	0.250	0 ==> 1
	456	1	0.190	0 ==> 1
	460	2	0.600	0 ==> 2
	493	1	0.200	1 --> 0
node_380 --> Adriosaurus sues	36	1	0.062	1 --> 0
	49	1	0.089	0 ==> 1
	460	1	0.600	2 ==> 3
	505	1	0.167	0 ==> 1
node_380 --> Pontosaurus	115	1	0.600	0 ==> 2
	499	1	0.143	1 --> 0
node_385 --> node_384	2	1	0.083	0 --> 1
	7	2	0.069	0 --> 2
	10	1	0.087	1 --> 2
	26	1	1.000	0 --> 1
	83	1	1.000	2 ==> 3
	94	1	0.062	0 ==> 2
	96	1	0.222	0 --> 2
	165	1	0.200	1 --> 0
	382	1	0.333	0 ==> 1
	393	1	0.250	1 --> 0
	405	1	0.250	0 --> 1
	531	1	0.125	0 --> 1
	546	1	0.100	1 ==> 0
	567	1	1.000	0 --> 1
node_384 --> Aigialosaurus da	529	1	0.286	1 ==> 2
node_384 --> node_383	50	1	0.167	0 ==> 1
	51	1	0.200	0 ==> 1
	78	1	0.571	1 ==> 3
	87	1	0.200	0 ==> 1
	124	1	0.077	0 ==> 1
	129	2	0.051	0 ==> 2
	158	1	0.333	0 --> 1
	389	1	0.200	0 --> 1
	418	1	0.083	1 ==> 2
	463	1	0.108	1 ==> 0
	522	1	1.000	0 ==> 2
	524	1	0.200	0 ==> 1
	527	1	1.000	0 ==> 1
	544	1	1.000	0 --> 1
node_383 --> node_382	283	1	0.133	1 --> 2
	333	1	0.333	0 ==> 1
	400	1	0.200	0 --> 1
	421	1	0.075	3 ==> 2
	456	1	0.190	0 --> 1
	475	1	0.300	2 --> 3
	478	1	0.250	1 ==> 0
	495	1	0.125	1 --> 0
node_382 --> Clidastes	49	1	0.089	0 ==> 1
	429	1	0.500	0 ==> 1
	564	1	0.500	0 ==> 1
	584	1	0.188	1 ==> 0
node_382 --> node_381	468	3	0.120	3 ==> 0
node_381 --> Plotosaurus	272	1	0.500	0 ==> 1
	273	1	0.062	0 ==> 1
	293	1	0.143	0 ==> 1
	355	1	0.059	0 ==> 1
	392	1	0.105	2 ==> 1
	420	1	0.085	2 ==> 3
	422	1	0.182	1 ==> 2
	423	1	0.100	0 ==> 1
	456	1	0.190	1 ==> 2
	499	1	0.143	1 ==> 0
	540	1	0.500	0 ==> 1
node_381 --> Tylosaurus	77	1	0.083	0 ==> 1
	143	1	0.200	0 ==> 1
	389	1	0.200	1 --> 0
	400	1	0.200	1 --> 0
	406	1	0.143	0 ==> 1
	456	1	0.190	1 --> 0
node_383 --> Platecarpus	77	1	0.083	0 ==> 1
	93	1	0.111	0 ==> 1
	283	1	0.133	1 --> 0
	307	1	0.125	0 ==> 1
	313	1	0.500	0 ==> 1
	337	1	0.136	0 ==> 1
	397	1	0.333	0 ==> 1
	422	1	0.182	1 ==> 0
	423	1	0.100	0 ==> 1
	505	1	0.167	0 ==> 1
	573	1	0.083	0 ==> 1
	584	2	0.188	1 ==> 3

Table 5.3. Skull and Snout-Vent Length (SVL) measurements of *Magnuviator ovimonsensis*, gen. et sp. nov. and nine Campanian-age iguanomorphs from Mongolia. "Measurement type" refers to the type of measurement made (SVL or skull straight-line measurements along skull midline). All Mongolian iguanomorph measurements are based on measuring figured specimens (see Ref. Figure #) using ImageJ. The SVL of *Saichangurvel davidsoni* was measured twice (measurement 1 and 2) to determine level of consistency in measurement. References are from three primary sources (Gao and Hou 1995; Gao and Norell 2000; Conrad and Norell 2007). Additional details of how specimens were measured are included under the column heading "Notes regarding measurements". All measurements are in mm.

Taxon	Specimen #	Holotype	Measurement type	mm	View	ImageJ	Reference	Ref. Figure #	Notes regarding measurements
Iguanomorpha (?stem Pleurodonta)									
Magnuviator ovimonsensis	MOR 6627	Yes	SVL	216	dorsal	Yes	this paper		
Magnuviator ovimonsensis	MOR 6627	Yes	straightline skull length along midline	40.7	ventral	No	this paper		measured using AmPro Electronic Digital Calipers (T74615): resolution 0.01mm; Accuracy ±0.02 mm (<100mm)
Magnuviator ovimonsensis	MOR 7042	No	SVL	160	dorsal	Yes	this paper		
Magnuviator ovimonsensis	MOR 7042	No	straightline skull length along midline	32.8	dorsal	No	this paper		measured using AmPro Electronic Digital Calipers (T74615): resolution 0.01mm; Accuracy ±0.02 mm (<100mm)
Magnuviator ovimonsensis	MOR 7042	No	straightline skull length along midline	34.2	ventral	No	this paper		measured using AmPro Electronic Digital Calipers (T74615): resolution 0.01mm; Accuracy ±0.02 mm (<100mm)
Saichangurvel davidsoni	IGM 3/858	Yes	straightline skull length along midline	25.4	dorsal	Yes	Conrad and Norell 2007	3A	measured from anterior margin of premaxilla to a line perpendicular to the posterior margin of the left supratemporal
Saichangurvel davidsoni	IGM 3/858	Yes	SVL; measurement 1	116.9	dorsal	Yes	Conrad and Norell 2007	1	measured from anterior margin of premaxilla along midline of vertebral column to ca. posterior margin of caudal 1; scale was derived from measuring skull length in Conrad and Norell 2007 fig. 3A and using that known measurement to estimate SVL
Saichangurvel davidsoni	IGM 3/858	Yes	SVL; measurement 2	116.9	dorsal	Yes	Conrad and Norell 2007	1	measured from anterior margin of premaxilla along midline of vertebral column to ca. posterior margin of caudal 1; scale was derived from measuring skull length in Conrad and Norell 2007 fig. 3A and using that known measurement to estimate SVL
Temujinia ellisoni	IGM 3/63	Yes	straightline skull length along midline	22.2	dorsal	Yes	Gao and Norell 2000	5a	measured from tip of snout to a line perpendicular to the posterior margin of the supratemporal process of the parietal
Temujinia ellisoni	IGM 3/63	Yes	straightline skull length along midline	22.9	ventral	Yes	Gao and Norell 2000	5b	measured from tip of snout to a line perpendicular to the posterior margin of right prearticular
Temujinia ellisoni	IGM 3/64	No	straightline skull length along midline	21.4	dorsal	Yes	Gao and Norell 2000	6b	measured from anterior margin of premaxilla to a line perpendicular to the posterior margin of the supratemporal process of the parietal
stem Pleurodonta									
Zapsosaurus sceliphros	IGM 3/71	Yes	straightline skull length along midline	29.2	dorsal	Yes	Gao and Norell 2000	7C	measured from anterior margin of left dentary to a line perpendicular to the posterior margin of the supratemporal process of the parietal
Zapsosaurus sceliphros	IGM 3/71	Yes	straightline skull length along midline	29.4	ventral	Yes	Gao and Norell 2000	7D	measured from anterior margin of left dentary to a line perpendicular to the posterior margin of the right prearticular
Isodontosaurus gracilis	IGM 3/84	Yes	straightline skull length along midline	15.5	dorsal	Yes	Gao and Norell 2000	12A	measured from tip of snout to a line perpendicular to the posterior margin of the paroccipital process of the right otooccipital
Isodontosaurus gracilis	IGM 3/84	Yes	straightline skull length along midline	16.5	ventral	Yes	Gao and Norell 2000	12B	measured from anterior margin of left dentary to a line perpendicular to the posterior margin of the right prearticular
Isodontosaurus gracilis	IGM 3/91	No	straightline skull length along midline	14.9	dorsal	Yes	Gao and Norell 2000	13A	measured from anterior margin of premaxilla to a line perpendicular to the posterior margin of the right supratemporal process of the parietal
Anchaurosaurus gilmorei	IVPP V10028	Yes	straightline skull length along midline	33.3	dorsal	Yes	Gao and Hou 1995	1A	measured from anterior margin of premaxilla to a line perpendicular to the posterior margin of the left supratemporal process of the parietal
Anchaurosaurus gilmorei	IVPP V10028	Yes	straightline skull length along midline	36.4	ventral	Yes	Gao and Hou 1995	1B	measured from anterior margin of premaxilla to a line perpendicular to the posterior margin of the prearticulars
stem Acrodonta (Chamaeleontiformes)									
Ctenomastax parva	IGM 3/62	No	straightline skull length along midline	20.6	dorsal	Yes	Gao and Norell 2000	4B	measured from anterior margin of premaxilla to a line perpendicular to the posterior margin of the supratemporal process of the parietal
Ctenomastax parva	IGM 3/61	Yes	straightline skull length along midline	19.9	ventral	Yes	Gao and Norell 2000	3A	measured from anterior margin of right dentary to a line perpendicular to the posterior margin of the right prearticular
Mimeosaurus crassus	IGM 3/76	No	straightline skull length along midline	24.1	dorsal	Yes	Gao and Norell 2000	9A	measured from anterior margin of premaxilla to a line perpendicular to the posterior margin of the left supratemporal process of the parietal
Priscagama gobiensis	IGM 3/80	No	straightline skull length along midline	25.0	dorsal	Yes	Gao and Norell 2000	10C	measured from anterior margin of right dentary to a line perpendicular to the posterior margin of the right supratemporal process of the parietal
Phrynosomimus asper	IGM 3/81	No	straightline skull length along midline	12.5	dorsal	Yes	Gao and Norell 2000	11A	measured from anterior margin of premaxilla to a line perpendicular to the posterior margin of the right supratemporal process of the parietal

CHAPTER 6:

CONCLUDING REMARKS

Below I highlight the major conclusions of my dissertation.

1. Caudates and allocaudates suffered minor extinctions during the K-Pg mass extinction, but revealed patterns of growing ecological stress during the last ca. 400 k.y. of the Cretaceous and across the K-Pg boundary.

Fifty-six percent of local caudate and allocaudate species were lost in a stepwise fashion during the last ca. 400 k.y. of the Cretaceous (ca. 200 k.y. based on new radiometric age determinations; Sprain et al. 2015) though only 22% represent extinctions. Significant changes in diversity and community structure also preceded the K-Pg boundary as indicated by significant declines in species evenness, steepening RAD slopes, and a significant increase in the relative abundance of the caudate *Opisthotriton kayi* that carried over into the earliest Paleocene. Those changes temporally correlated with similar changes in other components of the local vertebrate fauna, the regional paleoflora, the global marine biota, and proxies for global environmental conditions. Combined, these data favor a complex multiple-cause extinction scenario for the end-Cretaceous mass extinction.

2. Squamates underwent consistent and major taxonomic turnover during the last ca. 1.9 m.y. of the Cretaceous and across the K-Pg boundary.

Significant squamate turnover occurred throughout most of the depositional duration of the Hell Creek Formation with moderate rates of turnover occurring more than ca. 300 k.y. before the K-Pg boundary. Disappearance rates increased and peaked during the last ca. 200 k.y. of the Cretaceous which culminated into 81% species extinctions. Taxonomic composition among squamate assemblages is distinct between the lower and upper halves of the Hell Creek Formation and is coincident with the local loss of chamopsiids possessing monocuspid teeth and

platynotans possessing fang-like teeth. These lower and upper Hell Creek squamate faunas correlate to the mammalian "La1" and "La2" faunas of Wilson (2014) of the local section. Similar lower and upper restricted biostratigraphic ranges have been documented in other nonmammalian vertebrates of the area (euselachians, caudates, allocaudates, frogs, and turtles).

4. The earliest Paleocene caudate assemblage was species depauperate, predominated by a bloom taxon, and invaded by an immigrant species. Squamates are nearly absent from the local section during the Pu1 interval but two chamopsiids are present and may represent members of a "dead clade walking".

The species depauperate caudate assemblage in the Pu1 interval was predominated by the 'bloom taxon' *Opisthotriton kayi*. That taxon began its climb to predominance during the last ca. 200 k.y. of the Cretaceous (see above). A single caudate immigrant, *Proamphiuma cretacea*, joined *O. kayi* and the three other local survivors immediately above the K-Pg boundary. The Lazarus taxon, *Prodesmodon copei*, reappeared in the local section during the Pu2/3 interval less than ca. 925 k.y. after the K-Pg boundary. The squamate fauna during that interval possessed two chamopsiid lizards. Chamopsiids are part of a clade thought to have gone extinct during the K-Pg mass extinction. These new records suggest that chamopsiids were a "dead clade walking" as they failed to recover in abundance or diversity following the extinction.

3. The Hell Creek Formation of Garfield County, northeastern Montana contains the most species rich lissamphibian and squamate faunas of the latest Cretaceous of North America.

From the large collection of fossil lissamphibians and squamates investigated for *Chapters Two* and *Three*, two albanerpetontids, nine caudates, two snakes, and 28 lizards were

recorded from the Hell Creek Formation. Several of these taxa were previously documented from the study area (several with systematic updates) but many represent new paleobiogeographic, biostratigraphic, and/or temporal range extensions (see also DeMar 2011). Several taxa occurring in the lower portions of the Hell Creek Formation previously were restricted to the Campanian-age deposits of southern Alberta, Canada, central Wyoming, USA, or both including the sirenid salamander *Habrosaurus prodilatus* and the chamopsiids *Leptochamops thrinax* and *Socognathus unicuspis*. Snakes are the rarest component of the Hell Creek vertebrate faunas; only 18 vertebrae have been found to date from three localities. A few taxa known from outside the study area (e.g., BCA) or from other Lancian-age deposits of the Western Interior also appear in the study area for the first time including the albanerpetontid *Albanerpeton galaktion*, the chamopsiids *Meniscognathus altmani* and *Socognathus brachyodon*, the anguimorph *Colpodontosaurus cracens*, and the snake *Coniophis precedens*.

I also recognized several new taxa from the richly fossiliferous deposits of the Hell Creek Formation. Among these new taxa are the oldest proteid salamander, *Paranecturus garbanii* (DeMar 2013; *Chapter Four*), and an undescribed scapherpetontid salamander (Wilson et al. 2012b; *Chapter Two*; see Gardner and DeMar 2013 for two more additions to the Hell Creek caudate fauna of the local section). Most new taxa are lizards including an indeterminate iguanomorph, six scincomorphs (four chamopsiids, a doubtful chamopsiid, and an indeterminate scincomorph), and five anguimorphs (two anguids and three platynotans). Many of these new taxa are restricted to the lower portions of the Hell Creek Formation though one is found as high as 5.2 m below the K-Pg boundary. Most are small-bodied, but some are large including the heavily armored platynotan Platynota gen. et sp. undet. C.

In sum, a total of 11 diagnosable or potentially diagnosable caudates occur in the Hell Creek Formation of the local study area making it the most species rich caudate assemblage known from North America during the Late Jurassic to the end of the Paleocene (Gardner and DeMar 2013). Similarly, of the 44 diagnosable or potentially diagnosable Maastrichtian-age squamates known from the Western Interior of North America, 30 are known from the Hell Creek Formation in the local section.

5. A new Late Cretaceous stem iguanian from northwestern Montana has provided novel insights into the evolution of Iguanomorpha.

Two nearly complete skeletons of a Campanian-age iguanomorph from Montana have yielded a wealth of morphological, phylogenetic, and ecomorphological information for better understanding the fossil record of iguanomorphs in North America prior to the K-Pg boundary. The new taxon, *Magnuviator ovimonsensis*, gen. et sp. nov., represents the oldest unequivocal member of Iguanomorpha from the continent and is closely related to a pair of iguanomorphs known from the paracontemporaneous deposits of Mongolia. That sister-taxon relationship provides the first phylogenetically based evidence for iguanomorph exchange between the northern Laurasian landmasses of Asia and North America during the Cretaceous. Based on comparative measurements, *Magnuviator* was a relatively large Late Cretaceous iguanomorph which likely fed on wasps based on its dentition and the nearly ubiquitous occurrences of wasp pupae cases found throughout the type locality of *Magnuviator* (Egg Mountain).